
BINDING SERVICES
Tel +44 (0)29 2087 4949
Fax.+44 (0)29 2037 1921
E-Mail Bindery@Cardiff.ac.uk

# Studies of Myosin Light Chain-Dependent Modulation of Tight Junction Function through the Actions of Membrane-Permeant Peptides

**Siân-Eleri Owens**

**Bsc (Hons)**

**A thesis submitted to Cardiff University in partial fulfilment of the requirements for the degree of Doctor of Philosophy**

**Welsh School of Pharmacy,**

**Cardiff University,**

**Wales**





ProQuest LLC
789 East Eisenhower Parkway
P.O. Box 1346
Ann Arbor, MI 48106-1346

**Er cof tadcu, Vicky a Chris**

**Acknowledgements**

First and foremost I would like to thank my supervisor Prof. Randy Mrsny for his continued support and guidance throughout the course of this PhD.

I would also like to thank Dr. Arwyn Jones and all members of CPT, who have helped so much in the transition into a new group. Thanks also to Dr Jerry Taylor for his help with the biological assays performed in these studies.

Special thanks go to Dr. Dario Siccardi who helped me out so much with techniques such as peptide synthesis and LC-MS at the beginning of this PhD, Dr. Vicky Dickinson for being one of the biggest inspirational people in my life. A big thank you to Ian, Ross, Saly, Sioned and Steve for their help I couldn't have survived this PhD without you guys. Karen thanks for those endless nights of writing up, which seemed to go on forever.

Thanks to my friends Vick, Elin, Zoe and Ruth who have been terrific emotional support throughout this time.

To all my family whose constant support has been amazing, especially Mam who thinks tight junctions are like jam sandwiches, Dad for his continued support and Llini for her continuous haven't you finished yet! And finally Rhyds who has had to live with all the stress of this PhD, thank you for your endless encouragement and help I really could not have done this without you.

**Abstract**

Myosin light chain phosphorylation plays a central role in the regulation of paracellular permeability. The main objective of this study was to design and synthesise membrane-permeant peptide inhibitors of myosin light chain kinase and phosphatase that could potentially decrease and increase paracellular permeability, respectively.

Elevated myosin light chain kinase activity, as observed in a variety of inflammatory disease, phosphorylates myosin light chain, to increase paracellular permeability. Initial studies showed a peptide inhibitor of myosin light chain kinase (termed PIK) could rectify increased paracellular permeability in two different cell-based models of inflammation. PIK was also, however, shown to be too labile for use *in vivo*. From a series of PIK analogues, two candidates prepared using D-amino acids were identified that showed sufficient stability, membrane-permeant properties and retention of specific function of PIK for future *in vivo* studies.

Since the ratio of myosin light chain kinase to phosphatase activity regulates the degree of myosin light chain phosphorylation, it was hypothesised that inhibition of myosin light chain phosphatase would increase paracellular permeability. A membrane-permeant peptide designed to inhibit myosin light chain phosphatase activity (termed PIP) was identified in a screen of potential candidates through its capability to significantly decrease transepithelial electrical resistance in a polarized human intestinal epithelial cell system *in vitro* without any apparent cytotoxicity. Further studies will be required to determine the extent to which PIP increases paracellular permeability.

Using these novel membrane-permeant peptide inhibitors, studies were performed using polarized monolayers of human intestinal epithelial cells to assess the action of previously identified regulators of paracellular permeability *in vitro*. Previous studies demonstrated that the non-specific myosin light chain kinase inhibitor ML-7 prevented the absorption enhancing properties of sodium caprate. Treatment with PIK and sodium caprate simultaneously resulted in significant increases in the permeability of inert fluorescent probes while pre- and post-incubation with PIK inhibited sodium caprate effects. These surprising findings suggest a potential application for combination treatment with sodium caprate and PIK to increase paracellular permeability of poorly absorbed drugs.

## Index

## List of Figures

## List of Tables

**List of Abbreviations**

| | |
|---|---|
| Acetonitrile | ACN |
| Adenosine triphosphate | ATP |
| N-(6-aminohexyl)-5-chloro-1- napthalenesulphoamide | W7 |
| Angstrom | Å |
| Arachidonic acid | AA |
| Attach and efface | A/E |
| | |
| O-benzotriazole-N,N,N,N-tetramethyl-uronium hexaflurophosphate | HBTU |
| Benzotriazole-1-yl-oxy-tris-pyrrolidino-phosphonium hexaflurophosphate | PyBOP® |
| Blood-brain barrier | BBB |
| | |
| Calcium | $Ca^{2+}$ |
| Calmodulin | CaM |
| Calcium/calmodulin-dependent protein kinase II | CaMPKII |
| 1-(5-chloronaphthalene-1-sulphonyl)-1H-hexahydro-1,4-diazepine hydrochloride | ML-9 |
| Caspase recruitment domain | CARD |
| Cell-penetrating peptide | CPP |
| Crohn's disease | CD |
| Cyclooxygenase 2 | COX2 |
| | |
| Diacylglycerol | DAG |
| *N,N*-diisopropylethylamine | DIEA |
| 4-(2',4'-Dimethoxyphenyl-Fmoc-aminomethyl)-phenoxyacetamido-norleucyl-MBHA resin | Rink amide MBHA resin |
| Dimethylformamide | DMF |
| Dimethylsulfoxide | DMSO |
| (3-[4,5-dimethyl-thiazol-2-yl]-2,5-diphenyl-tetrazolium bromide | MTT |
| Dopamine- and cyclic AMP- regulated Phosphoproteins of 32,000 | DARPP-32 |
| Dulbecco's modified Eagle's media | D-MEM |

**List of Abbreviations continued**

| | |
|---|---|
| Enteropathogenic *Escherichia coli* | EPEC |
| Enzyme-Linked Immunosorbent Assay | ELISA |
| Electrospray ionisation | ESI |
| Ethylenediamine tetra-acetic acid | EDTA |
| Filamentous-actin | F-actin |
| Foetal bovine serum | FBS |
| $N^{\alpha}$-9-fluorenylmethoxycarbonyl | Fmoc |
| Fluoresceinisothiocyanate dextran | FD |
| Guanylate kinase-like | GUK |
| Hanks' balanced salt solution | HBSS |
| (2-1-H-benzotriazol-1-yl)-1,1,3,3-tetramethyl-uronium hexaflurophosphate | HBTU |
| High pressure-liquid chromatography | HPLC |
| Hydrogen Peroxide | $H_3PO_4$ |
| Hydroxybenzotriazole | HOBt |
| N-2-Hydroxyethylpiperazine-N'-2-ethanesulfonic acid | HEPES |
| Immunoglobulin | Ig |
| Inhibitory concentration for 50% cell population | $IC_{50}$ |
| Inflammatory bowel disease | IBD |
| Interferon γ | IFN-γ |
| Interleukin | IL |
| Inositol triphosphate | $IP_3$ |
| 1-(5-iodonapthalene-1-sulphonyl)-1H- hexahydro-1,4-diazepine hydrochloride | ML-7 |
| Junction adhesion molecule | JAM |
| Kilodalton | kDa |

**List of Abbreviations continued**

| | |
|---|---|
| Leucine-rich repeat | LRR |
| Lipopolysaccarides | LPS |
| Liquid chromatography-mass spectrometery | LC-MS |
| | |
| 4-methylmorpholine | NMM |
| Madin-Darby canine kidney | MDCK |
| Membrane-associated guanylate kinase | MAGUK |
| Membrane permeant inhibitor of myosin light chain kinase | PIK |
| Mucosa-associated lymphatic tissue | MALT |
| Myosin light chain | MLC |
| Myosin light chain kinase | MLCK |
| Myosin light chain phosphatase | MLCP |
| | |
| Nuclear factor-κB | NF-κB |
| Nuclear magnetic resonance | NMR |
| Nucleotide-binding domain | NBD |
| | |
| Perijunctional actin-myosin II ring | PAMR |
| Phosphate buffered saline | PBS |
| Phospholipase C | PLC |
| Phorbol 12-myristate 13-acetate | PMA |
| Potential of hydrogen | pH |
| Polyoxyethylene-sorbitan monolaurate | Tween-20 |
| Proteinase-activated receptor | PAR |
| Protein kinase C | PKC |
| Protein phosphatase type 1 | PP1 |
| PKC-potentiated inhibitory protein for heterotrimeric myosin light chain phosphatase of 17kDa | CPI-17 |
| Protein transduction domain | PTD |
| PSD95/dlg/ZO-1 | PDZ |
| | |
| Sodium caprate | C10 |

**List of Abbreviations continued**

| | |
|---|---|
| Sodium dodecyl sulphate- polyacrylamide gel electrophoresis | SDS-PAGE |
| Sodium-glucose co-transporter | SGLT-1 |
| Src homology 3 | SH3 |
| Standard deviation | SD |
| Standard error of the mean | SEM |
| Tight junction | TJ |
| Trans-activating transcriptional activator | TAT |
| Transepithelial electrical resistance | TER |
| Transforming growth factor β | TGF-β |
| Trifluoroacetic acid | TFA |
| Triisopropylsilane | TIPS |
| *N,N,N*-trimethyl chitosan chloride | TMC |
| Tris(hydroxymethyl)aminomethane hydrochloride salt | Tris-HCl |
| Tumour necrosis factor α | TNF-α |
| Type 1 helper-T-cell | $T_H1$ |
| Type 17 helper-T-cell | $T_H17$ |
| Type 2 helper-T-cell | $T_H2$ |
| Ulcerative colitis | UC |
| Weight-average molecular weight | Mw |
| Zonnula occluden | ZO |

**Amino Acid Abbreviations**

| | | |
|---|---|---|
| Alanine | A | Ala |
| Cysteine | C | Cys |
| Aspartic acid | D | Asp |
| Glutamic acid | E | Glu |
| Phenylalanine | F | Phe |
| Glycine | G | Gly |
| Histidine | H | His |
| Isoleucine | I | Ile |
| Lysine | K | Lys |
| Leucine | L | Leu |
| Methionine | M | Met |
| Asparagine | N | Asn |
| Proline | P | Pro |
| Glutamine | Q | Gln |
| Arginine | R | Arg |
| Serine | S | Ser |
| Threonine | T | Thr |
| Valine | V | Val |
| Tryptophan | W | Trp |
| Tyrosine | Y | Tyr |
| Any amino acid | X | Xaa |

# Chapter 1

# General Introduction

## 1.1 Introduction

An integral role of epithelia is to establish diffusion barriers, thereby establishing and preserving compartments with varying compositions. This is a vital requirement for the physiological functioning of organs (Balda and Matter 1998). The main functions of the intestinal epithelium are:

1) To protect the underlying tissue compartments from the luminal contents of the intestine, which may contain harmful substances such as bacteria (Kucharzik, *et al* 2001).
2) The digestion of dietary proteins into smaller components such as amino acids and di/tripeptides, resulting in their absorption by the intestine (Pauletti, *et al* 1997).
3) To allow the selective secretion and absorption of molecules such as ions and water (Wang 1996).

Molecules are able to traverse the intestinal epithelium by four main pathways which include the transcellular pathway, where molecules cross the cell membrane by passive diffusion and paracellular pathway, whereby molecules passively diffuse between adjoining cells. P-glycoprotein is part of the ATP binding cassette family of transporters, which functions as a drug efflux pump. Finally, molecules can also cross cells via carrier-mediated transport as depicted in figure 1.1 (Spring 1998). Lipophilic molecules cross cell membranes by transcellular diffusion, whereas those hydrophilic molecules that are not transported via carrier-mediated transport, are therefore unable to traverse the hydrophobic membrane, are transported via the paracellular pathway (Ward, *et al* 2000).

## 1.2 Epithelial cell adhesion

The paracellular pathway is regulated by a junctional complex composed of gap junctions, desmosomes, adherence junctions and tight junctions (TJs) (Farquhar and Palade 1963, Stevenson and Paul 1989). Gap junctions are responsible for communication between cells, while adherence junctions and desmosomes are believed to provide mechanical strength to tissues (Balda and Matter 2003). Tight junctions, which are located at the most apical part of this specialised complex, regulate the paracellular pathway diffusion (Denker and Nigam 1998).

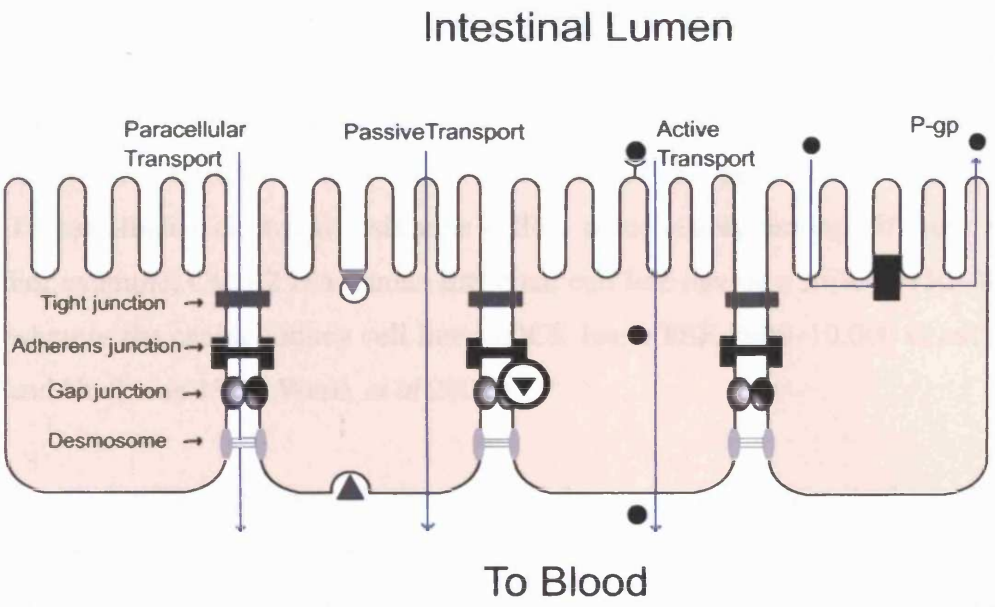


Figure 1.1 Schematic representation of molecule transport across intestinal epithelia. Molecules are able to traverse the intestinal epithelium by four main pathways which include the transcellular pathway, where molecules cross the cell membrane by passive diffusion and paracellular pathway, whereby molecules passively diffuse between adjoining cells. P-glycoprotein is part of the ATP binding cassette family of transporters, which functions as a drug efflux pump. Molecules can also cross cells via carrier-mediated transport.

## 1.3 Function of the tight junction

The TJ acts as a selective channel or pore that allows the movement of ions whilst limiting the passage of larger molecules. Tight junction pores have been shown to have a diameter of approximately 6 angstrom (Å) using impermeant tracers, which is comparable to some ion channels. Since the TJ regulates solute movement through the paracellular space, changes in transepithelial electrical resistance (TER) are used as an indicator of TJ permeability (Madara 1998). Transepithelial electrical resistance differs considerably among different cell lines. For example, Caco-2 is a human intestinal cell line having a TER of 150–300 $\Omega$ cm$^2$ whereas the canine kidney cell line MDCK has a TER 2000–10,000 $\Omega$ cm$^2$ (Quaroni and Hochman 1996, Ward, *et al* 2000).

Ion passage through the paracellular pathway as described previously is a passive process that is generated by electro-osmotic gradients. The TJ has many biophysical properties in common with ion channels. Indeed it appears that the development of intact TJs is required for paracellular ion selectivity. Tang and Goodenough hypothesised that within the TJ there are discrete ion channels that facilitate ion transport permitting regulated extracellular ion transport via the paracellular pathway. It has been hypothesised that the paracellular tight junction channels are established by adjacent extracellular domains of tight junction proteins contacting in the intercellular space thereby creating cross-bridges (Tang and Goodenough 2003).

## 1.4 Proteins of the tight junction

Tight junctions are composed of a variety of different proteins implicated in cell signalling, vesicle trafficking and cytoskeleton modulation. Additionally, TJs contain scaffolding proteins suggesting that the TJ plaque comprises of a complex system of interacting proteins (Lapierre 2000). The proteins of the TJ are thought to be important in the regulation of paracellular permeability. Schematic representation of currently known transmembrane TJ proteins can be seen in figure 1.2.

### *Occludin*

The first TJ transmembrane protein detected was the approximately 60 kDa

protein occludin. Sequence analysis suggests occludin to be a tetraspan protein, with both COOH and $NH_2$ termini located within the cytoplasm. Remarkably, 60 % of the first extracellular loop of occludin consists of the amino acids Y and G (Furuse, *et al* 1993). It has been suggested that occludin's second extracellular loop is involved in the establishment of the TJ barrier itself (Stevenson and Keon 1998). However, it is worth noting that occludin is not vital for the development of the TJ, since the development of functional strands is not prevented following occludin gene disruption in embryonic stem cells (Saitou, *et al* 1998). Generation of homozygous occludin null mice resulted in viable mice that seem to develop TJs. However, various abnormalities were evident. Occludin knockout mice exhibited growth retardation following birth, displayed defects in their salivary glands and testis, had compact bone thinning and gastric epithelium hyperplasia as well as deposition of calcium inside the brain and chronic gastritis. This suggests that although occludin is not required for the formation of TJs, it has an essential but as yet undefined role in mice (Harhaj and Antonetti 2004).

*Claudins*

Claudins, like occludin, have 4 transmembrane domains however they have comparatively short $NH_2$ and COOH termini located within the cytoplasm. Twenty-four claudin family members have been identified using genomic cloning and database searching. Genes from this family encode proteins of between 20 and 27 kDa (Schneeberger and Lynch 2004). Different claudins have diverse tissue distribution, thereby implying that these proteins are responsible for the different degrees of TER and paracellular ionic selectivity shown by different endothelia and epithelia (Gonzalez-Mariscal, *et al* 2003). Claudin 5, for example, is widely expressed whereas claudin 4 is expressed exclusively within the kidney and lung (Lapierre 2000). Induced expression of claudin-1 and 2 together in fibroblasts, which do not contain TJs, resulted in TJ strand formation indicating that claudins are important in the assembly of TJ strands (Tsukita and Furuse 1999). Mutations in the genes encoding claudin 14 and claudin 16 (paracellin-1) cause autosomal recessive deafness (DFNB29) and hereditary hypomagnesaemia respectively, thereby reiterating claudins importance in the function of TJ paracellular permeability (Simon, *et al* 1999, Wilcox, *et al* 2001).

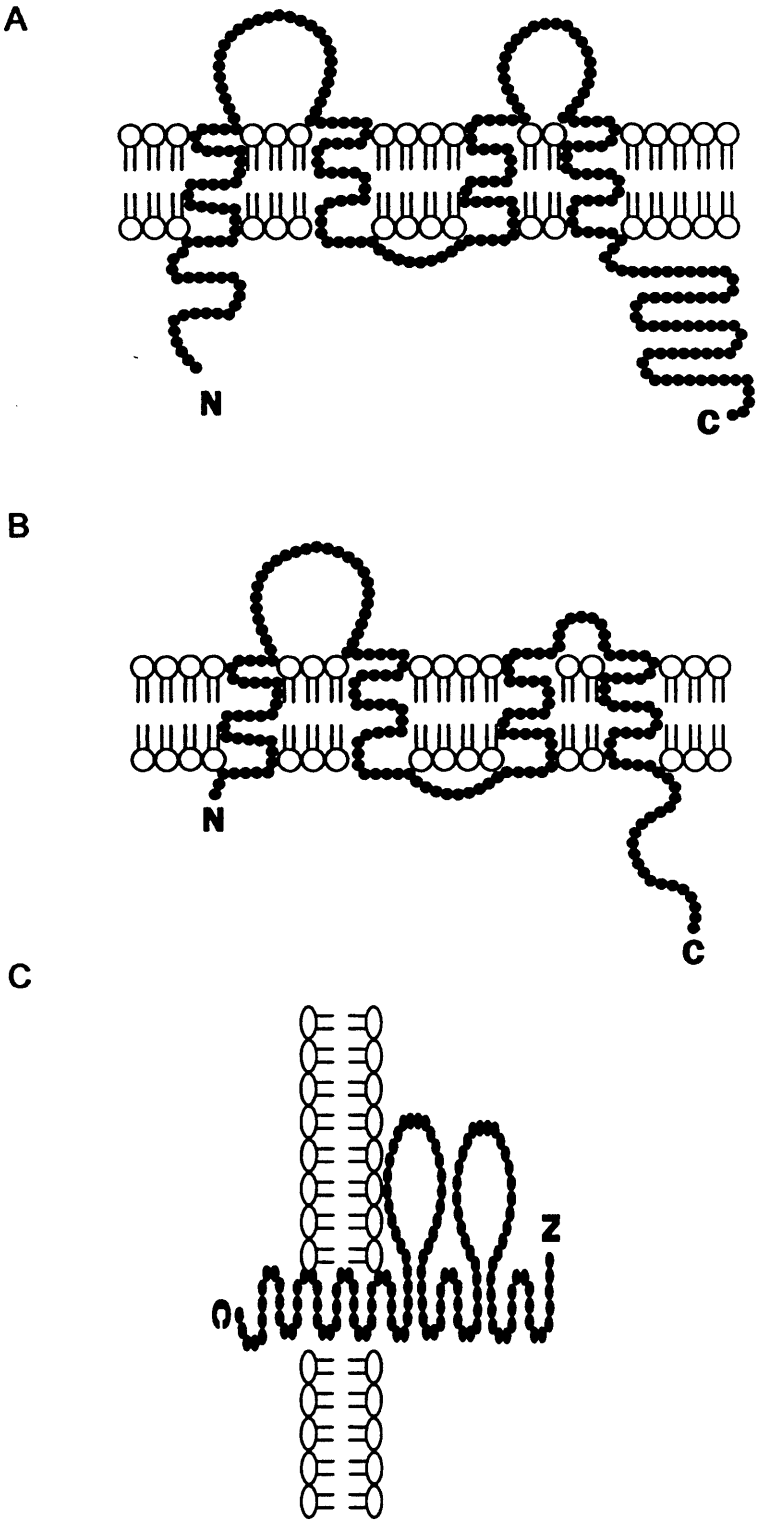


Figure 1.2 Schematic representation of the tight junction transmembrane proteins occludin (A), claudin (B) and junctional adhesion molecule (C).

*Human Junction Adhesion Molecule*

Human junctional adhesion molecule (JAM) is another transmembrane protein of the TJ. Several variants of JAM have been observed, all being 35-39 kDa and members of the immunoglobulin (Ig) superfamily. The amino acid sequence of human JAM predicts a highly polar region within the cytoplasm and 2 extracellular IgV loops with a single membrane-spanning domain. Junction adhesion molecules are expressed at epithelial and endothelial TJs, where they assist leukocyte diapedesis via the paracellular pathway. The first extracellular IgV domains of apposing JAM molecules create homophilic contact, thereby potentially stabilising the TJ (Liu, *et al* 2000).

*Zonnula Occludens*

Zonnula occluden (ZO) are cytoplasmic plaque proteins and members of the membrane-associated guanylate kinase (MAGUK) homologue family possessing the typical multi-domain structure consisting of the PSD95/dlg/ZO-1 (PDZ), guanylate kinase-like (GUK) and Src homology 3 (SH3) domains. Zonnula occluden proteins also include an acidic domain, a P rich region and a basic R rich domain not found in other MAGUK family members (Wittchen, *et al* 1999).

## 1.5 Tight junction protein interactions

Membrane-associated guanylate kinase proteins are typically regarded as the scaffolding proteins of the TJ as they connect different proteins together into particular membrane sub-domains, and are thought to serve as a link between the TJ transmembrane proteins and the actin cytoskeleton. They are also capable of binding to one another: ZO-1 binds to both ZO-2 and ZO-3. However, ZO-2 and ZO-3 do not interact to form complexes with each other (Wittchen, *et al* 1999). Filamentous actin (F-actin) binds directly to ZO-1 (Fanning, *et al* 1998), ZO-2 and ZO-3 (Wittchen, *et al* 1999) proteins in co-sedimentation studies. However, the actin-binding domain position has yet to be identified.

The final 150 amino acids of occludin tails are envisaged to form an α-helical coiled-coil structure (Ando-Akatsuka, *et al* 1996). Occludin is able to interact directly with ZO-1 (Furuse, *et al* 1993), ZO-2 (Itoh, *et al* 1999b) and ZO-3 (Haskins, *et al* 1998), as well as to F-actin (Wittchen, *et al* 1999) and occludin itself via the

coiled-coil domain (Nusrat, *et al* 2000a).

The COOH terminus of claudin bind directly to all three of the zonnula occludens proteins (Itoh, *et al* 1999a). The COOH terminus of JAM contains a PDZ domain that interacts with ZO-1 PDZ binding motif, an interaction thought to stabilise JAM at the TJ (Ebnet, *et al* 2000). *In vitro* binding analysis has shown that ZO-1 links claudins to JAM-1 through its PDZ1 and PDZ3 motifs (Bazzoni, *et al* 2000, Schneeberger and Lynch 2004) (figure 1.3).

Thus the scaffolding proteins have been shown to provide the link between the F-actin of the perijunctional actin-myosin ring (PAMR) and transmembrane TJ proteins, which have important functions in the regulation of the paracellular space. Therefore, the regulation of PAMR contraction may have a critical function in the ability to increase and decrease paracellular permeability.

Alterations in TJ permeability have been shown to be important in numerous pathophysiologiacal conditions such as inflammatory bowel disease (IBD), graft versus host disease and ischemic retinopathies (Harhaj and Antonetti 2004). Therefore, the ability to selectively open and close TJs could lead to novel therapeutics with various applications. For example, a therapeutic that could close intestinal epithelium TJs could be used for diseases such as IBD where intestinal TJ permeability is increased.

## 1.6 Inflammatory bowel disease

Inflammatory bowel disease has a prevalence of 10-200 cases per 100,000 in developed countries. Inflammatory bowel disease is a chronic inflammatory condition of the gastrointestinal tract of unknown, but apparently multifaceted origin. Inflammatory bowel disease comprises of 2 subsets, which include Crohn's disease (CD) and ulcerative colitis (UC). Crohn's disease and UC are both diseases of young adults, with the majority of cases occurring between the ages of 15 and 30 years (Bonen and Cho 2003). There are several resemblances between CD and UC; however, there are also numerous pathological and clinical differences (Bouma and Strober 2003).

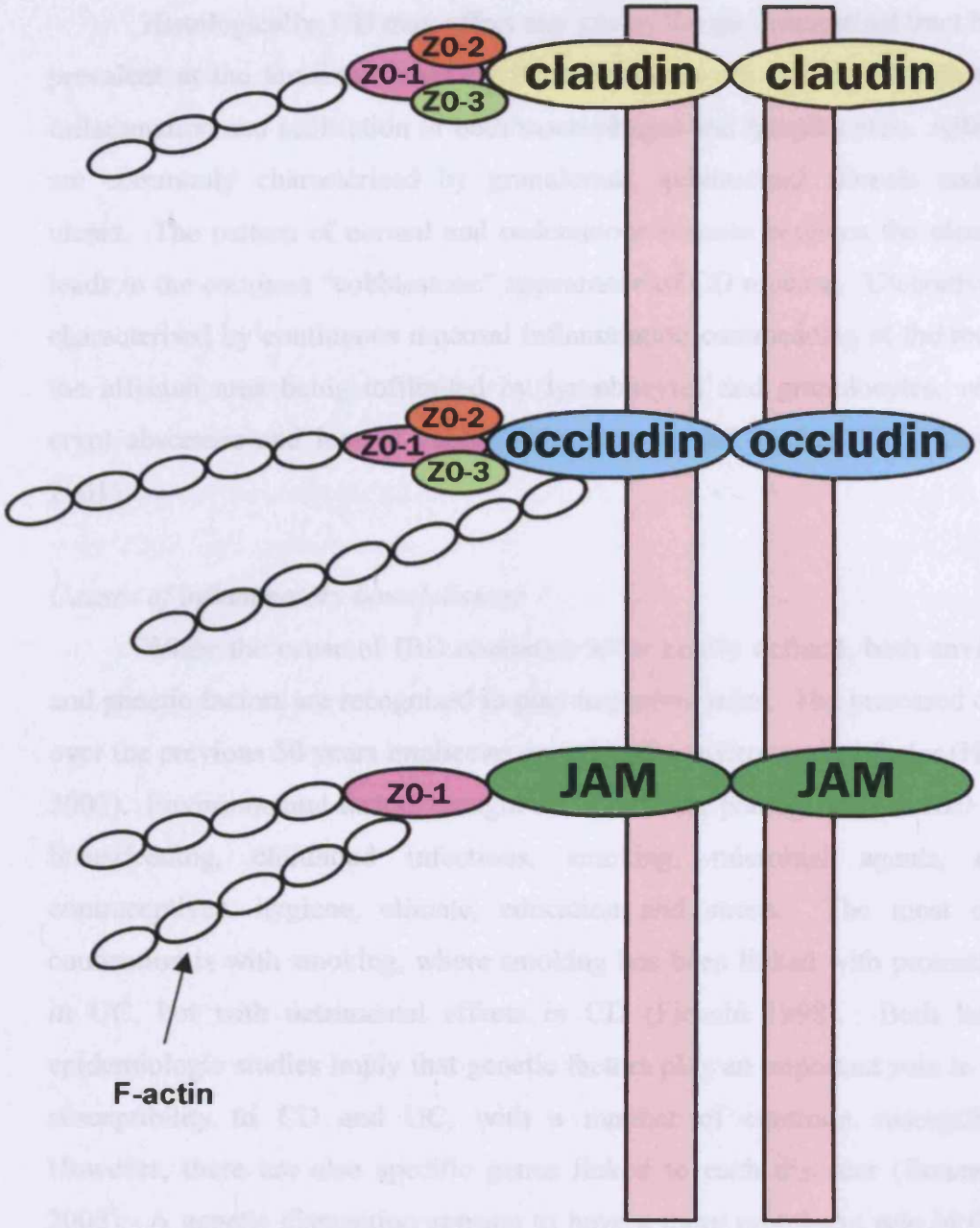


Figure 1.3 Known tight junction protein interactions

*Histology of the inflammatory bowel diseases*

Histologically, CD may affect any site of the gastrointestinal tract but is most prevalent at the terminal ileum. Affected regions are associated with transmural inflammation and infiltration of both macrophages and lymphocytes. Affected areas are commonly characterised by granulomas, submucosal fibrosis and fissuring ulcers. The pattern of normal and oedematous mucosa between the ulcerous areas leads to the common "cobblestone" appearance of CD mucosa. Ulcerative colitis is characterised by continuous mucosal inflammation commencing at the rectum, with the affected area being infiltrated by lymphocytes and granulocytes, with ulcers, crypt abscesses and loss of goblet cells (Bouma and Strober 2003, Gassler, *et al* 2001).

*Causes of inflammatory bowel disease*

While the cause of IBD continues to be poorly defined, both environmental and genetic factors are recognised to play important roles. The increased occurrence over the previous 50 years implicates an unknown environmental factor (Hugot, *et al* 2001). Environmental factors thought relevant in the pathogenesis of IBD include of breastfeeding, childhood infections, smoking, microbial agents, diet, oral contraceptives, hygiene, climate, education and stress. The most established connection is with smoking, where smoking has been linked with protective effects in UC, but with detrimental effects in CD (Fiocchi 1998). Both linkage and epidemiologic studies imply that genetic factors play an important role in governing susceptibility to CD and UC, with a number of common susceptible genes. However, there are also specific genes linked to each disorder (Bonen and Cho 2003). A genetic disposition appears to have a more prominent role in CD than in UC, as there is a greater occurrence of familial clustering in CD. Studies of the concordance rates in European twin pairs demonstrated a 37 % concordance rate of CD in monozygotic twin pairs with a reduced rate in dyzygotic twin pairs of 7 %. UC, on the other hand, has a 10 % concordance rate in monozygotic and 3 % in dyzygotic twins (Nakamura, *et al* 2003). Further evidence suggesting a genetic predisposition comprises of different frequency of CD between separate ethnic populations such as a high prevalence in Ashkenazi Jews (Shanahan 2002).

## 1.7 Crohn's disease and intestinal permeability

Intestinal paracellular permeability of different markers have been demonstrated to be increased in patients with active CD. Hollander suggested that the development of CD followed a period of increased TJ permeability. Using polyethylene glycol 400 as a probe, symptomless relatives of CD sufferers have been shown to have a 2-fold increase in permeability compared to individuals in the healthy control group (Hollander 1988). However, these results were controversial, as other groups could not replicate these findings. Nevertheless, May and co-workers demonstrated that there is a population of first-degree relatives that have increased intestinal permeability without any symptoms attributed to CD. The percentage of this subpopulation (10 %) is the same as that predicted to develop CD, suggesting that relatives may suffer from sub-clinical CD or have an intestinal permeability defect that occurs before the development of CD (May, *et al* 1993). It has been hypothesised that an increased intestinal permeability weakens the intestine's protective barrier from the external environment, thereby increasing mucosal immune system exposure to luminal antigens, which consequently results in an active inflammatory response and predisposes individuals to clinical symptoms of CD (Hilsden, *et al* 1996). These observations suggest that CD may be a consequence of a TJ defect causing increased paracellular permeability.

Further evidence supporting this hypothesis is the case of an asymptomatic girl of 13 whose intestinal permeability was investigated in 1989 as both her older brother and mother had CD. Her intestinal permeability to $^{51}$Cr-labelled EDTA was elevated even though there were no endoscopic, histologic, or radiographic signs of CD. Eight years later, at age 21, she was diagnosed with ileal CD. It is thought that the increased $^{51}$Cr-EDTA permeability is a primary phenomenon that corresponds to early stage development of CD. Although this is only 1 case, it demonstrates that increased permeability does precede the onset of CD (Irvine and Marshall 2000).

## 1.8 Genetics of crohn's disease

As previously described there is evidence that increased TJ permeability predisposes CD, and that a genetic link may also be associated with this predisposition. The first CD susceptibility locus was located at the pericentromeric region of chromosome 16, called IBD1 locus (Shanahan 2002). Studies have

identified that the nucleotide oligomerization domain (NOD2) gene is positioned on chromosome 16q12 and is part of the NOD1/APAF1 gene family. Members of this gene family are implicated in inflammatory responses to bacterial products, especially lipopolysaccarides (LPS) (Inohara, *et al* 2002).

Nucleotide oligomerization domain 2 protein is expressed predominantly in monocytes and is comprised of a nucleotide-binding domain (NBD), 2 caspase recruitment domains (CARD), and a L-rich repeat (LRR) responsible for LPS binding. Binding of bacterial products such as LPS to the LRR results in NOD2 activation of nuclear factor-κB (NF-κB) (Hugot, *et al* 2001). Nuclear factor-κB transcription factors regulate genes that are implicated in inflammatory and immune responses, growth factors, cell adhesion, inducible nitric oxide synthase and inducible enzymes including cyclooxygenase 2 (Hanada and Yoshimura 2002, Stancovski and Baltimore 1997).

Inactive NF-κB is complexed with the inhibitory protein κB (IκB) and is situated mainly in the cytoplasm of resting or unstimulated cells (Ma, *et al* 2004). Inhibitory protein κB degradation occurs in response to stimulation by external stimuli such as proinflammatory cytokines, leading to NF-κB activation and its translocation to the nucleus. Binding of nuclear NF-κB to DNA containing the NF-κB motif (GGGRNNYYCC, where R is purine and Y is pyrimidine) can instigate or control early-response gene transcription (Chen, *et al* 1999) (figure 1.4).

Truncation of the LRR due to NOD2 gene mutations prevents activation of NF-κB in response to LPS. Insufficient monocyte detection of bacteria may possibly instigate the inappropriate T-cell mediated response, aberrant cytokine production and tissue inflammation associated with CD (Inohara, *et al* 2002, Ogura, *et al* 2001). Since NOD2 variants only account for approximately 20 % of CD cases, there is a need to investigate other possible susceptibility genes. Further mapped putative loci include chromosomes 12 (IBD2), 6 (IBD3), and 14 (IBD4) (Shanahan 2002).

## 1.9 Cytokine involvement and inflammatory bowel disease

Although NOD2 gene mutations provide potential mechanisms for the inappropriate inflammatory response observed in CD, other stimuli may play a critical role. In CD, the mucosa of the gastrointestinal tract is infiltrated by $CD4^+$ type 1 helper-

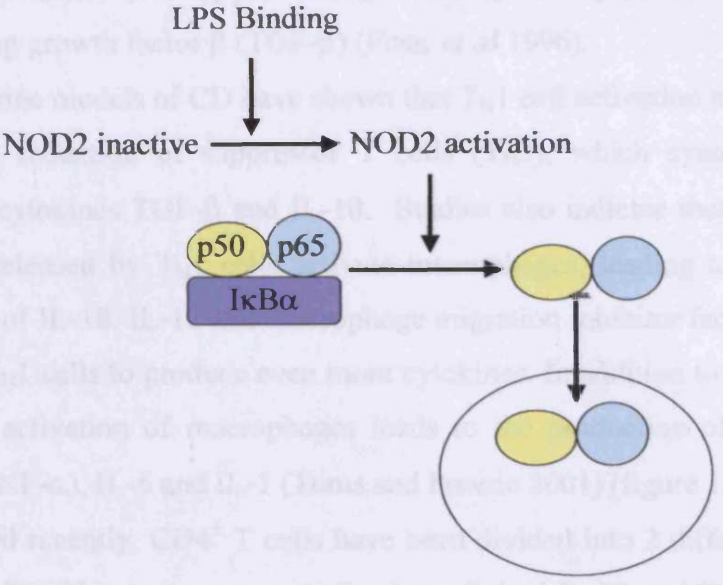


Figure 1.4 Activation of NF-κB. Activating stimuli including lipopolysaccharide promote degradation of IκBα and the subsequent release of NF-κB p65 into the cysolic compartment. NF-κB p65 translocates into the nucleus and forms dimmers as part of the activation process. NF-κB can then bind specific sites in inflammation gene promoter regions and initiate transcription.

T-cell ($T_H1$) lymphocytes capable of producing the proinflammatory cytokines interleukin (IL)-12 and interferon γ (IFN-γ). The mucosa of UC patients is thought to be predominantly permeated by $CD4^+$ lymphocytes expressing an atypical type 2 helper-T-cell ($T_H2$) phenotype, distinguished by the synthesis of both IL-5 and transforming growth factor β (TGF-β) (Fuss, *et al* 1996).

Murine models of CD have shown that $T_H1$ cell activation may be elevated due to the reduction of suppressor T cells ($T_H3$), which synthesise the down-regulatory cytokines TGF-β and IL-10. Studies also indicate that proinflammatory cytokines released by $T_H1$ cells activate macrophages, leading to the macrophage production of IL-18, IL-12 and macrophage migration inhibitor factor, which further stimulate $T_H1$ cells to produce even more cytokines. In addition to the stimulation of $T_H1$ cells, activation of macrophages leads to the production of tumour necrosis factor α (TNF-α), IL-6 and IL-1 (Toms and Powrie 2001) (figure 1.5).

Until recently, $CD4^+$ T cells have been divided into 2 different lineages $T_H1$ and $T_H2$ cells. However, recent studies have linked IL-23 and IL-17 to $T_H17$ cells and not to $T_H1$ cells as previously thought (Harrington, *et al* 2006). Current studies have shown that $T_H17$ cells produce IL-17A, IL17F, IL-6 and TNF-α, collectively these cytokines have been shown to recruit and activate neutrophils (Reinhardt, *et al* 2006). Increases in IL-17 expression has been demonstrated in the mucosa and serum of IBD patients, indicating that $T_H17$ cells play an important role in the pathogenesis of Crohn's disease as well as $T_H1$ cells (Fujino, *et al* 2003).

Patients with CD have increased levels of TNF-α in their intestinal tissue, serum and stools. Tumour necrosis factor α is an important proinflammatory cytokine in CD pathophysiology as it alters the integrity of endothelial and epithelial membranes. This subsequently results in an increased transmigration of inflammatory cells playing a central role in the formation of granuloma (commonly observed in CD patients) and in the maintenance of the inflammatory response in a self renewing cycle (Romagnani, *et al* 1997). Elevated TNF-α levels represent a potential therapeutic target for the treatment of CD. Indeed, recent studies have shown that administration of anti-TNF-α antibody to patients with active CD is an effective therapeutic (Suenaert, *et al* 2002).

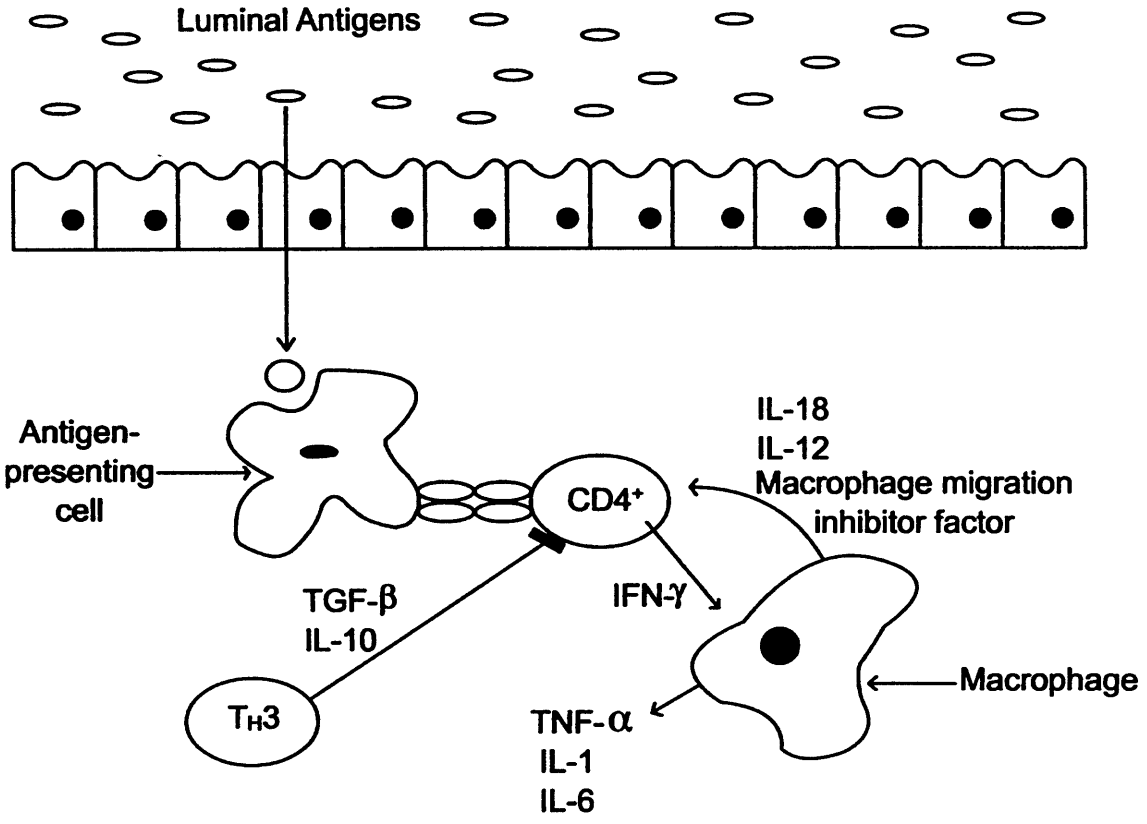


Figure 1.5 Schematic representation of cytokine involvement in Crohn's disease. Activation of $T_H1$ cells result in the production of the pro-inflammatory cytokines IL-12 and INF-γ. Release of INF-γ results in macrophage activation which leads to production of IL-18, IL-12 and macrophage migration inhibitor factor which further stimulate $T_H1$ cells. Activated macrophages also produce the pro-inflammatory cytokines TNF-α, Il-16 and IL-1. Additionally increased $T_H1$ has been shown to be due to a reduction in $T_H3$, which synthesise the down-regulatory cytokines TGF-β and IL-10.

Ma and co-workers demonstrated that increases in intestinal paracellular permeability induced by TNF-α were due to activation of NF-κB, which then binds to DNA as described previously. They also suggested that Caco-2 monolayer elevations in paracellular permeability caused by TNF-α were due to downregulation of the TJ protein ZO-1; decreased ZO-1 levels were accompanied by a change in junctional localisation of ZO-1. Nuclear factor-κB inhibitors prevented TNF-α induced alterations of ZO-1 expression and localisation within the TJ, thereby suggesting that activation of NF-κB is necessary for this process. This implies that NF-κB regulates TJ protein genes (Ma, *et al* 2004). This finding is contradictory to NOD2 mutations studies where an inappropriate immune response is due to inactivation of NF-κB in response to LPS.

*Interferon-γ disruption of the tight junction*

Interferon-γ levels are also increased in patients with CD, resulting in augmentation of the inflammatory responses leading to enhanced paracellular permeability. Interferon-γ down-regulates the expression of ZO-1 thereby disrupting the actin cytoskeleton (Youakim and Ahdieh 1999). Since ZO-1 is a scaffolding protein of the TJ, loss of this protein would lead to disorganisation of TJ proteins, such as occludin and ZO-2. As ZO-1 is important in linking the TJ to the PAMR, its loss also results in a loss of cytoskeleton control of the paracellular pathway. Therefore, increased IFN-γ levels associated with CD may be a cause of increased TJ permeability seen in these patients (Gonzalez-Mariscal, *et al* 2000). Thus, inappropriate IFN-γ activation can alter TJ function leading to increased TJ permeability, which can allow additional noxious materials to traverse the paracellular pathway to further elevate the inflammatory response. Such noxious materials can facilitate central immune-cell population activation that inevitably results in the synthesis of numerous non-specific stimulators of inflammation. These stimulators include a variety of cytokines, growth factors, chemokines, metabolites of arachidonic acid (such as leukotrienes and prostaglandins) and reactive oxygen metabolites such as nitric oxide (Podolsky 2002).

*Protein-activated receptors*

It has been demonstrated that increased cytokine and inflammatory mediator release is associated with CD. Cytokines not only stimulate inflammation; for example, TNF-α and IL-1 released upon macrophage activation, they also stimulate a 10-fold increase in the expression of PAR2 in endothelial cells (Kunzelmann and Mall 2002). Proteinase-activated receptors (PARs) are members of the 7 transmembrane domain G-protein-coupled receptors that are activated via proteolytic cleavage of their N-terminus. The free N-terminal sequence then binds to the receptor itself resulting in its activation (Cenac, *et al* 2003). Proteinase-activated receptor-2 is particularly prominent within the gastrointestinal tract where it is activated by trypsin and mast cell tryptase from the mucosa-associated lymphatic tissue (MALT) (Vergnolle 2000).

Located within the gastrointestinal tract MALT are mast cells which produce TNF-α and various other proinflammatory cytokines along with mast cell tryptase (Kunzelmann and Mall 2002). Inflammatory bowel disease is typified by the infiltration of mast cells; a key factor in the formation of intestinal granuloma. Mast cell degranulation leads to changes in ion transport within the intestine in both IBD and normal conditions (Vergnolle 2000). Inflammatory bowel disease is also associated with a decreased concentration of trypsin inhibitors. This along with the increased degranulation of mast cells, may lead to an increase in PAR2 activation (Cenac, *et al* 2003).

Proteinase-activated receptor 2 may be involved in the regulation of ion transport in gastrointestinal epithelia as mentioned previously. Basolateral PAR2 is responsible for trypsin-mediated activation of $Cl^-$ secretion and increases $Ca^{2+}$ concentration in human distal colon. Therefore, TNF-α may increase PAR2 expression, thereby contributing to the hypersecretion observed in IBD (Kunzelmann and Mall 2002, Mall, *et al* 2002).

## 1.10 Inflammatory bowel disease therapeutics

The treatment of CD and UC consists of inducing remission of active disease and then maintenance of remission. Current first-line treatments for UC and CD

include aminosalicyclates and cortiosteroids, which are used to reduce the inflammation associated with IBD. Whereas immunosuppressors such as azathioprine or 6-mercaptopurine, which contain thiopurine, are used in patients with refractory disease, newer immunomodulatory therapies, such as methotrexate and infliximab (a monoclonal antibody to TNF-α) are being administered more frequently to patients resistant to common treatments, especially in CD (table 1.1). However, these drugs are not universally effective and are coupled to a spectrum of serious adverse effects (Carty and Rampton 2003).

Side effects of patients receiving oral 5-aminosalicylates include headache, rash, pancreatitis, diarrhoea, nausea, with up to 5 % of patients suffering from blood dycrasias and approximately 1 in 500 presenting with interstitial nephritis (Rampton 1999). Corticosteroid use may lead to side effects in practically every system, including the central nervous system, dermatologic, metabolic and musculoskeletal systems; other side effects include infection, hypertension and retardation of development in children (Rutgeerts 2001). Therapeutic response to thiopurines often requires up to 4 months. One major side effect of taking these drugs is that approximately 0.2 % of people have a deficiency in the enzyme 6-thiopurine methyltransferase. This enzyme is responsible for the degradation of purine analogues and such a deficiency can potentially lead to serious side effects including acute pancreatitis, chronic hepatitis and bone marrow depression (Rampton 1999).

Side effects of methotrexate include hepatic fibrosis, bone marrow depression, opportunistic infections and pneumonitis. Side effects to infliximab comprise of nausea, headache, and upper respiratory tract infections (Rampton 1999). Despite all of the side effects caused by these drugs, these drugs are also not very effective with a relapse rate of approximately 50 % within 1 year for both types of IBD. Currently, no therapy cures IBD apart from colectomy for UC (Carty and Rampton 2003).

As described previously, TJ permeability is increased in CD, which is thought to be either a causative factor or an effect of some other factors. Elevations in paracellular permeability have been shown in healthy first-degree relatives of CD patients, while cytokines have been shown to alter the expression and locality of TJ

Table 1.1 Inflammatory bowel disease therapeutics*.

| Therapeutic | Mode of action | Implication for use |
|---|---|---|
| Aminosalicyclates | Inhibits arachidonic acid metabolism pathways, suppression of IL-1 release, inhibits leukocyte recruitment and protects against oxidant injury. | Mild to moderate CD and UC, Maintenance of remission CD and UC, |
| Corticosteroids | Reduction of transcription of multiple inflammatory genes and increasing transcription of anti-inflammatory genes. | Mild to moderate CD and UC, Moderate to severe CD and UC, |
| Azathioprine | Inhibits T and B lymphocytes and decreases cytotoxic T cells and plasma cell numbers. | Moderate to severe CD, Maintenance of remission CD and UC, |
| 6-mercaptopurine | Inhibits T and B lymphocytes and decreases cytotoxic T cells and plasma cell numbers. | Moderate to severe CD, Maintenance of remission CD and UC, |

Table 1.1 Continued*.

| Therapeutic | Mode of action | Implications of use |
|---|---|---|
| Methotrexate | Inhibits dihydrofolate reductase and other folate-dependent enzymes, decreases IL-1 production, neutrophil chemotaxis and eicosanoid production. | Moderate to severe CD |
| Infliximab | Neutralises soluble TNF-α, lyse TNF-α-expressing cells and induces apoptosis of activated T cells. | Moderate to severe CD |
| Adalimumab | Neutralises soluble TNF-α, lyse TNF-α-expressing cells and induces apoptosis of activated T cells. | Moderate to severe CD |
| Certolizumab pegol | Neutralises soluble TNF-α, lyse TNF-α-expressing cells and induces apoptosis of activated T cells. | In clinical trials |

* Compiled from (Arnott, *et al* 2003, Lofberg 2003, Lewis 2007, Rizzello, *et al* 2003, Shanahan and Targan 1992).

proteins within the TJ complex. Therefore, there is evidence suggesting that the TJ is important in the pathophysiology of CD and hence the TJ is a suitable target for the design of novel therapeutics for CD. This would be a novel approach as current therapeutics for CD are aimed at the inflammatory response itself. The ability to close TJs may result in the prevention of immune response activation in susceptible individuals or prevent further exposure to luminal antigens for patients with active CD.

Although TJ regulation is an important factor in the pathology of Crohn's disease, it is worth noting that the TJ plays an important role in the regulation of physiological processes such as $Na^+$-glucose co-transport in the small intestine (Pappenheimer and Reiss 1987)

## 1.11 Perijunctional actin-myosin II ring

Tight junctions are composed of numerous different proteins, all of which could potentially be targeted to reduce paracellular permeability of the intestinal epithelium. However, there is accumulating evidence demonstrating that the perijunctional actin-myosin II ring (PAMR) plays an important role in regulation of the paracellular permeability barrier. The PAMR is a ring of actin and myosin II located at the epithelial junctional complex. A direct connection between the PAMR and TJ barrier has been hypothesised, and that PAMR lateral tension within epithelial cells modifies paracellular transport. Several secondary signalling pathways have been demonstrated to affect the organisation of the perijunctional cytoskeleton organisation concurrently with alterations in paracellular permeability (Lapierre 2000, Madara 1998, Mitic and Anderson 1998).

### *Disruption of the perijunctional actin-myosin II ring using cytochalasins leads to increased paracellular permeability*

The fungal toxins cytochalasins have been used to demonstrate the PAMR role in intestinal paracellular permeability. These toxins work by disruption of the actin filament network and instigation of a cellular response (Ma, *et al* 2000, Turner 2000a). Ma and colleges demonstrated that *in vitro* treatment Caco-2 intestinal epithelial monolayers with 5 mg/ml of cytochalasin-B resulted in increased paracellular permeability. Protein synthesis inhibitors such as actinomycin-D or

cycloheximidie, or the microtubule inhibitor colchicine did not affect these elevations. However, addition of 2,4-dinitrophenol or sodium azide (metabolic energy inhibitors) prevented any increases in TJ permeability. Inhibitors of protein synthesis or microtubule function following cytochalasin-B removal did not affect paracellular permeability decreases. However, inhibition was observed following addition of metabolic energy inhibitors. These results suggest that the cytochalasin-B induced increases in paracellular permeability of Caco-2 monolayers are caused by the existing actin filaments that extend into the TJ from the PAMR (Ma, *et al* 1995).

*SGLT-1 activation increases tight junction permeability*

Cytochalasin disruption of the PAMR is an example of toxin-meditated disruption, while a physiological stimulus of TJ permeability includes $Na^+$-glucose co-transport in the small intestine. In 1987 Pappenheimer and Reiss found that the transport of glucose or amino acids was mainly via the paracellular pathway by solvent drag. As during glucose absorption the TJ permeability of solutes such as creatinine was increased. While the absorption of such insert hydrophilic solutes was reduced at low luminal glucose concentrations. They hypothesised that Na-coupled transport of hexoses or amino acids created osmotic forces for fluid absorption that induces increases paracellular permeability, thereby allowing bulk absorption of nutrients via solvent drag (Pappenheimer and Reiss 1987). It has been demonstrated that luminal glucose activation of SGLT-1 (a $Na^+$-glucose co-transporter) resulted in water absorption increasing to 91 %, whilst the absorption of creatinine, inulin and polyethylene glycol 4000 increased by 193 %, 100 % and 6 % respectively (Turner 2000b).

Determination of the role of SGLT-1 with regards to myosin light chain (MLC) phosphorylation has been demonstrated by the use of $^{32}P$ labelled SGLT-1 transfected Caco-2 cells. Three phosphoproteins were identified employing sodium dodecyl sulphate–polyacrylamide gel electrophoresis (SDS-PAGE) analysis, all of which were around 20 kDa. One of these bands was identified as MLC. Phosphorylation of the MLC band was assessed in whole cell lysates, which was increased 2.08-fold in Caco-2 monolayers transfected with SGLT-1 which were active, compared with those incubated with phloridzin (an inhibitor of SGLT-1-mediated $Na^+$-glucose co-transport). Thus, a mechanism exists whereby epithelial

paracellular permeability can be regulated by $Na^+$-glucose co-transport involving PAMR MLC phosphorylation (Turner, *et al* 1997).

## 1.12 Myosin light chain kinase

Myosin light chain phosphorylation has been shown to be important in the regulation of TJ permeability. The enzyme by which myosin II regulatory light chain is phosphorylated is a $Ca^{2+}$/calmodulin-dependent protein kinase called myosin light chain kinase (MLCK). Calmodulin (CaM) is a protein of 16-17 kDa with 4 helix-loop-helix motifs that has a high affinity and specificity binding to $Ca^{2+}$. Binding of $Ca^{2+}$ to CaM causes a conformational change resulting in the $Ca^{2+}$/CaM complex binding with MLCK. The phosphorylation at $S^{19}$ of MLC by MLCK is an important process in commencing contraction due to increased activity of myosin MgATPase (Soderling and Stull 2001) (figure 1.6).

Smooth muscle of the distal stomach, small intestine and colon has adjustable tone caused by rhythmic contractions instigated by membrane depolarisation and repolarisation cycles. Activation of voltage-gated $Ca^{2+}$ channels results in depolarisation, leading to $Ca^{2+}$ mobilisation into the cell and ultimately contraction. Excitatory neurotransmitters such as acetylcholine and tachykinins simultaneously activate rhythmic smooth muscle, thereby instigating further depolarisation with entry of $Ca^{2+}$ into the cell resulting in stimulation of signalling cascades leading to transient $Ca^{2+}$ release within the cell from the sarcoplasmic reticulum (Murthy 2005).

*Myosin light chain kinase and SGLT-1 activation*

Further work by Turner and co-workers demonstrated that addition of MLCK inhibitors 1-(5-iodonapthalene-1-sulphonyl)-1H-hexahydro-1, 4-diazepine hydrochloride (ML-7) and 1-(5-chloronaphthalene-1-sulphonyl)-1H-hexahydro-1,4-diazepine hydrochloride (ML-9) to monolayers led to an almost complete inhibition of TER decreases following $Na^+$-glucose co-transport activation. The TER of these monolayers were significantly different compared to those incubated with 25 mM glucose only; however, there was no significant difference between monolayers incubated with MLCK inhibitors and phloridzin. Indicating that SGLT-1 activation is linked to MLC phosphorylation via MLCK activation (Turner, *et al* 1997).

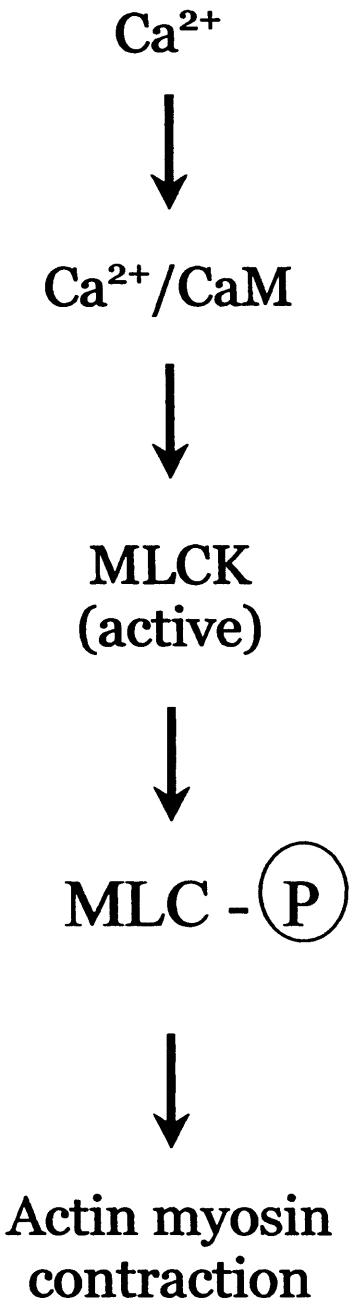


Figure 1.6 Calcium/calmodulin pathway activiation of myosin light chain

*Myosin light chain kinase and Enteropathogenic Escherichia coli colonisation*

Evidence supporting the importance of MLC phosphorylation includes intestinal epithelial models colonised by enteropathogenic *Escherichia coli* (EPEC). Enteropathogenic *Escherichia coli* is 1 of many different strains of *E.coli* that can cause diarrhoea. However, this strain differs to the others due to its capability to attach and efface (A/E) upon its host cells. Adherence of EPEC to epithelial cells causes distinctive changes in both *in vivo* and *in vitro* cells called A/E lesions. The loss of microvilli by host cells is termed effacement. Below the adherent EPEC the epithelial membrane is elevated forming pedestals. The formation of pedestals and possibly microvilli effacement is caused by the rearrangement of the host cell cytoskeleton. Beneath the pedestals various cytoskeletal components co-localise, including MLC and F-actin (Donnenberg, *et al* 1997).

Colonisation of EPEC has also been reported to activate many host signals, including increases in intracellular $Ca^{2+}$, inositol phosphate metabolism, tyrosine kinase and perhaps protein kinase C (PKC) activation (Yuhan, *et al* 1997). Manjarrez-Hernandez and co-workers demonstrated that EPEC adhesion to human laryngeal epithelial cells resulted in a 20-21 kDa phosphoprotein, with the most prominent being identified as MLC (Manjarrez-Hernandez, *et al* 1991). This has also been observed in EPEC infected Caco-2 cells and mucosal organ cultures of human small intestine. Increased TJ permeability is also observed during EPEC infection that is associated with a rise in MLC phosphorylation. Protein kinase C or MLCK are able to phosphorylate MLC. However, phosphorylation by MCLK alone instigates contraction by increasing the activity of myosin adenosine triphosphate (ATPase) (Yuhan, *et al* 1997). It has been shown that following 1 hour EPEC infection, the amount of cytosolic phosphorylated MLC was 90 %; however, 75 % was connected with the cytoskeleton at 4 hours (Manjarrez-Hernandez, *et al* 1991). Thus, EPEC infection activates MLCK within host cells over time and results in phosphorylation of myosin and relocation of cytoplasmic MLC to the cytoskeleton. Once phosphorylated, MLC binds with actin and activates myosin ATPase, leading to cytoskeletal contraction and ultimately increased paracellular permeability (Yuhan, *et al* 1997).

It is worth noting that although EPEC infection and SGLT-1 activation both involve MLCK phosphorylation of MLC, they involve different mechanisms. Activation of MLCK can be part of a physiological or pathophysiological process. As SGLT-1 induced increases in paracellular permeability are considerably faster, readily reversible and highly regulated compared to those caused by EPEC bacterial infection (Turner 2000b).

*Role of myosin light chain kinase in regulating tight junction permeability*

Hecht and colleagues demonstrated the importance of MLCK in the regulation of TJ permeability by infecting Madin-Darby canine kidney (MDCK) cells with the catalytic domain of MLCK (tMK). This mutant lacks the inhibitory domain required for CaM dependence and thus is constitutively active. Transfection with tMK led to an increase in MLC phosphorylation that was limited and consistent with a physiological process, resulting in a 90 % decrease in TER. In these studies, increased MLC phosphorylation did not increase permeability to large molecules such as the 40 kDa horseradish peroxidase but increased ion and small molecules (e.g. 3.6 Å mannitol) permeability, suggesting that this is a regulated, physiological process (Hecht, *et al* 1996).

## 1.13 Current inhibitors of myosin light chain kinase

As MLCK activation has been shown to be important in the opening of TJs, inhibition of MLCK appears to be a suitable means of TJ closure, and could reduce exposure of the mucosal immune system to luminal antigens. The MLCK inhibitors ML-7 and ML-9 have been utilised to determine the importance of MLCK in the regulation of TJ permeability: these are ATP-competitive cell-permeable inhibitors of MLCK (Turner, *et al* 1997). Studies by Bain and co-workers found that ML-9 inhibited PKA and PKC but did not inhibit smooth and skeletal muscle MLCKs potently and inhibited several other protein kinases such as Rho kinase II (ROCK-II). ML-7, derived from ML-9, had increased selectivity although weakly inhibited smooth muscle MLCK. (Bain, *et al* 2003). Therefore, a more potent and specific inhibitor of MLCK is required if inhibition of this enzyme is to be used as a mode of TJ closure in *in vivo* studies of IBD.

*Novel myosin light chain kinase inhibitor*

Lukas and colleagues identified an inhibitor of MLCK (RKKYNMARRK-$NH_2$) through functional genomics studies, which they further modified to the sequence of RKKYKYRRK-$NH_2$ (PIK) as seen in figure 1.7. This peptide was found to be a specific inhibitor of MLCK as it did not obstruct CaM kinase activation, significantly inhibit the activity of CaMKII or inhibit cAMP-dependent protein kinase (PKA) (Lukas, *et al* 1999). Protein kinase A (Murthy, *et al* 2003) and CaMKII (Stull, *et al* 1990) are both able to phosphorylate MLCK, resulting in its inhibition and smooth muscle relaxation.

*Myosin light chain kinase inhibitor and paracellular permeability*

Zolotarevsky and co-workers performed initial studies examining this MLCK inhibitor peptide as a potential therapeutic drug for IBD. The peptide inhibitor is derived from smooth muscle MLCK; however, confluent Caco-2 monolayers express a 215 kDa isoform of MLCK, which is larger than smooth muscle MLCK. Nevertheless, both their inhibitory and catalytic domains are highly conserved. Therefore, this should not affect the ability of PIK to inhibit Caco-2 MLCK (Zolotarevsky, *et al* 2002).

*Transport of the myosin light chain kinase inhibitor across membranes*

Initial studies showed that this peptide is membrane permeant, which is thought to be due to its sequence similarity to the HIV-1 TAT protein transduction domain (YGRKKRRQRRR), with 7 out of the 9 amino acids being either positively charged R or K. The transduction domain of HIV-1 TAT is thought to enable independent passage of proteins across cell membranes without specific transporters or receptors through a mechanism that is both quick and concentration-dependent (Schwarze, *et al* 1999).

The MLCK inhibitor was thought to passage in a similar way and studies using biotinylated PIK peptide showed that it crossed the cell membranes, entered the cytoplasm of Caco-2 cells and concentrated at the PAMR where F-actin is concentrated. Therefore, the oligopeptide was named PIK (membrane-permeant inhibitor of MLC kinase) (Zolotarevsky, *et al* 2002). It is worth noting, however, that more recent findings suggest that cell- penetrating peptides such as HIV-1 TAT

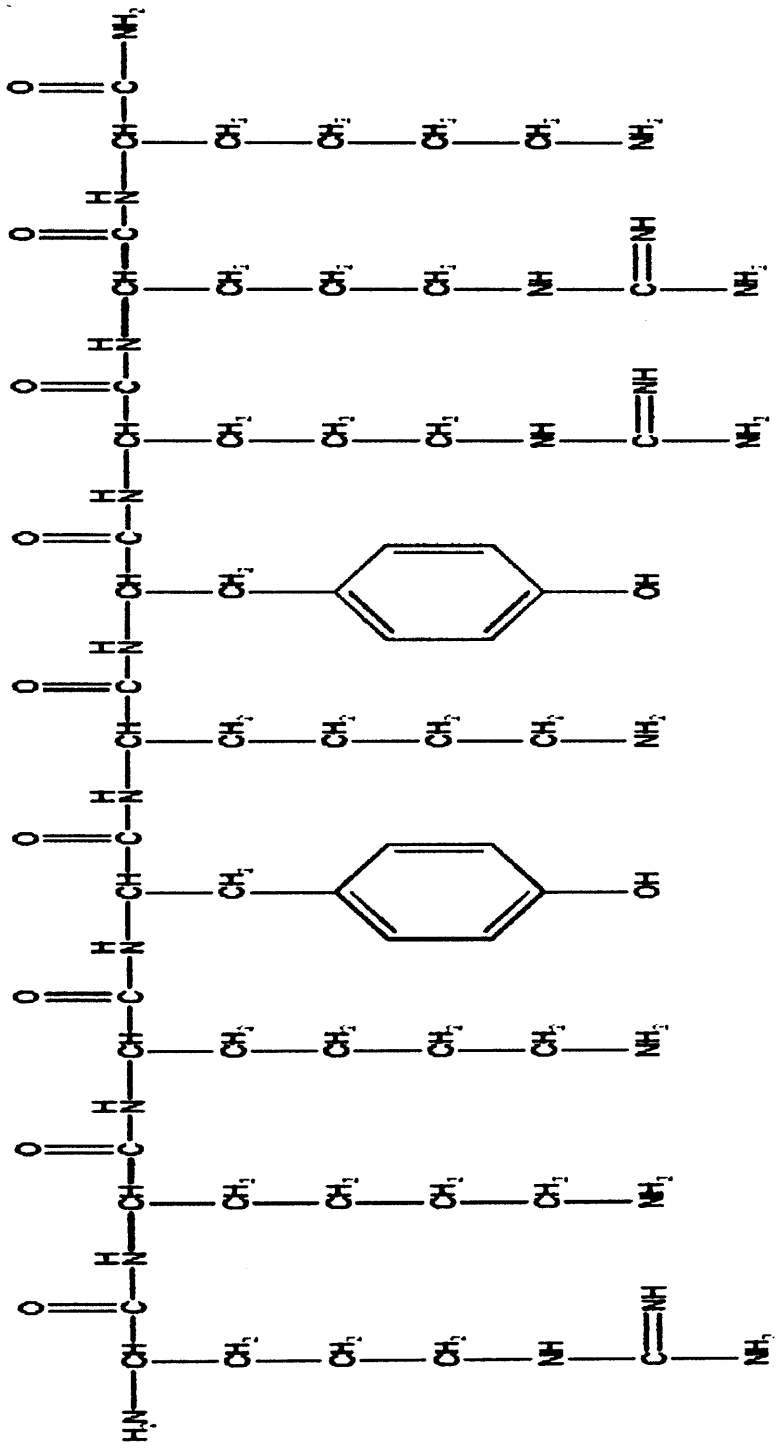

Figure 1.7 Chemical structure of PIK

do not directly pass through membrane lipid bilayers as originally thought but rather are internalised via the process of endocytosis (Richard, *et al* 2003). Therefore, the exact route and mechanism of PIK uptake is still undefined.

*Confirmation that PIK changes transepithelial electrical resistance via inhibition of myosin light chain kinase*

Two separate tests have been performed in order to ensure that PIK changed TER via inhibition of MLCK. The first compared the amount of PIK required to increase TER with that required for MLCK inhibition *in vitro*. Transepithelial electrical resistance increases paralleled inhibition of MLCK, thereby suggesting an association between MLCK inhibition and increases in TER. Second, modification of the PIK sequence was correlated with function. Substitution at position 5 and positions 4, 5 and 6 with cis-4-aminocyclohexanecarboxylic showed that monosubstituted PIK resulted in increases in TER comparable with those of PIK. It also showed that trisubstituted PIK was not as effective as PIK at inhibiting MLCK and hence did not increase TER. Both the dose-response data along with PIK peptide sequence substitution studies are consistent with the hypothesis that the effects on TER caused by PIK are mediated by inhibition of MLCK (Zolotarevsky, *et al* 2002).

*Mode of myosin light chain kinase inhibition*

The mechanism of MLCK inhibition by PIK is analogue to the function of the inhibitory domain of MLCK association with its catalytic domain (Lukas, *et al* 1999). When CaM interacts with the inhibitory domain of MLCK, binding between the catalytic and inhibitory domains are reduced resulting in MLCK activation (Tanaka, *et al* 1995). It is thought that PIK prevents activation of MLCK, despite the presence of CaM, through a direct binding to MLCK's catalytic domain in a manner similar to the inhibitory domain (Zolotarevsky, *et al* 2002).

*Efficiency of PIK at inhibiting increases in tight junction permeability in two in vitro cell models of inflammation*

Two different *in vitro* cell models of inflammation have been used to determine the effectiveness of PIK at inhibiting Caco-2 MLCK and hence the

regulation of paracellular permeability. One model used EPEC infected Caco-2 monolayers which, as mentioned previously, requires MLC phosphorylation by MLCK (Yuhan, *et al* 1997). Following 1 hour of infection of monolayers with EPEC, PIK was added; at this stage no barrier defects have yet to occur. Treatment of infected monolayers with PIK resulted in the decreases of TER being prevented by 57 % following 4 hours after infection. However, PIK was less effective in advanced infection, as following 6 hours of infection the decreases in TER were only prevented by 30 %. This could possibly be due to PIK degradation or the inability of PIK to prevent reduction of TER in advanced states of epithelial injury (Zolotarevsky, *et al* 2002).

The other model attempts to recreate changes in paracellular permeability seen in Crohn's disease. In this model, cultured Caco-2 monolayers were treated with IFN-γ and TNF-α, pro-inflammatory cytokines that have been demonstrated to be important in the pathogenesis of CD (Nusrat, *et al* 2000b). Caco-2 monolayers treated with both IFN-γ and TNF-α had a decrease of 25 % in MLC phosphorylation and the TER restored to 97 % following addition of PIK compared to monolayers not treated with PIK. However, PIK is not very effective in the prevention or correction of large permeability defects, such as decreases in TER of greater than 50 % caused by high concentrations of IFN-γ and TNF-α. This could potentially be due to other mechanisms being stimulated by IFN-γ and TNF-α, such as reduced expression of occludin and ZO-1 (Zolotarevsky, *et al* 2002).

*PIK as a candidate for oral drug delivery*

PIK appears to be a specific MLCK inhibitor, as it does not appreciably inhibit CaMKII or PKA (Lukas, *et al* 1999). These characteristics make PIK a potential oral drug candidate for CD as it has been demonstrated to cross the cell culture models of intestinal epithelium such as Caco-2 monolayers. The Caco-2 cell model however, does not represent the intestinal environment accurately as it lacks many elements such as pancreas-derived luminal proteases. Therefore, prior to *in vivo* experiments, further studies are required to determine PIK's stability in the intestinal environment (Zolotarevsky, *et al* 2002).

## 1.14 Absorption enhancers

Co-administration of drugs with absorption enhancers is one method of increasing the transport of drugs. Absorption enhancers are compounds that temporarily disrupt the intestinal barrier to improve the transport of drugs (Mahato, *et al* 2003). Transcellular transport of drugs requires the passage of the drug through both the apical and basolateral membrane. Thus, it is doubtful whether absorption enhancers can work effectively on a wide range of compounds by increasing transcellular transport without causing damage such as cell lysis or intestinal epithelium exfoliation. Absorption enhancers with general applications are thought to act by modifying TJs (Hochman and Artursson 1994). Mechanisms that maximise protein and peptide absorption through the paracellular pathway are being sought as it is hypothesised that the paracellular space does not pose a proteolytic barrier for proteins and peptides. Therefore, much research is being undertaken in order to discover novel modes of relaxing TJs and hence increase paracellular transport of poorly absorbed protein and peptide therapeutics (Lee, *et al* 1991).

*Classes of absorption enhancers*

Generally, absorption enhancers fall into two classes: calcium chelators, which include ethylenediamine tetra-acetic acid (EDTA) and citrate, and surfactants, which include sodium dodecyl sulphate (SDS), sodium salts of fatty acids, bile salts, and palmitoylcarnitine. Calcium chelators and surfactants have numerous drawbacks and hence their use must be considered carefully (Hochman and Artursson 1994). Calcium chelators can result in $Ca^{2+}$ depletion, which may potentially lead to global alterations in cells, such as disturbance of adherent junctions, actin filament disruption and reduction in cell adhesion (Lee, *et al* 1991, Mahato, *et al* 2003). Proposed modes of action of surfactants include increases in paracellular permeability, membrane fluidity increases, mucus viscosity decreases and leakage of proteins via the membranes (Fix 1996, Lee, *et al* 1991, Mahato, *et al* 2003). Therefore, the potential of epithelium exfoliation and the possibility of complications occurring due to the increased rate of intestinal repair due to surfactant use raises concerns about its use as an absorption enhancer (Hochman and Artursson 1994).

## 1.15 Myosin light chain phosphatase

Myosin light chain kinase has long been established as an important enzyme for smooth muscle contraction that is activated by the $Ca^{2+}$-calmodulin complex. Decreases in the concentration of intracellular $Ca^{2+}$ results in MLC dephosphorylation by myosin light chain phosphatase (MLCP) leading to relaxation of the smooth muscle (Huang, *et al* 2004).

Myosin light chain phosphatase was considered to be unregulated and therefore constitutively active as it was thought that there should be a fixed relationship between the concentration of $Ca^{2+}$, myosin phosphorylation, and contraction. However, this relationship was not demonstrated in studies performed on preparations of skinned or intact smooth muscle, hence indicating that another factor was involved (Ichikawa, *et al* 1996).

It has been shown that agonists can modify MLC phosphorylation at a constant $Ca^{2+}$ concentration, demonstrating that MLCP can regulate MLC phosphorylation independently of $Ca^{2+}$ concentration (Hartshorne, *et al* 1998). The balance between phosphatase to kinase activities has been shown to govern the degree of MLC phosphorylation and hence the level of contraction (a schematic representation can be seen in figure 1.8). As MLCP is regulated independently of $Ca^{2+}$ concentration, signalling pathways other than the $Ca^{2+}$/Calmodulin pathway must be involved in the regulation of MLCP activity and hence MLC phosphorylation.

*Myosin light chain phosphatase holoenzyme subunits*

Smooth muscle MLCP is a holoenzyme comprising of 3 subunits: a catalytic subunit of approximately 38 kDa that is the protein phosphatase type 1 (PP1) δ isoform, a small subunit of around 20 kDa (M20), whose function has not been established, and a 110 to 133 kDa myosin-targeting subunit (MYPT) (Brozovich 2002). It is hypothesised that regulation of MLCP holoenzyme activity is due to alterations in subunit interaction. The small subunit is not necessary for catalytic activity and is not required for PP1 activation. Hence, MYPT has been investigated in detail to determine its effects on MLCP activity (Hartshorne, *et al* 1998).

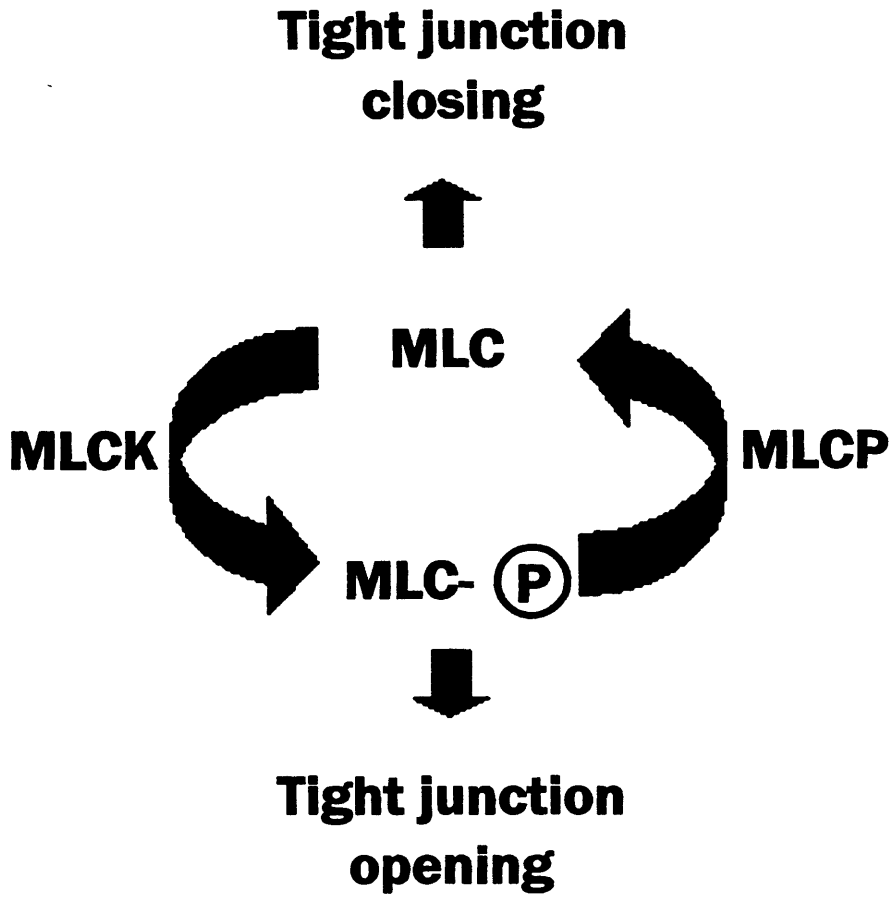


Figure 1.8 Schematic representation of the regulation of MLC phosphorylation. Adapted from (Somlyo and Somlyo 2003).

*Myosin-targeting subunit*

Myosin-targeting subunit is essential for PP1 binding and activation as well as for targeting myosin (Kitazawa, *et al* 2000). A variety of MYPT isoforms exist with comparatively minor distinctions situated at L zipper motifs at the C-terminus and/or central region inserts. Several regions of MYPT are highly conserved, such as the N-terminal ankyrin repeats and the sequence surrounding the phosphorylation site. Additionally, all isoforms have a PP1-binding motif that is 4 residues long consisting of RVXF (Ito, *et al* 2004).

The PP1 phosphatase activity is normally low, but is elevated upon MYPT binding. It is hypothesised that MYPT is a targeting subunit that interacts with both PP1 and myosin. Myosin-targeting subunit N-terminus is required for PP1 activation it also has 2 PP1 binding sites: the N-terminus, which has a strong binding site (possessing the 4-residue binding motif) and a binding site at the ankyrin repeats thought to be at repeats 5, 6, and 7 that are weaker. The exact site for MYPT binding to myosin is not yet known, as binding for this sequence has been reported on both the C- and N- terminal ends of the protein (Hartshorne, *et al* 1998).

## 1.16 Signalling pathways involved in myosin light chain phosphatase activity

Reduction of MLCP activity is known as $Ca^{2+}$ sensitisation, whereas an increase in activity is referred to as $Ca^{2+}$ desensitisation. Myosin light chain phosphatase activity regulation involves alterations in subunit interactions; however, the molecular mechanisms behind these interactions have not been fully characterised. Phosphatase inhibition as observed in increased $Ca^{2+}$ sensitivity induced by agonists is thought to occur by either Rho A, AA and PKC pathway acting either independently or in concert (Somlyo 1997) (figure 1.9).

*Rho A/Rho-Kinase*

Studies have revealed that the small GTP-binding protein RhoA plays a key function in $Ca^{2+}$ sensitisation. RhoA has been shown to target numerous proteins, such as Rho-kinase (ROCK) and MYPT of MLCP. Activation of ROCKs by RhoA, leads to the phosphorylation of the MYPT, thereby resulting in the inhibition of MLCP holoenzyme catalytic activity (Kitazawa, *et al* 2000, Ohama, *et al* 2003).

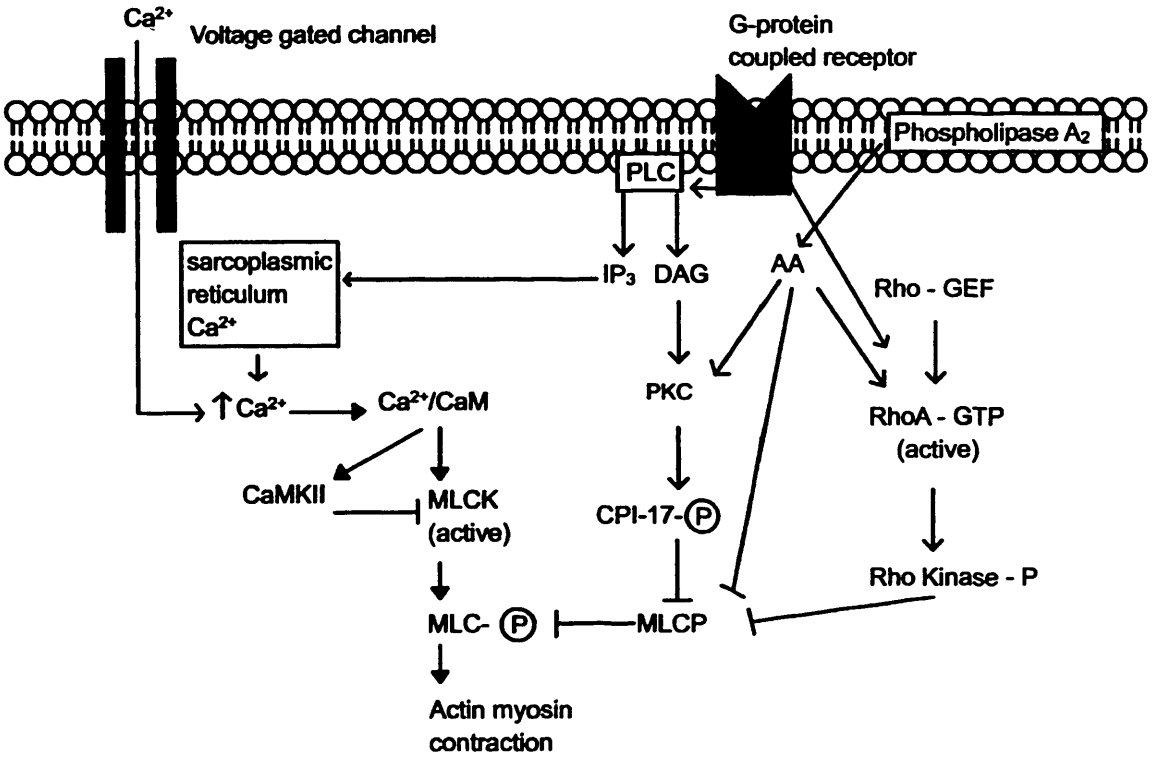


Figure 1.9 Signalling pathways involved in the regulation of myosin light chain phosphatase activity. Agonists via G-protein-coupled pathways activate phospholipase $A_2$ synthesis of AA by its action on phospholipids. Arachidonic acid inhibits MLCP through an unknown mechanism. G-protein-coupled receptor activation and AA activate RhoA, which stimulates ROCK leading to phosphorylation of MYPT, resulting in inhibition of MLCP holoenzyme catalytic activity. G-protein-coupled receptor activation of phospholipase C, results in the synthesis of DAG which activates PKC (AA also activates PKC) which phosphorylates CPI-17 an inhibitor of MLCP.

*Arachidonic acid*

Arachidonic acid is synthesised via the direct action of phospholipase $A_2$ on phospholipids. Phospholipase $A_2$ is activated by agonists and increases the synthesis of AA via a G-protein-coupled pathway. Additionally, PKC can be activated by AA and in numerous cell systems (Gong, *et al* 1992). Arachidonic acid could potentially bind directly with MYPT, leading to separation of the holoenzyme (thereby effectively decreasing phosphatase activity of MLCP to that of the PP1), or it may result in the activation of an undefined kinase that phosphorylates MYPT and results in myosin phosphatase inhibition (Gailly, *et al* 1997).

*Protein kinase C pathway*

Another pathway that increases $Ca^{2+}$ sensitisation is via PKC activation, which leads to phosphorylation of the MLCP inhibitor PKC-potentiated inhibitory protein for heterotrimeric myosin light chain phosphatase of 17kDa (CPI-17). Phosphorylation of CPI-17 at $T^{38}$ alone results in a 1000-fold increase in its inhibitory effect, thereby enabling MLCP inhibition *in situ* and *in vitro* without MYPT phosphorylation. The phosphorylation of CPI-17 results in an increase in the $Ca^{2+}$ sensitivity and hence a reduction in MLCP activity (Kitazawa, *et al* 2000).

## 1.17 Increasing paracellular permeability by inhibition of MLCP?

As previously described, current absorption enhancers have many potential side effects and hence are not widely utilised. A paracellular absorption enhancer with known function that has no side effects would therefore, be beneficial. It is known that the ratio of myosin light chain phosphatase to kinase activity regulates the degree of MLC phosphorylation and hence regulates TJ permeability. Therefore, if an inhibitor of MLCK closes TJs, then it could be possible that an inhibitor of MLCP would open TJs to allow the passage of impermeable drugs. This approach could produce fewer undesirable side effects due to its specific mode of action.

*Properties of an ideal absorption enhancer*

An ideal absorption enhancer would have reversible actions, work quickly and allow for the delivery of efficacious drug plasma concentrations. It is generally considered that an absorption enhancer with rapid and reversible actions would have

minimal toxicological issues since it would minimise the potential absorption of non-specific substances such as toxins that could result in adverse effects (Fix 1996).

## 1.18 Inhibitors of myosin light chain phosphatase

As well as regulatory subunits, there are numerous PP1-specific inhibitor proteins found within mammalian cells. Inhibitor proteins at nanomolar concentrations potently suppress the activity of purified PP1. The majority of inhibitory proteins are phosphoproteins, indicating that the activity of cellular PP1 is adapted due to kinase signalling by PP1 inhibitor protein phosphorylation (Eto, *et al* 2004).

Specific inhibitor proteins for PP1 include inhibitor-1 and inhibitor-2 (Huang and Glinsmann 1976), dopamine- and cyclic-AMP-regulated phosphoproteins of molecular weight 32,000 (DARPP-32) (Hemmings, *et al* 1984). However, they only inhibit monomeric PP1, not MLCP (Eto, *et al* 2001). Hence, it is generally considered that the PP1 interacts with inhibitor proteins following dissociation from the regulatory subunits. Coherent with this theory, evidence suggests that both inhibitor-1 and DARPP-32 have a KIQF sequence that interacts with the RVXF-binding motif utilised by numerous PP1 regulatory subunits (Hayashi, *et al* 2001).

## 1.19 PKC-potentiated inhibitory protein for heterotrimeric myosin light chain phosphatase of 17kDa

Eto and colleagues isolated CPI-17, an inhibitory protein of PP1 encoded from a porcine aorta cDNA library. PKC-potentiated inhibitory protein for heterotrimeric myosin light chain phosphatase of 17kDa is a phosphoprotein that inhibits the MLCP holoenzyme, which is highly expressed in smooth muscle with little expression found in non-muscle tissues, the heart and skeletal muscle (Eto, *et al* 1997). In response to agonist stimulation such as phenylepherine and histamine stimulation, intact smooth muscle CPI-17 is phosphorylated at $T^{38}$ whilst dephosphorylation simultaneously occurs with vasodilation generated by production of nitric oxide (Eto, *et al* 2004).

PKC-potentiated inhibitory protein for heterotrimeric myosin light chain phosphatase of 17kDa, unlike other protein inhibitors, does not contain a sequence similar to RVXF. Binding of MYPT to PP1 by the RVXF sequence, alters the PP1

active centre thereby, increasing MLC dephosphorylation. However, CPI-17 inhibits the MLCP holoenzyme as potently as PP1 alone, demonstrating that binding to PP1 RVXF site is not necessary for inhibition and that MYPT bound at this site does not obstruct inhibition by CPI-17. Hence, CPI-17 has an undefined interaction with PP1. (Hayashi, *et al* 2001).

Phosphorylation of CPI-17 by PKC enhances its inhibitory potency by 1000-fold, thereby presenting a separate pathway for MLCP inhibition *in situ* and *in vitro* without MYPT phosphorylation like other inhibitory proteins. Threonine$^{38}$ phosphorylation is enough to induce MLCP inhibition and a simultaneous elevation in $Ca^{2+}$ sensitivity and hence increase MLC phosphorylation resulting in smooth muscle contraction (Kitazawa, *et al* 2000).

Artery strip permeabilisation via treatment with Triton X-100 diminishes endogenous CPI-17 and abolishes the PKC induced contractile response. However, addition of recombinant CPI-17 to the permeabilised artery strips reinitiates PKC-induced contraction. These results confirm that CPI-17 is essential for contraction induced by PKC. Expression levels of CPI-17 between different smooth muscles are correlated with sensitivity of contraction induced by phorbol ester, supporting the idea that PKC acts through CPI-17 (Hayashi, *et al* 2001).

## 1.20 Aims and objectives

The main aims of this study were to investigate the modulation of TJ function via the action of myosin light chain phosphorylation/dephosphorylation. This will be achieved by the synthesis of membrane-permeant peptide inhibitors of MLCK and MLCP.

i) Initial studies suggest PIK as a promising inhibitor of MLCK that increases TER in two different inflammation cell models such as IBD. However, use of this peptide may be limited by its potential susceptibility to enzymatic destruction. Therefore, studies will be performed to identify relevant labile sites of PIK and to synthesise stable analogues, whilst maintaining specificity and biological activity. This will be achieved by Fmoc-solid phase peptide synthesis of PIK, followed by incubation of PIK in biological fluids and cell homogenates followed by liquid chromatography-mass spectrometry analysis

of the peptide and its degradation products. Peptides will then be designed based on PIK degradation pattern, the stability of these peptides will then be determined. Any potential candidates will then be further tested for biological activity by using a kinase assay using Caco-2 MCLK and recombinant intestinal epithelial MLC, additionally PIK analogues ability to increase TER in Caco-2 monolayers with activated $Na^+$-glucose co-transporters will be assessed. Specificity of the analogues will be tested by determination of their abilities to inhibit the serine/threonine kinases PKA and CaMKII by enzyme-linked immunosorbent based assays.

ii) Elevated MLC phosphorylation has been shown to enhance paracellular permeability. Therefore, inhibition of MLCP may result in increased TJ permeability hence augment the absorption of poorly absorbed drugs. Peptide inhibitors of MLCP will be synthesised by Fmoc-solid phase peptide synthesis. These peptide inhibitors will then be tested for their abilities to reduce TER in confluent Caco-$2_{BBe}$ monolayers. Any potential peptide candidates will then be tested for their ability to increase paracellular permeability of inert paracellular markers such as fluorescein isothiocyante-dextran.

iii) The mode of commonly used absorption enhancers will be investigated as their exact modes of action are undefined. Myosin light chain has been shown to be important in the regulation of paracellular permeability therefore PIK a specific inhibitor of MLCK will be used to determine the role of MLC phosphorylation in commonly used absorption enhancers. Such as sodium caprate whose increases in paracellular permeability are inhibited by the specific MLCK inhibitor ML-7. Therefore, confluent Caco-$2_{BBe}$ will be treated with sodium caprate and the specific MLCK inhibitor PIK ability to reduce sodium caprate enhancement effects on paracellular permeability will be measured.

# Chapter 2

# Materials & Methods

## 2.1 Materials

All chemicals, reagents and equipment used in these studies along with their suppliers are listed below.

*General chemicals and reagents*

Phosphate buffered saline (PBS) tablets, glycerol, acetic acid, bovine serum albumin and N-2-Hydroxyethylpiperazine-N'-2-ethanesulfonic acid (HEPES) were supplied by Sigma-Aldrich Company Ltd, UK. Ethanol, tris(hydroxymethyl)aminomethane hydrochloride salt (Tris-HCl), HPLC grade acetonitrile (ACN) and methanol were supplied by Fisher Scientific Laboratories, UK. Ethylenediamine tetracetic acid (EDTA) was purchased from Promega, UK. RC DC Protein Assay kit was obtained from Bio-Rad laboratories GmbH, Germany.

*Chemicals and reagents for $N^{\alpha}$-9-fluorenylmethoxycarbonyl solid phase peptide synthesis*

$N^{\alpha}$-9-fluorenylmethoxycarbonyl (Fmoc)-amino acids, (2-1-H-benzotriazol-1-yl)-1,1,3,3-tetramethyl-uronium hexaflurophosphate (HBTU), benzotriazole-1-yl-oxy-tris-pyrrolidino-phosphonium hexaflurophosphate (PyBOP®), hydroxybenzotriazole (HOBt) and 4-(2′,4′-Dimethoxyphenyl-Fmoc-aminomethyl)-phenoxyacetamido-norleucyl-MBHA resin (rink amide MBHA resin) were from CN Biosciences Ltd., UK. Solvents were either peptide synthesis grade or highest grade available *N,N*-dimethylformamide (DMF), dichloromethane (DCM) and acetic acid were supplied from Fisher Scientific Laboratories, UK. Trifluoroacetic acid (TFA), *N*-methylmorpholine (NMM), piperdine, acetic anhydride, ether, pyridine and *N,N*-diisopropylethylamine (DIEA) were obtained from Aldrich, UK, whereas, triisopropylsilane (TIPS) was supplied by Fluka, UK and d-biotin and dimethylsulfoxide (DMSO) were from Sigma-Aldrich Company Ltd, UK.

*Cell culture*

Caco-2 and Caco-$2_{BBe}$ cells were purchased from American Type Culture Collection, USA. High glucose Dulbecco's modified Eagle's medium (D-MEM) with 4500 mg/L glucose and L-glutamine, D-MEM with 1000 mg/L glucose and L-glutamine, foetal bovine serum (FBS), cell culture freezing medium–DMSO

(prepared in D-MEM and calf sera) and 0.05 % trypsin–0.53 mM EDTA were supplied by Invitrogen Life Technologies, UK. Penicillin/streptomycin was purchased from Gibco, UK. Trypan blue solution (0.4 % w/v) was obtained from Sigma-Aldrich Company Ltd, UK. Medical grade $CO_2$ (all 95 % v/v) and liquid nitrogen were supplied by BOC, UK.

*Mycoplasma screening of cell cultures*

Mycoplasma Plus™ PCR primer set was purchased from Stratagene, USA. Agarose, Tris-Borate-EDTA buffer and DirectLoad™ wide range DNA marker were from Sigma-Aldrich Company Ltd, UK. Deoxynucleotide triphosphates, ethidium bromide and 10 x TAQ reaction buffer were purchased from Promega, UK, whereas TAQ polymerase was from Cancer Research UK, UK.

*Enzyme-linked immunosorbent based assays*

Protein assay kit non-radioactive, peroxidase-conjugated streptavidin, horseradish peroxidase, *o*-Phenylenediamine and $Ca^{2+}$/calmodulin kinase II inhibitor 281-309, protein kinase A inhibitor 6-22 amide, Calcium-calmodulin dependent protein kinase II were from Calbiochem, UK. Polyoxyethylene-sorbitan monolaurate (Tween-20), hydrogen peroxide ($H_3PO_4$), streptavidin, protein kinase catalytic subunit from bovine heart and monoclonal anti-phosphoserine-biotin clone PSR-45 were supplied by Sigma-Aldrich Company Ltd, UK.

*Thiophosphorylation experiments*

Protein kinase C, catalytic subunit from rat brain was obtained from Merck, UK. Magnesium chloride, adenosine 5'-[γ-thio] triphosphate tetralithium salt (ATPγS), 1,2-diolein and 4-Morpholinepropane sulfonic acid sodium salt (MOPS-NaOH) were purchased from Sigma-Aldrich Company Ltd, UK.

*Caco-$2_{BBe}$ monolayer permeability studies*

Hanks' Balanced Salt Solution (HBSS), HBSS (without calcium chloride and magnesium sulphate), sodium decanoate, phorbol 12-myristate 13-acetate (PMA), fluorescein sodium salt, fluorescein isothiocyante-dextran (FD) average molecular weight 4,000 and 77,000 were purchased from Sigma-Aldrich Company Ltd, UK as

were type I collagen from rat-tail and chloroform for coating of Transwell® inserts. *N,N,N*-trimethylation chitosan chloride (77 % degrees of trimethylation) was a kind gift from Thomas Kean, Centre of Polymer Therapeutics, Cardiff University, UK.

*Colorimetric cytotoxicity assay*

3-[4,5-dimethylthiazol-2-yl]-2,5-diphenyltetrazolium bromide (MTT), analytical grade DMSO, polyethylenimine (PEI; MW 750,000 Da; 50 % w/v in $H_20$) and dextran (MW = 68,800 Da) were purchased from Sigma-Aldrich Company Ltd, UK.

## 2.2 Equipment

*General laboratory equipment*

A Heraeus Multifuge 3 S-R with a BIOshield rotor was obtained from Kendro, UK. Eppendorf centrifuge 5417R was from Eppendorf, Germany. Weighing scale Sartorius CP124S was purchased from Sartorius, Germany. A Grant USD prima dry block heater and Jenway 3510 pH meter were supplied by Fisher Scientific Laboratories, UK.

*$N^{\alpha}$-9-fluorenylmethoxycarbonyl solid phase peptide synthesis*

Peptides were synthesised on an automated Symphony Quartet Peptide Synthesiser with the Quartet multiplex peptide synthesizer version 2.0 software from Zinsser analytic, UK. A Büchi rotavapor R-205 from Fisher Scientific Laboratories, UK was used to evaporate solvents and a Thermo savant MicroModulyo Lyophiliser purchased from Thermo Electron Corporation, UK were used to lyophilise peptides to dryness.

*High-pressure liquid chromatography*

Purification of desired peptides from crude material was achieved by semi-preparative HPLC system consisting of a SCL-10A system controller, LC-10AD pumps, SPD-M10A diode array detector CLASS-VP version 6.1 chromatography data system all from Shimadzu, Japan. Peptide separation was performed using a Vydac 218TP $C_{18}$ reversed-phase silica gel column (10 x 250 mm, 300 Å pore size,

5-μm particle size) (Grace Vydac, California, USA). The flow rate was 2 ml/min and the gradient conditions were used as follows: solvent A was 0.3 % TFA in water and solvent B was 0.3 % TFA in ACN. The gradient started at t = 0 min, B = 0 %; t = 0.1 min, B = 70 %; t = 10 min, B = 60 %; t = 15 min, B = 10 %; t = 20 min, B = 5 %; T = 25 min, B = 0 %. Separation was monitored at a wavelength of 214 nm.

*Liquid chromatography-mass spectrometry*

Peptides were separated on a 218TP $C_{18}$ reversed-phase silica column (4.6 x 250 mm, 300 Å pore size, 5 μm particle size) from Grace Vydac, USA. Peptides and degradation products were separated using the spectrasystem AS3000 autosampler and spectrasystem P4000 gradient pump and detected using UV6000LP UV detector and on a Thermo Finnigan LCQ DECA mass spectrometer and analysed using Thermo Finnigan Xcalibar software from Thermo Separation Products, USA.

*Cell culture*

Costar cell culture consumables were purchased from Corning Inc, USA, with the exception of kwill filling tubes and BD plastipak syringes, which were obtained from Western Laboratory Service Ltd, UK and Ministart® 0.2 μm filters from Sartorius, Germany. The Heraeus Hera Cell incubator and the Heraeus safe type II laminar hood were supplied by Jencons PLS, UK. For routine cell culture work an inverted Nikon Eclipse TS100 microscope was used (Jencons PLS, UK) with a Neubauer haemocytometer (Marienfeld, Germany) for cell counts.

*Mycoplasma screening of cell cultures*

Techne Flexigene PCR machine was purchased from Jencons PLS, UK. The horizontal gel unit and electrophoresis power supply FB300 were supplied by Fisher Scientific Laboratories, UK.

*Enzyme-linked immunosorbent based assays*

Ninty-six well polystyrene flat bottom microtiter plates were supplied by Corning Inc, USA. Colorimetric detection of the microtiter plates was measured using a plate reader from Anthos HTII from Fisher Scientific Laboratories, UK.

*Caco-2$_{BBe}$ monolayer permeability studies*

Six well plate Tranwells with 24 mm diameter, 0.4 μm pore size, collagen-coated polytetrafluoroethylene membranes, 6 well plate Tranwells with 24 mm diameter, 0.4 μm pore size, polycarbonate membranes and black 96 well polystyrene flat bottom microplates were supplied by Corning Inc, USA. EVOM™ epithelial voltohmmeter with STX2 "chopstick" electrodes from World Precision Instruments Inc, USA were used to measure TER. The STX2 electrode is composed of a fixed pair of double electrodes. The outer electrodes silver pads conduct current across the membrane sample, whilst the inner electrodes composed of silver/silver-chloride pellets measure voltage. Fluorescence was measured using the Flurostar optima from BMG Labtechnologies, Germany.

*Colorimetric cytotoxicity assay*

A Sunrise UV-absorbance plate reader from Tecan, Australia was used to measure absorbance. Ninety six well polystyrene flat bottom microtiter plates were purchased from Corning Inc, USA and a U300 ultrasonic cleaning bath from Ultrawave Ltd, UK.

## 2.3 Methods

The methods used in this thesis are described below, though where necessary specific details are given in the forthcoming experimental chapters.

### *2.3.1 $N^{\alpha}$-9-fluorenylmethoxycarbonyl solid phase peptide synthesis*

Peptides were synthesised by solid-phase peptide synthesis techniques using Fmoc chemistry. Amino acid side chains were protected as in table 2.1. Rink amide MBHA resin 100 mg (0.78 mmol/g) was swollen with DCM for 30 min. De-protection of Fmoc-amino acids was accomplished by treatment with 20 % (v/v) piperdine/DMF for 20 min. Initial coupling reactions were performed by adding resin/amino acid/HOBt/PyBOP®/DIEA in equivalents of 1/5/5/4.9/10 and mixing for 2 h. Each subsequent coupling reaction was performed by mixing 0.05 M Fmoc-amino acids dissolved in DMF with 0.1 M of HBTU and 0.4 M of NMM for 30 min followed by resin washing the $N^{\alpha}$-Fmoc group was cleaved at following each step with 20 % (v/v) piperdine: DMF for 12 min. N-terminal acetylation was performed

Table 2.1 Side chain protection groups of the amino acids.

| Amino Acid | Protection Group |
|---|---|
| Ala | No protection group |
| Arg | 2,2,4,6,7-pentamthyldihydrobenzofuran-5-sulfonyl |
| D-Arg | 2,2,4,6,7-pentamthyldihydrobenzofuran-5-sulfonyl |
| Asp | *Tert*-butyl ester |
| Gln | Trityl |
| Glu | *Tert*-butyl ester |
| Lys | *Tert*-butoxycarbonyl |
| D-Lys | *Tert*-butoxycarbonyl |
| Thr | No protection group |
| Tyr | *Tert*-butyl |
| D-Tyr | *Tert*-butyl |
| Val | No protection group |

on some peptides prior to cleavage from the resin by treatment with 50 % acetic anhydride, 25 % pyridine and 25 % DMF (v/v) for 30 min. Other peptides had their N-terminus biotinylated this was achieved by addition of resin/biotin/HBTU/HOBt/DIEA in equivalents of 1/3/3/3/5 and mixing for 3 h. Schematic representation of Fmoc solid phase peptide synthesis can be seen in figure 2.1.

Crude peptides were cleaved from the resin for 3 h in 95 % TFA, 2.5 % TIPS and 2.5 % $H_2O$ (v/v) due to the presence of multiple R within the peptide sequence. The crude peptide was then roto-evaporated to remove solvents, precipitated in cold ether, washed and then extracted with 2 % ACN 2 % acetic acid in $H_2O$ (v/v) and then lyophilised to dryness. Peptides were then kept in an airtight container at – 20 °C until required

### *2.3.2 Purification of peptides*

Purification of desired peptides from crude material following lyosphilisation was achieved by dissolving the peptide with water, followed by separation using a semi-preparative HPLC Vydac 218TP $C_{18}$ reversed-phase silica gel column. Crude mixtures were then separated using a gradient elution as shown in table 2.2. Separation of crude peptide mixtures was monitored at a wavelength of 280 nm due to the presence of multiple R within the PIK peptide sequence. Collected peptide fractions were analysed using mass spectrometry, fractions containing the peptide were pooled, concentrated, and verified by liquid chromatography and mass spectrometry analysis.

### *2.3.3 Liquid chromatography-mass spectrometry analysis*

Verification of peptide purification was done by HPLC separation of peptides on a 218TP $C_{18}$ reversed-phase silica column (using a linear gradient from 98 % A/2 % B to 50 % A/50 % B in 1 h (flow rate 0.5 ml/min) where eluent A was 0.1 % TFA in water and eluent B was 0.1 % TFA in ACN. Peptides were monitored at a wavelength of 214 nm and/or 280 nm by positive electrospray ionisation (ESI).

### *2.3.4 Rat intestinal flush and determination of protein content*

The rats intestine (duodenum to the rectum) was removed as soon as possible following death, and was flushed with 10 ml of 20 mM of HEPES buffer, pH 7.4. Discharged contents were then centrifuged at 3000 rpm for 20 min at 4 °C to remove

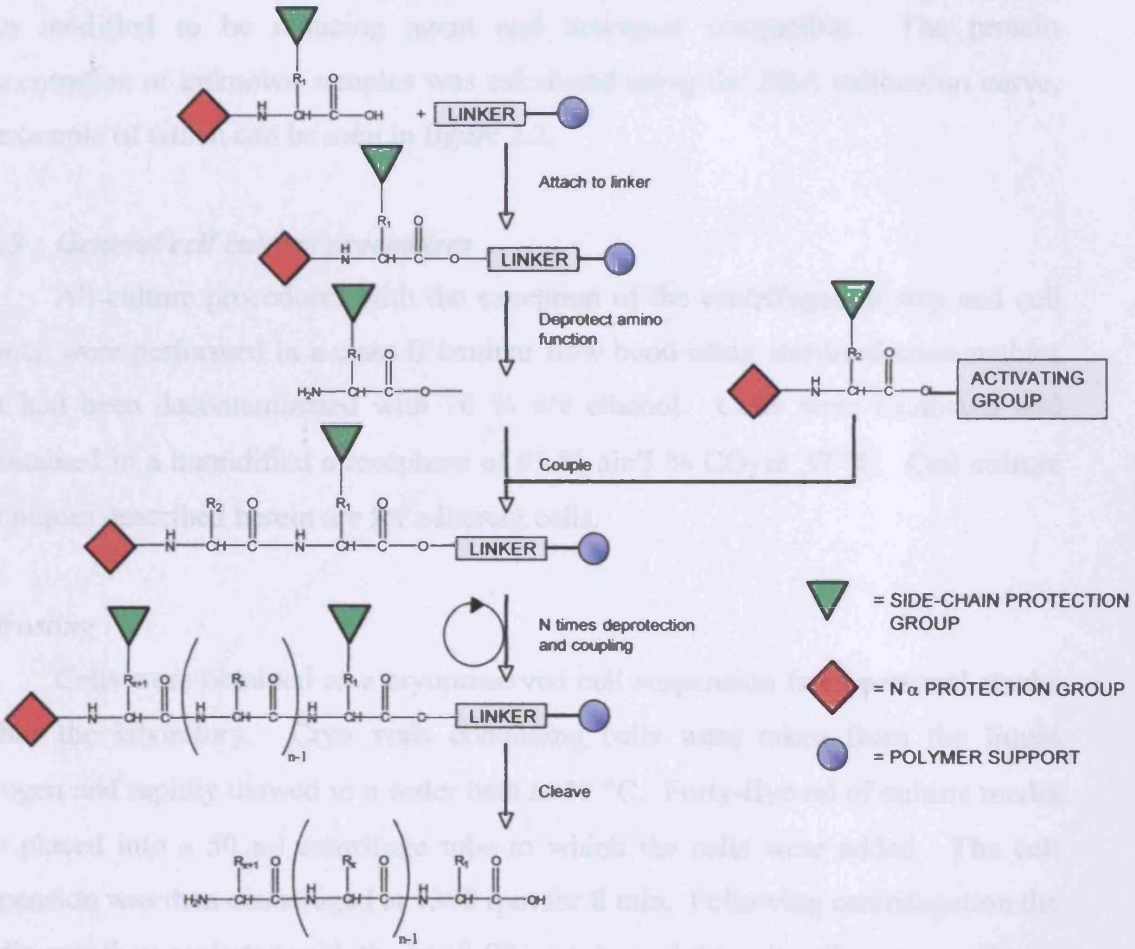


Figure 2.1 Schematic representation of Fmoc-solid phase peptide synthesis.

solids and the supernatant filtered using a 0.20 μm filter, prior to protein content determination. The intestinal juice protein content was then determined using the RC DC Bio-Rad Protein Assay as manufacturers guidelines. The RC DC Protein Assay is a colorimetric assay for protein quantification based on the Lowry assay but has been modified to be reducing agent and detergent compatible. The protein concentration of unknown samples was calculated using the BSA calibration curve, an example of which can be seen in figure 2.2.

### *2.3.5 General cell culture procedures*

All culture procedures with the exception of the centrifugation step and cell counts, were performed in a class II laminar flow hood using sterilised consumables that had been decontaminated with 70 % v/v ethanol. Cells were incubated and maintained in a humidified atmosphere of 95 % air/5 % $CO_2$ at 37 °C. Cell culture techniques described herein are for adherent cells.

*Defrosting*

Cells were obtained as a cryopreserved cell suspension from personal stocks within the laboratory. Cryo vials containing cells were taken from the liquid nitrogen and rapidly thawed in a water bath at 37 °C. Forty-five ml of culture media was placed into a 50 ml centrifuge tube to which the cells were added. The cell suspension was then centrifuged at 1300 rpm for 8 min. Following centrifugation the media was then aspirated with the kwill filling tube and the cell pellet was gently re-suspended in 5 ml of culture media. The resulting cell suspension was then transferred into a 25 $cm^2$ culture flask and allowed to grow for 3 days, before culture media was changed.

*Maintenance*

Cells were supplemented with fresh media every other day. Cells were subcultured weekly when they were approximately 80 % confluent. This was achieved by removing the culture media from the flask, washing the cells twice with 0.1 M PBS (pH 7.4) followed by addition of 1 ml of trypsin/EDTA, the flask was then incubated for 20 min. Media was added to the cells and the cells where re-suspended vigorously and centrifuged at 1300 rpm for 8 min. The supernatant was

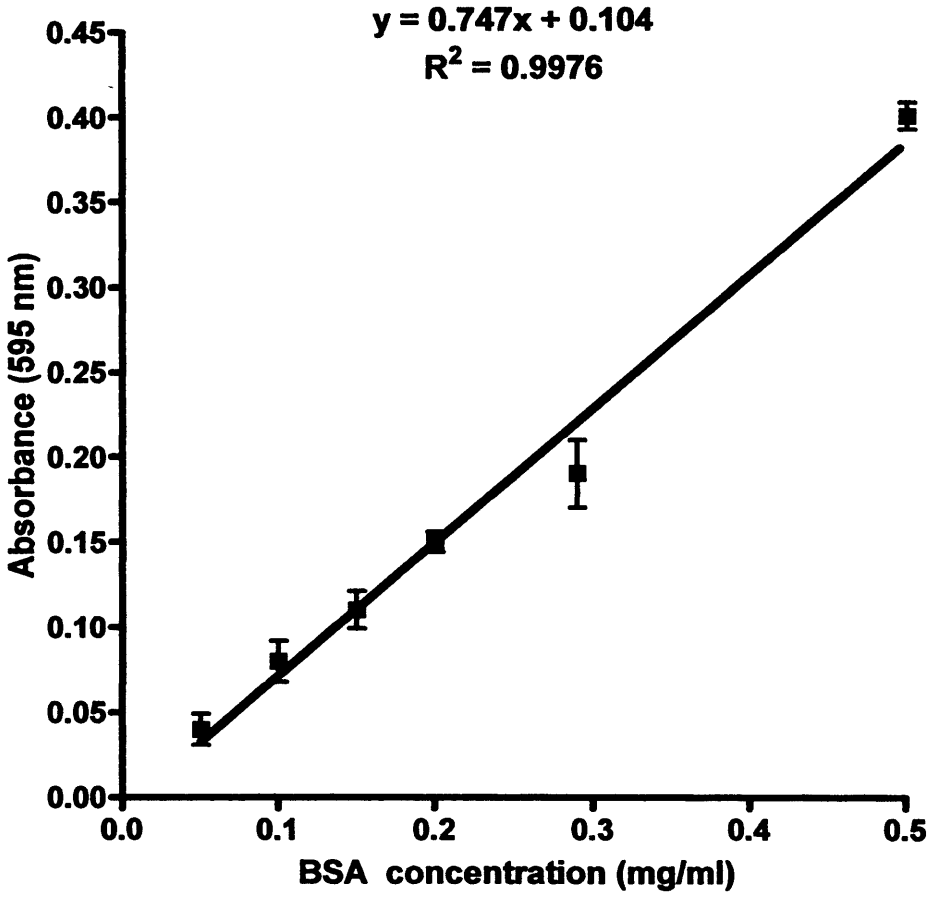


Figure 2.2 An example of a calibration curve used for the estimation of total protein concentration. (Data represents mean ± SD n=3, error bars are within plot symbols when not visible).

Table 2.2 Summary of routine culture conditions for Caco-2 cells*.

| Cell Line | Origin | Medium | Split Ratio | Freezing Media |
|---|---|---|---|---|
| Caco-2 | Human Caucasian colon adenocarcinoma | D-MEM | 1 : 10 | DMSO (prepared in D-MEM and calf sera) |
| Caco-$2_{BBe}$ | Cloned from the Caco-2 cell line by limiting dilution | High glucose D-MEM | 1 : 10 | DMSO (prepared in D-MEM and calf sera) |

* Media was supplemented with 10 % filtered FBS, 50 units penicillin and 50 μg/ml streptomycin.

decanted and cells were re-suspended in 5 ml of media. The resulting cell suspension was then used to subculture the cells at a 1 in 10 split ratio. Cells at passage numbers 58-68 were used for all experiments used in these studies.

*Counting*

Cells were washed, trypsinised, and re-suspended in a known volume of media as described previously. A haemocytometer and trypan blue exclusion assay was used to count viable cells. The reactivity of this dye is based on the fact that the chromaphore is negatively charged and does not interact with the cell unless the membrane is damaged hence, all cells that exclude the dye are viable. To 50 µl of cell suspension 100 µl of trypan blue was added, and allowed to stand for 5-15 min to allow staining of non-viable cells. The counting chamber was filled with the cell suspension and placed under an inverted light microscope. A total of 8 squares 0.1 $mm^3$ were counted according to manufacturers guidelines, taking into account the dilution factor, cell concentrations were determined.

*Cryopreservation*

Cells were regularly cryopreserved to sustain stock levels. Following cell counts, cells were centrifuged and the cell pellet was re-suspended in cell culture freezing medium at 1 x $10^6$ viable cells/ml. One ml aliquots of cell suspension were then placed into cryovials. The cryovials were then placed in a freezing container, filled with isopropanol (to achieve a - 1 °C/min rate of cooling) and then placed in the – 80 °C for a minimum of 4 h. The cryo vials where then transferred in liquid nitrogen for long-term storage.

*Mycoplasma screening of cell cultures*

Cell cultures and materials were routinely tested for Mycoplasma infections, cultures were tested by removal of 100 µl aliquot of the cell culture supernatent, method as per manufacturers guidelines. An example of routine mycoplasma test can be seen in figure 2.3.

### *2.3.6 Homogenisation of Caco-2 cells*

Caco-2 cells (a human intestinal epithelial cell line) were grown to

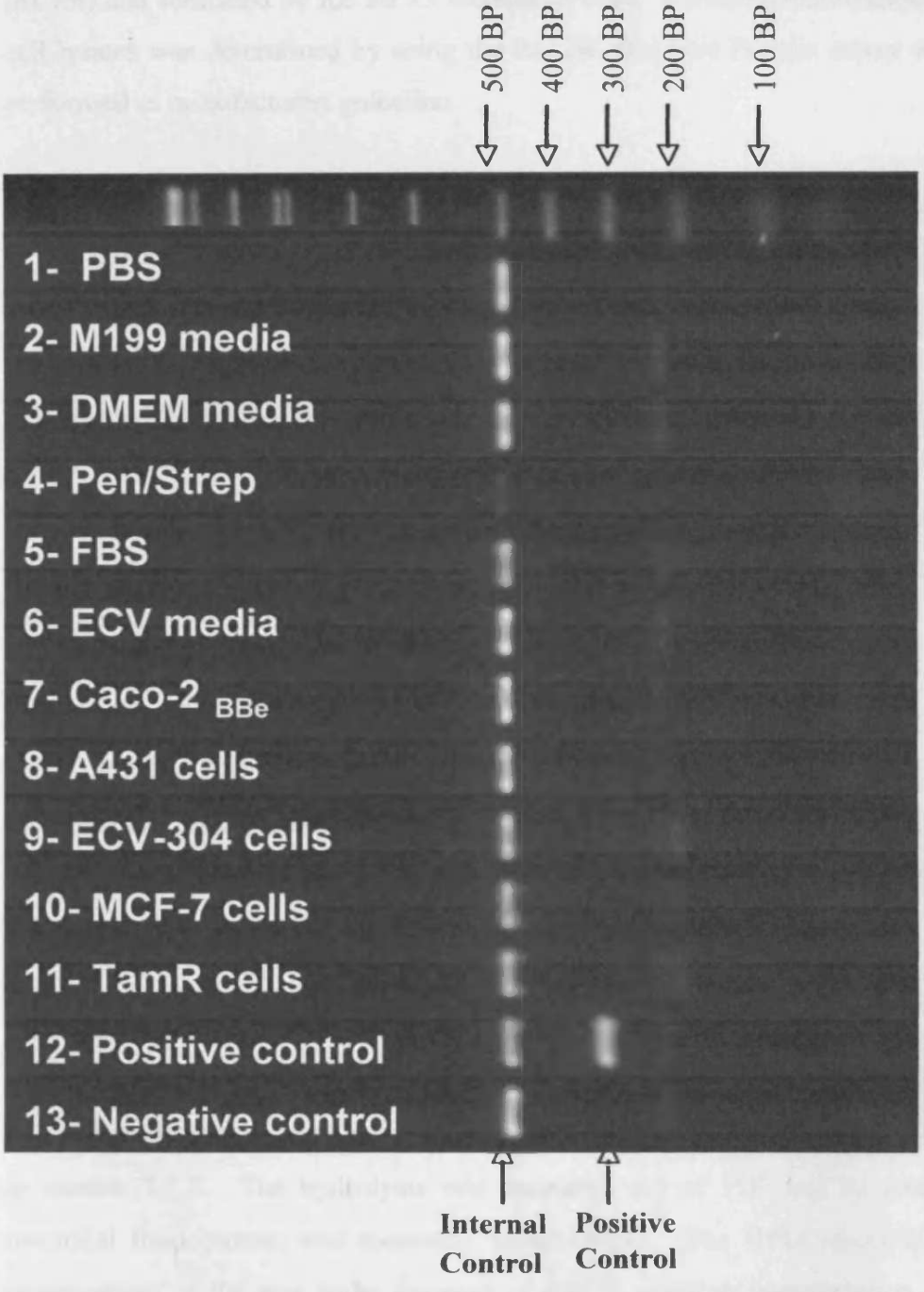


Figure 2.3 Example of a routine mycoplasma test agarose gel.

confluence, rinsed in PBS and detached from the flask with trypsin into a small volume of D-MEM. Suspended cells were pelleted by centrifugation at 1500 rpm, re-suspended in PBS and washed twice. Following the final wash, the cell pellet was re-suspended in a small volume of lysis buffer (50 mM Tris-HCl, 2 mM EDTA, 20 % glycerol at pH 7.4) and sonicated on ice for 15 seconds in total. Protein concentration of whole cell lysates was determined by using the RC DC Bio-Rad Protein Assay which was performed as manufacturers guideline.

### *2.3.7 Liquid chromatography-mass spectrometry analysis*

To validate the LC-MS method, Ac-PIK an end-terminal protected PIK peptide was incubated with trypsin a pancreatic protease, as this would result in a more predictable degradation pattern compared with incubation with multiple peptidases and proteases. Then 100 µl aliquots were withdrawn at different time points, diluted with the same volume of 0.5 % TFA (ACN/water), to terminate the enzymatic reaction. Samples were then centrifuged at 1200 rpm for 10 min at 4 °C and supernatants analysed by LC-MS analysis as in section 2.3.3. to determine the cleavage pattern of Ac-PIK.

### *2.3.8 Determination of peptide degradation patterns*

PIK and PIK peptide analogues (1 mg/ml) in PBS, were mixed with either 0.1 mg intestinal juice protein or 0.2 mg homogenised Caco-2 cell protein on ice. The reaction mixtures were then incubated at various times and temperatures and treated and analysed as section 2.3.7.

### *2.3.9 Determination of peptide half-lives*

PIK and PIK analogues were incubated with rat intestinal fluid protein at 37 °C. Aliquots were taken at various time points and treated and analysed as described in section 2.3.7. The hydrolysis rate constants (κ) of PIK and its analogues in intestinal fluid protein was measured using HPLC. The HPLC method involved measurement of the area under the peak of PIK to calculate concentration. The rate constant was then calculated using a first-order rate equation shown below.

$$\text{Log } [A]_t = \log [A]_0 - \kappa t/2.303$$

Where $[A]_t$ is the concentration of PIK at time $_t$ and $[A]_0$ is the concentration of PIK at time zero: $\kappa$ is the first-order rate constant. The plot of log $[A]_t$ versus decay time should be linear for a first-order reaction and $\kappa$ values were calculated from the slope (slope = $-\kappa t/2.303$). The degradation half-life was calculated using the equation.

$$t_{1/2} = 0.693/\kappa$$

### *2.3.10 Enzyme-linked immunosorbent based assays*

The specificity of PIK for MLCK was determined by performing enzyme-linked immunosorbent assays based assays. These were performed for PKA and CaMPKII enzymes to determine their activities in the presence of the 3 different D-amino acid PIK peptides. Protein kinase A activity was determined by using a non-radioactive protein kinase assay kit by adding 20 units of PKA to 0.5, 1, 2.5 and 5 mM PIK peptides and following manufacturers instructions, the principal of which can be seen in figure 2.4. The protein kinase A inhibitor 6-22 amide at a concentration of 4 nM was used as a positive control.

Calcium/calmodulin dependent protein kinase II activity was determined using a peptide pseudo-substrate for CaMPKII (Biotin-PLSRTLSVSS-$NH_2$) prepared by Fmoc solid-phase peptide synthesis and purification as described in sections 2.3.1. and 2.3.2. (Pearson, *et al* 1985). Biotinylated pseudo-substrate (0.5 μg/ml in PBS) was fixed to 96-well polystyrene microtiter plate wells previously coated with 100 μl of streptavidin (3 μg/ml in PBS) by overnight incubation at 4 °C. Wells were then washed 3 times with 100 μl of tris buffered saline containing 0.05 % Tween-20 to remove any unbound pseudo-substrate peptide.

After 5 min pre-incubation at 30 °C, 12 μl of the CaMPKII-PIK peptide sample and $Ca^{2+}$/Calmodulin kinase II inhibitor 281-309 (4 μM) were added to pseudo-substrate-coated wells. This was then incubated for 20 min at 30 °C. Following incubation 100 μl of 20 % $H_3PO_4$ was added to each well. The wells were then washed 5 times with PBS, after the final wash, the plates were inverted and blotted on paper towels to remove the liquid from each well, whilst avoiding drying

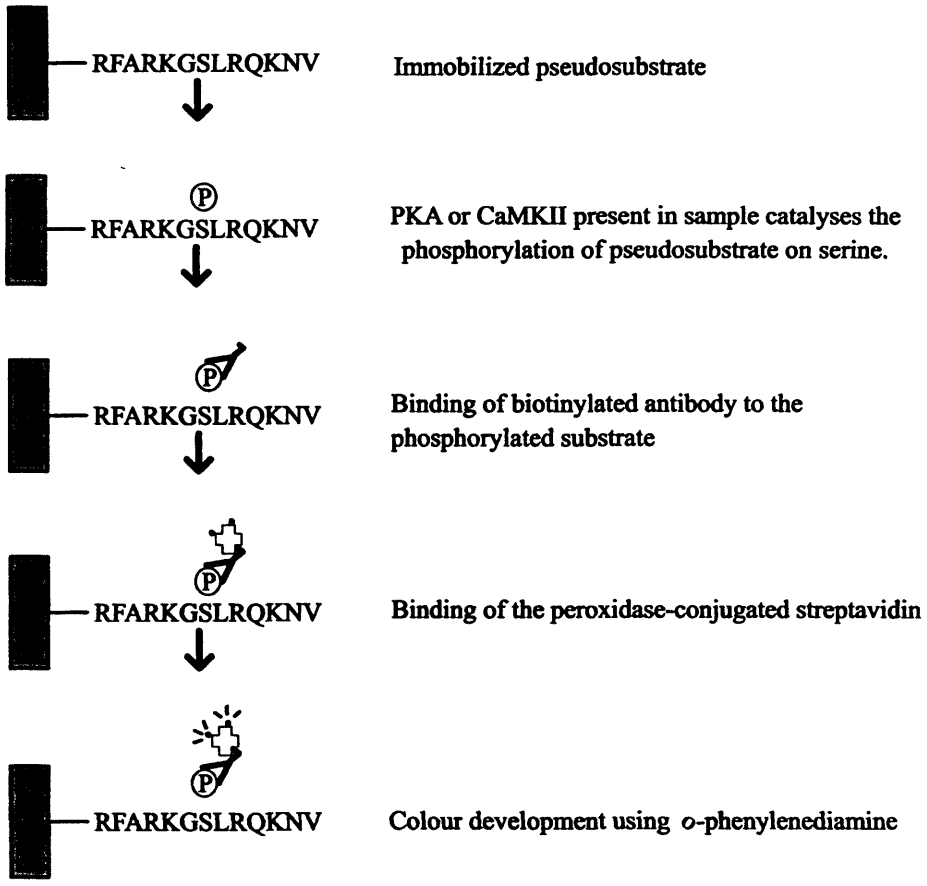


Figure 2.4 Outline of the PKA enzyme-linked immunosorbent based assay protocol.

the wells out. Then 100 µl of 1 in 50,000 of monoclonal anti-phosphoserine-biotin (clone PSR-45) was added to each well and incubated for 1 h at 30 °C. Following this incubation the wells were washed 5 times with PBS as described previously. Then the wells were incubated with 100 µl of peroxidase-conjugated streptavidin and incubated for 1 h at 30 °C. The wells were then washed again 5 times with PBS and then 100 µl of horseradish peroxidase conjugated to streptavidin. *o*-phenylenediamine was added to each well and incubated for 5 min at 30 °C. Then 100 µl of 20 % $H_3PO_4$ was added each well and the optical density read at 492 nm in a microplate reader.

### *2.3.11 Extracellular matrix coating of Transwell inserts*

Type I collagen was added to 0.1 M acetic acid to obtain a 0.1 % w/v collagen solution, which was then stirred at room temperature for 2 h until dissolved. Once dissolved the collagen solution was transferred to a glass bottle (with a screw cap) and chloroform (approximately 10 % of the volume of collagen solution) was carefully layered underneath. Without shaking or stirring the bottle was placed at 4 °C overnight. Aseptically the top layer containing the collagen was removed. The polycarbonate culture surface was coated with 10 µg/cm$^2$ collagen as manufacturers guidelines. Protein was allowed to bind for 3 h at room temperature. Excess fluid was aspirated from the coated surface, and allowed to dry for an additional hour, before being left overnight under an ultraviolet (UV) lamp in a type II laminar hood for sterilisation. Immediately prior to the introduction of cells and media each well was rinsed with sterile PBS.

### *2.3.12 Culture of Caco-2$_{BBe}$ monolayers on permeable supports*

Caco-2$_{BBe}$ cells were subcultured and counted as described in section 2.3.5, before seeding on Transwell inserts (figure 2.5). Two and a half ml of media was added to the lower compartments of the 6 well plates. The Transwells filters were then seeded at a density of 10,000 Caco-2$_{BBe}$ cells/cm$^2$ (Borchard, *et al* 1996). The cells were then grown for 21 days to allow the development of TJs and ion channels this was confirmed by measurement of the TER which in cells with functional TJs is between 150-300 Ω cm$^2$. Since the TJ regulates the movement of solutes through the

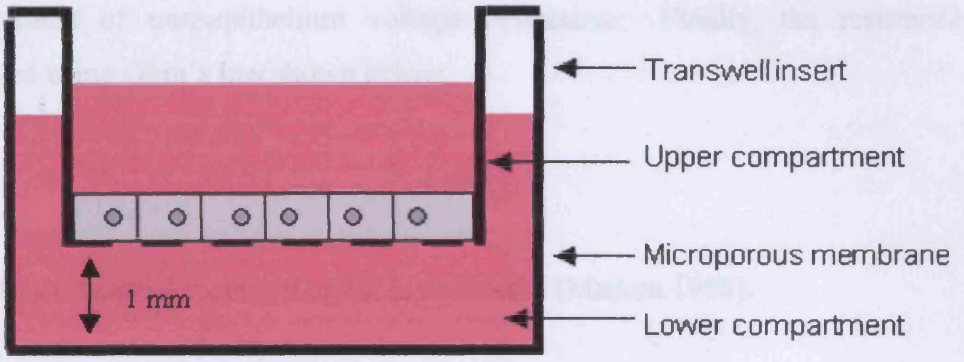


Figure 2.5 Schematic representation of the Transwell permeable support. Media volume inside of the upper compartment of the Transwell insert was 2.5 ml and 2.5 ml in the lower compartment.

paracellular space, changes in TER are used as an indicator of TJ permeability. This method is therefore widely used in cell culture. The method essentially involves the passage of a pulse of defined amplitude across the epithelium and subsequent measurement of transepithelium voltage deflection. Finally, the resistance is calculated using Ohm's law shown below

$$V=IR$$

where $V$ is voltage, $I$ is current and $R$ is resistance (Madara 1998).

### *2.3.13 Effects of absorption enhancers on TER*

Caco-$2_{BBe}$ cells were cultured as described in section 2.3.12. Monolayers were firstly incubated with pre-warmed HBSS (buffered to pH 7.4 with 25 mM HEPES) for 20 min. Then the absorption enhancers were added to the apical compartments and the TER measured at time zero and then the TER measured at various time points. The TER was then expressed as a percentage of the initial TER value.

### *2.3.14 Inhibition of absorption enhancement by PIK*

Caco-$2_{BBe}$ cells were cultured as described in section 2.3.12. Monolayers were firstly incubated with pre-warmed HBSS (buffered to pH 7.4 with 25 mM HEPES) for 20 min. Cells were then incubated with absorption enhancers with and without PIK and the paracellular transport was measured using fluorescent probes, 50 µl aliquots were taken from the basolateral side of the filter and replaced with HBSS at various time points. The fluorescence of the aliquots were measured at excitation 485 nm and emission 520 nm. And the permeability coefficients were calculated using the equation.

$$P_{app} = (dQ/dt)/(Co*A)$$

Where $P_{app}$ equals the apparent permeability coefficient (cm/s), dQ/dt is the amount of fluorescent marker transported, A is the diffusion area of the monolayer ($cm^2$), and Co is the initial concentration of the marker in the donor compartment (Lindmark, *et*

*al* 1998).

### *2.3.15 Colorimetric cytotoxicity assay*

The assay involves the cleavage of the tetrazolium salt of MTT by mitochondrial dehydrogenase into formazan a dark blue product in living but not dead cells (figure 2.6). Consequently toxic insult resulting in the death of the cell inhibits this process and thus allowing the use of the MTT as a cellular toxicity assay. Detection of crystal formation is achieved by dissolving the crystals in DMSO, and measurement of absorbance at 550 nm (Mosmann 1983).

Firstly the wells surrounding the outer edge of the 96 well plate were filled with 100 µl of PBS to prevent dehydration of the cells. Caco-$2_{BBe}$ cells were then seeded at a density of 15,528 cells/$cm^2$ to the remaining wells and cultured for 48 h. The wells were subsequently washed with PBS and peptide was added to the wells. As a negative control no peptide/polymer was added to the wells. Following addition of the peptide/polymer, Caco-$2_{BBe}$ cells were incubated at 37 °C for the relevant time required for increases in paracellular enhancement. The peptide/polymer was then aspirated followed by addition of a 5 mg/ml MTT solution in PBS to each well, cells were then incubated for a further 5 h at 37 °C. The MTT solution was then removed from each well and the reaction product was then solubilised in DMSO and the colour of the reaction product measured using a microplate reader at 550 nm. Each experiment was performed in triplicate (Bromberg and Alakhov 2003). Data from these experiments were expressed as a percentage of the viability seen in the control (untreated) cells. The $IC_{50}$ calculation was performed using the Hill equation (below) using Biograph v1.2c for Microsoft Windows 1995:

$$y = R_{min} + (R_{max} - R_{min})/(1+(x/IC_{50})^P)$$

Where $R_{max}$ is fixed at 100 and $R_{min}$ at 0, weighted for standard error. The $IC_{50}$ of a compound is the concentration of the compound needed to reduce population growth of cells by 50 % *in vitro* (Kean, *et al* 2005).

### *2.3.16 Statistics*

Statistical significance was assigned to $p \leq 0.05 - 0.001$ and calculated using

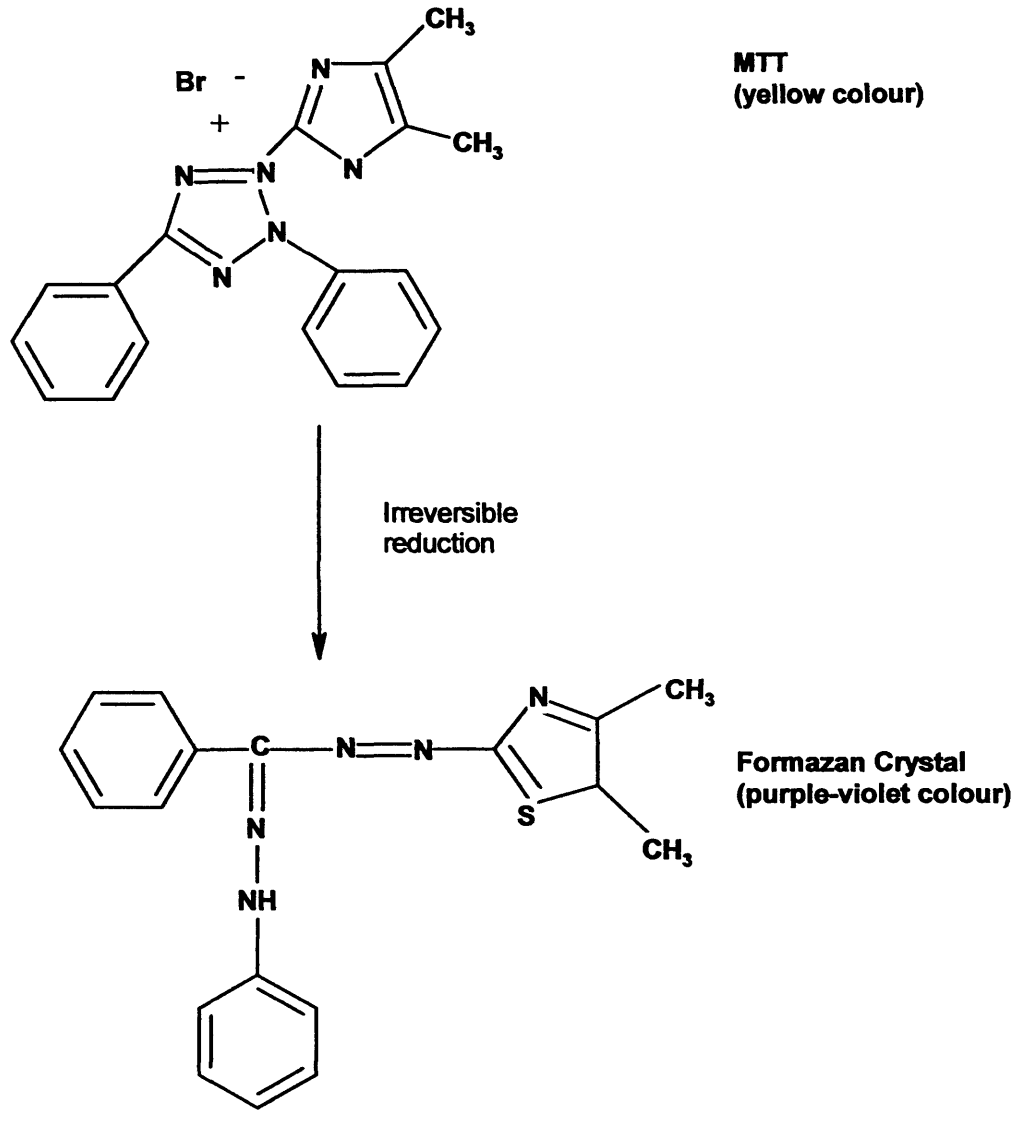


Figure 2.6 Outline of the reduction of MTT. Reduction of MTT to formazan is irreversible and catalysed by enzymes of the respiratory chain and thus an indicator of mitochondrial activity.

a Student's t-test (paired/unpaired as indicated) for the comparison of 2 samples, and one-way or two-way analysis of variance (ANOVA) when more than 2 samples were compared, followed by Bonferroni post-hoc analysis. Where indicated, standard error of the mean (SEM) for data points were calculated and the number (n) of experiments/replicates are given as indicated.

# Chapter 3

# Identification of Stable PIK Analogues

## 3.1 Introduction

The main functions of the gastrointestinal tract are to protect the underlying tissue from the potentially noxious contents of the intestinal lumen, digestion, and selective secretion and absorption of substances such as electrolytes and water (Wang 1996). Digestion of proteins and peptides in this organ are mediated by a number of different enzymes which specifically cleave peptide bonds. These enzymes, called proteases and peptidases, have different substrate specificities and hence are important factors preventing absorption of peptide-based drugs due to cleavage (Pauletti, *et al* 1997).

*Gastrointestinal tract peptidases*

There are 2 classes of peptidases, including endopeptidases such as chymotrypsin and pepsin, which are capable of hydrolysing peptide bonds within peptides. Meanwhile, exopeptidases such as carboxypeptidases and aminopeptidases cleave amino acids from the terminal ends of peptides. Proteins and peptides are usually vulnerable to more than 1 specific peptidase, resulting in the degradation of nutritional proteins and peptide drugs into small, easily absorbed molecules (Woodley 1994).

*Exocrine pancreatic proteases*

The exocrine pancreatic secretions contain many proteases including trypsin, α-chymotrypsin and elastase, as well as the exopeptidase carboxypeptidases, all of which have optimum activity at about pH 8. α-chymotrypsin hydrolyses peptide bonds close to amino acids that are hydrophobic, which include, Y, M, L, W, and F, whereas trypsin specifically cleaves bonds at the carboxyl sides of K and R residues. Elastase hydrolyses peptide bonds of small, non-polar amino acids such as V, A, L, I and G. Whereas carboxypeptidase A cleaves peptide bonds at the C-terminus; its substrates must have an unblocked C-terminal L isomer amino acid (Lee 1988). Table 3.1 shows some of the different proteases located within the intestinal lumen along with their cleavage specificities.

*Brush-border and cytosolic proteases*

Brush-border and cytosolic proteases of enterocytes are possibly the biggest

Table 3.1 Substrate specificity of luminally secreted enzymes*

| Enzyme | Cleavage sites | Specificity |
|---|---|---|
| Trypsin | ↓<br>$H_2N$-O-O-O-●-O-O-COOH | R, K |
| Chymotrypsin | ↓<br>$H_2N$-O-O-O-●-O-O-COOH | F, Y |
| Elastase | ↓<br>$H_2N$-O-O-O-●-O-O-COOH | A, G, I, L, V, S |
| Carboxypeptidase A | ↓<br>$H_2N$-O-O-O-O-O-●-COOH | Y, F, I, T, E, H, A |
| Caboxypeptidase B | ↓<br>$H_2N$-O-O-O-O-O-●-COOH | R, K |

Table 3.2 Substrate specificity of brush border membrane-bound enzymes*

| Enzyme | Cleavage sites | Specificity |
|---|---|---|
| Endopeptidase 24.11 | ↓<br>$H_2N$-O-O-O-●-O-O-COOH | Hydrophobic amino acids |
| Endopeptidase 24.18 | ↓ ↓<br>$H_2N$-O-O-O-●-O-O-COOH | Aromatic amino acids |
| Aminopeptidase N | ↓<br>$H_2N$-●-O-O-O-O-O-COOH | Many especially A, L |
| Aminopeptidase A | ↓<br>$H_2N$-●-O-O-O-O-O-COOH | D, E |
| Carboxypeptidase P | ↓<br>$H_2N$-O-O-O-O-O-●-COOH | P, G, A |
| Carboxypeptidase M | ↓<br>$H_2N$-O-O-O-O-O-●-COOH | R, K |

* Specificity indicated by filled circle.

obstacles in the absorption of intact small peptide drugs. These include endopeptidase 24.11, which cleaves peptides containing a peptide bond on the N-terminal side of hydrophilic residues and endopeptidase 24.18, which hydrolyses bonds adjacent to aromatic residues. Exopeptidases such as aminopeptidase N hydrolyse peptides with N-terminal L-amino acids. Meanwhile, aminopeptidase A cleaves peptides with an N-terminal L-D or L-E, whilst carboxypeptidase P cleaves peptides with P as the penultimate residue from the free N-terminus.

Table 3.2 shows some of the proteases located on the brush border membrane. These proteases are commonly attached to the cell's apical membrane, with their active sites protruding into the extracellular environment. In addition to these proteases, luminal fluid pancreatic proteases such as trypsin are absorbed onto the enterocytes brush-border, thus aiding the degradation of proteins and oligopeptides. However, brush-border peptidases are capable of the degradation of peptides of between 3 to 10 amino acids in length, whereas intracellular peptidases such as dipeptidase hydrolyses neutral dipeptides (Lee 1988, Pauletti, *et al* 1997, Woodley 1994).

*Prediction of PIK stability within the intestine*

As PIK functions at an intracellular site of epithelial cells and is envisaged to be taken orally, its amino acid sequence of RKKYKYRRK is likely to be cleaved by a number of different proteases within the intestinal lumen. Some potential cleavage sites of PIK by the different proteases located within the intestinal environment are shown in figure 3.1.

Therefore, it is likely that unmodified PIK peptide taken orally will be degraded within minutes of reaching the gut due to enzymatic degradation, resulting in a loss of activity. Hence, it may be necessary to perform chemical modifications that increase enzymatic stability whilst simultaneously maintaining the selectivity and effectiveness of the bioactive peptide in order to bioactive peptide in order to be able to perform *in vivo* studies to determine PIK's efficiency at treating animal models of CD.

*Methods to increase peptide stability*

Enhancement of peptide drug candidate *in vivo* stability can be achieved by

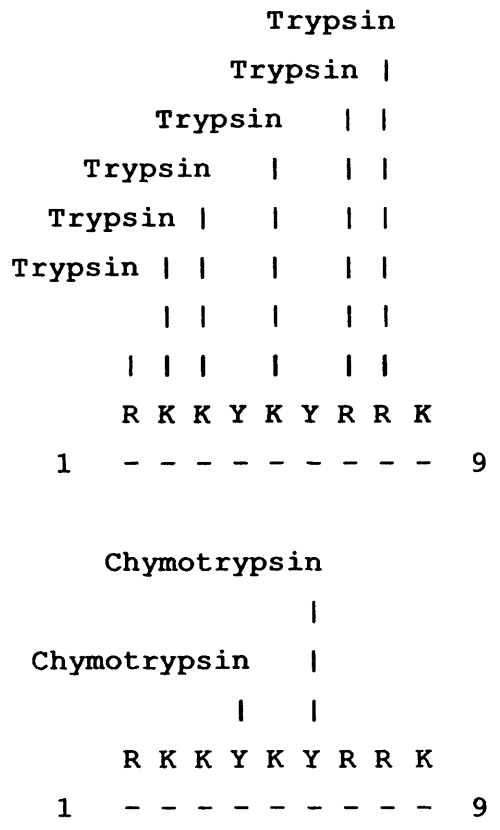


**Figure 3.1 Calculated cleavage sites of PIK with the proteases trypsin and chymotrypsin. Line 1 represents the prominent cleavage sites, line 2 amino acid composition of peptide and line 3 the peptide sequence number.**

chemical modifications of peptide bonds at possible enzymatic cleavage sites. It is possible to identify potential cleavage sites by observation of the peptide sequence. However, confirmation of these cleavages experimentally is necessary. Incubation of peptides in a mixture of purified peptidases generally does not imitate the metabolic behaviour of these peptidases *in vivo*. Therefore, peptides can be incubated *in vitro* with various membrane preparations and tissue homogenates as well as serum and plasma as these reflect the physiological environment more closely (Fauchere and Thurieau 1992). Peptide degradation kinetics and the emergence of metabolites at different time points may be monitored by liquid chromatography separation-mass spectrometry analysis (LC/MS). This technique separates biological materials via HPLC followed by identification of different components by MS (Aebersold and Mann 2003). The information generated can then be used to identify the peptide vulnerable peptide bonds and determine which peptide bonds to protect (Adessi and Soto 2002).

*Protection of the peptides end termini*

L-amino acid peptides containing unprotected N- and C-termini are typically degraded rapidly by exopeptidases. Acetylation and amidation of neuropeptides has previously been shown to improve their biological stability and activity. Hence, end-protection of peptides has been extensively used in the development of peptide drugs to increase their enzyme stability. Although this strategy has been widely used, it seldom prevents degradation of peptides. Rather, it increases the peptide half-life: degradation typically arises through cleavage of peptide bonds within the sequence by specific endopeptidases (Adessi and Soto 2002).

*Alteration of peptide chirality*

If end-protection of PIK is not sufficient to increase its stability, another potential method commonly used to improve peptide drug stability is to alter its chirality. Replacing all or even certain L-amino acids with their equivalent D-amino acids within a peptide sequence may provide resistance from proteolytic degradation. However, loss of activity is a common disadvantage of using D-analogues as a consequence of conformational changes. Improvement of D-amino acid peptide biological activity can be overcome by synthesising a retro-inverso-isomer peptide, where the original sequence is reversed and the chiralility of each amino acid is

changed. These peptides correspond to the original peptide structure better than the D-analogue and hence maintain biological activity (Chorev and Goodman 1995).

*Aims of the study*

Therefore, this chapter will firstly develop the Fmoc solid-phase peptide synthesis and purification methods also the ability of the LC-MS protocols to detect peptide fragments will be determined. Once this is achieved then the stability and location of any labile peptide bonds within the PIK peptide sequence will be assessed. This will be achieved using methods such as incubation of the peptide within biological fluids and cell homogenates (such as rat intestinal fluid protein and human intestinal epithelial cell line homogenates), followed by LC-MS to determine the degradation pattern and the half-life of PIK.

Following detection of the labile peptide bonds cleaved by incubation with biological fluid and cell homogenates, chemical modifications such as end terminal protection and alteration of amino acid chirality will be used to attempt to increase PIK peptide stability. These peptide analogues will then be tested for increases in stability by determination of peptide degradation patterns and half lives. Any potential candidates will then be tested further to determine if they specifically inhibit MLCK this will be achieved by ELISA based assays. PIK analogues with increased stability and specifically inhibit MLCK will be tested for their abilities to inhibit MLCK as effectively and specifically as the parent PIK and their ability to increase TER in a cell model of CD will then be tested by our collaborator J. Turner.

## 3.2 Methods

Peptides were synthesised by Fmoc solid-phase peptide techniques and purified by the procedures outlined in sections 2.3.1 and 2.3.2.

Validation of the LC-MS method was performed by incubation of Ac-PIK with the pancreatic protease trypsin. One mg/ml Ac-PIK was incubated with 1.25 µg, 2.5 µg, 5 µg, 10 µg, 15 µg, 20 µg and 25 µg/ml trypsin solutions. Following this, 100 µl aliquots were withdrawn at time 0 and 15 min, and the enzymatic reactions were then terminated by dilution with the same volume of 0.5 % TFA (ACN/water). The samples were then centrifuged at 1200 rpm for 10 min at 4 °C

and the supernatants analysed by LC-MS as outlined in section 2.3.7.

The conditions for determination of PIK and PIK analogues degradation patterns within rat intestinal fluid and homogenised Caco-2 cell extracts are outlined as described in table 3.3. Aliquots were treated as described in section 2.3.8.

As PIK is susceptible to cleavage in rat intestinal fluid protein, the half-lives of PIK and PIK analogues were determined by incubation of 0.1 mg/ml of peptide with 0.2 mg/ml of rat intestinal fluid protein. One hundred µl aliquots were taken at various time points and then treated and analysed as described in section 2.3.7. Peptide decay was monitored by LC-MS, with the percentage of peptide remaining at each time point being used to calculate half-life values as described in section 2.3.9.

Protein kinase A activity was determined by using the non-radioactive protein kinase assay kit, as described in section 2.3.10, by adding 20 units of PKA to 0, 0.5, 1, 2.5 and 5 mM of D-amino acid PIK analogues. The experiment was conducted as per the manufacturer's guidelines. The protein kinase A inhibitor 6-22 amide at a concentration of 4 nM was used as a positive control.

Calcium/calmodulin dependent protein kinase II activity was determined as depicted in section 2.3.10. Calcium/calmodulin dependent protein kinase II (20 U) was mixed with 0, 0.5, 1, 2.5 and 5 mM of the PIK analogues in 108 µl of the CaMKII reaction buffer (50mM Tris-HCl, 10mM $MgCl_2$, 2 mM dithiothreitol, 0.1 mM $Na_2$ EDTA, 100 µM ATP, 1.2 µM CaM and 2 mM $CaCl_2$). After 5 min pre-incubation at 30 °C, 12 µl of the kinase-PIK peptide sample was added to pseudo-substrate-coated wells. The inhibitor $Ca^{2+}$/calmodulin kinase II inhibitor 281-309 was used as a control at a concentration of 4 µM.

## 3.3 Results

### *3.3.1 Validation of $N^{\alpha}$-9-fluorenylmethoxycarbonyl peptide synthesis and high pressure liquid chromatography analysis methods*

The methods by which the peptides were synthesised, purified and detected were initially assessed before commencement of PIK stability studies. The semi-preparative HPLC chromatogram of Ac-PIK can be seen in figure 3.3. To validate

Table 3.3 Determination of PIK and PIK analogues half-lives, conditions of incubations.

| **Peptide** | **Biological Fluid** | **Time Points (min)** | **Temp (°C)** |
|---|---|---|---|
| PIK | Intestinal fluid protein | 0, 1, 2, 4, 8, 10, 20 & 30 | 4 |
| PIK | Caco-2 cell extracts | 0, 15, 30, 60 & 120 | 37 |
| Ac-PIK | Intestinal fluid protein | 0, 5, 8, 10, 15, 20 & 30 | 4 |
| Ac-PIK | Caco-2 cell extracts | 0, 15, 30, 60 & 120 | 37 |
| Dpalindrome PIK | Intestinal fluid protein | 0, 1, 2, 4, 8, 10, 20 & 30 | 4 |
| Dpalindrome PIK | Caco-2 cell extracts | 0, 15, 30, 60, 120 & 240 | 37 |
| D PIK | Intestinal fluid protein | 0, 30, 60, 120, 240 & 360 | 37 |
| D PIK | Caco-2 cell extracts | 0, 60, 120, 240 & 360 | 37 |
| Dreverse PIK | Intestinal fluid protein | 0, 30, 60, 120, 240 &360 | 37 |
| Dreverse PIK | Caco-2 cell extracts | 0, 60, 120, 240 & 360 | 37 |

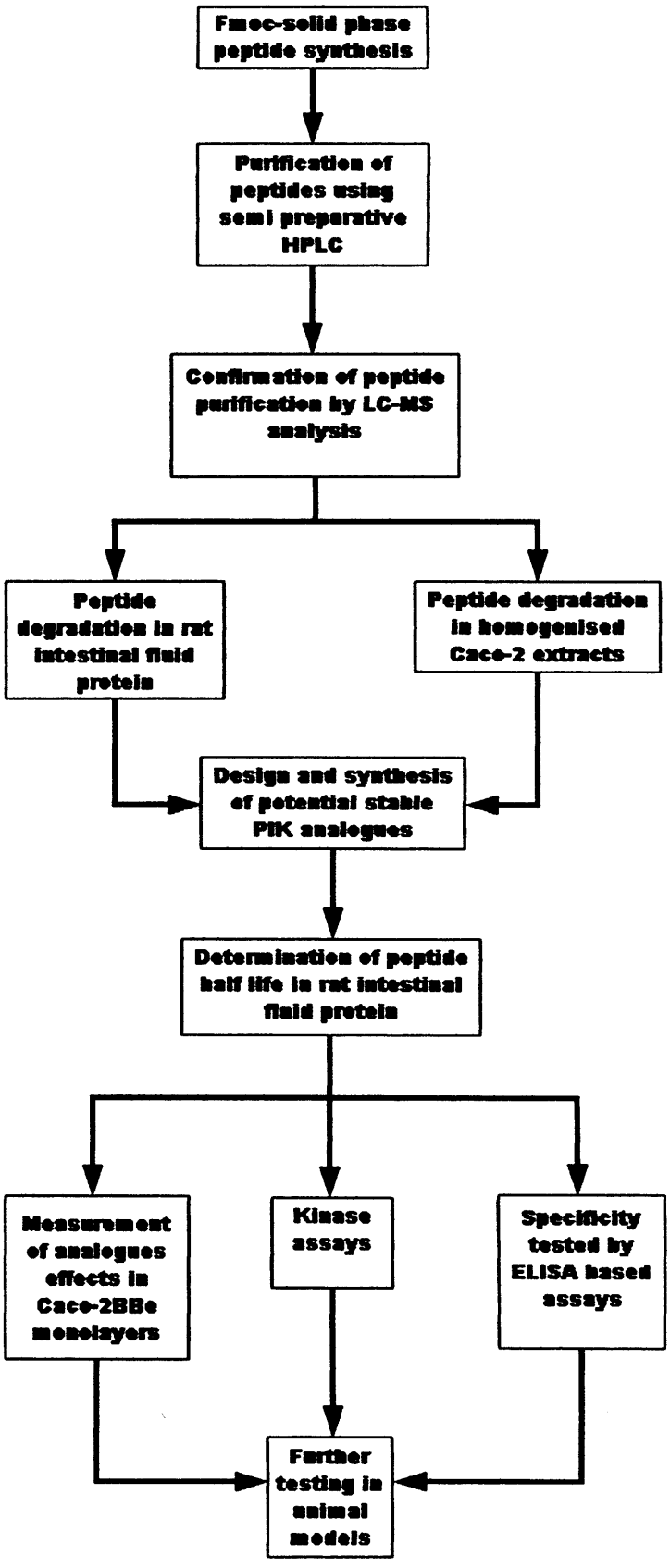


Figure 3.2 Summary of the methods used to synthesise stable PIK analogues for testing in animal models of intestinal epithelial inflammation.

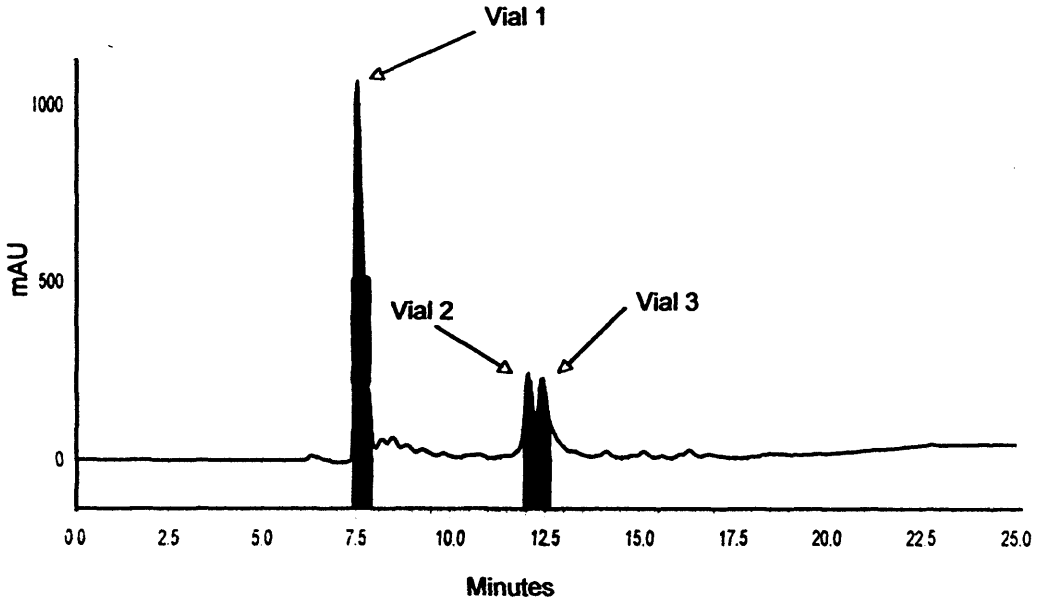


Figure 3.3 Semi-preparative HPLC chromatogram of Ac-PIK. Pepide was separated on a semi-preparative HPLC Vydac 218TP $C_{18}$ reversed-phase silica gel column, absorbance was measured at a wavelength of 280 nm. Vials 1 to 3 were analysed by MS analysis, vial 1 was shown to contain Ac-PIK, these vials were collected and pooled, concentrated, and verified.

the Fmoc solid-phase peptide synthesis and purification methods, utilised acetylated PIK (Ac-PIK; Ac-RKKYKYRRK-$NH_2$), was analysed by LC-MS. The HPLC chromatogram measured at 280 nm demonstrated 1 prominent component with the predicted molecular mass of 1366 Da as analysed by MS analysis (figure 3.4.). The mass spectrometry chromatogram also detected peaks at molecular weights 684 and 456 Da. These peaks are due to the fact that MS do not measure mass but the mass to charge ratio (m/z). Each peak represents Ac-PIK carrying a different number of charges. This indicated that the Fmoc-solid phase peptide synthesis method was successful and that the LC-MS analysis method used detects peptides synthesised successfully.

To determine if the LC-MS method used for the detection of purified peptides was also able to detect degradation products, Ac-PK, which has end-terminal protection (acetylation at its N-terminus and amidation at its C-terminus) was incubated with the pancreatic protease trypsin. Incubation of 1 mg/ml Ac-PIK with 2.5 μg/ml trypsin for 15 min at 37 °C resulted in the formation of several new peaks that could be identified as Ac-RKKYK (763 Da), Ac-RKKYKYR (1083 Da), and Ac-RKKYKYRR (1239 Da) (figure 3.5.a). The chromatograms are measured using the base peak function; the peaks measured are the mass spectrum corresponding to the mass–to-charge value that has the greatest intensity. The peptide cleavage map of Ac-PIK demonstrated that 4 peptide bonds were initially cleaved when Ac-PIK was incubated with trypsin (figure 3.5.b).

### *3.3.2 Stability of unmodified PIK*

Firstly, the stability of PIK needed to be assessed to determine how stable/unstable the peptide was within the intestinal environment. This could then be used as a reference point when studying the degradation patterns of different PIK analogues. Liquid chromatography-mass spectrometry analysis of the purified peptide confirmed PIK to have the expected mass of 1324 Da, and a positive ion breakdown map that was consistent with its composition (figure 3.6.).

Following verification of PIK's molecular mass, the peptide was incubated with rat intestinal fluid, which contains a mixture of pancreatic and brush border proteases and peptidases. Incubation of 1 mg/ml PIK with 0.1 mg/ml rat intestinal fluid protein at 4 °C for 4 min resulted in several cleavage products. The cleavage map showed that 4 peptide bonds were cleaved to achieve these degradation products

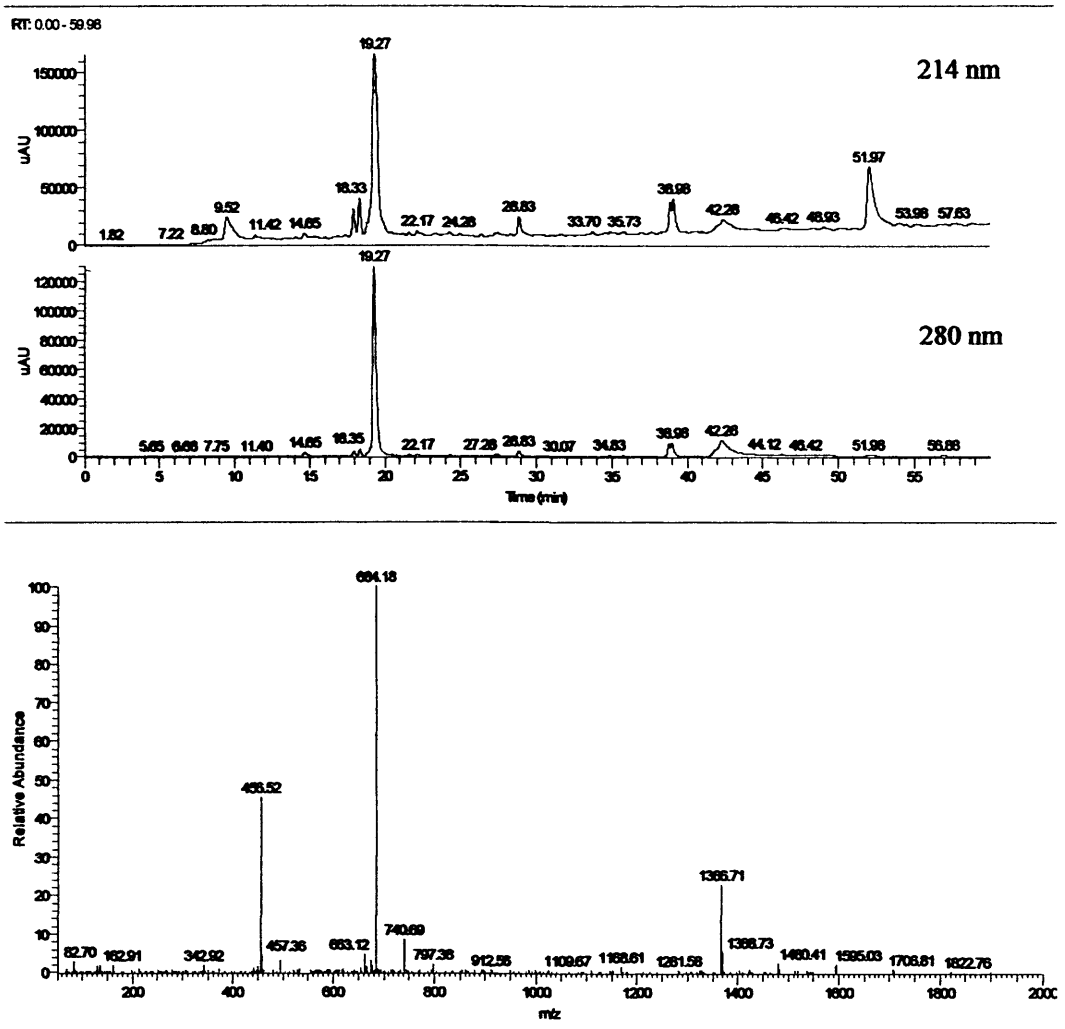


Figure 3.4 LC-MS analysis of Ac-PIK. HPLC analysis of Ac-PIK detected at 214 and 280 nm along with LC-MS analysis of Ac-PIK showing breakdown pattern in positive ion mode.

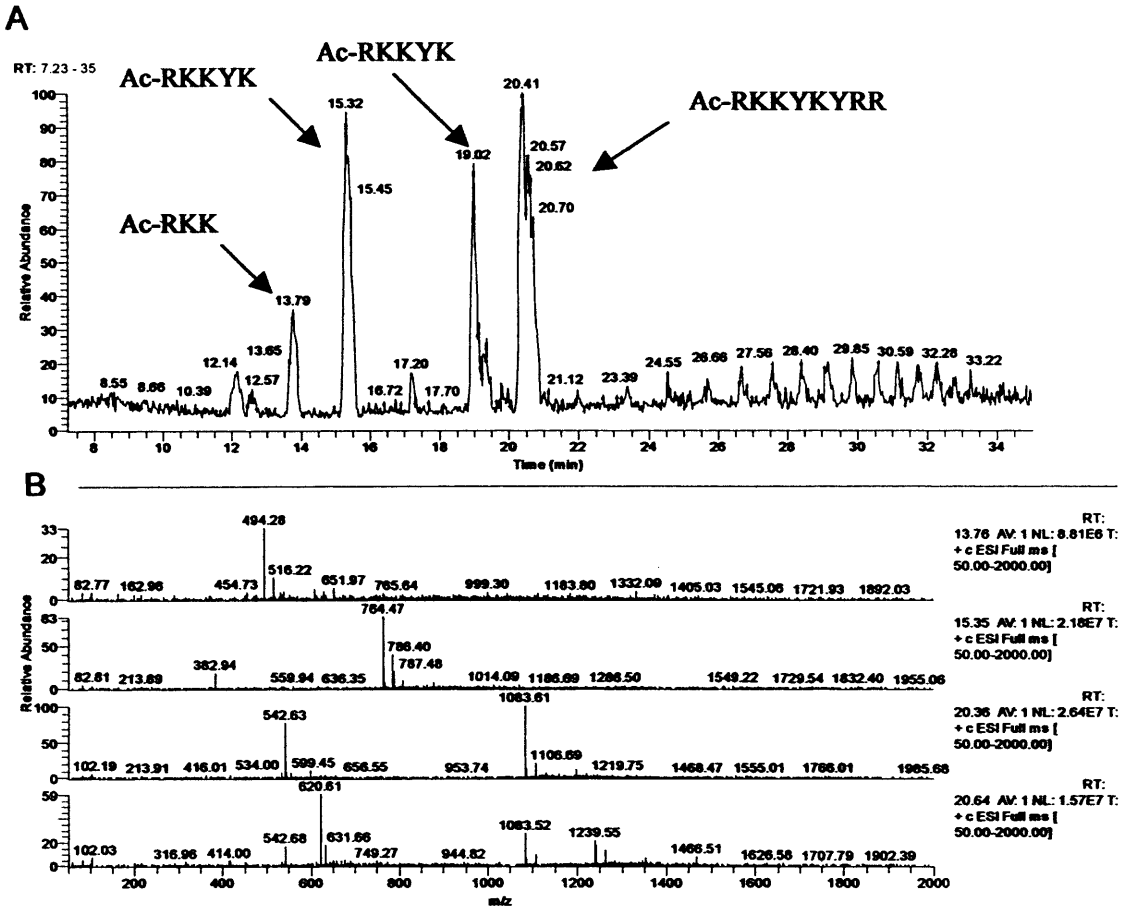


C

Line 1 ↓ ↓ ↓ ↓

Line 2 AC -R K K Y K Y R R K- $NH_2$

Line 3 1 2 3 4 5 6 7 8 9

Figure 3.5 Ac-PIK cleavage pattern when incubated with trypsin.

A) Hydrolysis pattern determined by HPLC analysis of 1 mg/ml Ac-PIK following a 15 min incubation at 37 °C with 2.5 µg/ml trypsin.

B) Mass spectrometry analysis of HPLC peaks.

C) Peptide site map of Ac-PIK showing initial sites of cleavage identified by LC-MS. Line 1 represents the prominent cleavage sites, line 2 amino acid composition of the peptide and line 3 the peptide sequence number.

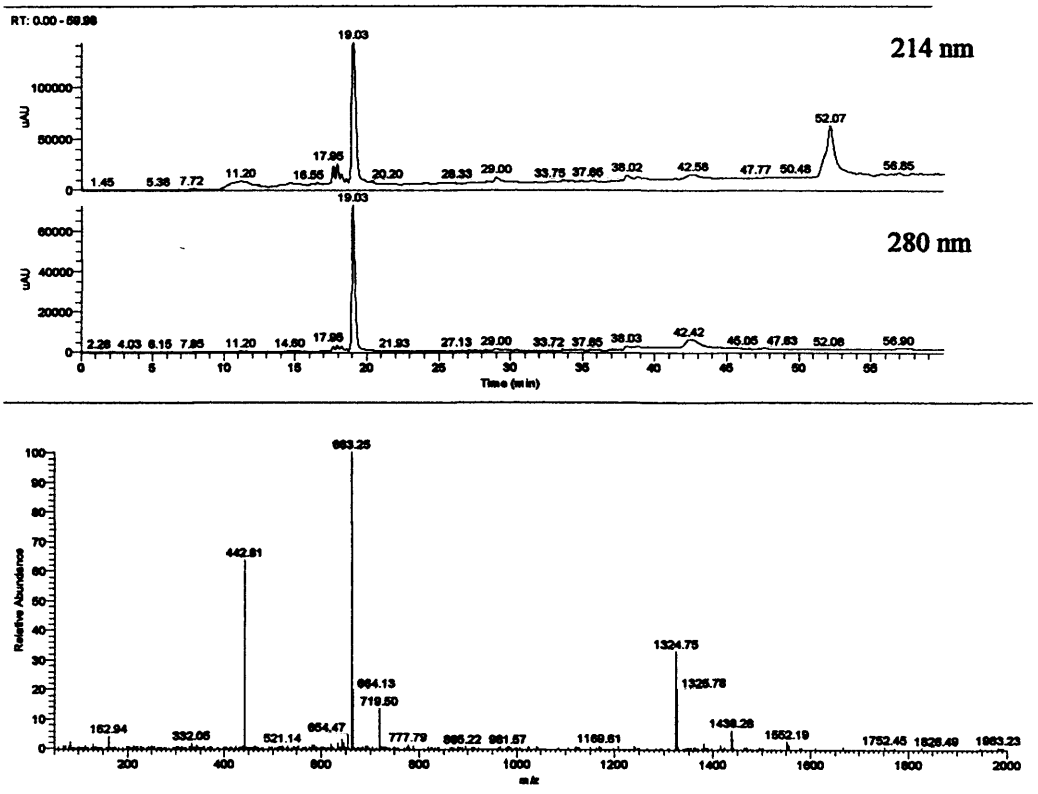


Figure 3.6 LC-MS analysis of PIK. HPLC analysis of PIK detected at 214 and 280 nm along with MS analysis of PIK showing breakdown pattern in positive ion mode.

A

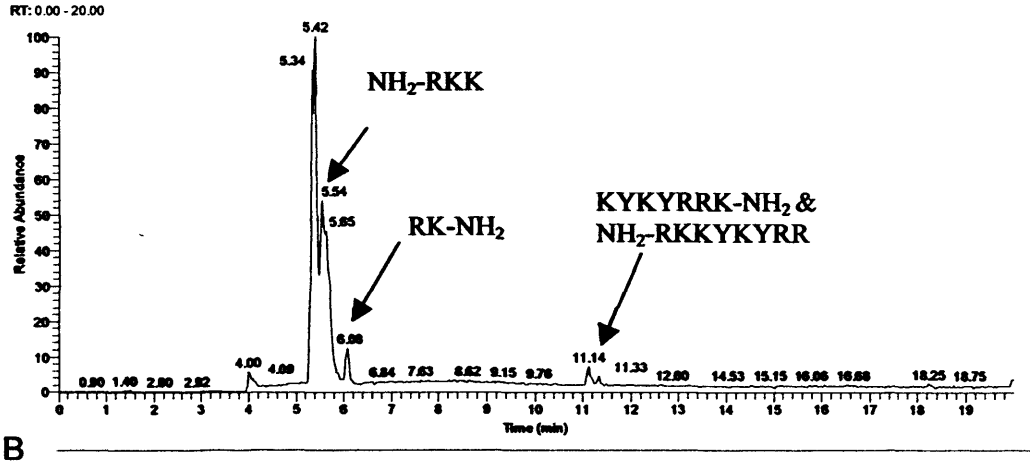


B

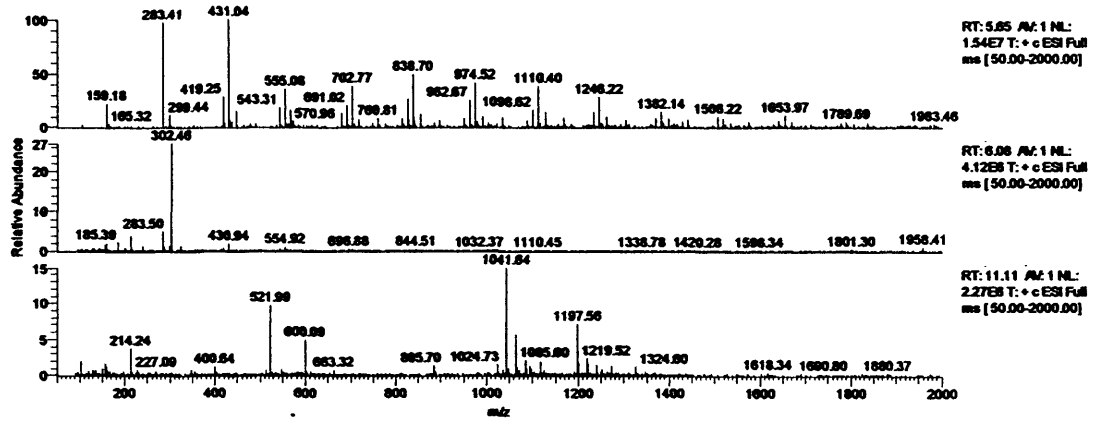


C

Line 1 ↓ ↓ ↓

Line 2 $NH_2$ -R K K Y K Y R R K- $NH_2$

Line 3 1 2 3 4 5 6 7 8 9

Figure 3.7 LC-MS analysis of PIK incubated with rat intestinal fluid. Reaction mixture incubated for 8 min at 4 °C.

A) HPLC analysis of 1mg/ml PIK cleavage pattern in rat intestinal fluid protein. Reaction mixtures initially contained 1 mg/ml PIK and 0.1 mg/ml rat intestinal fluid and incubated at 4 °C for 8 min.

B) Mass spectrometry analysis of HPLC peaks.

C) Peptide site map of PIK showing initial sites of cleavage identified by LC-MS. Line 1 represents the prominent cleavage sites, line 2 amino acid composition of the peptide and line 3 the peptide sequence number.

(figure 3.7.b). Extended incubations at 4 °C (figure 3.8) and incubation at 37 °C (figure 3.9) resulted in near total hydrolysis of the peptide with only 1 peptide fragment being detected $NH_2$-RKK (431 Da). Next, the stability of PIK in Caco-2 intestinal epithelial cell extracts, which contain a mixture of brush border and cytosolic proteases, was characterised. Incubation of 1 mg/ml PIK with 0.2 mg/ml homogenised Caco-2 cell extracts at 37 °C for 2 h followed by LC-MS analysis identified the cleavage products $NH_2$-RKKYK (722 Da) and YRRK-$NH_2$ (621 Da) (figure 3.10.a). The peptide site map of PIK showed that only 2 peptide bonds were initially cleaved (figure 3.10.b).

### *3.3.3 Stability of end-terminal protected PIK*

Incubation of 1 mg/ml of end terminal protected PIK (Ac-PIK) with 0.1 mg/ml rat intestinal fluid protein at 4 °C for 5 min resulted in numerous cleavage products comprising of Ac-RKKYKYRR (599 Da), RKKY (297 Da), KRR-$NH_2$ (430 Da) and Ac-RKKYKYRRK-$NH_2$ (445 Da) as detected by LC-MS analysis (figure 3.11.a). The cleavage map showed that 4 peptide bonds were initially cleaved when Ac-PIK was incubated with rat intestinal fluid (figure 3.11.b). Incubation of 1 mg/ml Ac-PIK with 0.2 mg/ml homogenised Caco-2 cell extracts at 37 °C for 1 h resulted in several cleavage products identified as Ac-RKKYKYRR (1240 Da), Ac-RK (345 Da), RK-$NH_2$ (302 Da), KYKYRRK-$NH_2$ (1040 Da), and KKYKYRRK-$NH_2$ (1139 Da) (figure 3.12.a). The degradation map again showed that 4 peptide bonds were initially cleaved when Ac-PIK was incubated with homogenised Caco-2 cell extracts (figure 3.12.b).

### *3.3.4 Determination of PIK and PIK analogues half-lives*

PIK appears to be more vulnerable to degradation in rat intestinal fluid protein than in homogenised Caco-2 extracts, indicating that the gut lumen would be the main site of PIK degradation *in vivo*. Therefore, the half-life of PIK was determined in rat luminal secretions; this could then be used a reference point to determine if any chemical modifications were successful in increasing PIK stability.

A representative liner plot of the log concentration versus time (figure 3.13) indicates that peptide degradation is a pseudo-first order reaction. The slope of the plot was then used to calculate the peptide half-life.

A

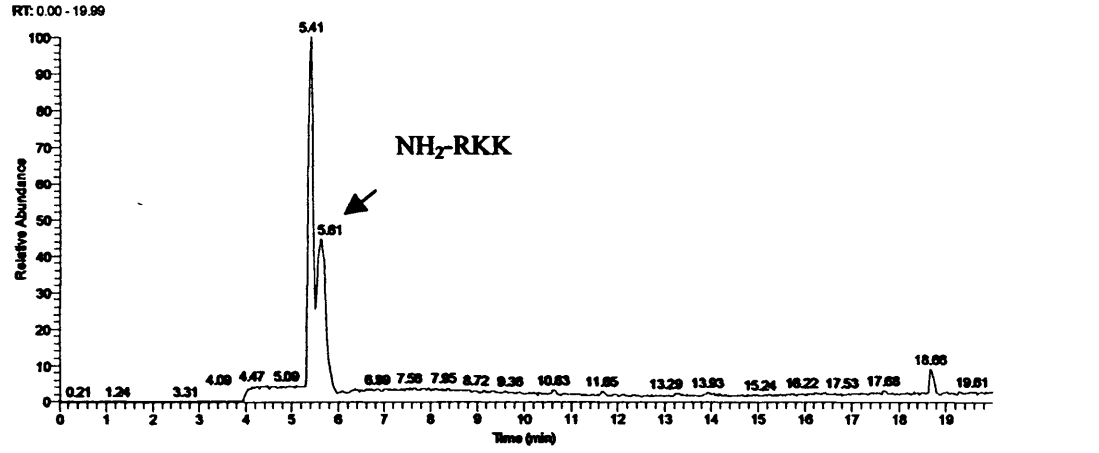


B

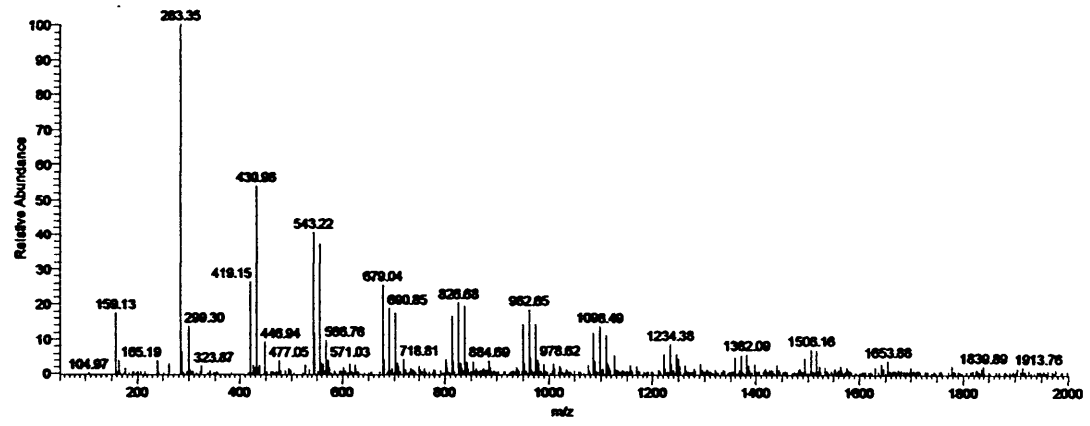


C

Line 1 ↓
Line 2 $NH_2$ -R K K Y K Y R R K- $NH_2$
Line 3 1 2 3 4 5 6 7 8 9

Figure 3.8 LC-MS analysis of PIK incubated with rat intestinal fluid at 4 °C for 15 min.

A) HPLC analysis of 1mg/ml PIK cleavage pattern in rat intestinal fluid protein. Reaction mixtures initially contained 1 mg/ml PIK and 0.1 mg/ml rat intestinal fluid and incubated at 4 °C for 15 min.

B) Mass spectrometry analysis of HPLC peaks.

C) Peptide site map of PIK showing initial sites of cleavage identified by LC-MS. Line 1 represents the prominent cleavage sites, line 2 amino acid composition of the peptide and line 3 the peptide sequence number.

A

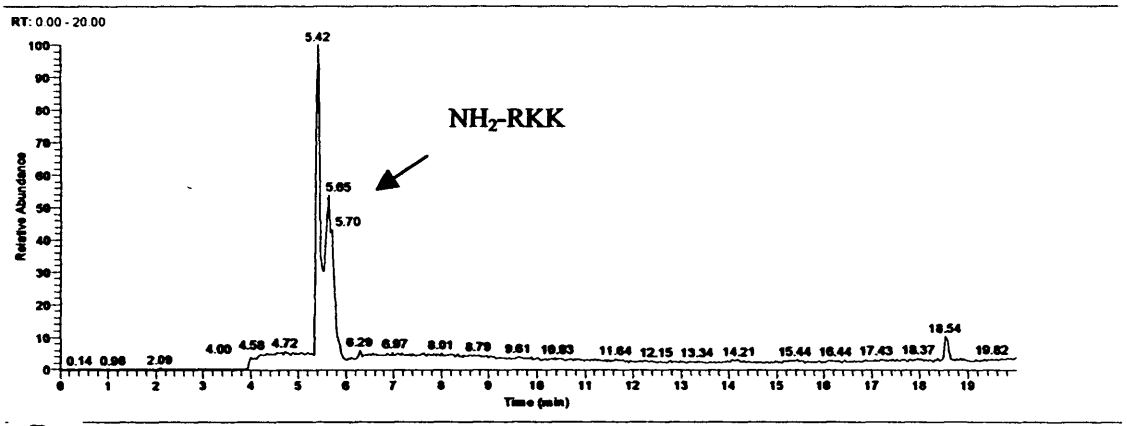


B

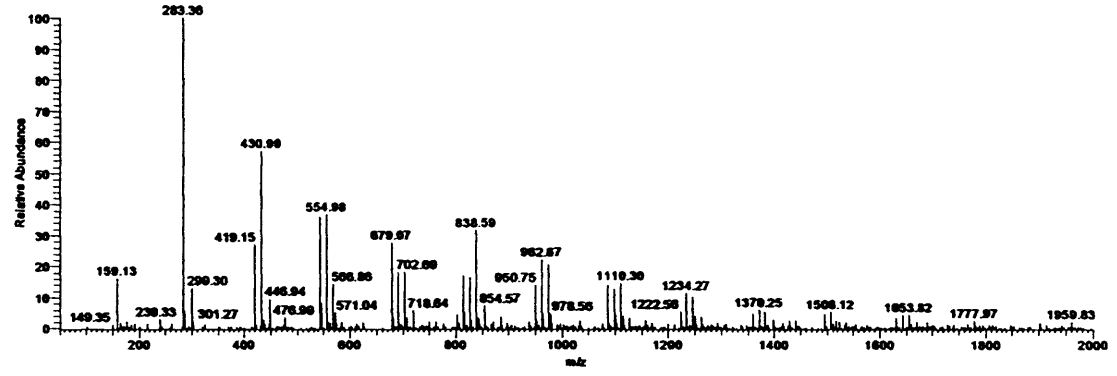


C

Line 1 ↓
Line 2 $NH_2$ -R K K Y K Y R R K- $NH_2$
Line 3 1 2 3 4 5 6 7 8 9

Figure 3.9 LC-MS analysis of PIK incubated with rat intestinal fluid. Peptide incubated at 37 °C for 1 min.

A) HPLC analysis of 1mg/ml PIK cleavage pattern in rat intestinal fluid protein. Reaction mixtures initially contained 1 mg/ml PIK and 0.1 mg/ml rat intestinal fluid and incubated at 37 °C for 1 min.

B) Mass spectrometry analysis of HPLC peaks.

C) Peptide site map of PIK showing initial sites of cleavage identified by LC-MS. Line 1 represents the prominent cleavage sites, line 2 amino acid composition of the peptide and line 3 the peptide sequence number.

A

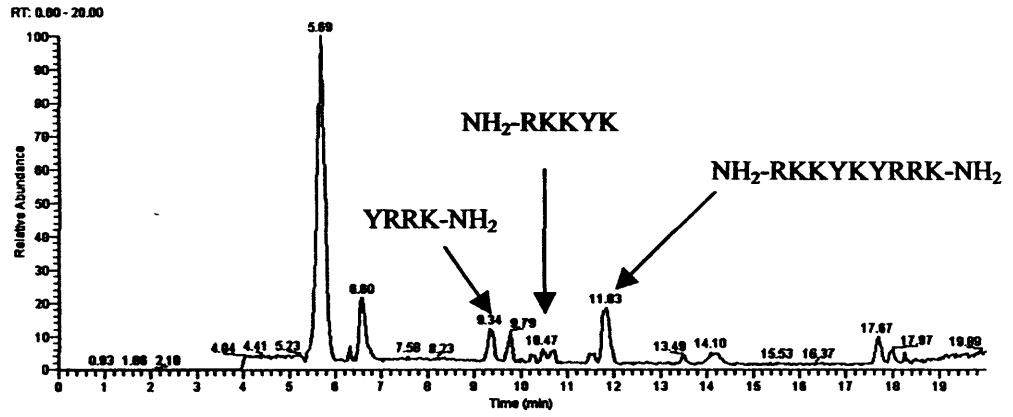


B

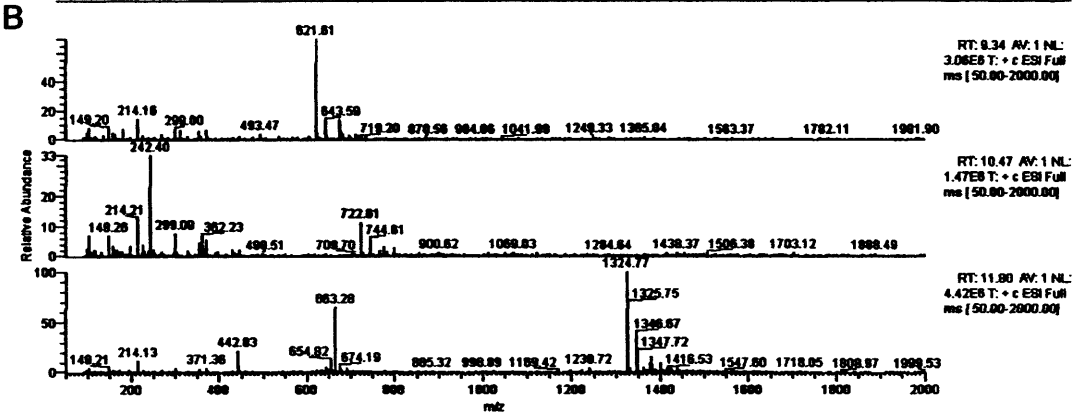


C

Line 1 ↓ ↓
Line 2 $NH_2$ -R K K Y K Y R R K- $NH_2$
Line 3 1 2 3 4 5 6 7 8 9

Figure 3.10 LC-MS analysis of PIK incubated with homogenised Caco-2 cell extracts.

A) HPLC analysis of 1 mg/ml PIK hydrolysis pattern in Caco-2 lysate monitored at 214 nm. Reaction mixtures initially contained 1 mg/ml PIK and 0.1 mg/ml Caco-2 cell lysate protein and were incubated at 37 °C for 15 min.

B) Mass spectrometry analysis of HPLC peaks.

C) Peptide site map of PIK showing initial sites of cleavage identified by LC-MS. Line 1 represents the prominent cleavage sites, line 2 the amino acid composition of the peptide and line 3 the peptide sequence number.

A

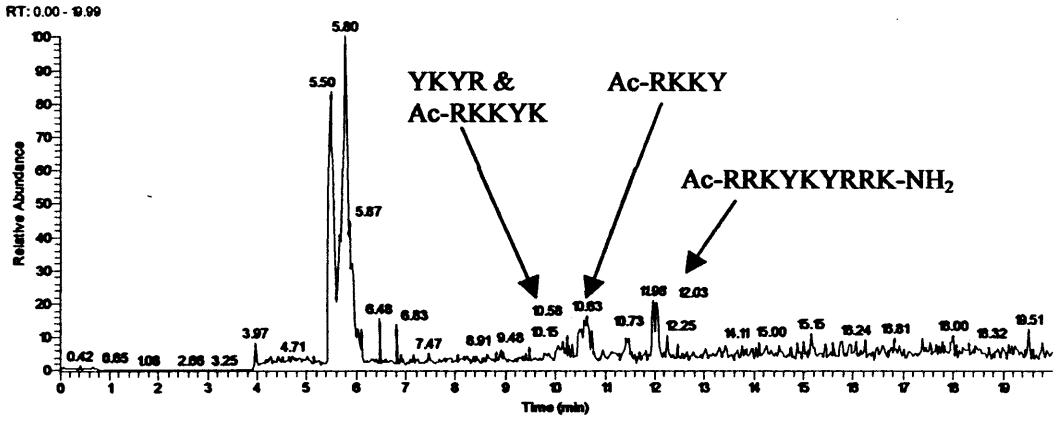


B

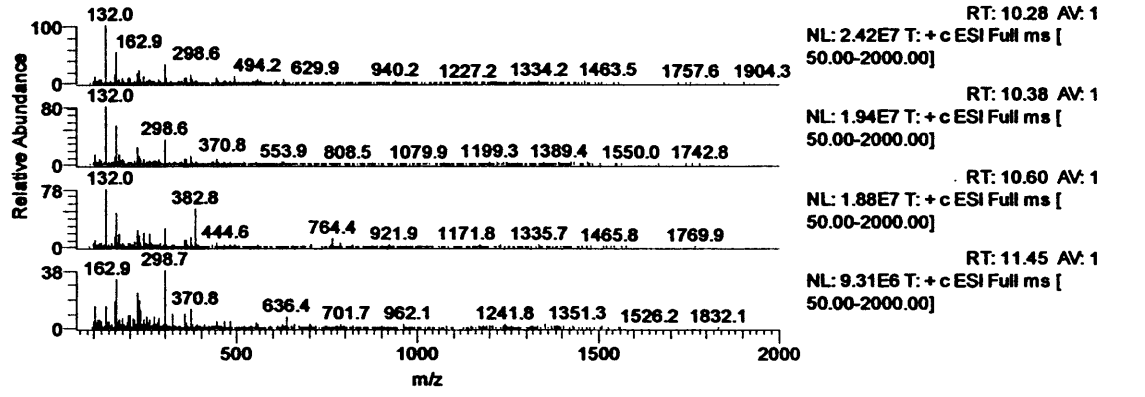


C

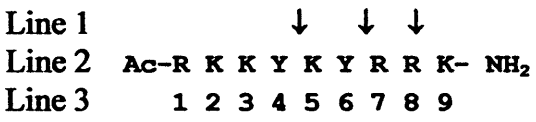


Figure 3.11 LC-MS analysis of Ac-PIK incubated with rat intestinal fluid protein.

A) HPLC analysis of Ac-PIK hydrolysis pattern in rat intestinal fluid at 214 nm. Initial reaction mixtures contained 1 mg/ml PIK and 0.1 mg/ml intestinal fluid protein and were incubated at 4 °C for 1 h.

B) Mass spectrometry analysis of HPLC peaks.

C) Peptide site map of Ac-PIK showing initial sites of cleavage identified by LC-MS. Line 1 represents the prominent cleavage sites, line 2 the amino acid composition of the peptide and line 3 the peptide sequence number.

A

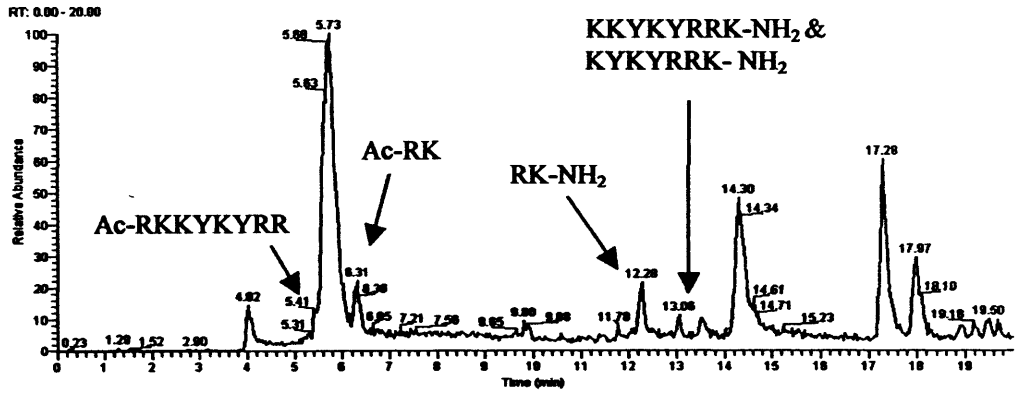


B

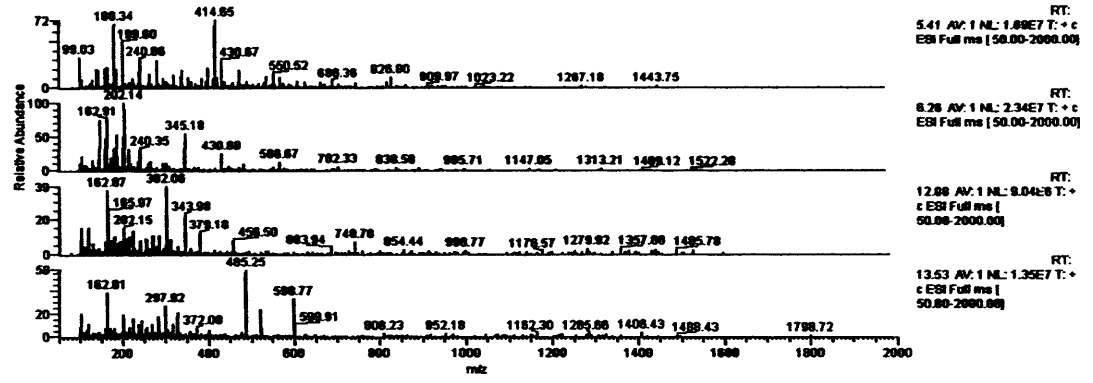


C

| | | | | | | | | | | |
|---|---|---|---|---|---|---|---|---|---|---|
| Line 1 | | ↓ | ↓ | | | | ↓ | ↓ | | |
| Line 2 | Ac-R | K | K | Y | K | Y | R | R | K- | $NH_2$ |
| Line 3 | | 1 | 2 | 3 | 4 | 5 | 6 | 7 | 8 | 9 |

Figure 3.12 LC-MS analysis of Ac-PIK incubated with Caco-2 cell lysate.

A) HPLC analysis of 1 mg/ml Ac-PIK hydrolysis pattern in homogenised Caco-2 lysate monitored at 214 nm. Reaction mixtures initially contained 1 mg/ml Ac-PIK and 0.2 mg/ml Caco-2 cell lysate protein and were incubated at 37 °C for 1 h.

B) Mass spectrometry analysis of HPLC peaks.

C) Peptide site map of Ac-PIK showing initial sites of cleavage identified by LC-MS. Line 1 represents the prominent cleavage sites, line 2 the amino acid composition of the peptide and line 3 the peptide sequence number.

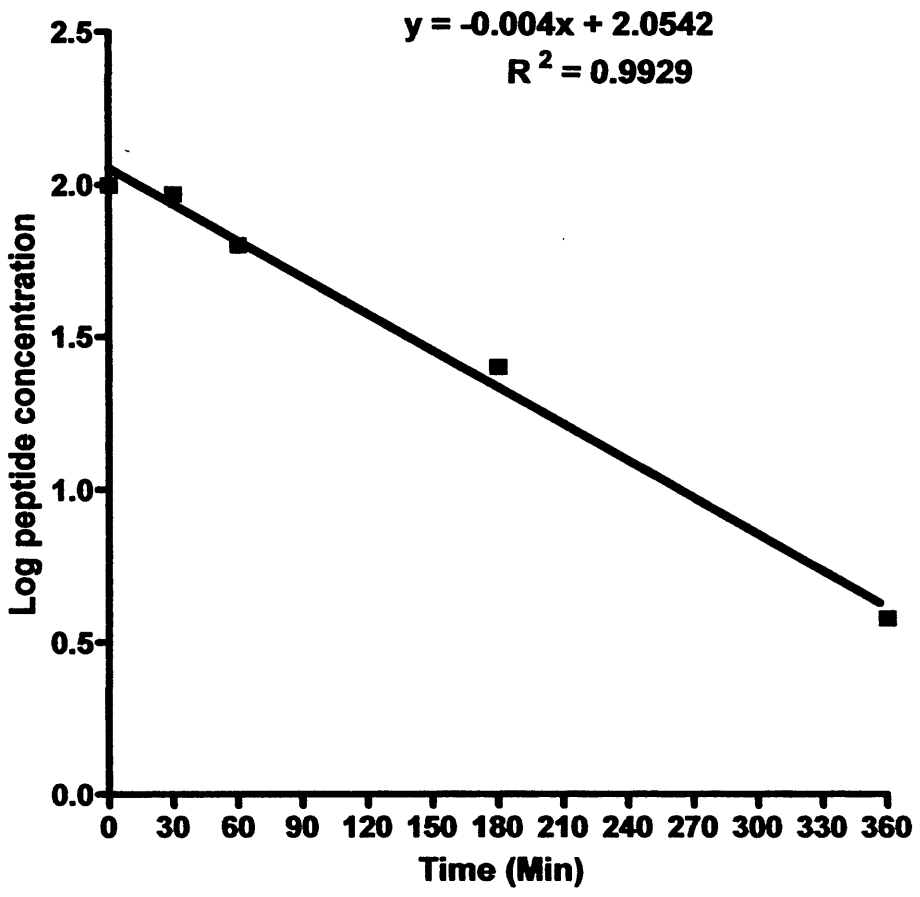


Figure 3.13 Representative linear plot of the log concentration verses time indicating a pseudo-first order hydrolysis of the peptide. The slope was used to calculate the peptide half-life.

The half-lives of PIK and Ac-PIK (0.2 min) in rat intestinal fluid protein were very short (table 3.4). Based on their pattern of protease/peptidase susceptibility, a series of PIK analogues were required in an effort to obtain molecules with improved stability to protease and peptidase activities found in the intestinal luminal secretions and associated intestinal epithelial cells.

Therefore, PIK analogues were synthesised using D-amino acids. Dpalindrome PIK (RKKykyRRK-$NH_2$) was synthesised first. However, protection of the central inhibitory domain did not increase its half-life (0.2 min ± 0.21 min). PIK analogues synthesised entirely from D-amino acids were then prepared; these included D PIK (rkkykyrrk-$NH_2$) and Dreverse PIK (krrykyrrk-$NH_2$), which had much longer half-lives of 3.6 h ± 2.6 h and 13.4 h ± 8.4 h respectively.

### *3.3.5 Identification of the D-Amino acid containing PIK peptides cleavage patterns*

Liquid chromatography-mass spectrometry analysis of 1 mg/ml Dpalindrome PIK incubated with 0.1 mg/ml rat intestinal fluid at 4 °C for 20 min resulted in only 3 cleavage products including RKKykyRR (599 Da), KykyRRK-$NH_2$ (521 Da) and RKK (430 Da) (figure 3.14.a). Incubation of 1 mg/ml Dpalindrome PIK with 0.2 mg/ml homogenised Caco-2 cell extracts identified the cleavage products KKykyRRK-$NH_2$ (585 Da), KykyRRK-$NH_2$ (521 Da), RKK-$NH_2$ (430 Da) and RK (303 Da) (figure 3.15.a).

One mg/ml of D PIK incubated with 0.1 mg/ml rat intestinal fluid at 37 °C for 30 min produced four cleavage products, including $NH_2$-rkk (430 Da), $NH_2$-rkkykyr (521 Da), kykyrrk-$NH_2$ (521 Da) and $NH_2$-rkkykyrrk-$NH_2$ (figure 3.16.a). Incubation of 0.2 mg/ml of homogenised Caco-2 cell extracts with 1 mg/ml D PIK at 37 °C for 6 h resulted in 4 degradation products: $NH_2$-rkk (430 Da), kkykyrrk-$NH_2$ (585 Da), kkykyr (884 Da), kkykyrrk-$NH_2$ (1168) (figure 3.17.a). In addition, there was a relative high abundance of un-cleaved PIK peptide rkkykyrrk (442, 663 and 1324).

Incubation of 1 mg/ml Dreverse PIK with 0.1 mg/ml rat intestinal fluid protein at 37°C for 3 h resulted in the formation of only 1 detectable cleavage product by LC-MS analysis. The cleavage product was the 430 Da KKR-$NH_2$, additionally there was also a relatively high abundance of $NH_2$-RKKYKYYRRK-

Table 3.4 Half-lives of PIK and PIK analogues incubated in rat intestinal luminal secretions*.

| Peptide | Half-Life |
|---|---|
| PIK | 0.2 min ± 0.01 min |
| Acetylated (Ac) PIK | 0.2 min ± 0.01 min |
| Dpalindrome PIK | 0.2 min ± 0.21 min |
| D PIK | 3.6 h ± 2.6 h |
| Dreverse PIK | 13.4 h ± 8.4 h |

* Data represents the mean half-lives ± SD n=3.

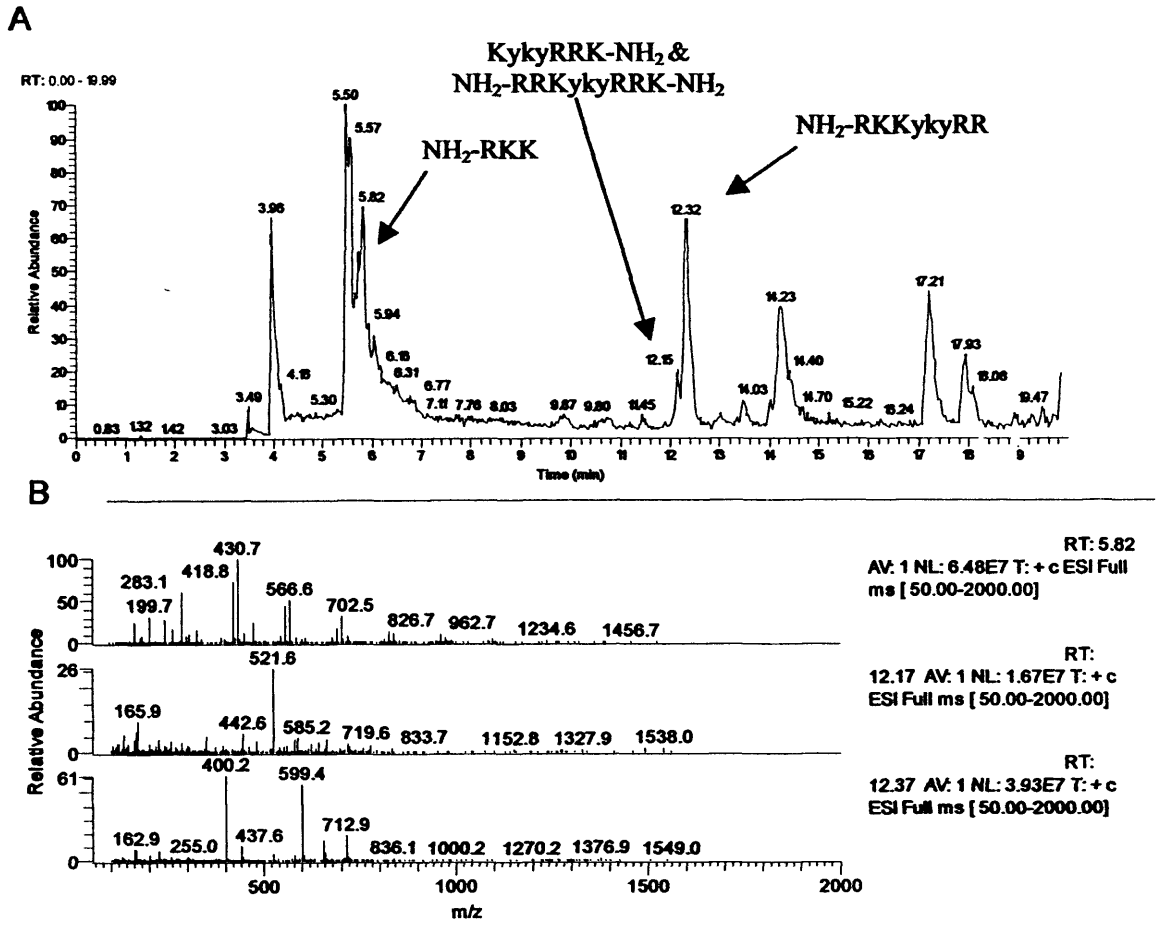


C

Line 1 ↓ ↓ ↓

Line 2 $NH_2$-R K K y k y R R K- $NH_2$

Line 3 1 2 3 4 5 6 7 8 9

Figure 3.14 LC-MS analysis of Dpalindrome PIK incubated with rat intestinal fluid.

A) HPLC analysis of 1 mg/ml Dpalindrome PIK hydrolysis pattern in rat intestinal fluid protein monitored at 214 nm. Reaction mixtures initially contained 1 mg/ml Dpalindrome PIK and 0.1 mg/ml rat intestinal fluid protein and were incubated at 4 °C for 4 min.

B) Mass spectrometry analysis of HPLC peaks.

C) Peptide site map of Dpalindrome PIK showing initial sites of cleavage identified by LC-MS. Line 1 represents the prominent cleavage sites, line 2 the amino acid composition of the peptide and line 3 the peptide sequence number.

A

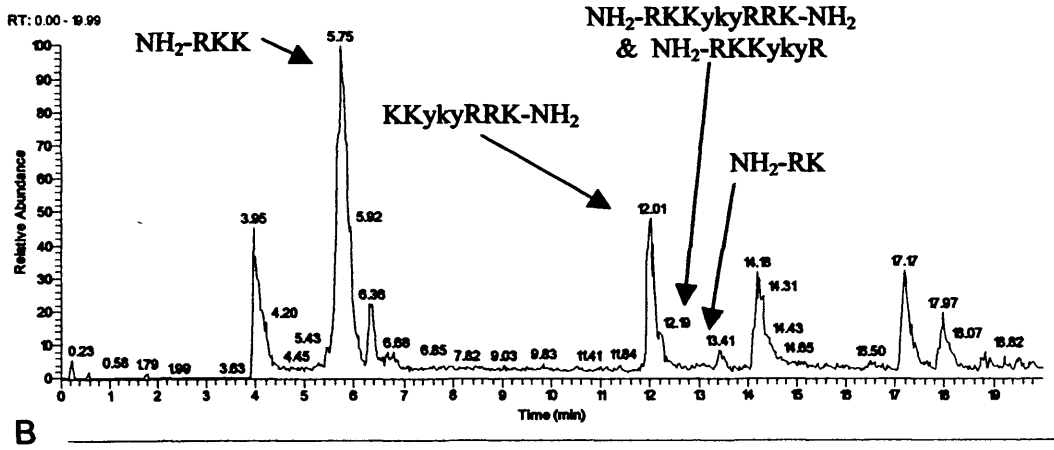


B

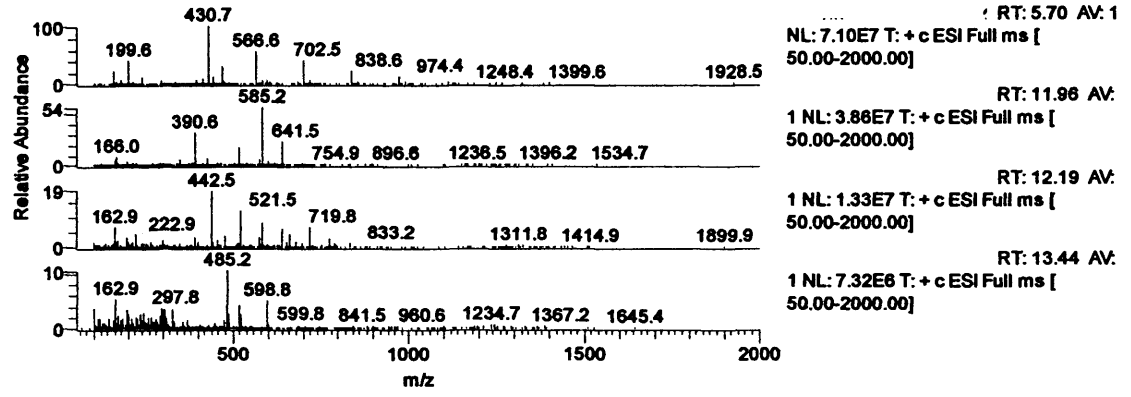


C

Line 1 ↓ ↓ ↓
Line 2 $NH_2$-R K K y k y R R K- $NH_2$
Line 3 1 2 3 4 5 6 7 8 9

Figure 3.15 LC-MS analysis of Dpalindrome PIK incubated with homogenised Caco-2 cell extracts.

A) HPLC analysis of 1 mg/ml Dpalindrome PIK hydrolysis pattern in Caco-2 lysate monitored at 214 nm. Reaction mixtures initially contained 1 mg/ml Dpalindrome PIK and 0.2 mg/ml Caco-2 cell lysates protein and were incubated at 37 °C for 4 h.

B) Mass spectrometry analysis of HPLC peaks.

C) Peptide site map of Dpalindrome PIK showing initial sites of cleavage identified by LC-MS. Line 1 represents the prominent cleavage sites. Line 2 the amino acid composition of the peptide and line 3 the peptide sequence number.

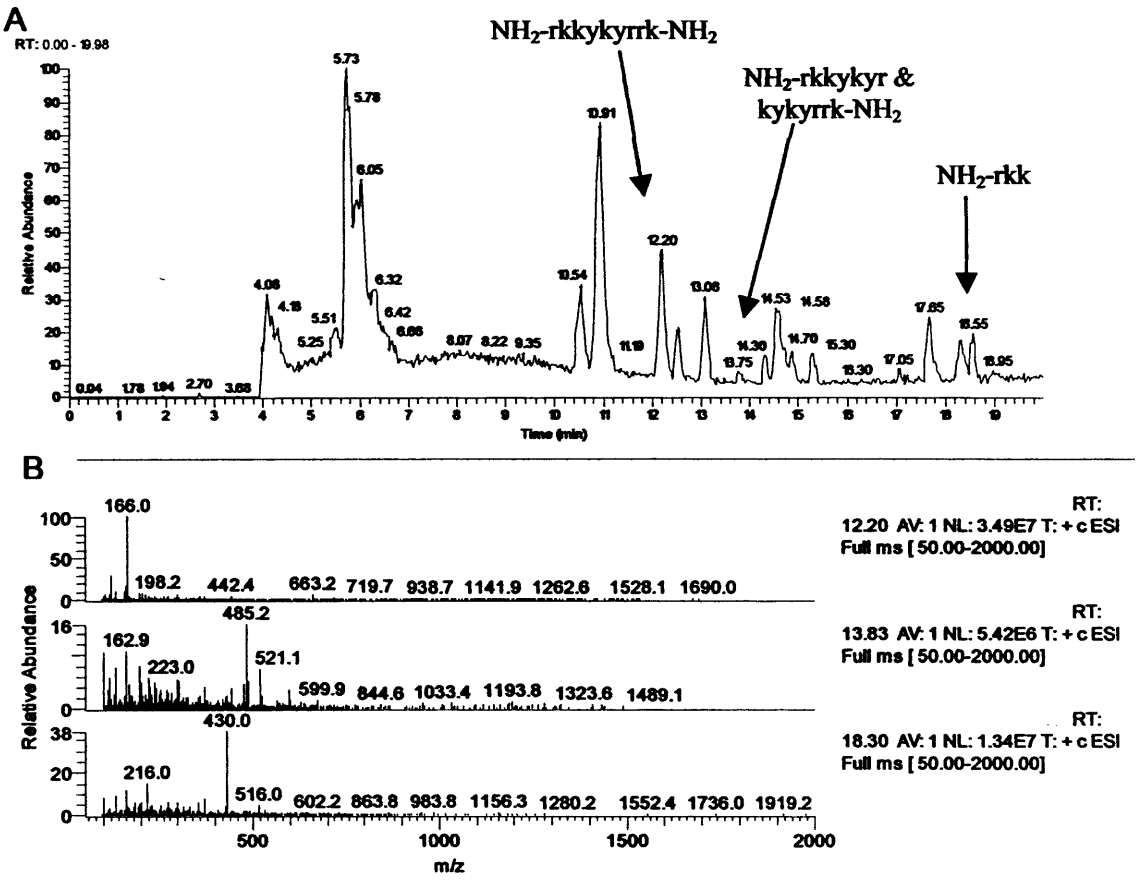


C

Line 1 ↓ ↓ ↓

Line 2 $NH_2$-r k k y k y r r k- $NH_2$

Line 3 1 2 3 4 5 6 7 8 9

Figure 3.16 LC-MS analysis of D PIK incubated with rat intestinal fluid protein.

A) HPLC analysis of 1 mg/ml D PIK hydrolysis pattern in rat intestinal fluid protein monitored at 214 nm. Reaction mixtures initially contained 1 mg/ml D PIK and 0.2 mg/ml rat intestinal fluid protein and were incubated at 37 °C for 30 min.

B) Mass spectrometry analysis of HPLC peaks.

C) Peptide site map of D PIK showing initial sites of cleavage identified by LC-MS. Line 1 represents the prominent cleavage sites. Line 2 the amino acid composition of the peptide and line 3 the peptide sequence number.

A

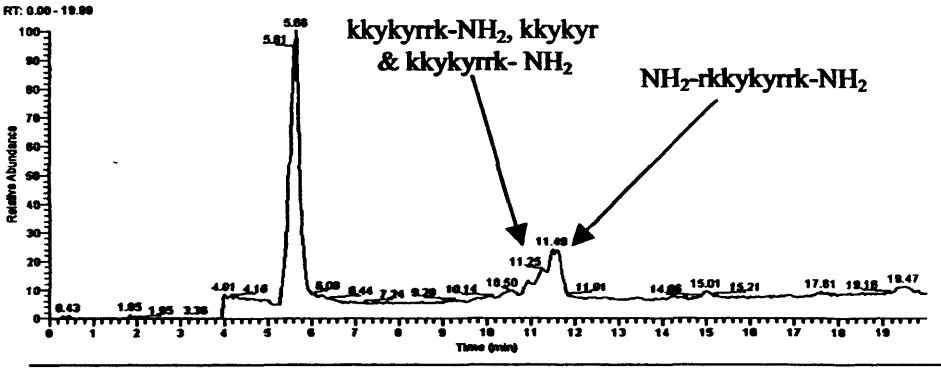


B

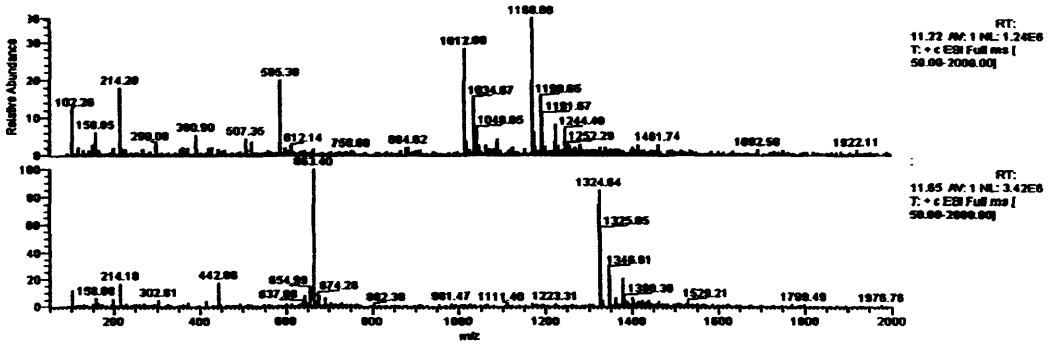


C

Line 1 ↓ ↓
Line 2 $NH_2$-r k k y k y r r k- $NH_2$
Line 3 1 2 3 4 5 6 7 8 9

Figure 3.17 LC-MS analysis of D PIK incubated with homogenised Caco-2 cell extracts.

A) HPLC analysis of 1 mg/ml D PIK hydrolysis pattern in Caco-2 lysate monitored at 214 nm. Reaction mixtures initially contained 1 mg/ml D PIK and 0.2 mg/ml Caco-2 cell lysate protein and were incubated at 37 °C for 2 h.

B) Mass spectrometry analysis of HPLC peaks.

C) Peptide site map of D PIK showing initial sites of cleavage identified by LC-MS. Line 1 represents the prominent cleavage sites, line 2 amino acid composition of the peptide and line 3 the peptide sequence number.

$NH_2$ (442, 663 and 1324) (figure 3.18.a). Dreverse PIK (1 mg/ml) incubated with 0.2 mg/ml homogenised Caco-2 cell extracts at 37 °C for 6 h led to the production of 5 cleavage products. These were identified as $NH_2$-kkr (430 Da), $NH_2$-krrykykk (1169 and 585 Da), ykykkr (884 Da) and $NH_2$-krrykykk (1168 Da) (figure 3.19). In addition, there was a relatively high abundance of krrykykkr- $NH_2$.

### *3.3.6 Specificity of PIK analogues*

Incubation of PKA with Dreverse PIK resulted in a 2-fold increase of PKA activity (figure 3.20). Therefore, a different batch of synthesised Dreverse PIK was used and the experiment was performed again. Once the new batch of Dreverse PIK was used there was no significant inhibition of PKA (figure 3.1). Neither D PIK nor Dreverse PIK nor Dpalindrome PIK demonstrated significant inhibitory effects toward PKA or CaMKII at concentrations of up to 5 mM (figure 3.22). Protein kinase A inhibitor 6-22 amide reduced PKA activity to 43 % and the $Ca^{2+}$/Calmodulin inhibitor 281-309 reduced CaMKII activity to 52 %.

## 3.4 Discussion

The amino acid sequence of PIK suggests vulnerability as a potential substrate for trypsin- and chymotrypsin-like hydrolysis, as the entire sequence is composed of R, K and Y residues. Due to the desire to administer PIK orally to target intestinal epithelial cells, PIK susceptibility to degradation in intestinal luminal secretions and in the presence of enzyme activities associated within intestinal epithelial cells was determined. To achieve this objective, the LC-MS method used to detect peptides and degradation products needed to be validated. For this study, Ac-PIK was used as end-terminal protection of peptides has been previously been shown to reduce susceptibility to amino- and carboxy-peptidases, thereby making its degradation pattern more predictable (Adessi and Soto 2002).

The breakdown pattern of Ac-PIK was consistent with the anticipated tryptic proteolysis of Ac-PIK, as trypsin cleaves at the C-terminal side of positively charged amino acids such as R and K (the main components of PIK). These data also confirm trypsin susceptibility of Ac-PIK, a pancreatic protease located within the intestinal lumen. The results show that the method utilised is a reliable way of detecting peptides as well as the smaller degradation products created by incubation of peptides with proteases and peptidases.

A

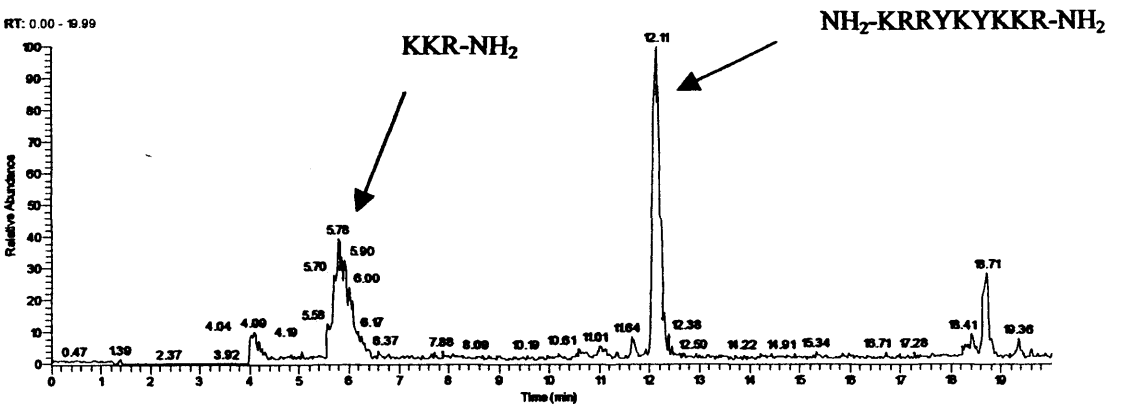


B

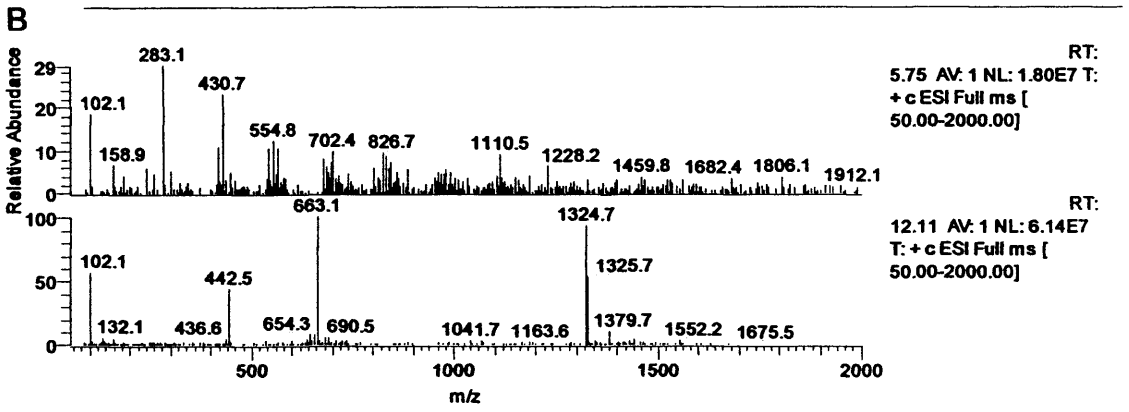


C

Line 1 ↓
Line 2 $NH_2$-k r r y k y k k r- $NH_2$
Line 3 1 2 3 4 5 6 7 8 9

Figure 3.18 LC-MS analysis of Dreverse PIK incubated with rat intestinal fluid protein.

A) HPLC analysis of 1 mg/ml Dreverse PIK hydrolysis pattern in rat intestinal fluid protein monitored at 214 nm. Reaction mixtures initially contained 1 mg/ml Dreverse PIK and 0.1 mg/ml rat intestinal fluid protein and were incubated for 3 h.

B) Mass spectrometry analysis of HPLC peaks.

C) Peptide site map of Dreverse PIK showing the initial site of cleavage identified by LC-MS. Line 1 represents the prominent cleavage site. Line 2 the amino acid composition of the peptide and line 3 the peptide sequence number.

A

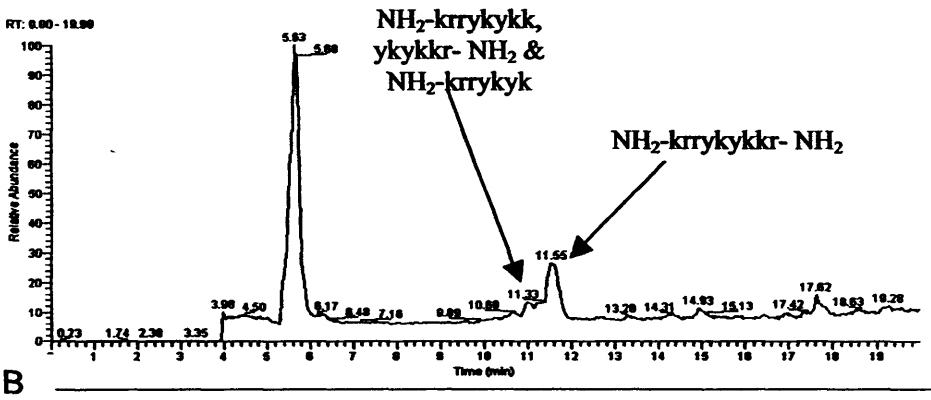


B

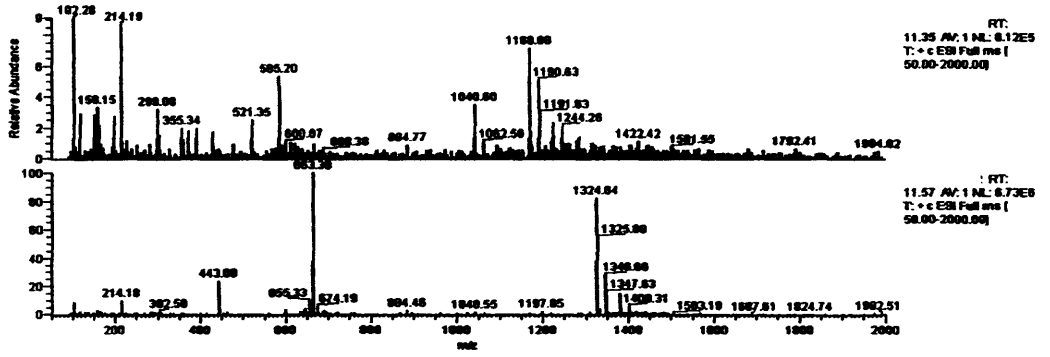


C

Line 1 ↓ ↓ ↓

Line 2 $NH_2$-k r r y k y k k r- $NH_2$

Line 3 1 2 3 4 5 6 7 8 9

Figure 3.19 LC-MS analysis of Dreverse PIK incubated with homogenised Caco-2 cell extracts.

A) HPLC analysis of 1 mg/ml Dreverse PIK hydrolysis pattern in Caco-2 lysate monitored at 214 nm. Reaction mixtures initially contained 1 mg/ml Dreverse PIK and 0.2 mg/ml Caco-2 cell lysate protein and were incubated at 37 °C for 2 h.

B) Mass spectrometry analysis of HPLC peaks.

C) Peptide site map of Dreverse PIK showing initial sites of cleavage identified by LC-MS. Line 1 represents the prominent cleavage sites, line 2 the amino acid composition of the peptide and line 3 the peptide sequence number.

Table 3.5 Summary of PIK and PIK analogues degradation products incubated in rat intestinal fluid protein

| Peptide | Incubation Conditions | Peptide Fragments Detected by LC-MS Analysis |
|---|---|---|
| PIK | 8 min at 4 °C | $NH_2$-RKK, RK-$NH_2$, KYKYRRK-$NH_2$ and $NH_2$-RKKYKYRR |
| Ac-PIK | 4 min at 4 °C | Ac-RKKYK, Ac-RKKY, YKYR and Ac-RKKYKYRRK-$NH_2$ |
| Dpalindrome PIK | 4 min at 4 °C | $NH_2$-RKK, KykyRRK-$NH_2$, $NH_2$-RKKykyRRK-$NH_2$ and $NH_2$-RKKykyRR |
| D PIK | 30 min at 37 °C | $NH_2$-rkkykyrrk-$NH_2$, $NH_2$-rkkykyr, kykyrrk-$NH_2$ and $NH_2$-rkk |
| Dreverse PIK | 3 h at 37 °C | kkr-$NH_2$ and $NH_2$-krrykykkr-$NH_2$ |

Table 3.6 Summary of PIK and PIK analogues degradation products incubated in homogenised Caco-2 cell extracts

| Peptide | Incubation Conditions | Peptide Fragments Detected by LC-MS Analysis |
|---|---|---|
| PIK | 15 min at 37 °C | YRRK-$NH_2$, $NH_2$-RKKYK and $NH_2$-RKKYKYRRK-$NH_2$ |
| Ac-PIK | 1 h at 37 °C | Ac-RKKYKYRR, Ac-RK, RK-$NH_2$, KKYKYRRK-$NH_2$ and KYKYRRK-$NH_2$ |
| Dpalindrome PIK | 4 h at 37 °C | $NH_2$-RKK, KKykyRRK-$NH_2$, $NH_2$-RKKykyRRK-$NH_2$, $NH_2$-RKKykyR and $NH_2$-RK |
| D PIK | 2 h at 37 °C | kkykyrrk-$NH_2$, kkykyr, kkykyrrk-$NH_2$ and $NH_2$-rkkykyrrk-$NH_2$ |
| Dreverse PIK | 2 at 37 °C | $NH_2$-krrykyrr, ykyrrk-$NH_2$, $NH_2$-krrykyk and $NH_2$-krrykykkr-$NH_2$ |

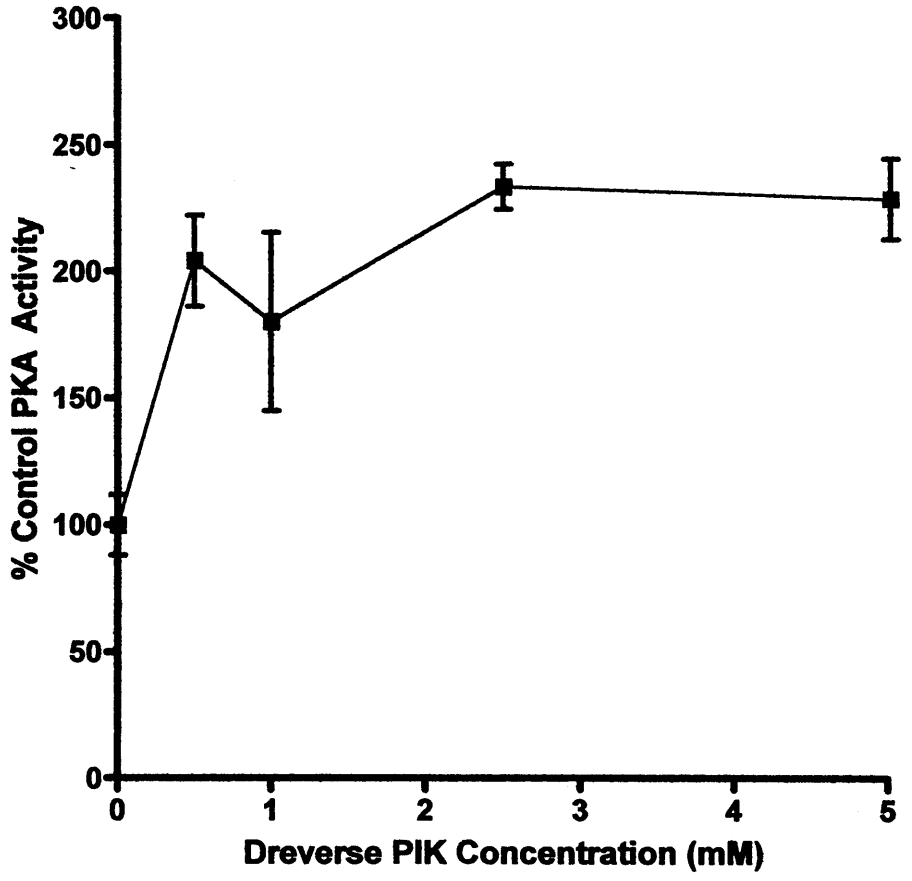


Figure 3.20 ELISA based assay of Dreverse PIK's effect on PKA activity at different concentrations. (Data represents mean ± SEM n=3, error bars are within plot symbol if not visible).

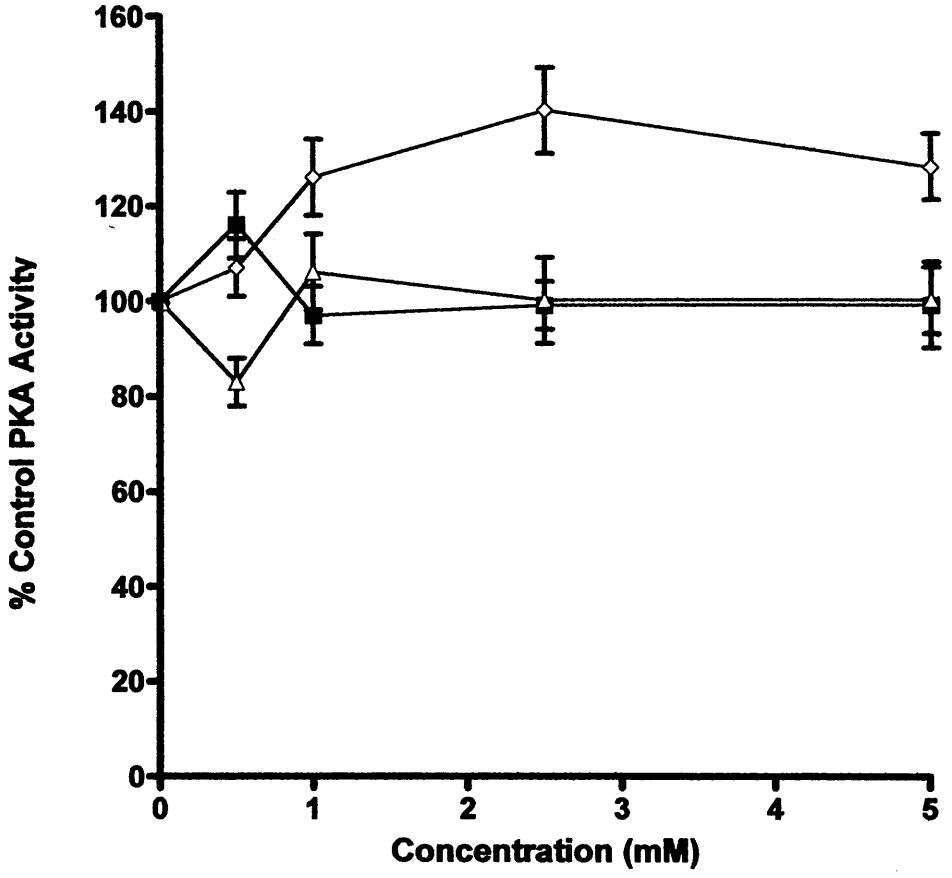


Figure 3.21 ELISA based assay of D-amino acid PIK peptide effect on PKA activity at increasing concentrations. Dreverse PIK (■), D PIK (◇) and Dpalindrome PIK (△). Protein kinase A inhibitor 6-22 amide reduced PKA activity to 43 % ± 9 %. (Data represents mean ± SEM n=3, error bars are within plot symbols when not visible).

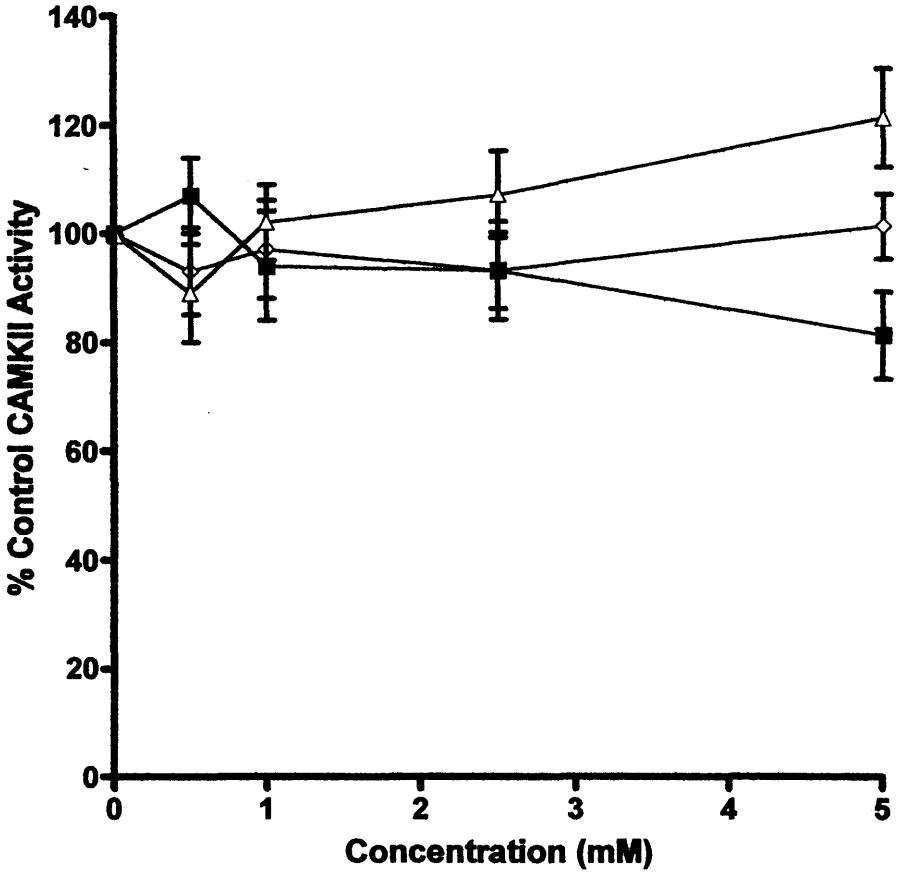


Figure 3.22 ELISA based assay of D-amino acid PIK peptide effect on CAMKII activity at increasing concentrations. Dreverse PIK (■), D PIK (◇) and Dpalindrome PIK (△). $Ca^{2+}$/Calmodulin kinase II inhibitor 281-309 reduced CAMKII activity to 52 % ± 8 %. (Data represents mean ± SEM n=3, error bars are within plot symbols when not visible).

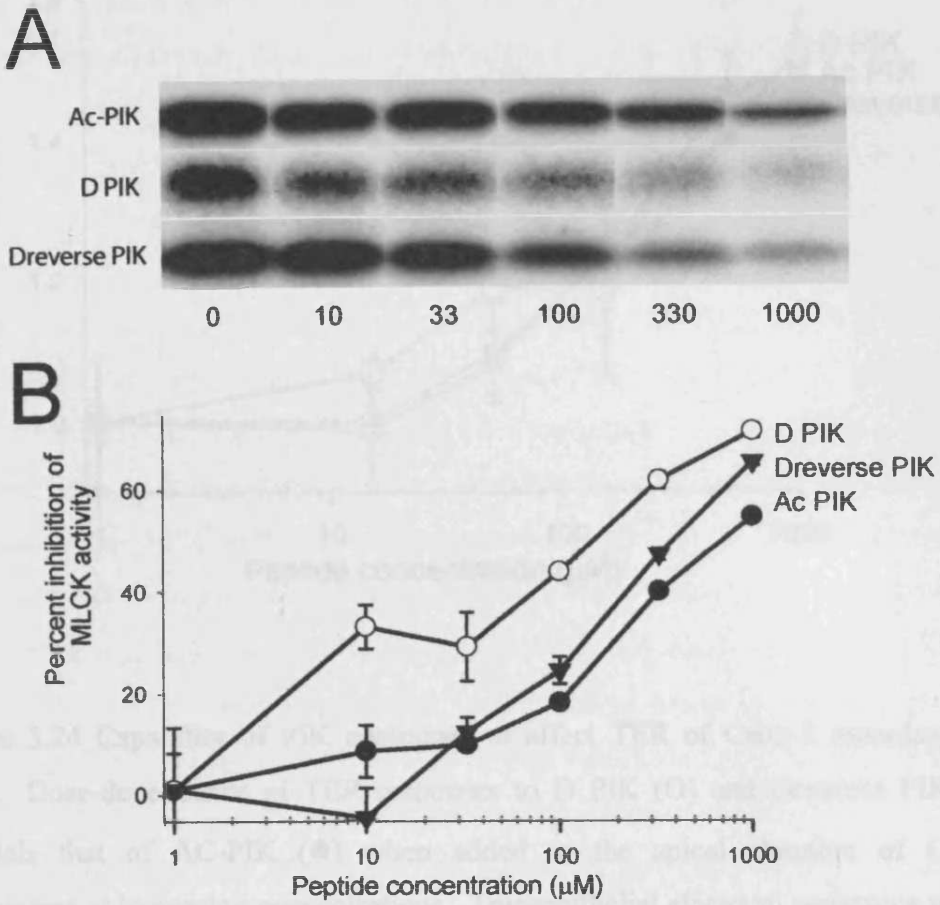


Figure 3.23 Action of PIK analogues on MLCK function .

A) Representative example of experiment comparing MLCK activity for Ac-PIK to that observed using D PIK and Dreverse PIK. Increasing concentrations of peptide (0-1000 μM) were introduced into an *in vitro* kinase reaction with recombinant human enterocyte MLC and $\gamma$-$^{32}$P-ATP. Reaction mixtures were separated by SDS-PAGE and MLC phosphorylation assessed by autoradiography.

B) Percent inhibition of MLCK activity, D PIK (O) and Dreverse PIK (▼) and AC-PIK (●), demonstrated as a reduction of MLC incorporation of $\gamma$-$^{32}$P, from triplicate studies was averaged and normalised to $\gamma$-$^{32}$P incorporation in the absence of peptide.

Performed by J Turner at the Department of Pathology, University of Chicago, Chicago, Illinois.

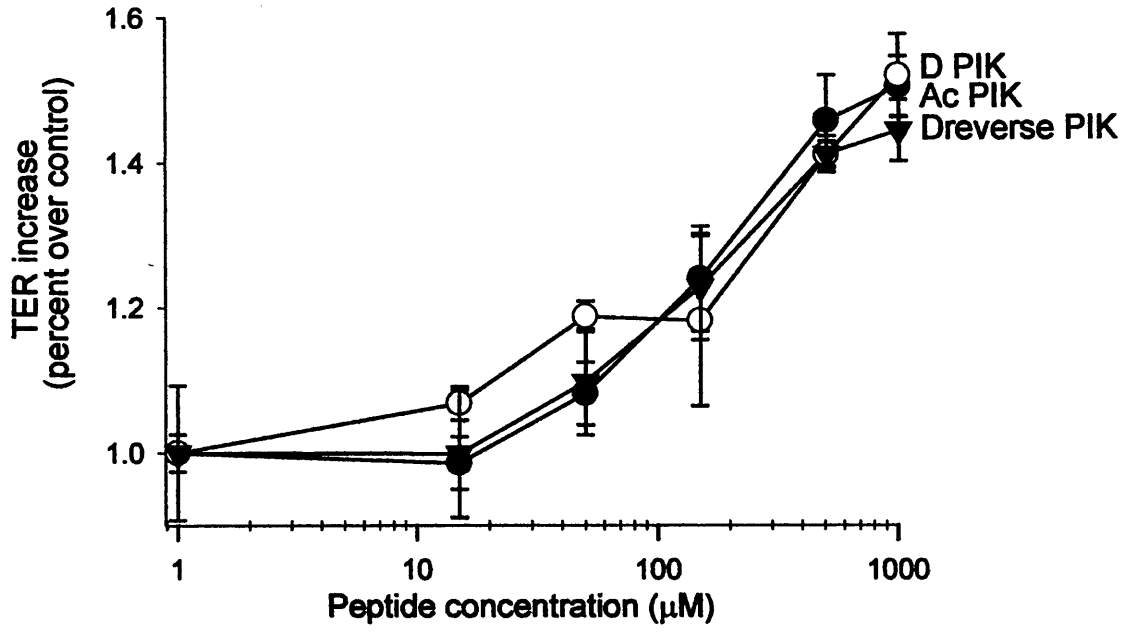


Figure 3.24 Capability of PIK analogues to affect TER of Caco-2 monolayers *in vitro*. Dose-dependence of TER responses to D PIK (O) and Dreverse PIK (▼) parallels that of AC-PIK (●) when added to the apical chamber of Caco-2 monolayers at increasing concentrations. Transepithelial electrical resistance values, determined 60 min after peptide addition, were normalised to those obtained after addition of vehicle alone. (Data show mean ± SEM).

Performed by J Turner at the Department of Pathology, University of Chicago, Chicago, Illinois.

As a method of detecting peptides and their cleavage products had been established it was then possible to determine the stability of PIK (RKKYKYRRK-$NH_2$) in luminal fluids isolated from rat intestines. This model of the intestinal environment was used as it reflects the physiological environment more closely than a mixture of purified peptidases such as trypsin and chymotrypsin (Fauchere and Thurieau 1992). Liquid chromatography-mass spectrometery analysis of the purified peptide confirmed PIK to have the expected mass (1324 Da), and a positive ion breakdown map was consistent with its composition. Incubation of PIK with rat intestinal fluid protein resulted in several cleavage products. Peptide bonds at the C-terminal sides of K and R residues were initially cleaved to produce the degradation products observed. The cleavage map generated for the most sensitive sites of PIK when incubated in rat intestinal fluid protein were characteristic of trypsin-like endopeptidase(s) hydrolysis. Extended incubations and incubations at 37 °C in rat intestinal fluid led to the total hydrolysis of PIK with no detectable cleavage products remaining. This indicates that hydrolysis of PIK within the intestinal environment is rapid, with multiple peptide bonds being cleaved. Based on the amino acid sequence of PIK, it is likely that non-trypsin-like proteases and peptidases participated in subsequent hydrolysis steps. PIK cleavage in rat intestinal fluid is, however, dominated initially by trypsin-like endopeptidase(s) that would act to cleave PIK at positively charged residues of the peptide.

Next, the stability of PIK in Caco-2 intestinal epithelial cell extracts was assessed, which contains a mixture of brush border and cytosolic proteases. Incubation of PIK with Caco-2 extract identified fewer cleavage products when compared with incubation with rat intestinal fluid protein. Analysis of the cleavage map suggested that proteolysis was performed by a chymotrypsin–like endopeptidases(s) that cleave PIK at the C-terminal sides of $K^5$ and $Y^6$. The central palindrome sequence $Y^4K^5Y^6$ of PIK is essential for effective inhibition of MLCK (Zolotarevsky, *et al* 2002). Therefore, these protease/peptidase activities cleave the central palindrome sequence of PIK, thereby neutralising its potential to inhibit MLCK and reduce TER. However, this could also be advantageous as it could prevent PIK from accumulating in cells. Any toxic effects of excessive decreased paracellular permeability could subsequently be prevented, which could potentially include dehydration as water is transported via the paracellular route.

PIK appears to be more vulnerable to degradation in rat intestinal fluid protein than in homogenised Caco-2 cell extracts, indicating that the gut lumen would be the main site of PIK degradation *in vivo*. Therefore, the half-life of PIK was determined in rat luminal secretions; this could then be used as a reference point to determine if any chemical modifications were successful in increasing PIK stability.

The half-life of PIK, 0.2 min, is very short and consistent with rapid, multiple degradation events. The end-terminal protected Ac-PIK had an equally short half-life of 0.2 min. This demonstrates that, in this case, blockage of PIK termini offers no protection from proteases/peptidases present within the rat intestinal lumen. This suggests that specific endopeptidases cleave PIK, which could potentially result in unprotected termini for non-specific exopeptidases to cleave the remaining peptide.

Based on the pattern of PIK protease/peptidase susceptibility, a series of PIK analogues were required in an effort to obtain molecules with improved stability to protease and peptidase activities found in intestinal luminal secretions and associated intestinal epithelial cells. Due to the failure of end-terminal protection of PIK to increase stability, it was decided that the peptide bonds within PIK sequence needed to be protected in order to increase stability.

Replacing all or even certain L-amino acids with their equivalent D-amino acids within a peptide sequence may reduce recognition by mammalian enzymes and hence increase stability (Chorev and Goodman 1995). Based on the degradation of PIK in Caco-2 lysates where the central palindrome $Y^4K^5Y^6$ of PIK was cleaved, the central palindrome sequence was substituted to D-amino acids to create Dpalindrome PIK (RKKykyRRK-$NH_2$). The $Y^4K^5Y^6$ sequence of PIK has been shown to be important in its ability to inhibit MLCK, as cis-4-aminocyclohexanecarboxylic acid substitutions at these positions led to a reduction in PIK activity (Zolotarevsky, *et al* 2002). Loss of activity from use of D-amino acids should be prevented; as this sequence is palindromic, alteration of chirality should therefore not alter its structure greatly. However, the half-life of Dpalindrome PIK was similar to that of PIK. These data indicate that the positively charged residues flanking the central palindrome sequence of PIK are extremely sensitive to proteolysis within rat intestinal fluid protein.

As end-terminal protection and altering the chirality of the central palindrome sequence did not increase stability, 2 PIK analogues in which all of the L-amino acids

were replaced by D-amino acids were synthesised: D PIK (rkkykyrrk-$NH_2$), the D-analogue of PIK, which has the same amino acid sequence as PIK, while Dreverse PIK (krrykykkr-$NH_2$) has the PIK sequence of amino acids in reversed order (retro-inverso-isomer of PIK). This strategy to identify a stable PIK analogue was guided by observations that peptide synthesis using D-amino acids can result in loss of function that can be regained by sequence reversal (Chorev and Goodman 1995). D PIK and Dreverse PIK showed approximately 1000 - and 4000 - fold increases in half-life of 3.6 h and 13.4 h respectively relative to the other PIK analogues when incubated in rat intestinal fluids. The standard deviation of D PIK and Dreverse PIK could be high due to the fasting state of the rats. The rats used for this study were non fasting. Therefore, if they had just eaten, their intestinal luminal secretions would contain increased concentrations of the pancreatic proteases such as trypsin and chymotrypsin compared to fasting animals, which would result in a shorter half-lives of the peptides. It would therefore be advantageous to repeat these studies in fasting animals as PIK is more labile within intestinal fluid protein. Hence, PIK is likely to be taken without food for optimal effectiveness.

Since stable PIK analogues had been synthesised, their degradation patterns within the intestinal environment needed to be determined in order to predict the outcome of oral intake of these peptides. Incubation of Ac-PIK with rat intestinal fluid protein resulted in 4 cleavage products being produced. The cleavage of Ac-PIK appears to be performed by both trypsin- and chymotrypsin-like endopeptidases. This is different to PIK, which was predominantly cleaved by trypsin-like endopeptidases. Therefore, it appears that protection of the end-terminus of PIK increases its susceptibility to chymotrypsin-like endopeptidases. Incubation of Ac-PIK with homogenised Caco-2 lysate resulted in several cleavage products. Acetylation of PIKs N-terminus and amidation of the C-terminus appears to alter degradation of the peptide by chymotrypsin-like proteases as observed when PIK is incubated in homogenised Caco-2 cell extracts to a trypsin-like hydrolysis. Therefore, protection of PIKs N-terminus and C-terminus appears to alter its susceptibility to the peptidases and proteases located within the intestinal lumen and within intestinal cells.

Incubation of Dpalindrome PIK with rat intestinal fluid resulted in only 3 cleavage products. These results show that substitution of the central palindrome

sequence for D-amino acids did not prevent degradation of the positively charged K and R flanking the palindrome; however, the central palindrome sequence was not cleaved. The cleavage of Dpalindrome PIK appears to be undertaken by trypsin-like endopeptidases. Incubation of Dpalindrome PIK with homogenised Caco-2 cell extracts resulted in protection of the central palindrome with the positively charged amino acids surrounding this area being cleaved. This corroborates with the half-life results that suggest that protection of PIKs central palindrome does not increase its stability within the intestinal environment.

Enzymatic cleavage of D PIK was by trypsin-like endopeptidases in both the rat intestinal fluid and homogenised Caco-2 cell extract proteins. The cleavage of Dreverse PIK in rat intestinal fluid was also trypsin-like although only 1 cleavage product was observed following 3 h incubation, which in concurrence with Dreverse PIK much longer half-life compared with D PIK which had 4 cleavage products following incuabtaation with rat intestinal fluid for 30 min. Dreverse PIK was also cleaved by a trypsin-like endopeptidase within the Caco-2 cell extracts. The HPLC chromatograms show a relatively high abundance of the intact peptide when the all D - amino acid peptides are incubated within different intestinal environments also longer time periods are required to observe the degradation products thereby corroborating with the half-life studies.

The central palindrome of all modified PIK peptides appeared to have greater protection from cleavage within homogenised Caco-2 cell extracts compared to PIK, as incubation of PIK with Caco-2 cell protein at 37 °C for 2 h led to cleavage of this domain. However, this did not occur when the modified PIK peptides were incubated for an equal amount of time or longer under the same conditions. The central palindrome sequence is important for PIK's ability to inhibit MLCK. This suggests that these peptides would have much longer activities within intestinal cells. The half-lives of PIK and its analogues were determined within rat intestinal fluid protein as PIK was more labile within this protein extract. It has been hypothesised that PIK, is rapidly internalised into cells due to its sequence similarity to HIV-TAT, a known cell penetrating peptide (Jones, *et al* 2005). If so, PIK may not be exposed for long periods of time to intestinal luminal enzymes. Perhaps the half-life within Caco-2 cell extracts would have been valuable to determine the potential length of PIK activity within Caco-2 cells. Additionally, it would be interesting to evaluate whether cleaved PIK would retain MLCK inhibitory activity. This could be

achieved by cleavage of PIK with rat intestinal fluid protein and the addition of this to Caco-2 cells then investigating whether this reduces its ability to inhibit MLCK.

Along with MLCK, PKA and CaMKII are 2 other serine/threonine kinases that interact with CaM-mediated pathways (Murthy, *et al* 2003, Stull, *et al* 1990). The PIK peptide sequence has previously been shown to discriminate between these kinases and specifically inhibit MLCK (Lukas, *et al* 1999). If the more stable PIK analogues identified in these studies are to be useful *in vivo*, it is important that they also selectively inhibit MLCK only. Incubation of PKA with Dreverse PIK resulted in a 2-fold increase activity. It was speculated that this increase could be due to a contaminant salt in the purified peptide or the Dreverse PIK itself. Therefore, to determine if a contaminant was the cause of increased activity, a different batch of Dreverse PIK was used, which resulted in neither inhibition or increased activity of PKA, indicating that a contaminant was present in the first batch of Dreverse PIK which caused an increase in PKA activity. Neither D PIK nor Dreverse PIK nor Dpalindrome PIK demonstrated significant inhibitory effects toward PKA or CaMKII at concentrations up to 5 mM. Thus, both D PIK and Dreverse PIK, which were shown to have increased stability in rat intestinal fluid and Caco-2 cell lysates, were able to specifically inhibit MLCK without affecting PKA or CaMKII activities.

PIK has previously been shown to inhibit Caco-2 MLCK activity in a dose-dependent fashion (Zolotarevsky, *et al* 2002). To determine if D PIK and Dreverse PIK shared this MLCK-inhibitory activity, kinase assays using Caco-2 MLCK and recombinant intestinal epithelial MLC were performed by our collaborators. The activity of Dreverse PIK was indistinguishable from Ac-PIK, whereas D PIK appeared to have slightly enhanced MLCK inhibitory activity. These results suggest that in the case of PIK, the use of D-amino acids does not require sequence reversal (Owens, *et al* 2005). This is contrary to published literature which states that use of D-amino acids often leads to a loss of function while retro-inverso-isomers maintains the activity of the parent peptide (Chorev and Goodman 1995).

PIK has also been shown to reduce paracellular permeability in a dose-dependent manner using an *in vitro* Caco-2 monolayer system where enhanced activity of $Na^+$-glucose co-transport results in a decrease in TER (Zolotarevsky, *et al* 2002). Having identified 2 PIK analogues with enhanced stability that each retained the ability to inhibit MLCK *in vitro*, our collaborators assessed the ability of these

PIK analogues to increase TER of similar Caco-2 monolayers. In this assay, Ac-PIK, D PIK and Dreverse PIK each produced similar increases in TER at concentrations up to 1 mM. The results demonstrated that PIK analogues produced using D-amino acids (D PIK and Dreverse PIK) can produce a physiological outcome similar to PIK molecules prepared entirely from L-amino acids (Ac-PIK). Because this effect on paracellular permeability requires PIK to be membrane permeant, these data also show that D PIK and Dreverse PIK are membrane permeant in a manner similar to PIK (Owens, *et al* 2005).

## 3.5 Conclusions

PIK represents a unique peptide-based drug candidate for the correction of paracellular permeability defects associated with intestinal disease. PIK is composed of a central palindrome sequence YKY sequence that is required for MLCK inhibition. This sequence is flanked by positively charged amino acids that possibly act to properly position the central YKY sequence of PIK at a crucial site on MLCK (Lukas, *et al* 1999). Presumably, the R and K residues also make PIK membrane permeant, thereby allowing it to access intracellular MLCK (Zolotarevsky, *et al* 2002). However, as predicted, PIK in its original form is highly susceptible to protease and peptidase hydrolysis, making it unsuitable for oral use. The half-life studies demonstrated that L-amino acid containing PIK analogues (Ac-PIK and Dpalindrome PIK) had half-lives equal to that of PIK. However, the all D-amino acid containing PIK analogues D PIK and Dreverse PIK had much longer half-lives when compared to PIK. These findings are consistent with previous studies demonstrating that peptides derived from D-amino acids have greater stability (Chorev and Goodman 1995). These peptides also specifically inhibited MLCK with no appreciable inhibition of PKA or CaMKII, therefore making these peptides suitable for further studies in animal models of IBD.

PIK has a half-life of approximately 13 h; therefore, it is predicted to be administered twice or thrice daily without food to prevent degradation by pancreatic proteases. As PIK works by closing TJs, thereby preventing the paracellular passage of toxins and hence reducing inflammation, it is predicted to work in a similar manner as the anti-inflammatory glucocosteroids. Glucocosteroids suppress inflammation by several mechanisms, including inhibition of numerous

inflammatory gene expression, whilst increasing the transcription of anti-inflammatory genes (Barnes 1998). Therefore, PIK is estimated to take approximately 2 to 3 weeks for anti-inflammatory effects to occur. PIK could be taken in solution for CD, thus covering the lining of the gastrointestinal tract, or as enemas or foam for UC that is limited to the lower part of the colon.

PIK potentially has advantages over current CD therapeutics, as it might prevent the onset of CD. A case study showed that an asymptomatic female of 13 years had increased TJ permeability even though there were no signs of CD. This individual was then diagnosed with CD 8 years later, indicating that increased permeability is a primary phenomenon that corresponds to early stage development of CD (Irvine and Marshall 2000). This implies that prevention of elevated permeability may reduce the possibility or delay the onset of disease. This suggests that prescribing PIK to individuals with a high risk of developing CD (such as those with first degree relatives with the disease) and that have increased intestinal permeability could be beneficial. Further studies could also assess the ability of PIK to prevent the onset of disease in those with increased intestinal permeability.

Identification of these stable PIK peptide analogues now provides the opportunity to examine the role of MLCK modulators in various *in vivo* models of epithelial inflammation and inflammation-associated diseases such as CD.

# Chapter 4

# Synthesis of MLCP Inhibition Peptides

## 4.1 Introduction

Drug delivery systems should ideally deliver the correct drug concentration to its target site at the desired rate and timing, to maximise its therapeutic response. However, if this cannot be achieved the effectiveness of the drug is reduced, which in some instances prevents their use (Aungst 2000).

New oral drug delivery methods are continually being sought after, as this method of drug delivery is most favourable due to its relative simplicity compared with other routes (Fasano 1998). Drugs can be absorbed either by the transcellular or paracellular pathways. Absorption via the paracellular pathway is relatively small due to the regulation of this space by TJs. Therefore, absorption enhancers have been used to increase TJ permeability of hydrophilic drugs via this route. Nevertheless, use of absorption enhancers that increase paracellular permeability is limited as it is difficult to establish whether the enhancer acts in a physiological or pathological manner (Hayashi, *et al* 1999). Sodium caprate (C10) used in ampicillin suppositories in Japan, Sweden and Denmark is the only absorption enhancer currently licensed (Lindmark, *et al* 1998, Lindmark, *et al* 1997). Current research is focusing on the design of absorption enhancers whose effects are reversible, that are either selective against target cells only or their intercellular junctions, and do not activate an inflammatory response (Lee, *et al* 1991). Although transport this route is relatively small, luminal glucose activation of SGLT-1 results in water absorption increasing to 91 %, whilst the absorption of creatinine, inulin and polyethylene glycol 4000 increasing to 193 %, 100 % and 6 % respectively via the paracellular pathway (Turner 2000). Demonstrating that increases in TJ permeability is possible in a physiological manner without adverse side affects.

The ratio of myosin light chain phosphatase to kinase activity regulates the degree of MLC phosphorylation (Somlyo and Somlyo 2003). Myosin light chain kinase activity is important in the regulation of the paracellular space (Hecht, *et al* 1996). The MLCK inhibitor PIK closes TJs in 2 different models of intestinal epithelial inflammation (Zolotarevsky, *et al* 2002). Therefore, an inhibitor of MLCP is hypothesised to open TJs to allow the passage of drugs and hence development of a novel absorption enhancer of known function.

Regulation MLCP activity involves alterations in subunit interactions, figure 4.1 shows the subunit structure of smooth muscle myosin phosphatase. Phosphatase

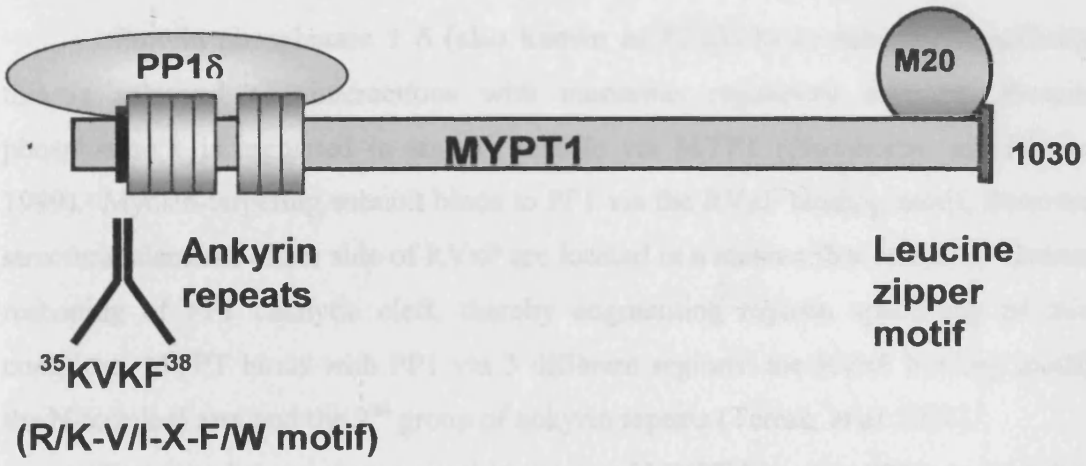


Figure 4.1 Subunit structure of smooth muscle myosin phosphates (adapted from Ito, *et al* 2004).

inhibition as observed in increases in $Ca^{2+}$ sensitivity induced by agonists is thought to occur by either Rho A, AA and PKC pathways acting independently or collectively (Somlyo and Somlyo 2003).

*MLCP inhibition by PP1*

Protein phosphatase 1 δ (also known as PP1β) lacks substrate specificity this is achieved via interactions with numerous regulatory subunits. Protein phosphatase 1 is regulated in smooth muscle via MYPT (Hartshorne and Hirano 1999). Myosin-targeting subunit binds to PP1 via the RVxF binding motif, however structural elements either side of RVxF are located in a manner that results in distinct reshaping of PP1 catalytic cleft, thereby augmenting myosin specificity of this complex. MYPT binds with PP1 via 3 different regions: the RVxF binding motif, the N-terminal arm and the $2^{nd}$ group of ankyrin repeats (Terrak, *et al* 2004).

Terrak and co-workers crystal structure of MYPT bound to PP1δ showed that $E^{300}$ to $E^{309}$ of PP1δ are positioned between 2 ankyrin repeats of MYPT, in particular the ankyrin repeats bind with $Y^{305}$ and $Y^{307}$. Suggesting that the C terminus of PP1δ is important for regulatory subunit interaction and to mediate isoform specificity. Therefore, a peptide corresponding to this area may prevent MYPT ability to bind to PP1δ and hence diminish myosin specificity of the MYPT/PP1δ complex (Terrak, *et al* 2004).

*MLCP inhibition via CPI-17*

The MLCP PP1 subunit inhibitor CPI-17 is widely expressed in smooth muscle (Eto, *et al* 1997). The structural determinants and potential method by which CPI-17 inhibits MLCP was first characterised by Hayashi and co-workers. Phosphorylation or thiophosphorylation of $T^{38}$ is required for potent inhibition as substitution to a E residue resulted in a loss of inhibitory activity. Therefore, E negative charge does not mimic phosphorylated $T^{38}$. $Tyrosine^{41}$ substitution to A residue transformed CPI-17 into a MLCP substrate. Suggesting that the mutation subtly but significantly changes the binding of CPI-17 with the PP1 active site. It has been proposed that $Y^{41}$ side chain interacts with PP1 to increase binding additionally it is thought that it may prevent hydrolysis of the phosphorylated $T^{38}$.

The N-terminal side residues such as $K^{32}$ and $R^{33}$ of phosphorylated $T^{38}$ were not essential for inhibition, as substitutions at these sites did not affect the $IC_{50}$ value of phosphorylated CPI-17. However residues located at the C-terminal side of phosphorylated $T^{38}$ (e.g. $Y^{41}$, $D^{42}$, $R^{43}$ and $R^{44}$) are necessary for generating potent inhibition. As substitution of these amino acids with A greatly increased $IC_{50}$ values, the YDRR sequence is also important in halting dephosphorylation of phosphorylated $T^{38}$ (figure 4.2) (Hayashi, *et al* 2001).

*Minimal functional domain of CPI-17*

Deletion mutants containing amino acids 1-120, 10-147, 22-147 and 35-147 of CPI-17 sequence had $IC_{50}$ values similar to that of wild type CPI-17, in living fibroblasts and biochemical assays. Whereas mutant proteins (1-102) and (1-89) with 45 and 58 residues deleted from the C-terminus of CPI-17 had $IC_{50}$ values 22-fold greater than the wild type. Further deletions resulting in shorter proteins (1-76) and (1-67) did not inhibit MLCP even though they possess phosphorylated $T^{38}$ and the YDRR sequence. Indicating that the C-terminal region of the inhibitory domain is also important for CPI-17 function. Therefore, amino acids 35–120 of CPI-17 inhibitory domain are essential for MLCP inhibition (Hayashi, *et al* 2001).

*CPI-17 nuclear magnetic resonance structure*

The solution nuclear magnetic resonance structure of CPI-17 is comprised of 4 helices. Between helix A (residues 46 to 63) and helix D (residues 105 to 115) an anti-parallel helix pair is formed. Thereby explaining why the 103-120 domain is essential for CPI-17 function and is consistent with deletion analysis studies. The N-terminal loop called the P-loop is long and unstructured, which includes the important functional YDRR sequence and $T^{38}$. The P-loop is not exposed to the surface but underneath the molecular surface created by helices A and B. During activation of CPI-17 a conformational change is hypothesised to expose the P-loop, thereby allowing it to bind with MLCP active site (Hayashi, *et al* 2001, Ohki, *et al* 2001).

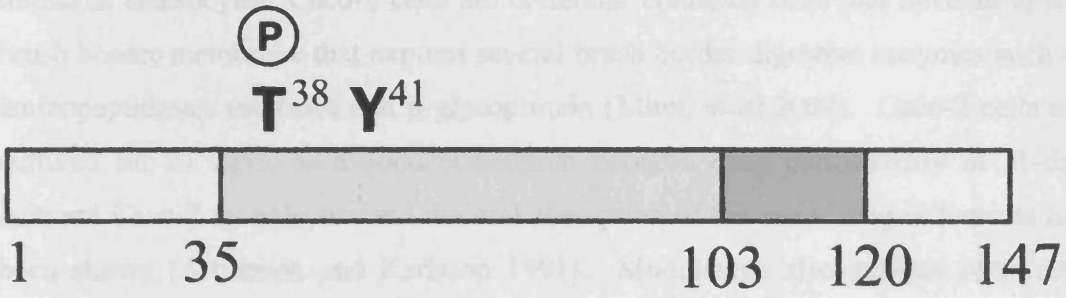


Figure 4.2 CPI-17 amino acid sequence represented as a bar. Amino acids 35 to 120 are the minimal inhibitory domain. Residues 103 to 120 are necessary for potent MLCP inhibition. Phosphorylated $T^{38}$ is required for MLCP recognition and $Y^{41}$ prevents the dephosphorylation of $T^{38}$ (adapted from Hayashi, et al 2001).

*Rational for selecting the Caco-2 cell culture model*

Cell culture models offer a useful platform to investigate intestinal drug uptake and transport. There are numerous human colonic cell models including T84 (Dharmsathaphorn, *et al* 1984), HT-29 (Zweibaum, *et al* 1985) and Caco-2 (Hilgers, *et al* 1990). With Caco-2 being the most extensively used as an intestinal permeability model. The human intestinal epithelial cell line Caco-2 was isolated from a primary colonic tumour in a 72-year old Caucasian male. Although they are derived from colonic cells they exhibit morphological and functional similarities to intestinal enterocytes. Caco-2 cells are columnar epithelial cells that have an apical brush border membrane that express several brush border digestive enzymes such as aminopeptidases, esterases and p-glycoprotein (Miret, *et al* 2004). Caco-2 cells are cultured for 21 days, as a good correlation between drug permeability in 21-day cultured Caco-2 monolayers and the oral absorption of the same drug in humans has been shown (Artursson and Karlsson 1991). Monolayers also express junctional complexes; indeed in confluent Caco-2 cell cultures domes are observed indicating the occurrence of TJs and active ion transport processes. Formation of TJs on Caco-2 cells cultured on Milipore filters has been confirmed by electrical measurements with a TER of about 150–300 $\Omega$ $cm^2$ making them ideal models for intestinal TJ function (Quaroni and Hochman 1996).

Caco-2 was shown to be highly morphologically heterogeneous, some cells did not express brush borders, and those that did often lost this ability following numerous passages. Therefore, Peterson and Mooseker cloned Caco-2 $_{BBe}$ cells from the Caco-2 cell line by limiting dilution. Studies showed that these cells express brush border cytoskeleton that is comparable to that of the human enterocyte and have little morphological heterogeneity (Peterson and Mooseker 1992). And hence are more suitable as a model for the investigation of MLCP inhibition peptides.

*Aims of the chapter*

The main aims of this chapter are to determine whether inhibition of MLCP will open TJs thereby allowing absorption of impermeable drugs such as polymers and peptide drugs through the paracellular space. Myosin light chain phosphatase inhibition peptides will be based on both the PP1$\delta$ and CPI-17 protein sequences. These peptides will be synthesised by Fmoc solid-phase peptide synthesis followed

by HPLC purification. Then the ability of these peptides to increase paracellular permeability will be determined. This will be achieved by incubation of confluent Caco-$2_{BBe}$ monolayers with the MLCP inhibition peptides and monitoring any changes in TER. If any of the peptides are successful in decreasing TER then this peptide will be further tested for cytotoxicity and determination of any increases in permeability of different molecular weight fluorescein isothiocyanate dextrans will be measured.

## 4.2 Methods

First MLCP inhibition peptides (shown in table 4.1) were synthesised by Fmoc solid-phase peptide synthesis techniques and purified as described in the protocols outlined in sections 2.3.1 and 2.3.2.

Thiophosphorylation of the CPI-17 based inhibitor peptides were perfomed by incubating peptide with protein kinase C, catalytic subunit (PKC-M) was used as it is catalytically active but does not require $Ca^{2+}$ or phosphatidylserine for its activity. Thiophosphorylation of these peptides was done by dissolving the peptide in Tris, pH 7.2 containing 1 mM DTT to which 0.8 units/ml PKC-M, 20 mM and 1 mM ATPγS were added (VanRenterghem, *et al* 1994). Reaction mixtures were then incubated at 30 °C for 60 min, and terminated by heating at 70 °C for 20 min. The reaction mixtures were then centrifuged and the supernatant collected for MS analysis to confirm weather the T was thiophosphorylated.

Before examining the effects of the MLCP inhibition peptides on the TER of Caco-$2_{BBe}$ monolayers, a comparison between the TER measurements of monolayers grown on different inserts was performed. Caco-$2_{BBe}$ cells were cultured on Transwell-COL inserts (which have a PTFE membrane that have been treated with an equimolar mixture of types I and III bovine placental collagens) and Transwell inserts coated with type I collagen as described in section 2.3.11. Membranes were seeded as described in section 2.3.12 and the TER measured every other day for 21 days to compare the TER of Caco-$2_{BBe}$ monolayers grown on the different inserts.

Table 4.1 PP1δ and CPI-17 based MLCP inhibitor peptides.

| Peptide Acronym | Peptide Sequence |
|---|---|
| PP1δ based inhibitor | RKAKYQYRRK |
| CPI-17 based inhibitor 1 | RRVT*VKYDRR |
| CPI-17 based inhibitor 2 | RRKT*VKYKRR |
| CPI-17 based inhibitor 3 | RRKT*VKYDRR |
| CPI-17 based inhibitor 4 | RRVT*VKYKRR |

Amino acids are identified by single letter symbols and * indicates thiophosphorylation of threonine.

To determine the effectiveness of the synthesised peptides at reducing Caco-$2_{BBe}$ monolayer TER, complete media was removed and monolayers were washed with pre-warmed HBSS (buffered to pH 7.4 with 25 mM HEPES) the final wash with HBSS was left on the cells for 20 min. This mild "washing" step and 20 min incubation allows the monolayers to adapt to the new buffer and eliminates any residual enzyme activity from the serum. HBSS was used to maintain the pH of the solution during the experiment. Peptide was dissolved in HBSS at desired concentrations and added to the apical compartment and the TER measured at times 0.5, 1, 2, 3, 4, 5, 10, 20, 25, 30, 35, 40, 60 and 120 min. At 120 min the monolayers were washed gently with HBSS and fresh HBSS containing no peptide was added to the monolayers and the TER measured at times 140, 160, 180, 195, 210 and 240 min to determine if the reduction in TER caused by the peptide was reversible.

To determine whether the decreases in TER caused by the peptides were due to inhibition of MLCP and not via peptide cytotoxicity. The MTT assay as described in section 2.11.4 was used. Briefly the peptide at the concentration ranges used in the permeability studies were added to the Caco-$2_{BBe}$ monolayers for 1 h (the time taken for the peptide to reduce TER), wells were then washed with PBS and the MTT reagent added and cells incubated for a further 5 h. Then the media was removed and replaced with DMSO incubated for 30 min and absorbance read at 550 nm.

## 4.3 Results

### *4.3.1 Effects of collagen coating of Transwell inserts on TER*

The effect of different collagen coatings of Transwell inserts on Caco-$2_{BBe}$ monolayers TER was initially assessed before commencement of TER and transport studies. The TER of Caco-$2_{BBe}$ monolayers grown on both the collagen coated Transwell filters and Transwell-COL inserts began to plateau at day 12. The TER of Caco-$2_{BBe}$ cells monolayers at day 21 cultured on Transwell-COL inserts was 223 $\Omega$ $cm^2$ were not significantly different to the TER of the monolayers cultured on polycarbonate inserts coated with type I collagen which was 224 $\Omega$ $cm^2$ (figure 4.4).

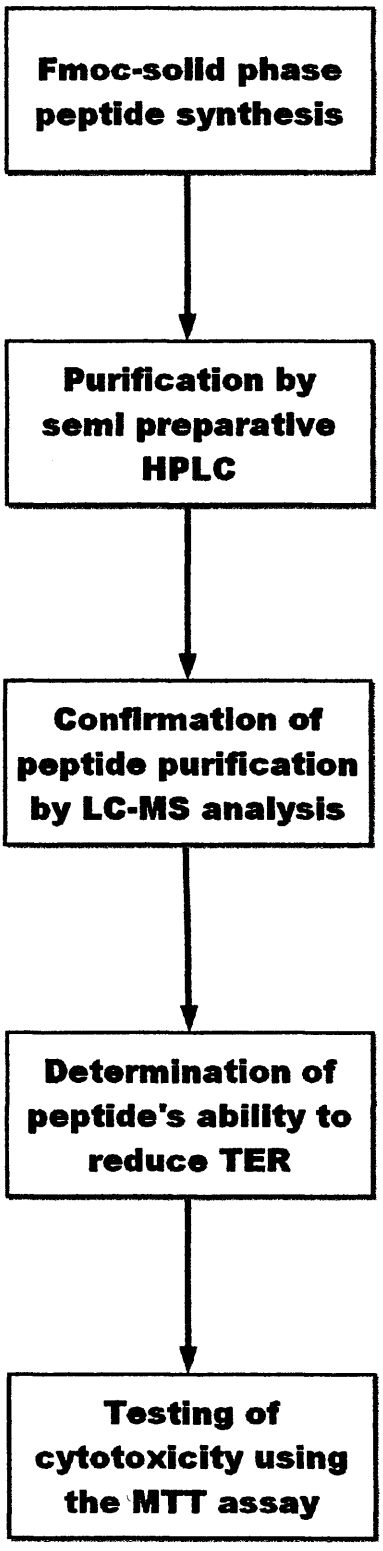


Figure 4.3 Summary of the techniques used to synthesise MLCP inhibition peptides.

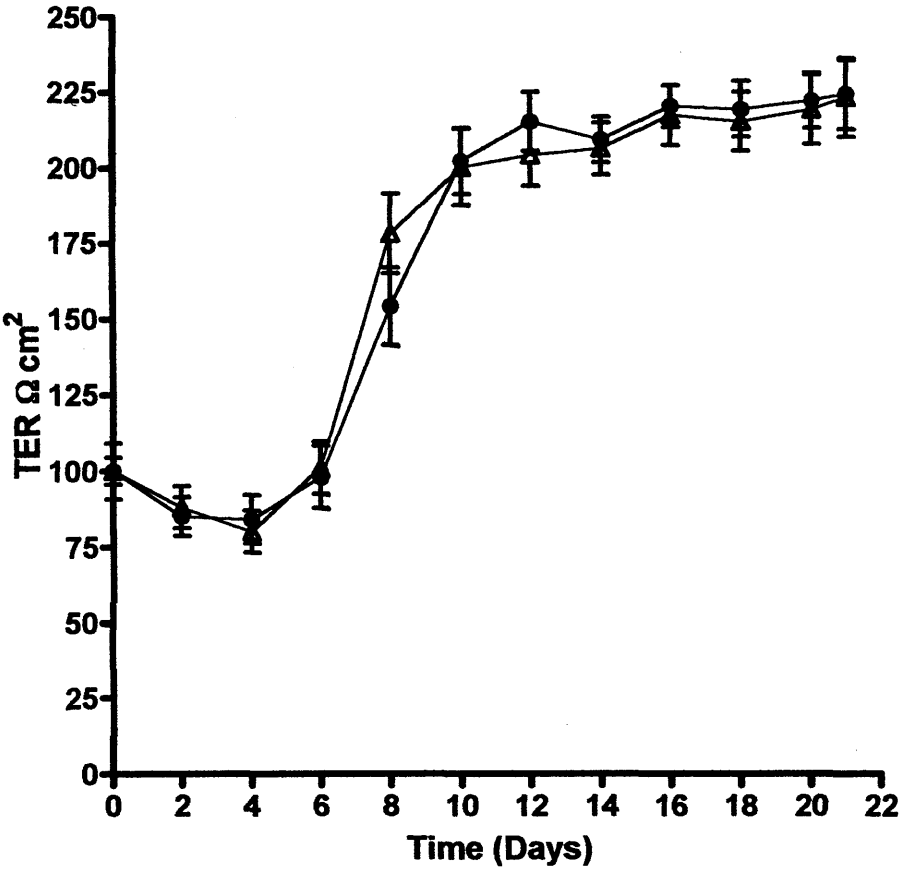


Figure 4.4 Effects of Transwell insert coating on the TER of Caco-$2_{BBe}$ monolayers. TER values for Caco-$2_{BBe}$ cells cultured on Transwell-COL inserts (△) and Transwells coated with type I collagen (●). Statistical analysis between monolayers cultured on Transwell-COL inserts and Transwells coated with type I collagen was determined using a student's t-test. (Data represents mean ± SD n=3, error bars are within plot symbols when not visible).

### 4.3.2 Design of a MLCP inhibition peptide based on PP1δ and its ability to reduce of TER

Since the synthesis of thiophosphorylated peptides was unsuccessful it was decided to design an alternative MLCP inhibitor. Protein phosphatase 1δ amino acids 300 to 309 have been shown to be important in binding to MYPT1, in particular $Y^{305}$ and $Y^{307}$ (Terrak, *et al* 2004), therefore RKAKYQYRRK which contains $^{301}$KAKYQY$^{306}$ of PP1δ with additional R and K residues was synthesised. The dose response of RKAKYQYRRK peptide (figure 4.5A) was assessed, these results show that incubation of Caco-$2_{BBe}$ monolayers with 5 mM RKAKYQYRRK peptide resulted in a significant reduction of TER compared to control monolayers to approximately 50 % of the initial TER within 30 sec of its addition. This reduction was maintained for the 2 h of the experiment. Addition of 1 mM to the monolayers led to a reduction in TER to approximately 20 % of the original TER although the reduction was not significant. Incubation of 0.5, 0.25 and 0.125 mM of RKAKYQYRRK peptide did not result in significant alterations in TER compared to the control monolayers.

Following 2 h incubation of the Caco-$2_{BBe}$ monolayers with peptide the monolayers were washed and the TER monitored for recovery for an additional 2 h (figure 4.5B). These results show that there was a very small recovery of TER following addition of 5 mM of RKAKYQYRRK peptide however the TER did not reach to 50 % of the initial value. There appeared to be no recovery of TER of monolayers incubated with 1 mM.

### 4.3.3 Assessment of RKAKYQYRRK peptide cytotoxicty

The MTT assay was used initially to determine the growth rate of Caco-$2_{BBe}$ cells in different conditions used in these studies. Wells were seeded at a density of 15,528 cells/cm$^2$ and cultured for 2 days (Bromberg and Alakhov 2003) and at 10,000 cells/cm$^2$ and cultured for 21 days as used for the culture of Transwell inserts (figure 4.6). Before commencement of peptide cytotoxicity assessment, the cytotoxicity of the commonly used cytotoxic and non-toxic polymers polyethylenimine (PEI) and dextran respectively in Caco-$2_{BBe}$ cells was assessed. Cytotoxicty was assessed at 2 and 21 days post seeding at seeding densities of 15,528 cells/cm$^2$ (Bromberg and Alakhov 2003) and 10,000 cells/cm$^2$ respectively. Dextran

A

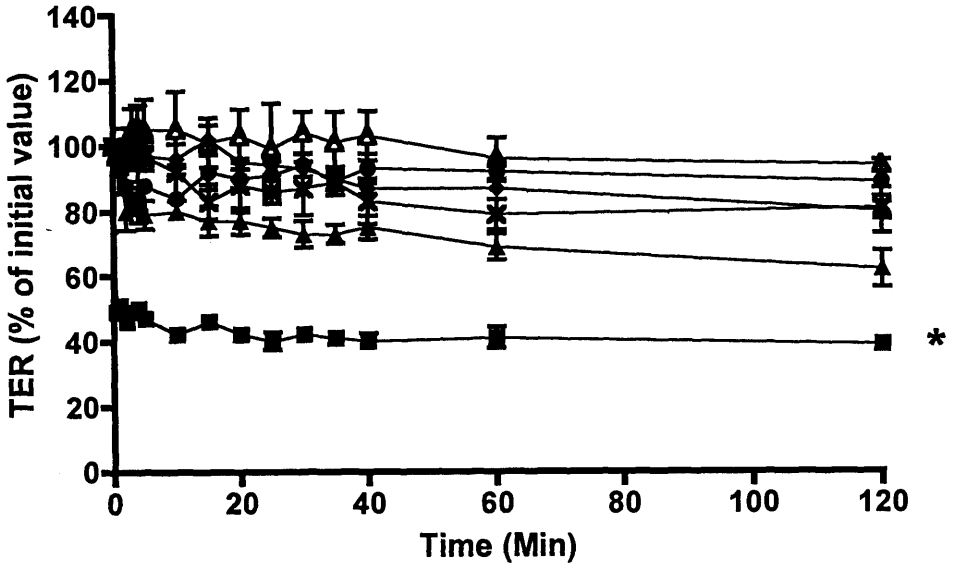


B

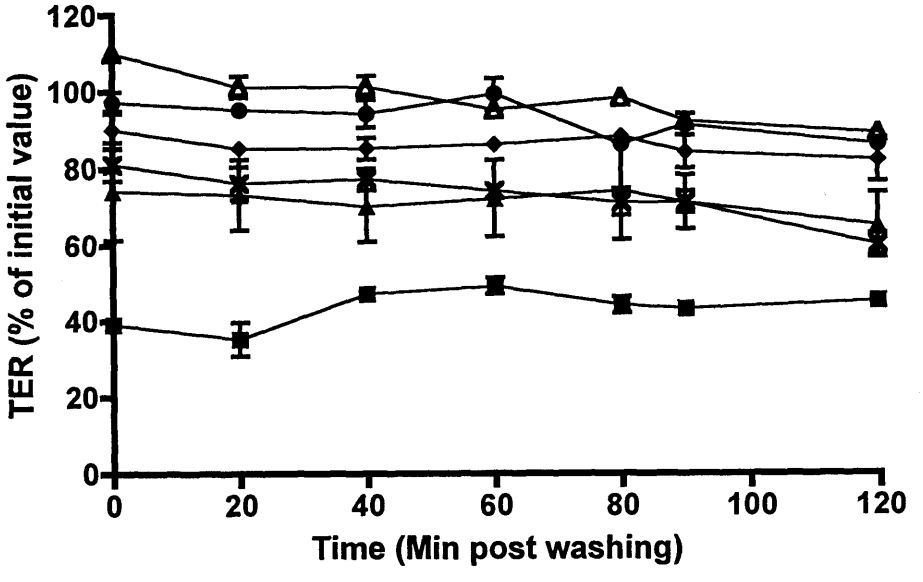


Figure 4.5 Decreases in TER induced by RKAKYQYRRK peptide. TER following incubation with RKAKYQYRRK peptide for 2 h (A) and TER post washing (B). Control (◆), 0.125 mM (●), 0.25 mM (△), 0.5 mM (✕), 1 mM (▲) and 5 mM (■). Statistical analysis between concentrations were determined at $p < 0.001$ (*) using two-way ANOVA and Bonferroni post hoc test. (Data represents mean TER normalised to the value at time zero ± SEM n=3, error bars are within plot symbols when not visible).

A

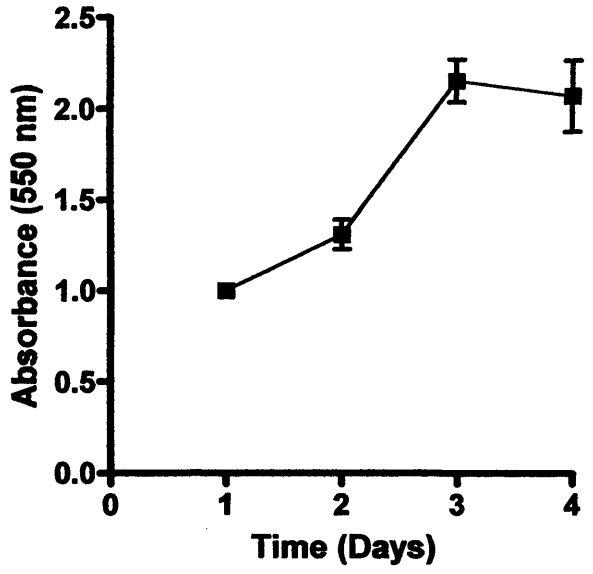


B

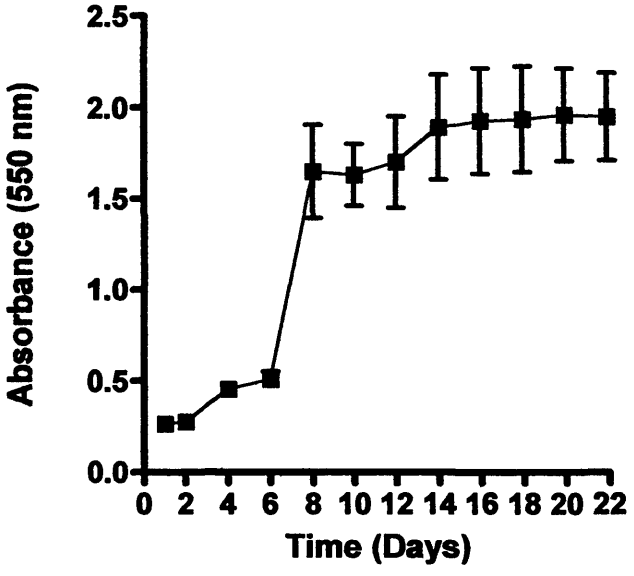


Figure 4.6 Cell proliferation of Caco-$2_{BBe}$ cells measured with the MTT assay. Cells were seeded at a density of 15,528 cells/cm$^2$ (A) and 10,000 cells/cm$^2$ (B). (Data represents mean ± SD n = 3. Error bars are within plot symbols when not visible).

was not toxic at concentrations of up to 1 mg/ml with no significant difference between cells seeded for 2 or 21 days prior to cytotoxicity testing. There was also no significant difference between PEI cytotoxicity of cells grown for 2 or 21 days (figure 4.7). The calculated 2 day $IC_{50}$ value of 0.08 mg/ml and a 21 day $IC_{50}$ value 0.06 mg/ml (table 4.2).

As there was little recovery of the TER when monolayers were incubated with RKAKYQYRRK, a MTT assay was performed to test for cytotoxicity. These results show that RKAKYQYRRK peptide is toxic at the concentrations required for TER reduction with an $IC_{50}$ value of 0.72 mM (figure 4.8). As observed in chapter 3 PKA activity studies, contaminants within the peptide not detected by LC-MS alter the function of the peptide. Therefore, a new batch of the RKAKYQYRRK peptide was synthesised then a MTT assay was performed. This peptide had an increased $IC_{50}$ value of 2.61 mM (figure 4.9). This peptide was then added to the Caco-$2_{BBe}$ monolayers at concentrations of 0.125 mM, 0.25 mM, 0.5 mM, 1 mM and 5 mM, peptide concentrations of up to 1 mM did not significantly reduce TER, only the cytotoxic concentration of 5 mM resulted in a significant decrease in TER (figure 4.10).

### *4.3.4 Design of MLCP inhibition peptide based on CPI-17*

Amino acids $T^{38}$ and $^{41}YDRR^{44}$ have been shown to be important in the inhibitory function of CPI-17 (Hayashi, *et al* 2001), therefore peptides were designed based on the $^{34}RVTVKYDRR^{44}$ sequence of CPI-17 which can be seen in table 4.1. CPI-17 based inhibitor 1 was identical to amino acids 34 to 44 with an extra R added to the C-terminal end. CPI-17 based inhibitor 2 was based on CPI-17 based inhibitor 1 except that $V^{37}$ and $D^{42}$ were changed to K and CPI-17 based inhibitor 3 where $V^{37}$ has been changed to K, finally CPI-17 based inhibitor 4 where $D^{42}$ was substituted for K. Thiosphosphorylation of these peptides as described in the methods was not successful at various concentrations of peptide an example of which can be seen in figure 4.11. In this reaction 0.5 mg of CPI-17 based inhibitor 1 peptide was incubated with 0.8 units/ml PKC-M.

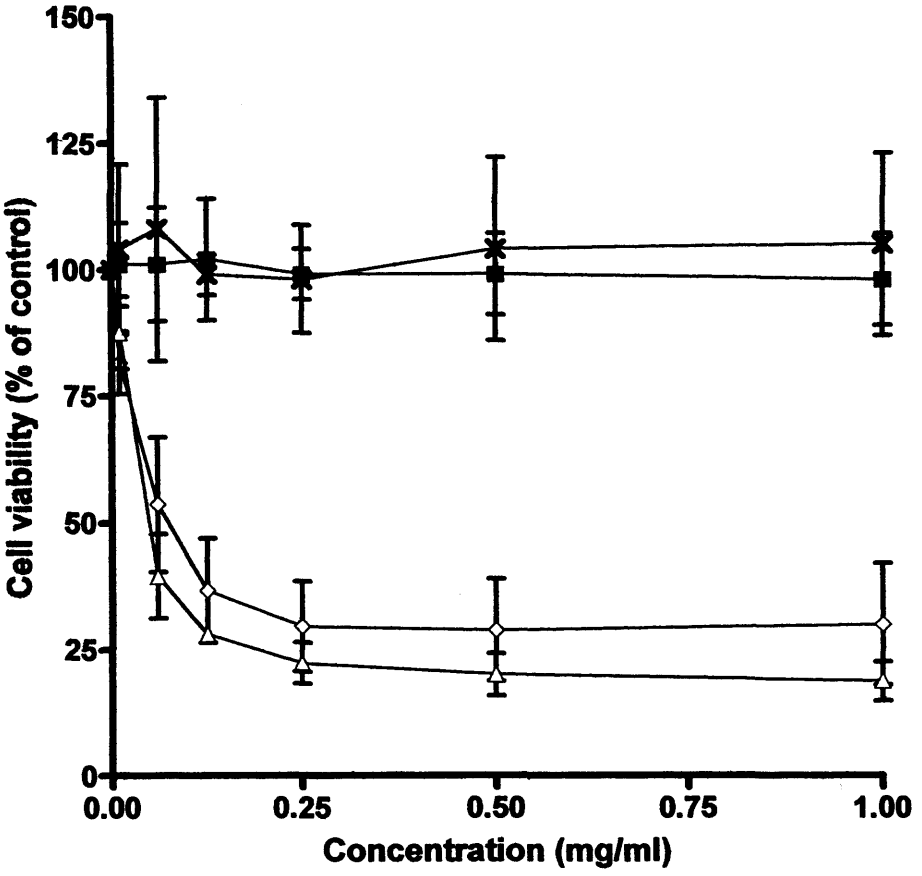


Figure 4.7 Cytotoxicity of PEI and dextran. Cells 2 days following seeding incubated with PEI (◇) and dextran (✕) and 21 post seeding incubated with PEI (△) and dextran (■). Statistical difference between the toxicity of PEI and dextran on cells cultured for 2 and 21 days was determined using a student's t-test. (Data show cell viability as percentage of untreated control cells and represent mean ± SD n=3, error bars are within plot symbols when not visible).

Table 4.2 Summary of $IC_{50}$ values[†] for PEI and dextran in Caco-$2_{BBe}$ cells[*].

| Seeding density (cells/cm$^2$) | Days post confluence | Compound | $IC_{50}$ values in mg/ml (± SEM) |
|---|---|---|---|
| 15,528 | 2 | PEI | 0.08 (0.02) |
| 10,000 | 21 | PEI | 0.06 (0.01) |
| 15,528 | 2 | Dextran | > 1 |
| 10,000 | 21 | Dextran | > 1 |

[*] Inhibitory concentration at which 50 % cell death occurs calculated using the MTT assay following 2 h exposure to polymer.

[†] Data show the mean (n=3)

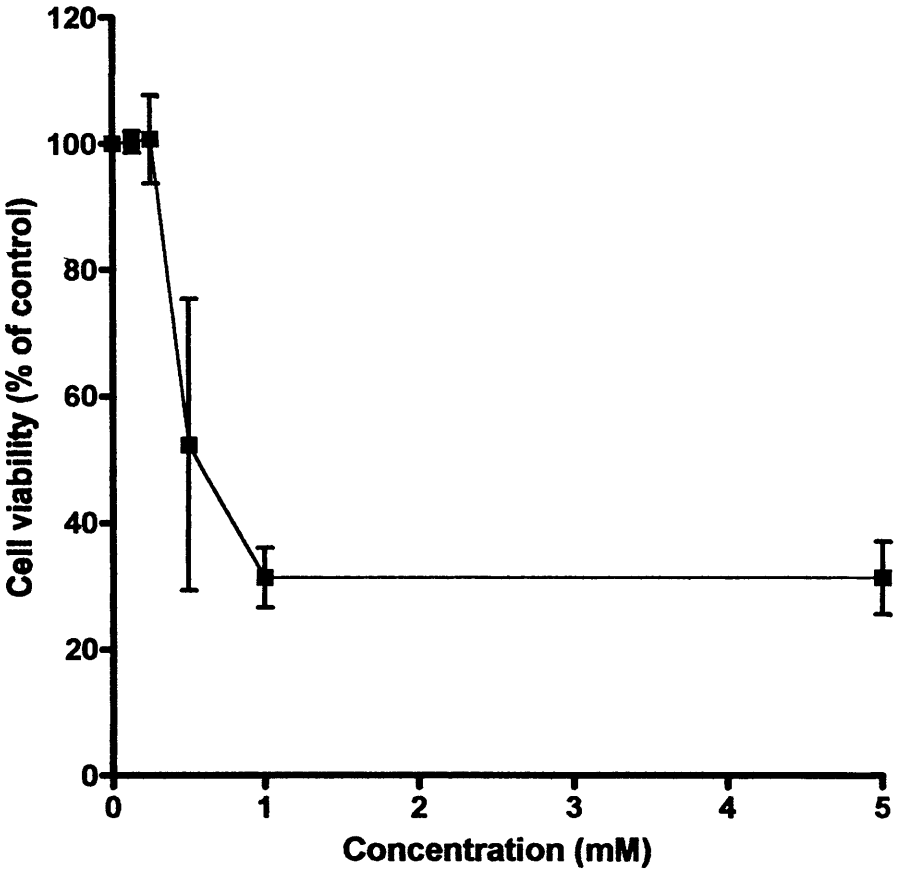


Figure 4.8 Effects of RKAKYQYRRK peptide on Caco-$2_{BBe}$ cell viability. Inhibitory concentration at which 50 % cell death occurs calculated as 0.72 mM (± 0.20 SD) using the MTT assay following 1 h exposure to RKAKYQYRRK peptide. (Data show cell viability as percentage of untreated control cells and represent mean ± SD n=3, error bars are within plot symbols when not visible).

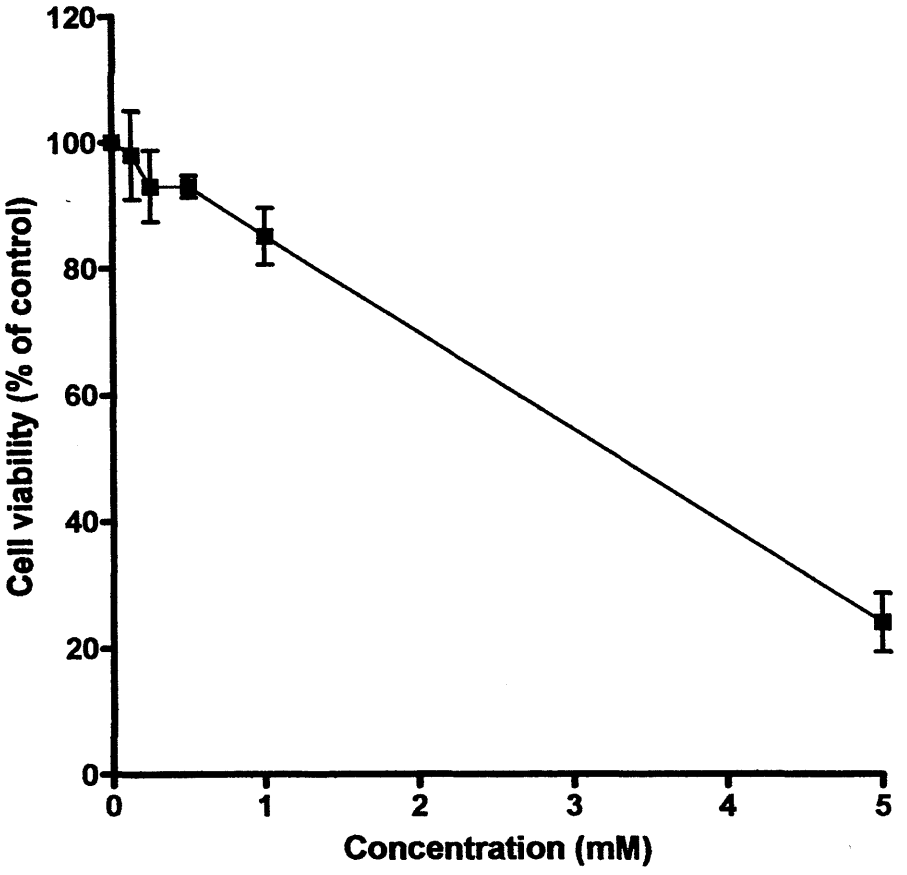


Figure 4.9 Effects of new batch RKAKYQYRRK peptide on Caco-$2_{BBe}$ cell viability. Inhibitory concentration at which 50 % cell death occurs calculated as 2.61 mM (± 0.16 SD) using the MTT assay following 1 h exposure to new batch RKAKYQYRRK peptide. (Data show cell viability as percentage of untreated control cells and represent mean ± SD n=3, error bars are within plot symbols when not visible).

A

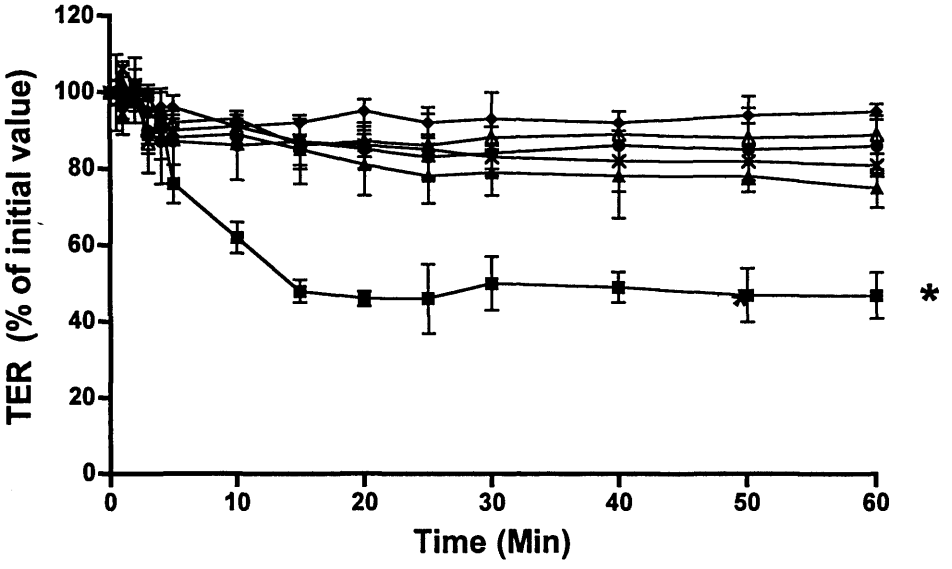


B

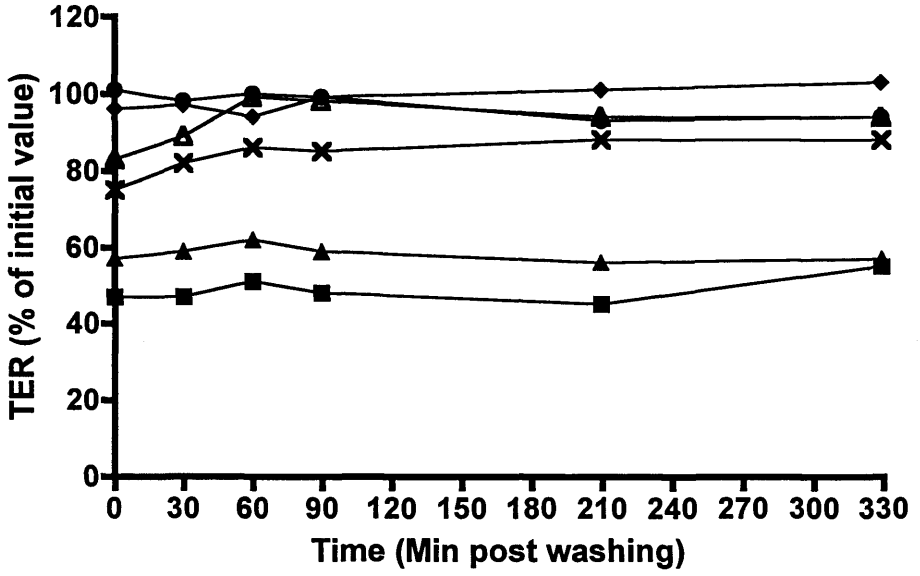


Figure 4.10 Alterations of TER by the new batch of RKAKYQYRRK peptide. TER following incubation with peptide for 1 h (A) and post washing (B). Control (◆), 0.125 mM (●), 0.25 mM (△), 0.5 mM (✕), 1 mM (▲) and 5 mM (■). Statistical analysis between concentrations were determined at $p < 0.001$ (*) using two-way ANOVA and Bonferroni post hoc test. (Data represents TER normalised to the value at time zero ±SD n=3, error bars are within plot symbols when not visible).

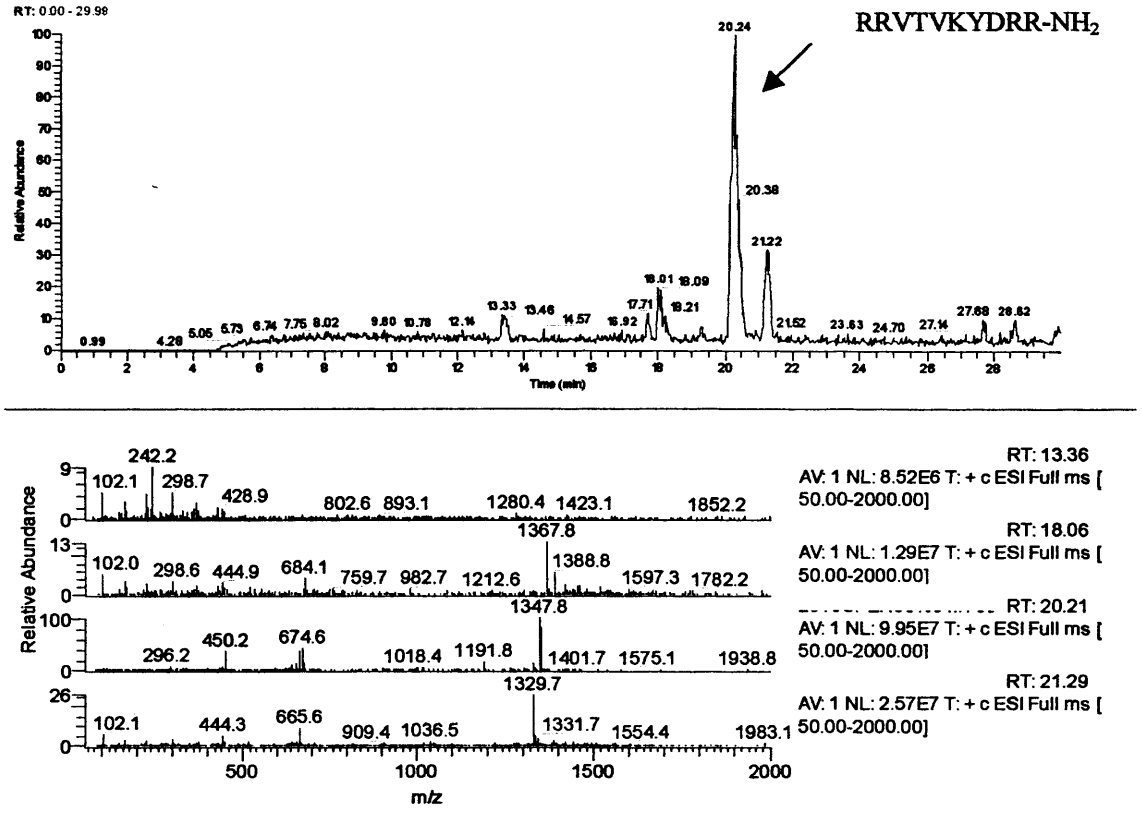


Figure 4.11 LC-MS analysis thiophosphorylation reaction of CPI-17 based inhibitor 1. Reaction mixture contained 0.5 mg CPI-17 based inhibitor 1 incubated with 0.8 units/ml PKC-M for 60 min at 30 °C.

### *4.3.5 Investigation of RRVEVKYDRR peptide as a potential absorption enhancer*

Initially biotin labelled RRVEVKYDRR peptide was synthesised as described in section 2.3.1, the HPLC chromatogram detected 1 prominent component with a predicted molecular mass of 1601 Da as analysed by MS analysis (figure 4.12). The MS also detected a peak at 801 Da (biotin- RRVEVKYDRR carrying 2 charges.

Following the experience of the above peptide it was decided to perform MTT assays before commencement of TER studies. RRVEVKYDRR peptide (PIP) was not toxic at concentrations of up to 5 mM (figure 4.13). Then this peptides effect on Caco-$2_{BBe}$ monolayer TER was measured (figure 4.14). These results show that 5 mM PIP resulted in a significant decrease in TER compared to the control monolayers. PIP reduced TER to approximately 50 % following 30 min incubation, which stabilised for the remaining 30 min of the experiment. There was no significant difference in TER values between the control and addition of 1 mM PIP to the Caco-$2_{BBe}$ monolayers. Following 60 min incubation the monolayers were washed gently and the TER measured at 24 h, the TER of the monolayers incubated with 5 mM PIP at 24 h increased from approximately 50 % before removal of the peptide to 80 %.

### *4.3.6 Increasing the permeability of RRKEVKYDRR across cell membranes*

As relatively high concentrations of RRVEVKYDRR peptide were required for significant reductions in TER. Valine[3] was substituted for the positively charged K giving RRKEVKYDRR peptide ($PIP_{K3}$). $PIP_{K3}$ was not toxic at concentrations of up to 5 mM like PIP (figure 4.15). The effect of RRKEVKYDRR peptide on Caco-$2_{BBe}$ monolayer TER was then assessed (figure 4.14). Five mM of $PIP_{K3}$ resulted in a reduction in TER to approximately 80 %, whereas 1 mM reduced TER to approximately 75 % within 60 min of addition to monolayers. However, $PIP_{K3}$ at concentrations of up to 5 mM did not produce significant reductions in TER when compared to control monolayers.

## 4.4 Discussion

Different methods have been used to culture Caco-$2_{BBe}$ cells on Transwell inserts, some coat the polycarbonate Transwells inserts with type I rat tail collagen

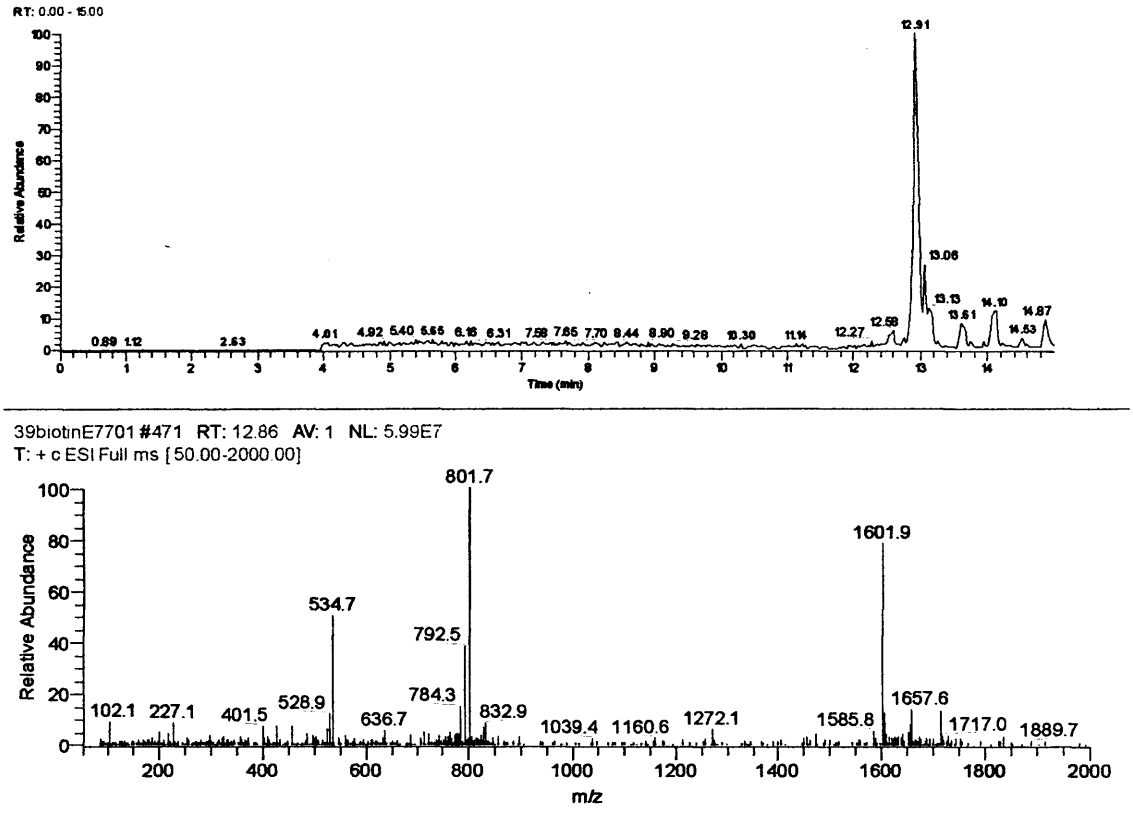


Figure 4.12 LC-MS analysis of biotin labelled RRVEVKYDRR peptide. LC-MS analysis of biotin-RRVEVKYDRR showing breakdown pattern in positive ion mode.

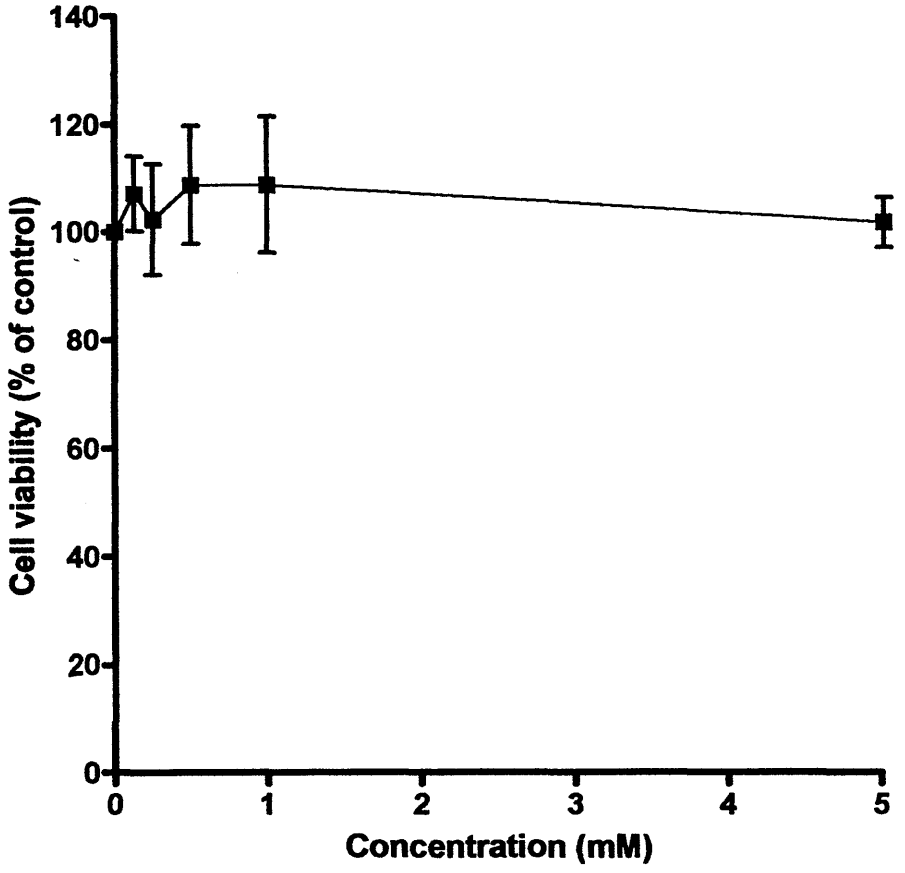


Figure 4.13 RRVEVKYDRR peptide effects on Caco-$2_{BBe}$ cell viability. Inhibitory concentration at which 50 % cell death occurs calculated as > 5 mM using the MTT assay following 1 h exposure to RRVEVKYDRR peptide. (Data show cell viability as percentage of untreated control cells and represent ± SD n=3, error bars are within plot symbols when not visible).

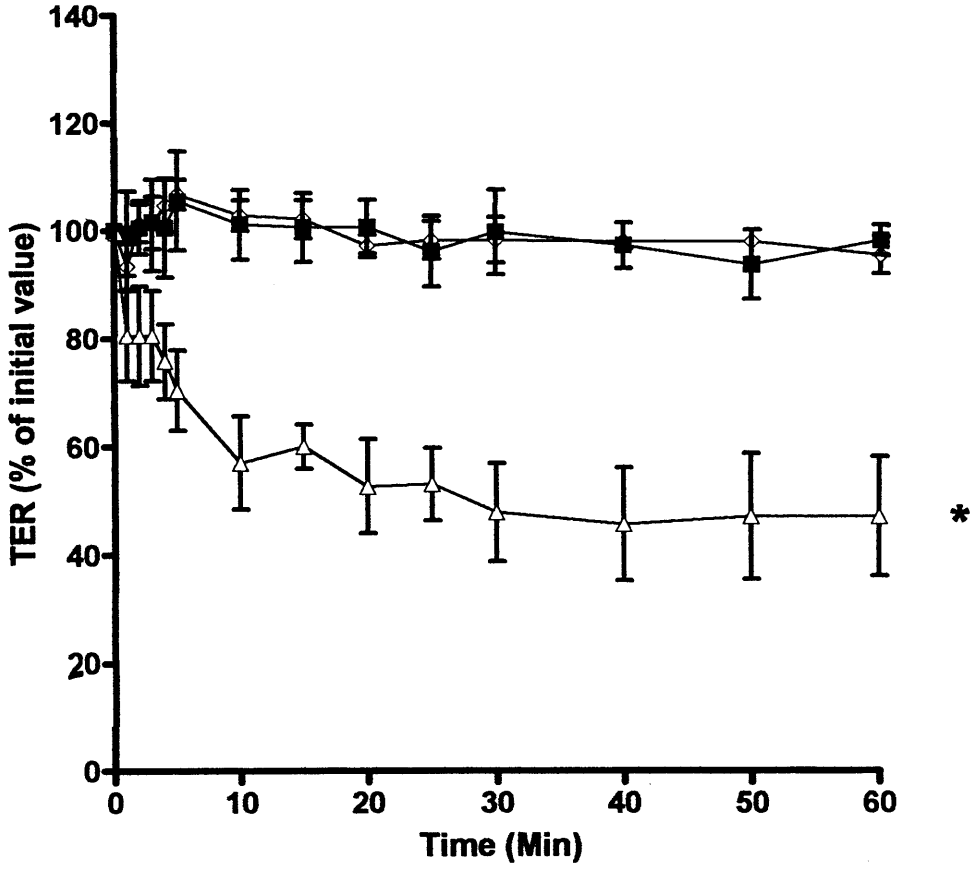


Figure 4.14 Effect of PIP on TER of Caco-$2_{BBe}$ monolayers. Control (◇), 1 mM (■) and 5 mM (△). The TER of monolayers incubated with 5 mM PIP returned to 80 % of the initial value 24 h after washing the monolayers. Statistical analysis between the concentrations were determined at $p < 0.001$ (*) using two-way ANOVA and Bonferroni post hoc test. (Data represents TER normalised to the value at time 0 ± SD n=3, error bars are within plot symbols when not visible)

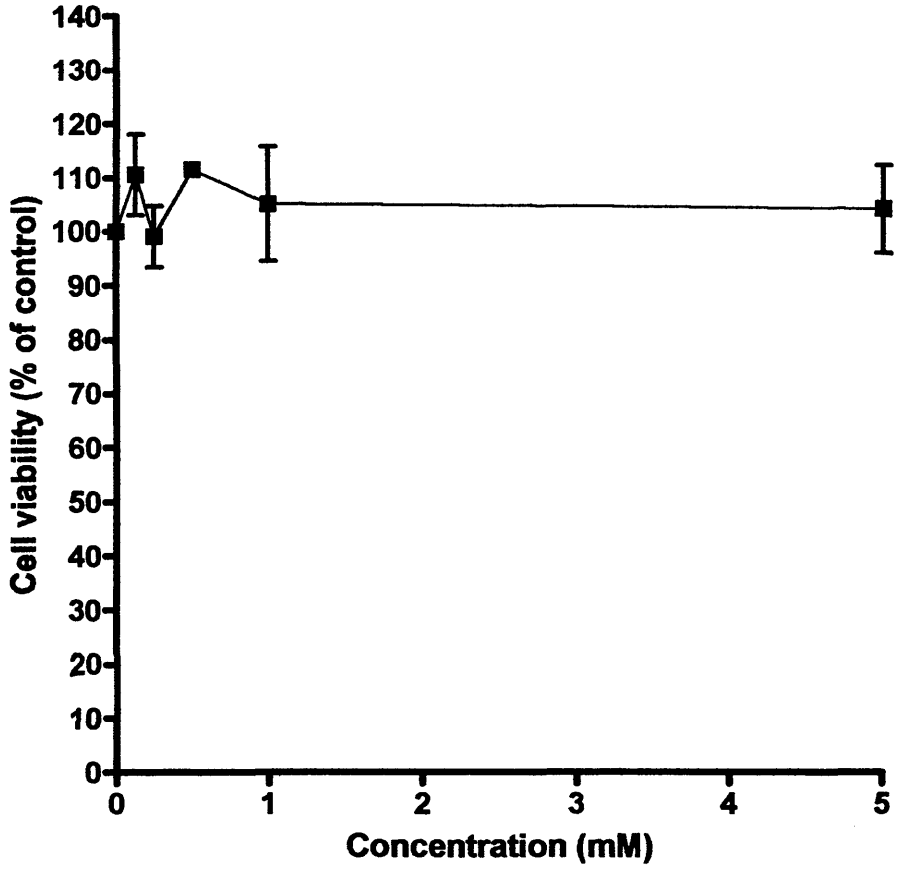


Figure 4.15 $PIP_{K3}$ effects on Caco-$2_{BBe}$ cell viability. Inhibitory concentration at which 50 % cell death occurs calculated as > 5 mM using the MTT assay following 1 h exposure to $PIP_{K3}$. (Data show cell viability as percentage of untreated control cells and represent ± SD n=3, error bars are within plot symbols when not visible).

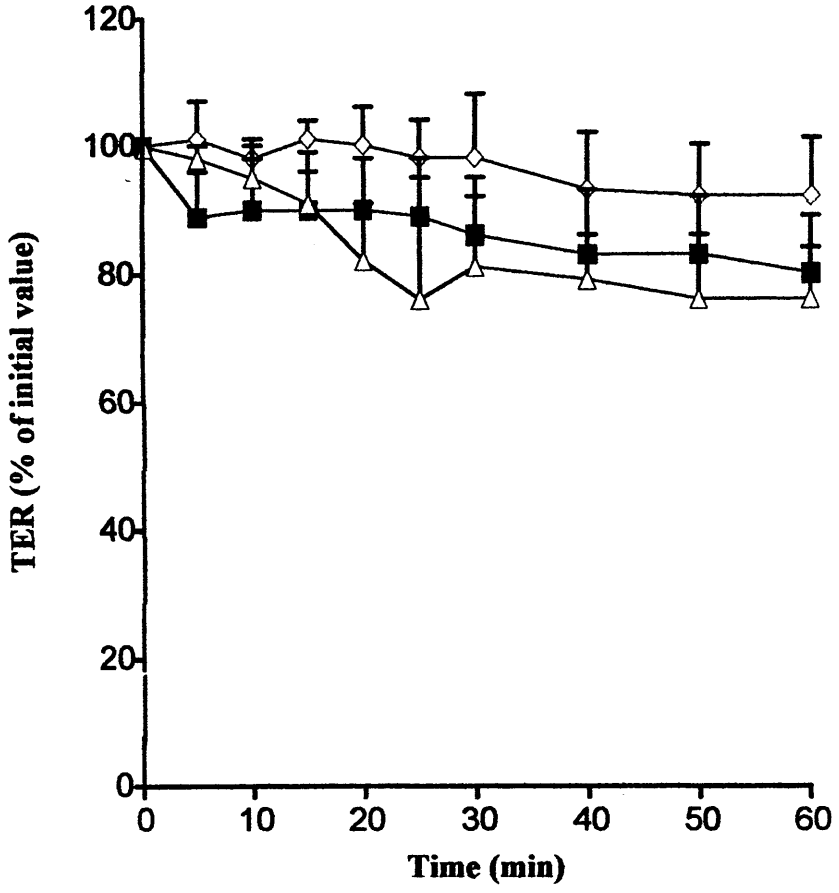


Figure 4.16 Effect of $PIP_{K3}$ on TER of Caco-$2_{BBe}$ monolayers. Control (◇), 1 mM (■) and 5 mM (△). Statistical analysis between the concentrations were determined at $p < 0.001$ (*) using two-way ANOVA and Bonferroni post hoc test. (Data represents TER normalised to the value at time 0 ± SD n=3, error bars are within plot symbols when not visible).

others purchase Transwell-COL (PFTE inserts coated with type I and III bovine placental collagens). Coating of Transwell filters is important, as extracellular matrix proteins such as collagen, improve the rate of cell attachment and spreading on the insert surface. The method by which the Transwells inserts were coated with collagen did not affect the Caco-$2_{BBe}$ monolayer TER. By day 12 the TER of the monolayers on both types of Transwells began to plateau. By day 21 the TER of the Caco-$2_{BBe}$ monolayers grown on the Transwell-COL inserts was 223 $\Omega$ $cm^2$, whilst the monolayers grown on the polycarbonate insert coated with type 1 collagen was 224 $\Omega$ $cm^2$. The TER value of Caco-$2_{BBe}$ monolayers obtained were comparable to those published (Zolotarevsky, *et al* 2002). This value also established the TER of confluent Caco-$2_{BBe}$ monolayers, so that the TER of the Caco-$2_{BBe}$ monolayers would have to reach this value before they would be used for experiments. Caco-2 cells are cultured for 21 days, as a good correlation between drug permeability in 21-day cultured Caco-2 monolayers and the oral absorption of the same drug in humans has been shown (Artursson and Karlsson 1991).

In order for a MLCP inhibition peptide to be effective it must first be able to cross biological membranes. Peptides that can rapidly transfect primary non--dividing cells without the aid of active transport are called cell-penetrating peptides (CPP). These peptides have cationic sequences of 10 to 30 amino acids in length. HIV-1 TAT was the first CPP to be discovered during investigation of HIV-1 TAT transactivation protein (a protein 86 amino acids in length) ability to internalise into cells (Jones, *et al* 2005). Other examples of identified CPPs and their amino acid sequences can be seen in table 4.3.

The ability of CPPs to cross cell membranes is not fully understood as these peptides are basic and hydrophilic, whereas the cell membrane is a hydrophobic barrier and hence considered to be impermeable to hydrophilic molecules without the aid of active transport (Futaki, *et al* 2003). There are no sequence similarities between the different CPPs (table 4.3) except that they contain numerous R residues (Suzuki, *et al* 2002). Mitchell and co-workers demonstrated that polyarginine peptides entered cells more effectively than peptides containing poly K, ornathine or H residues. Peptides containing less than 5 R residues internalised into cells less effectively than those containing between 6 and 15 residues. Whereas peptides with greater than 15 R residues had reduced cellular internalised (Mitchell, *et al* 2000).

Table 4.3 Amino acid sequences of characterised CPPs.

| Peptide | Origin | Amino acid sequence | Reference |
|---|---|---|---|
| HIV-1 TAT | HIV-1 TAT transactivation protein. | YGRKKRRQRRR | (Vives, *et al* 1997) |
| Antennapedia | *Drosophila* transcription factor. | RQIKIWFQNRRMKWKK | (Derossi, *et al* 1994) |
| VP22 | Herpes simplex virus structural protein. | DAATATRGRSAASRPTERPRA-PARSASRPRRPVE | (Elliott and O'Hare 1997) |
| Transportan | The 12 functional amino acids from the N-terminus of the neuropeptide galanin linked with a K residue to the 14 amino acids of the wasp venom mastoparan. | GWTLNSAGYLLGKINLKALA-ALAKKIL | (Pooga, *et al* 1998) |
| pVEC | Derived from the murine cell adhesion molecule vascular endothelial cadherin | LLIILRRRIRKQAHAHSK | (Elmquist, *et al* 2001) |

The RKAKYQYRRK peptide, a peptide sequence corresponding to the C terminus of PP1δ (figure 4.15) was synthesised. Protein phosphatase 1 δ (also known as PP1β) lacks substrate specificity this is achieved via interactions with numerous regulatory subunits. Protein phosphatase 1 is regulated in smooth muscle via MYPT (Hartshorne and Hirano 1999). Myosin-targeting subunit binds to PP1 via the RVxF binding motif, however structural elements either side of RVxF are located in a manner that results in distinct reshaping of PP1 catalytic cleft, thereby augmenting myosin specificity of this complex. MYPT binds with PP1 via 3 different regions: the RVxF binding motif, the N-terminal arm and the 2$^{nd}$ group of ankyrin repeats (Terrak, *et al* 2004).

Terrak and co-workers crystal structure of MYPT bound to PP1δ showed that $E^{300}$ to $E^{309}$ of PP1δ are positioned between 2 ankyrin repeats of MYPT, in particular the ankyrin repeats bind with $Y^{305}$ and $Y^{307}$. Suggesting that the C terminus of PP1δ is important for regulatory subunit interaction to mediate isoform specificity. Therefore, a peptide corresponding to this area may prevent MYPT binding to PP1δ and hence diminish myosin specificity of the MYPT/PP1δ complex (Terrak, *et al* 2004). Therefore, RKAKYQYRRK corresponds to $^{301}$KAKYQY$^{306}$ of PP1δ. Where an extra R residue was placed on the C terminus and RRK to the N terminus, to increase the amount of positively charged residues of the peptide, in particular R residues, which has been shown to increase the internalisation of CPPs (Wender, *et al* 2000).

Addition of 5 mM RKAKYQYRRK peptide to monolayers resulted in a significant reduction in TER to approximately 50 % within 30 sec of addition. Whilst addition of 1 mM led to a non significant decrease in TER to about 20 % within 5 min. Addition of 0.5, 0.25 and 0.125 mM did not significantly alter TER when compared to control monolayers. After 2 h incubation with the peptide the monolayers were washed and monitored for an additional 2 h for recovery. There was no significant recovery in TER, this could be due to the fact that the peptide is toxic to the cells or that the cells need to synthesise new proteins, in hindsight the TER should have been measured at 12 and 24 h to determine if the cells required time for protein synthesis.

| | | | | | |
|---|---|---|---|---|---|
| 1 | MADGELNVDS | LITRLLEVRG | CRPGKIVQMT | EAEVRGLCIK | SREIFLSQPI |
| 51 | LLELEAPLKI | CGDIHGQYTD | LLRLFEYGGF | PPEANYLFLG | DYVDRGKQSL |
| 101 | ETICLLLAYK | IKYPENFFLL | RGNHECASIN | RIYGFYDECK | RRFNIKLWKT |
| 151 | FTDCFNCLPI | AAIVDEKIFC | CHGGLSPDLQ | SMEQIRRIMR | PTDVPDTGLL |
| 201 | CDLLWSDPDK | DVQGWGENDR | GVSFTFGADV | VSKFLNRHDL | DLICRAHQVV |
| 251 | EDGYEFFAKR | QLVTLFSAPN | YCGEFDNAGG | MMSVDETLMC | SFQILKPSEK |
| 301 | **KAKYQY**GGLN | SGRPVTPPRT | ANPPKKR | | |

Figure 4.15 Amino acid sequence of PP1δ catalytic subunit (Shimizu, *et al* 1994). The amino acids used to synthesise the RKAKYQYRRK peptide are in bold and underlined.

Numerous studies have shown that polycations such as poly-L-lysine and poly-L-arginine induce cellular damage in various cultured cells (Schirmbeck, *et al* 2003). As RKAKYQYRRK peptide contains many R and K the cytotoxicity of the peptide was assessed using the MTT assay. This assay measures the activity of mitochondrial dehydrogenase, indicating the amount of viable cells compared to the untreated control cells (Mosmann 1983).

In order to determine if the MTT assay was suitable for cytotoxicity studies in Caco-$2_{BBe}$ cells, the cytotoxicity of the commonly used positive control polyethylenimine (PEI) was established. This polymer is highly branched synthetic polycation that has a high charge density compared to most polycations of the same size. High molecular weight PEI was used as polymer cytotoxicity increases with polymer molecular weight and that polycations are more cytotoxic than polyanions. High molecular weight PEI flexible structure allows it to electrostatically interact with the cell membrane, inducing curvature, thereby destroying the integrity of the cell membrane (Fischer, *et al* 2003). The highly water-soluble polysaccharide dextran was used as a negative control. Dextrans are biologically inert due to their poly-(α-D-1,6-gluocse) linkages, which are resistant to the majority of cellular glycosidases.

To determine the seeding density of cells used for this experiment, 2 different methods were used. Cells were seeded at a density of 15,528 cells/cm$^2$ and grown for 2 days as per Bromberg and Alakhov (Bromberg and Alakhov 2003), and at a density of 10,000 cells/cm$^2$ and grown for 21 days as for culture of cell on Transwell inserts. As expected PEI was cytotoxic towards the Caco-$2_{BBe}$ cells with the 2-day $IC_{50}$ of PEI was 0.08 mg/ml and the 21-day PEI was 0.06 mg/ml, whereas dextrean was not cytotoxic at concentrations of up to 1 mg/ml. These results show that the seeding densities and the duration of culture used did not significantly alter the $IC_{50}$ of PEI. Therefore the method described by Bromberg and Alakhov is a rapid way of determination of peptide cytotoxicity.

The $IC_{50}$ value of RKAKYQYRRK peptide was 0.72 mM, however 5 mM was the minimum concentration required to see a significant reduction of TER. Therefore, a pathophysiological process rather than a physiological one caused RKAKYQYRRK peptide effect on TER. Another batch synthesis of RKAKYQYRRK peptide was performed, this batch of peptide had a $IC_{50}$ value of

2.61 mM which is higher than that of the original batch ($IC_{50}$ value 0.72 mM). This could be due to batch-to-batch difference. The second batch of this peptide when added to Caco-$2_{BBe}$ monolayers only produced a significant reduction of TER at 5 mM, a concentration higher than the $IC_{50}$ value. In conclusion, RKAKYQYRRK peptide does not reduce TER in a physiological manner and hence is not suitable for use as an absorption enhancer.

As the PP1δ peptide was toxic at the concentrations required for reduction in TER, the MLCP inhibition peptides based on CPI-17 based inhibitors were synthesised. These peptides were based on the $^{34}$RVTVKYDRR$^{44}$ sequence of CPI-17. CPI-17 based inhibitor 1 (RRVTVKYDRR) where a R residue on the C-terminal end was added to increase the peptide cationic charge. CPI-17 based inhibitor 2 (RRKTVKYKRR) where $V^{37}$ and $D^{42}$ where substituted for the positively charged K to further increase cationic charge. However, substitution of 2 amino acids may result in a loss of any peptide activity, especially $D^{42}$ which has been shown to be important in CPI-17 inhibitory activity. Therefore CPI-17 based inhibitor 3 (RRKTVKYDRR) and CPI-17 based inhibitor 4 (RRVTVKYKRR) have only 1 amino acid substituted $V^{37}$ and $D^{42}$ to K respectively. Threonine residues were thiophosphorylayed with ATPγS as they are more resistant to phosphatase activity than T phosphorylated only (Gratecos and Fischer 1974). The peptides designed proved difficult to thiosphosphorylate and many different concentrations of peptide were used ranging from 1 mg to 0.1 mg. Rat brain PKC has been used to thiophosphorylate CPI-17 by Eto and colleagues, however their study involved the use of CPI-17 protein not just a peptide fragment (Eto, *et al* 1997). Perhaps there are important amino acids that are involved in the binding of PKC to CPI-17 which are not present in the peptide sequence.

As the initial CPI-17 based inhibitory peptides where difficult to thiophosphorylate and the RKAKYQYRRK peptide (based on PP1δ MYPT binding domain) was toxic at the concentration required for TER reduction. Another peptide was designed this peptide RRVEVKYDRR was again based on the $^{34}$RVTVKYDRR$^{44}$ sequence, however $T^{38}$ was altered to the negatively charged E in order to mimic the negative charge of thiophosphorylated T. As the previous CPI-17 sequence based inhibition peptides, 2 R residues were added to the C terminus.

However, studies by Hayashi and colleagues demonstrated that substitution of $T^{38}$ to E resulted in a loss of CPI-17 inhibitory activity (Hayashi, *et al* 2001). Phosphorylation of T is thought to induce a conformational change of CPI-17 and the phosphate binds to PP1 active site (Matsuzawa, *et al* 2005). However, $T^{38}$ is not required for conformational change of the RRVEVKYDRR peptide like the CPI-17 protein and hence may remain active.

PIP was not toxic at concentrations up to 5 mM according to the MTT assay. Incubation of Caco-$2_{BBe}$ monolayers with 5 mM PIP reduced TER by 50 % within 25 min of its addition, after which the TER remained constant. Following gentle washing of the monolayer the TER recovered to 80 % 24 h post washing. These studies show that PIP decreases TER of Caco-$2_{BBe}$ monolayers in a physiological manner and not a pathological one, as the peptide was not toxic according to the MTT assay. As PIP was able to cross biological membranes and inhibit MLCP, this peptide was called membrane **P**ermeant **I**nhibitor of myosin light chain **P**hosphatase (PIP). It is envisaged that PIP binds at the active site of PP1, as Matsuzawa *et al,* phospho-pivot models predicts that $T^{38}$ of CPI-17 binds to PP1 active site as a competitive inhibitor, additionally the positive charges of both $R^{33}$ and $R^{36}$ of CPI-17 are near to $E^{274}$ of PP1, a sequence unique to Ser/Thr phosphatases (Matsuzawa, *et al* 2005). Thereby, suggesting that PIP binds directly to PP1 active site thereby inhibiting its activity, this data also indicates that the phosphate group is essential for conformational change of CPI-17 but not for its ability to bind to PP1 active site.

To determine the importance of $V^3$ in PIP inhibitory activity this amino acid was substituted for a K residue. Normally amino acids are substituted for an A residue. However, as PIP decreased the TER of Caco-$2_{BBe}$ monolayers at a relatively high concentration of 5 mM, possibly due to the fact that PIP is not readily internalised into cells. $Valine^3$ was substituted for the positively charged K (RRKEVKYDRR), in order to attempt to increase cell permeability by increasing cationic charge (Mitchell, *et al* 2000). Incubation of $PIP_{K3}$ with the Caco-$2_{BBe}$ monolayers at the concentrations 1 mM and 5 mM, resulted in a non-significant reduction in TER compared to the control monolayers, indicating that PIP is a more potent inhibitor of MLCP. This result was surprising as substitutions of the $K^{32}$ and $R^{33}$ to A at N-terminal side of phosphorylated $T^{38}$ showed that these residues were not critical for inhibition, whereas the YDRR motif at the C-terminal side had been

shown to be important in CPI-17 ability to inhibit PP1 (Hayashi, *et al* 2001). These results demonstrate that the $V^3$ is important in PIP ability to inhibit MLCP therefore other strategies to increase PIP cell penetration will need to be investigated. These investigations would include the synthesis of D-amino acid PIP analogues as PIP could be cleaved by proteases and peptidases, hence why a large concentration required. Esterification of peptide side chains has been shown to increase peptide permeability and stability, the ester bonds are then readily hydrolysed by cellular esterases (Kahns, *et al* 1993). This pro-drug strategy has been extensively used in the production of many different drugs such as aspirin (Williams 1985). Therefore, esterification of PIP E acidic side chain could increase both PIP permeability and stability.

Although PIP decreased TER of Caco-$2_{BBe}$ monolayers it is important to actually measure the permeability of molecules through the paracellular space. As TER and paracellular permeability are not absolutely linked. Transepithelial electrical resistance corresponds to movement of both paracellular and transcellular ions in response to an applied current. Alterations in one can result in compensatory modifications of the other that may enhance or reduce the overall effect. Additionally TER measures at that precise moment in time, whereas paracellular permeability measures over a longer time period (Balda, *et al* 1996). Therefore, the absorption enhancement property of PIP was measured by the paracellular transport of FD-4K and FD-70K.

## 4.5 Conclusions

The main aim of this chapter was to determine whether MLCP inhibition would increase paracellular permeability. Numerous peptides were designed and synthesised and tested for their abilities to increase TER. PIP was the only peptide to decrease TER without any apparent cytotoxicity. Further studies are currently being performed to determine whether PIP increases the permeability of inert paracellular markers such as FD-4K and FD-70K.

The main advantage of PIP over other absorption enhancers is that its precise mode of action is known, many absorption enhancers currently being researched have undetermined modes of action and hence are not widely used. Another

advantage of using peptides to increase paracellular permeability is the fact that the peptide is likely to be degraded within the cell hence the absorption enhancement effects would be transient.

Its main disadvantages is the fact that such a high concentration (5 mM) is required for increases in permeability, although this is lower than the concentrations required by other absorption enhancers such as 10 mM sodium caprate (Lindmark, *et al* 1998). Additionally PIP is likely to be cleaved within the intestinal environment (similar to PIK) in its current form, accounting for the high concentrations required. Hence further studies would include the determination of PIP degradation pattern within the intestinal environment and in Caco-2 $_{BBe}$ cells and synthesis of stable PIP analogues. Stable analogues could be synthesised by use of D-amino acids as performed on PIK or by esterfication of E residue, this could potentially make the peptide more cell permeable also. The effect of PIP on the phosphorylation state of would be need to be assessed in order to ensure that PIP effects on permeability are due to MLCP inhibition.

# Chapter 5

# Studies of known absorption enhancers mechanisms of action

## 5.1 Introduction

Absorption enhancers are compounds which disrupt the intestinal barrier to improve the transport of drugs (Mahato, *et al* 2003). However, these compounds are not widely utilised, as they have numerous side effects and their modes of action are not fully understood. The method by which some commonly used absorption enhancers increase TJ permeability will therefore be investigated.

*Sodium caprate*

Sodium caprate, the sodium salt of the medium chain fatty acid capric acid, is licensed for use as part of a suppository in Sweden (Doktacillin™, which consists of C10 and a triglyceride base containing sodium ampicillin). Sodium caprate is also marketed in Japan and Denmark as an absorption enhancer (Lindmark, *et al* 1998, Lindmark, *et al* 1997). Sodium caprate has been shown to enhance the paracellular permeability in Caco-2 monolayers (Anderberg, *et al* 1993) in rat (Sawada, *et al* 1991) and human intestinal segments (Shimazaki, *et al* 1998).

Sodium caprate has been shown in rats and humans to increase the permeability of FD-4K; this effect was inhibited by the CaM inhibitor W7 (Shimazaki, *et al* 1998). It was proposed that the mechanism of W7 inhibition of permeation clearance is via inhibition of MLCK which results a reduction in TJ permeability (Hayashi, *et al* 1999). Elevated intracellular $Ca^{2+}$ levels leads to increased MLCK phosphorylation, consequently resulting in increased paracellular permeability (Turner, *et al* 1997). However, W7 is not a specific inhibitor of MLCK, but of CaM. Therefore the effects seen by W7 could be due to inhibition of a different $Ca^{2+}$/calmodulin-dependent protein kinase (Hidaka, *et al* 1981).

Lindmark and co-workers found that incubation of C10 on Caco-2 monolayers had time-dependent effects on permeability. This can be divided into an initial phase characterised by a rapid increase in permeability occurring between 10 to 20 min, followed by a later-phase at 20 to 40 min characterised by slow but more prolonged elevations in permeability. They found that the phospholipase C (PLC) inhibitor U73122 and the $Ca^{2+}$ chelator BAPTA-AM did not inhibit the short-term effects of C10. However, the long-term effects were inhibited, thereby suggesting that $Ca^{2+}$ is involved in the process of TJ opening and hence increased permeability (Lindmark, *et al* 1998).

Phospholipase C converts phosphatidylinositol 4,5-bisphosphate into the $Ca^{2+}$ mobilising secondary messenger inositol 1,4,5-triphosphate ($IP_3$) and the PKC-activating second messenger diacylglycerol (DAG) (Patterson, *et al* 2005). The $IP_3$ pathway was investigated using the N-(6-aminohexyl)-5-chloro-1-napthalenesulphonamide (W7) a $Ca^{2+}$/calmodulin antagonist, CaMPKII inhibitor KN62 and ML-7, a MLCK inhibitor. None of these inhibitors affected the short-term effects of C10; however, KN62, W7 and ML-7 inhibited the long-term increases in permeability, suggesting that permeation enhancement by these compounds is mediated via MLCK (Lindmark, *et al* 1998).

To investigate the effects of C10 on the DAG pathway, Lindmark *et al.* used a synthetic cell-permeable DAG analogue dioactanolglycerol, which inhibited both the short and long-term effects of C10. The PKC inhibitors H7 and calphostin C had opposing effects; H7 resulted in an additive effect to that of C10, increasing its long-term increases in permeability, whereas calphostin C did not increase C10 long-term effects. This demonstrated that activation of the DAG pathway leads to the down-regulation of TJ permeability, whereas $IP_3$ results in an up-regulation of TJ permeability. A summary of the pathways involved in C10 regulation of the paracellular space are shown in (figure 5.1) (Lindmark, *et al* 1998).

Incubation of C10 for 12 min did not result in an alteration of ZO-1 or occludin distribution, whereas longer incubations of 60 min with C10 changed the appearance of both ZO-1 and occludin distribution (Lindmark, *et al* 1998). Therefore, these results show that MLCK, ZO-1 and occludin are important in the long-term effects of C10, proteins that have been shown to be important in the regulation of the TJ space.

*Chitosan*

Chitosans are high molecular weight cationic linear polysaccharides that are synthesised by chitin *N*-deacetylation, a biopolymer found in abundance in crab and shrimp shells (figure 5.2a) (Schipper, *et al* 1997). Chitosan is considered to be a biocompatible, slowly biodegradable polymer of natural-origin that is used by the food industry, with various molecular weights, viscosity grades and degrees of deacetylation of chitosan available (Schipper, *et al* 1996). Numerous groups have found that chitosan salts increase the permeability of Caco-2 monolayers by

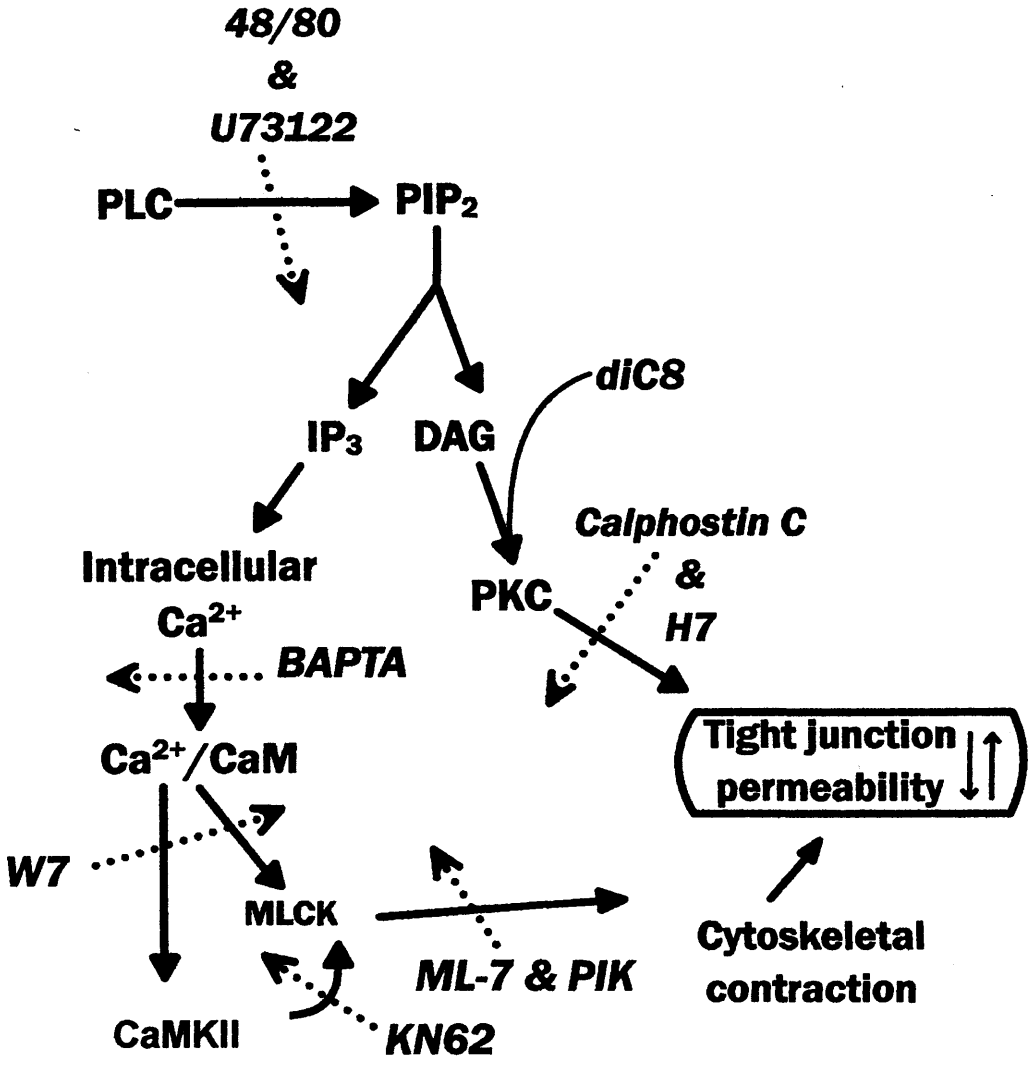


Figure 5.1 Pathways involved in the regulation of the paracellular space by C10. Studies have shown that C10 increases paracellular permeability of Caco-2 monolayers by activation of PLC. Activated PLC cleaves $PIP_2$ into $IP_3$ and DAG. Inositol 1,4,5-triphosphate releases $Ca^{2+}$ from intracellular stores, resulting in the phosphorylation of MLC by $Ca^{2+}$/calmodulin-activated MLCK. Dashed arrows represent inhibitors used in the study by Lindmark, et al 1988. (Diagram modified from Lindmark, et al 1998).

A

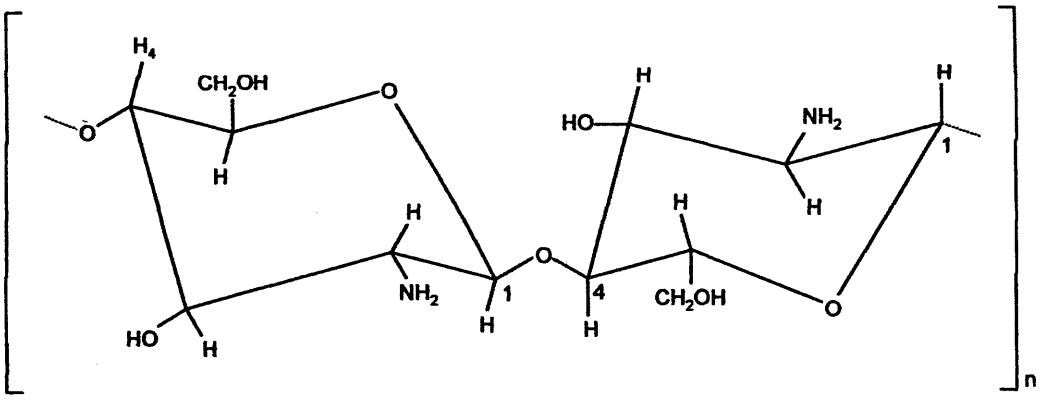


B

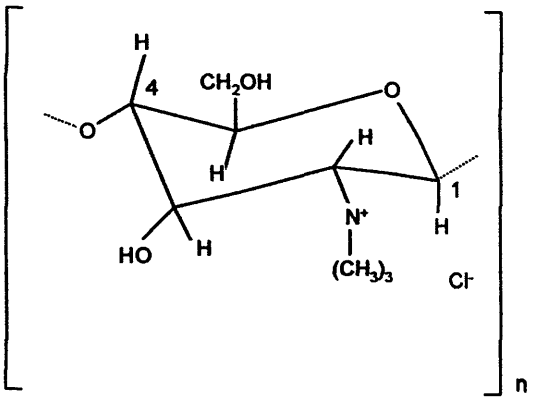


Figure 5.2 Chemical structures of chitosan (A) and TMC (B).

measurement of TER or by the permeability of paracellular markers (see table 5.1).

The main obstacle to using chitosan as an absorption enhancer is the fact that it aggregates in solution at neutral pH values and above, and hence only protonated chitosan (uncoiled chitosan) can be used in the intestinal environment. However, the chitosan derivative *N,N,N*-trimethyl chitosan chloride (TMC) is much more soluble than the parent chitosan at wider pH and concentration ranges (figure 5.2b). Different TMCs have been synthesised with various degrees of trimethylation (table 5.2). *N,N,N*-trimethyl chitosan chloride with a 60 % trimethylation has been shown to significantly increase the permeability of $^{14}$C-mannitol across Caco-2 monolayers, suggesting that the charge density of the polymer is important in its ability to open TJs at neutral pH values. Due to a lack of significant cytotoxicity, and their solubility at pH values observed in the jejunum of the small intestine, TMC polymers with a high degree of trimethylation have been hypothesised to be suitable for human use (Thanou, *et al* 2001).

Chitosan regulation of the paracellular space in not fully understood, Dodane *et al*, found that chitosan reduced fluorescent intensity staining of occludin with additional redistribution of ZO-1 and F-actin shown by confocal microscopy (Dodane, *et al* 1999). This suggests that chitosan enhances paracellular permeability via disruption of TJs, although the exact mechanism by which this occurs has not been fully identified.

The role of actin ring reorganisation in increases of permeability by chitosan is as yet still undetermined. Some groups have found that chitosan does not effect the actin ring of Caco-2 cells (Dodane, *et al* 1999, Smith, *et al* 2004). However, numerous groups have found a redistribution of F-actin from the actin ring of Caco-2 cells following incubation with chitosan chloride and glutamate respectively (Artursson, *et al* 1994, Ranaldi, *et al* 2002). Smith *et al*. found that treatment of Caco-2 cells with the PKC inhibitor (Ro318220) led to the inhibition of chitosan glutamate effects on TER (Smith, *et al* 2005). Protein kinase C has been shown to be an upstream regulator of MLC phosphorylation. Activation of PKC leads to phosphorylation of the MLCP inhibitor CPI-17 (Kitazawa, *et al* 2000). Myosin light

Table 5.1 Chitosan effects on Caco-2 permeability

| Chitosan | Concentration (w/v) | Effect on Caco-2 permeability | Reference |
|---|---|---|---|
| Chitosan hydrochloride (Seacure CL110, degree of acetylation 20 %) | 0.01% | TER decreased by 50 % in 15 min and by 75 % after 1 h. | (Dodane, *et al* 1999) |
| Chitosan (poly-D-glucosamine hydrochloride) with a degree of acetylation of 22.3 % | 0.002 – 0.01 % | Concentration decrease in TER and an increase in the passage of inulin. | (Ranaldi, *et al* 2002) |
| Chitosan glutamate (Protasan UP G113, degree of deacetylation = 85 %, Mw = 128,000 Da) | 0.05, 0.1 & 0.5 % | 0.05, 0.1 & 0.5 % solutions of chitosan resulted in reductions of TER by 12, 54, and 83 % respectively, after 60 min. | (Smith, *et al* 2004) |
| Chitosan glutamate (Seacure 210+) | 0.1 – 0.5 % | 0.25 % and 0.5 % gave a maximum 7-fold increase in $^{14}$C-mannitol permeability after 1 h. | (Artursson, *et al* 1994) |

Table 5.2 *N,N,N*-trimethyl chitosan chloride effects on Caco-2 permeability

| TMC | Concentration (w/v) | Effect on Caco-2 permeability | Reference |
|---|---|---|---|
| TMC with 40 and 60 % degrees of trimethylation. | 1.0 % | TMC 40 and TMC 60 induced a 17- and 46-fold enhancement of the transport of buserelin. | (Thanou, *et al* 2000). |
| TMC with a degree of quaternization of 12.28 % | 1.5, 2.0 and 2.5 % | 1.5, 2.0 and 2.5 % w/v resulted in a reduction of TER by 9, 52 and 79 % respectively after 20 min.<br><br>1.5 and 2.5 % w/v increased the transport rates of $^{14}$C-mannitol (32-60-fold), FD-4K (167-373-fold) and buserelin (28-73- fold) respectively. | (Kotze, *et al* 1997) |
| TMC-L degree of quaternization of 12.3 %. | 0.5 % | At pH 6.2 TER decreased by 37.3 % after 2 h whilst $^{14}$C-mannitol transport increased by 18-fold after 4 h. | (Kotze, *et al* 1999) |

Table 5.2 Continued

| TMC | Concentration (w/v) | Effect on Caco-2 permeability | Reference |
|---|---|---|---|
| TMC-H degree of quaternization of 61.2 %. | 0.1 – 1.5 % | At pH 6.2 TER was by 55.9 % after 2 h and $^{14}$C-mannitol increased by 20-fold after 4 h.<br><br>At pH 7.4 incubation with 0.1 %, 0.25 %, 0.5 %, 1 % and 1.5 % w/v led to a 43.1 %, 45.6 %, 58.6, 60.1 % and 63.1 % reduction in TER after 2 h. $^{14}$C-mannitol transport was increased by 31- and 48-fold when treated with 0.05 and 1.5 % w/v respectively. | (Kotze, *et al* 1999) |

chain phosphatase regulates dephosphorylation of MLC; therefore, its inhibition would result in TJ opening and hence decrease TER (Huang, *et al* 2004). Smith, *et al* compared the effects of chitosan to those of the PKC activator PMA. In these studies PMA reduced TER within 5 min of addition (Smith, *et al* 2005). Therefore, as PMA stimulates the effects of chitosan, it was decided to determine the effects of MLCK inhibition on PMA induced reductions in TER.

*Sodium caprate and chitosan effects on tight junction proteins*

Chitosan and C10 have been shown to alter the distribution of ZO-1 and occludin (Dodane, *et al* 1999, Lindmark, *et al* 1998). Zonnula occluden proteins are the scaffolding proteins of the TJ, and are thought to link the transmembrane TJ proteins to the actin cytoskeleton. Zonnula occludens-1 binds to both ZO-2 and ZO-3 (Wittchen, *et al* 1999), F-actin (Fanning, *et al* 1998), occludin (Furuse, *et al* 1993), claudin (Itoh, *et al* 1999a) and JAM (Ebnet, *et al* 2000). Occludin, however, binds directly with ZO-1 (Furuse, *et al* 1993), ZO-2 (Itoh, *et al* 1999b), ZO-3 (Haskins, *et al* 1998), F-actin (Wittchen, *et al* 1999) and to occludin via the coiled-coil domain (Nusrat, *et al* 2000). Occludin's second extracellular loop is thought to be important in the establishment of the TJ barrier (Stevenson and Keon 1998).

Therefore, alteration of ZO-1 and occludin distribution due to the long-term effects of C10 or treatment with chitosan may result in a loss of PAMR control of the paracellular pathway. It has been previously shown that TNF-α down-regulates and relocalises ZO-1 (Ma, *et al* 2004) and IFN-γ also down-regulates ZO-1, resulting in disruption of the actin cytoskeleton (Youakim and Ahdieh 1999). Since ZO-1 is a scaffolding protein, loss of this protein would lead to disorganisation of other TJ proteins, such as occludin and ZO-2. Additionally, ZO-1 is important in linking the TJ proteins to the PAMR; its loss would also result in a lack of cytoskeletal control of the paracellular pathway (Gonzalez-Mariscal, *et al* 2000). The specific MLCK inhibitor PIK has been shown to prevent decreases in TER caused by treatment of Caco-2 cells with TNF-α and IFN-γ. However, in this case the decreases in paracellular permeability were pathological, although this example demonstrates that PIK can prevent decreases in TER associated with the re-distribution and down-regulation of ZO-1 (Zolotarevsky, *et al* 2002).

*Aims of the chapter*

Therefore, the main aims of this chapter are to determine whether C10 and TMC enhance paracellular permeability via MLCK activation. Sodium caprate absorption enhancement effects are inhibited by the MLCK inhibitor ML-7 (Lindmark, *et al* 1998). However, as previously mentioned, ML-7 is not a potent inhibitor of MLCK (Bain, *et al* 2003). Dreverse PIK a specific and potent inhibitor of MLCK, will therefore be used to determine whether C10 absorption enhancement effects are via MLCK. This will be achieved by incubating confluent Caco-$2_{BBe}$ monolayers with C10 and Dreverse PIK along with fluorescent markers. The apparent permeability coefficients of the markers will then be calculated to determine whether MLCK inhibition by Dreverse PIK reduces the permeability of the markers.

The mode of TMC paracellular enhancement will also be investigated. Chitosan has been shown to alter the distribution of the TJ proteins F-actin, ZO-1 and occludin (Dodane, *et al* 1999). These proteins have been shown to be important in the regulation of the paracellular space and hence disruption of their expression and/or location may lead to chitosan absorption enhancement effects. As TMC is thought to have similar mode of action as chitosan it is hypothesised that inhibition of MLCK via Dreverse PIK may prevent the absorption enhancement effects of TMC. Initially the ability of the TMC to reduce TER without any cytotoxicity will be assessed. Then Caco-$2_{BBe}$ monolayers will be incubated with TMC and Dreverse PIK to determine whether MLCK activity is important in TMC ability to reduce TER.

The PKC activator PMA has been shown to mimic the effects of chitosan in Caco-2 monolayers (Smith, *et al* 2005). Therefore, the ability of PMA to reduce Caco-$2_{BBe}$ monolayers TER will be measured. The monolayers will then be treated with Dreverse PIK before addition of PMA to determine whether PMA ability to reduce TER is via MLCK activation.

## 5.2 Methods

To determine the concentration of C10 to be used in the permeability studies, Caco-$2_{BBe}$ cells were cultured on Transwells as explained in section 2.3.11. Prior to the experiments, the monolayers were washed twice and then incubated with HBSS

buffered to pH 7.4 with 25 mM HEPES for 20 min. HBSS without $Ca^{2+}/Mg^{2+}$ were used in the apical compartments to prevent the salt precipitating with C10. Integrity of the monolayers is not affected due to the presence of $Ca^{2+}/Mg^{2+}$ in the basolateral compartment (Anderberg, *et al* 1993). The epithelial monolayers were then incubated with 0, 2.5, 5, 7.5,10 and 13 mM C10, and the TER measured at times 0, 5, 10, 20, 30, 40, 50 and 60 min using an epithelial voltohmeter. The resistance was then expressed as percentage of the initial TER value.

The apparent permeability coefficients ($P_{app}$) of different inert fluorescent labels in Caco-$2_{BBe}$ monolayers incubated with C10 were determined along with the inhibition of C10 effects by Dreverse PIK. Prior to the experiments, the monolayers were incubated with HBSS buffered to pH 7.4 with 25 mM HEPES for 20 min. HBSS without $Ca^{2+}/Mg^{2+}$ were used in the apical compartments. Monolayers were then incubated with 2 mg/ml Flu, 0.5 mg/ml FD-4K or FD-70K with 13 mM C10 with or without 330 μM Dreverse PIK. Also, fluorescent marker was incubated without any C10 (control) and another monolayer was incubated with Dreverse PIK alone to determine its effects on the paracellular permeability of the fluorescent markers. One hundred μl aliquots were taken from the basolateral side of the membrane at times 0, 5, 10, 15, 20, 25, 30, 35 and 40 min which were then replaced with fresh HBSS. Samples were collected into black 96-well plates, and were protected from light using silver foil. Plates were measured at excitation value 485 and emission value 520 nm. The gain on the plate reader was always kept at 1000. The $P_{app}$ ratios were calculated using the equation below

$$P_{app}\ \text{ratio} = P_{app}\ \text{test}/P_{app}\ \text{control}$$

Following the increase of C10 effects on permeability when the monolayers were incubated with Dreverse PIK, the short- and long-term effects of C10 when incubated with the MLCK inhibitors Dreverse PIK and ML-7 was determined. Following pre-equilibration of the monolayers for 20 min in HBSS, the inserts were placed into wells containing fresh HBSS (time 0). Fluorescein isothiocynate-dextran 4,000 (0.5 mg/ml) with 13 mM C10 with or without the MLCK inhibitors 330 μM Dreverse PIK or 10 μM ML-7 were then added to the monolayers. At 12 min, the

inserts were moved into new chambers containing fresh HBSS and samples taken from the well to measure the short-term effects (time 0 to 12 min). The monolayers were then left for a further 48 min to measure the long-term effects (time 12 to 60 min). Samples (100 µl) were collected into black 96-well plates, and were protected from light using silver foil. Plates were measured at excitation value 485 and emission value 520 nm. The gain on the plate reader was always kept at 1000.

To determine if pre-incubation of Caco-$2_{BBe}$ monolayers with Dreverse PIK and ML-7 also resulted in increases in C10 short- and long-term epithelial permeability, monolayers were pre-incubated for 30 min with either 330 µM Dreverse PIK or 10 µM ML-7 before addition of C10. The experiment then proceeded as per the previous experiment. Additionally, the consequence of post-incubation of monolayers with Dreverse PIK and ML-7 on the long-term C10 effects on permeability was studied. This was determined by addition of the MLCK inhibitors (Dreverse PIK or ML-7) to the monolayers after 12 min incubation with C10 in order to establish the $P_{app}$ of the long-term effects of C10.

The concentration effect on Caco-$2_{BBe}$ monolayer TER by TMC was measured, before Dreverse PIK effects on the increases in TJ permeability induced by TMC could be assessed. Two hours before commencement of the experiment, the media was changed to DMEM buffered to pH 7.4 with 25 mM HEPES. The TER was measured at 1 h and 30 min before addition of TMC. *N,N,N*-trimethyl chitosan chloride was dissolved in water at 2 % stock solution which was kept at - 20 °C. *N,N,N*-trimethyl chitosan chloride at concentrations of 0, 0.05, 0.1, 0.5, 1, 1.5, 2 and 2.5 % w/v were then added to the apical side of the monolayers, and TER measured every 30 min for 2 h. Following 2 h incubation, the media was removed from the apical side and the monolayers washed gently to avoid detachment of cells from the filter. The resistance was measured for an additional 1 h to measure reversibility (Kotze, *et al* 1999). The resistance was then expressed as percentage of the initial TER value.

The cytotoxicity of TMC was measured using the MTT assay as described in section 2.3.15. Briefly, 96 well plates were seeded at a density of 15,528 cells/$cm^2$

and cultured for 48 h (Bromberg and Alakhov 2003). Wells were incubated with TMC at the concentrations used in the TER experiments and incubated for 2 h. The wells were then washed with PBS and MTT reagent added to them and incubated for a further 5 h, when the MTT was aspirated and the reaction product solubilised in DMSO for 30 min. The plate was then read in a colorimetric plate reader.

The effect of phorbol 12-myristate 13-acetate (PMA) on the TER of Caco-$2_{BBe}$ monolayers were determined, as Smith *et al.* have shown that PMA decreases TER in a similar manner to chitosan. The monolayers were incubated with HBSS buffered to pH 7.4 with 25 mM HEPES for 20 min prior to PMA addition (which was dissolved in DMSO at a concentration of 16 mM and stored at – 20 °C). Phorbol 12-myristate 13-acetate was added to the monolayers at 1.6 nM, 16.2 nM and 162 nM and the TER measured at times 0, 5, 15, 30, 60 and 120 min using an epithelial voltohmeter (Smith, *et al* 2005). The resistance was then expressed as percentage of the initial TER value.

## 5.3 Results

### *5.3.1 Effects of C10 on the TER of Caco-$2_{BBe}$ monolayers*

Incubation of the apical side of Caco-$2_{BBe}$ monolayers with 10 and 13 mM C10 resulted in a significant decrease in TER to approximately 80 % and 60 % of the initial value when compared to the control monolayer TER within 5 min of its addition. The TER further decreased to approximately 75 % and 45 % at 20 min, which was maintained for the entirety of the 1 h experiment (figure 5.3). Incubation with 2.5, 5 and 7.5 mM C10, however, did not significantly reduce TER compared to the control monolayers.

### *5.3.2 Effects of C10 on epithelial permeability of different molecular weight fluorescent probes*

The effects of C10 on the epithelial permeability of Flu, FD-4K and FD-70K, along with the effect of MLCK inhibition by Dreverse PIK on epithelial permeability were measured. Firstly the fluorescence intensity of the fluorescent markers used in this experiment needed to be measured in order to obtain accurate results. Fluorescence quenching is a process that reduces the intensity of the fluorescence

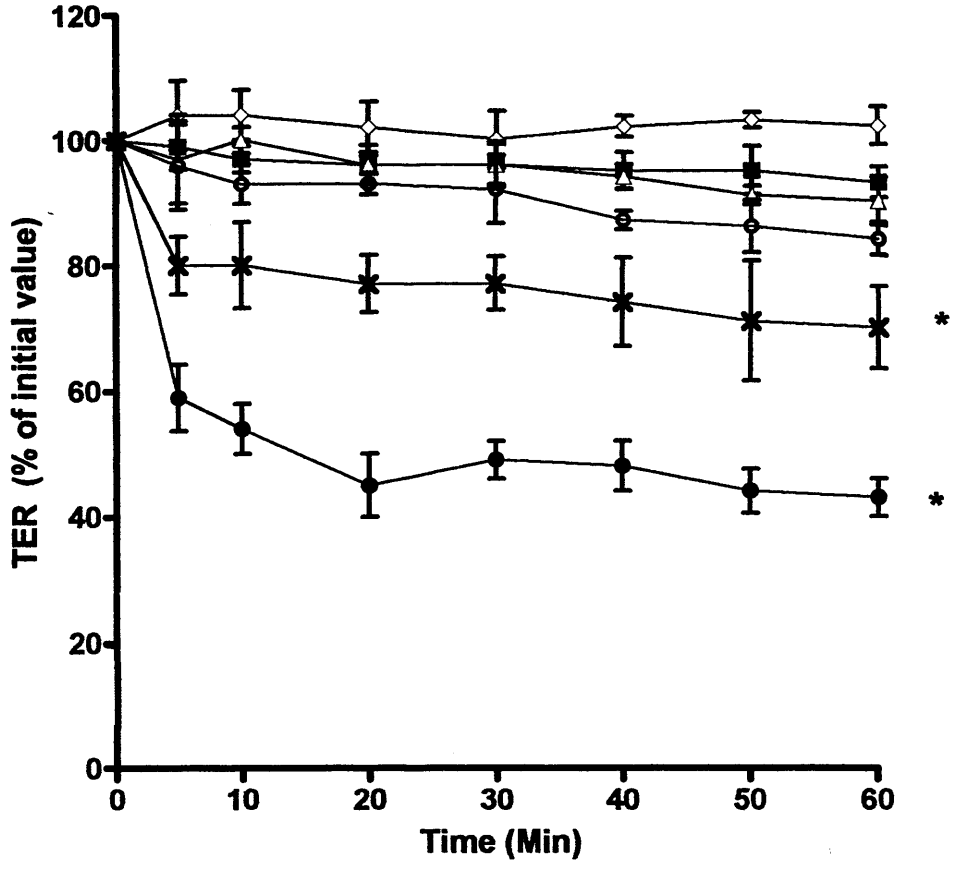


Figure 5.3 Sodium caprate effects on Caco-$2_{BBe}$ monolayers TER. Control (◇), 2.5 mM (■), 5 mM (△), 7.5 mM (o), 10 mM (×) and 13 mM (●). Statistical differences between the concentrations were determined at $p < 0.001$ (*) using two-way ANOVA and Bonferroni post hoc test. (Data represents mean TER normalised to the value at time zero ± SD n=3, error bars are within plot symbols when not visible).

emission at higher concentrations. Hence, standard curves of the markers were generated, and diluted if required in order to prevent quenching of fluorescence intensity (figure 5.4).

Following 10 min incubation of epithelial monolayers with C10 the $P_{app}$ of Flu was significantly increased to 3.2 x $10^{-7}$ cm/s (4-fold increase) when compared to the control monolayers (figure 5.5). The $P_{app}$ at 20 min had decreased to 2.3 x $10^{-7}$ cm/s and remained fairly constant thereafter to the end of the 40 min experiment. Addition of Dreverse PIK to the monolayers incubated with C10 resulted in a significant increase in the $P_{app}$ of Flu to 6.4 x$10^{-7}$ cm/s (10-fold increase) at 10 min compared to the control monolayers, and had a 2-fold increase when compared to C10 alone. At 20 min, the $P_{app}$ decreased to 3.6 x $10^{-7}$ cm/s the $P_{app}$, then plateaued for the remainder of the experiment. Incubation of monolayers with Dreverse PIK only did not significantly increase the $P_{app}$ of Flu across Caco-$2_{BBe}$ monolayers compared to the control.

After 10 min treatment of Caco-$2_{BBe}$ monolayers with C10, the $P_{app}$ of the epithelia to FD-4K was significantly increased to 3.4 x $10^{-7}$ cm/s (approximately 3-fold greater) compared with the control (FD-4K only) (figure 5.6). The $P_{app}$ gradually increased further to 3.9 x $10^{-7}$ cm/s at 30 min; thereafter, the permeability remained at a fairly constant value to the end of the experiment. Incubation of C10 with Dreverse PIK resulted in a significant increase of FD-4K $P_{app}$ to 8.7 x $10^{-7}$ cm/s (approximately 16-fold increase) compared to FD-4K alone at 10 min, with an approximately 3-fold increase of permeability compared to monolayers treated with C10 alone. At 20 min the $P_{app}$ reduced to 6.8 x $10^{-7}$ cm/s, where it remained comparatively constant for the remaining 20 min of the experiment. Although the $P_{app}$ had decreased from its value at 10 min, it remained higher than that of C10 alone. Incubation of monolayers without enhancer but with Dreverse PIK alone did not significantly increase epithelial permeability compared with the control.

The effect of C10 on the $P_{app}$ of FD-70K follows a similar pattern to that of Flu and FD-4K, although at a much lower rate. The $P_{app}$ of FD-70K incubated with C10 increased rapidly within the first 10 min 1.2 x $10^{-7}$ cm/s (C10 alone increased approximately 6-fold) and then stabilised at 30 min to approximately 1.6 x $10^{-7}$ cm/s

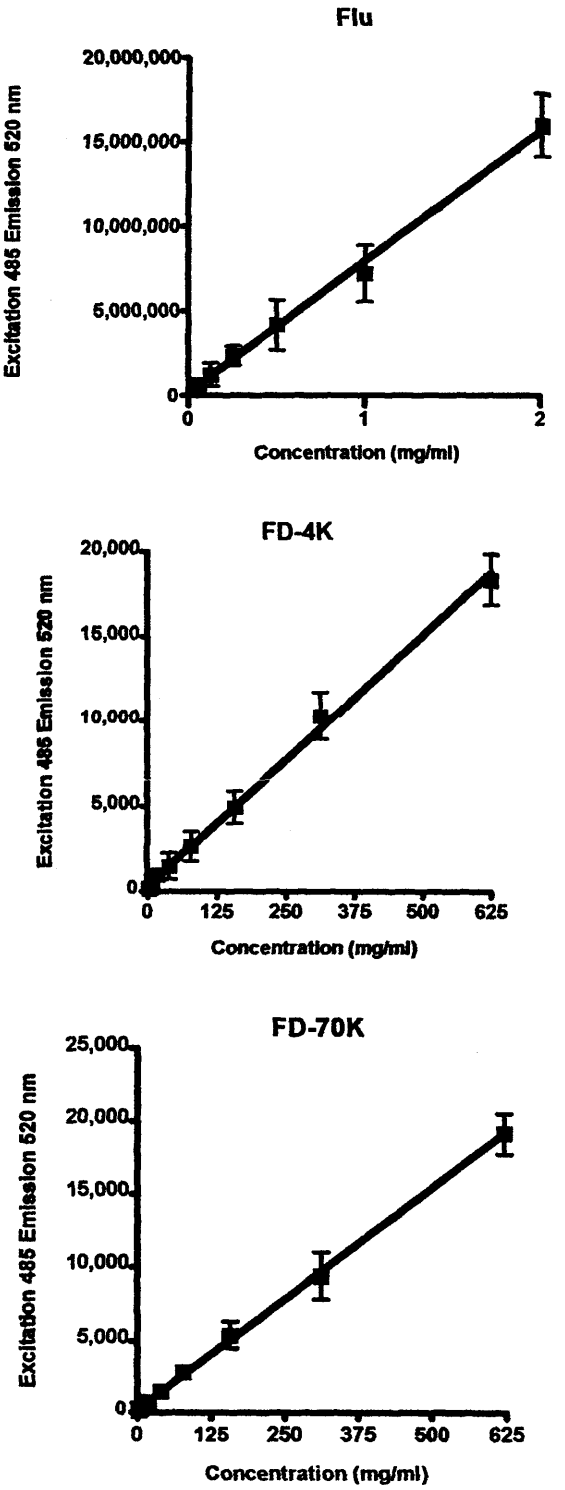


Figure 5.4 Concentration dependent fluorescence of the flu, FD-4K and FD-7K used in Caco-$2_{BBe}$ permeability studies.

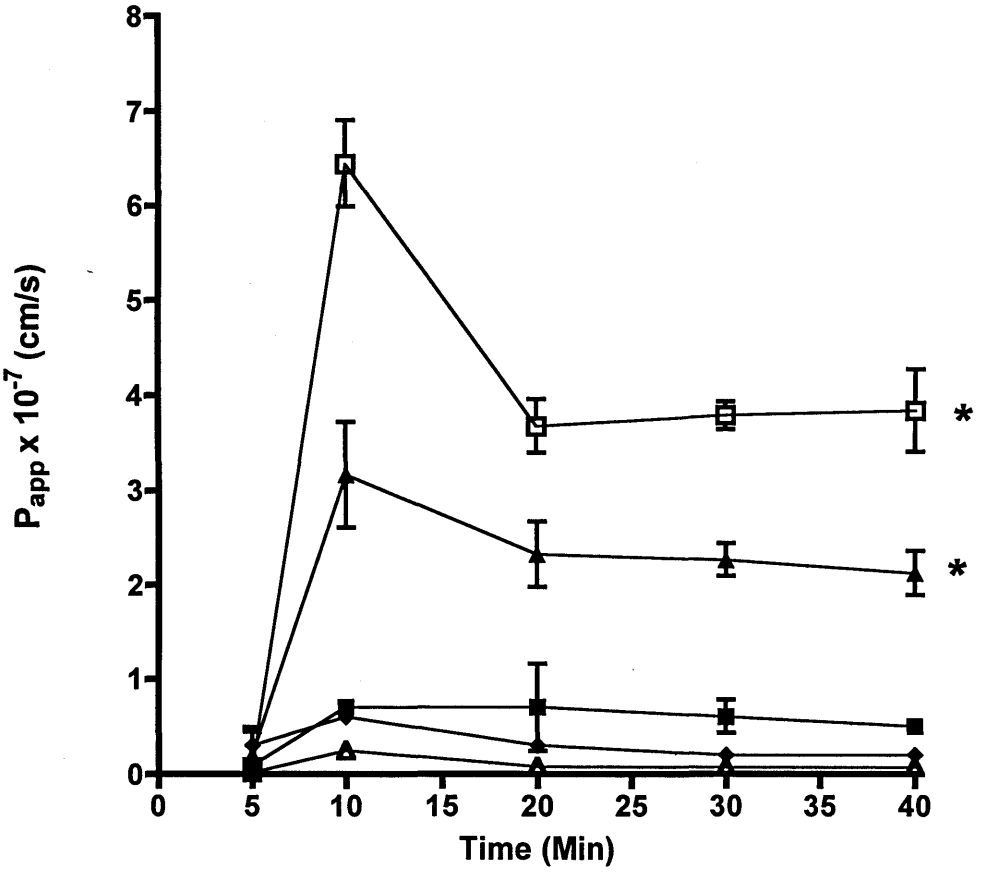


Figure 5.5 Effects of C10 on the apparent permeability coefficient ($P_{app}$) of Flu in Caco-$2_{BBe}$ monolayers. Control (△), Flu (◆), Dreverse PIK (■), C10 (▲) and C10 and Dreverse PIK (□). Statistical differences between the concentrations were determined at $p < 0.001$ (*) using two-way ANOVA and Bonferroni post hoc test. (Values are mean ± SD n=3, error bars are within plot symbols when not visible).

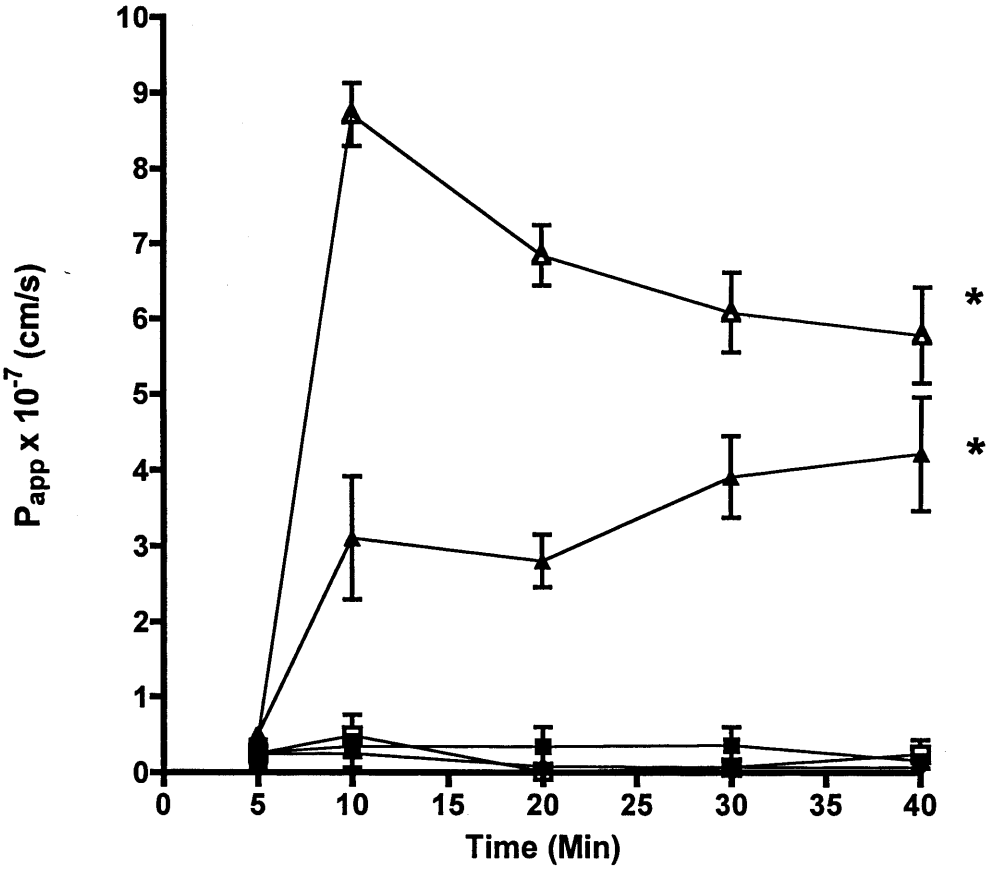


Figure 5.6 Consequences of C10 incubation on FD-4K $P_{app}$ of Caco-$2_{BBe}$ monolayers. Control (◆), FD-4K (■), C10 (▲), Dreverse PIK (□) and C10 and Dreverse PIK (△). Statistical differences between the concentrations were determined at $p < 0.001$ (*) using two-way ANOVA and Bonferroni post hoc test. (Values are mean ± SD n=3, error bars are within plot symbols when not visible).

for the remainder of the experiment (figure 5.7). Incubation of the monolayers with C10 and Dreverse PIK resulted in an increased $P_{app}$ of FD-70K by approximately 13-fold compared to control monolayers, with an approximately 2-fold increase compared to monolayers incubated with C10 only. After the initial 10 min increase ($2.5 \times 10^{-7}$ cm/s) the $P_{app}$ decreased to $1.7 \times 10^{-7}$ cm/s at 30 min, when the $P_{app}$ lowered to a value similar to that of C10 alone ($1.6 \times 10^{-7}$ cm/s).

### 5.3.3 *Inhibition of MLCK and its effects on C10 increases in epithelial permeability*

As the previous results showed that incubation of Caco-$2_{BBe}$ monolayers with and C10 resulted in elevation of epithelial permeability, the short- and long-term interval permeability of FD-4K when MLCK was inhibited by Dreverse and ML-7 was measured in order to compare these results with those of Lindmark and colleagues. Incubation of C10 with Dreverse PIK and ML-7 led to FD-4K permeability significantly increasing to 292 % and 252 % respectively when C10 alone was taken as 100 % over the short-term interval (figure 5.8a). The long-term interval permeability of FD-4K when Caco-$2_{BBe}$ monolayers were treated with C10 and Dreverse PIK significantly increased to 171 % and ML-7 to 196 % when compared to incubation with C10 alone (figure 5.8b).

### 5.3.4 *Effect of pre-incubating Caco-$2_{BBe}$ monolayers with MLCK inhibitors on C10 increases in epithelial permeability*

Incubation of Caco-$2_{BBe}$ monolayers with both C10 and ML-7 simultaneously led to increases in epithelial permeability, contradictory to previous findings by Lindmark and co-workers (Lindmark, *et al* 1998). Therefore, it was decided to pre-incubate the Caco-$2_{BBe}$ monolayers with Dreverse PIK and ML-7 for 30 min before the addition of C10. Pre-incubation of the monolayers with Dreverse PIK resulted in a significant increase of FD-4K short-term permeability to 139 %, whereas the short-term effects of C10 were significantly inhibited by ML-7 to 79 % (figure 5.9a). The long-term interval effect of C10 was significantly inhibited by both Dreverse PIK and ML-7 to 45 and 38 % respectively when compared to C10 alone (when C10 alone was taken as 100 %) (figure 5.9b).

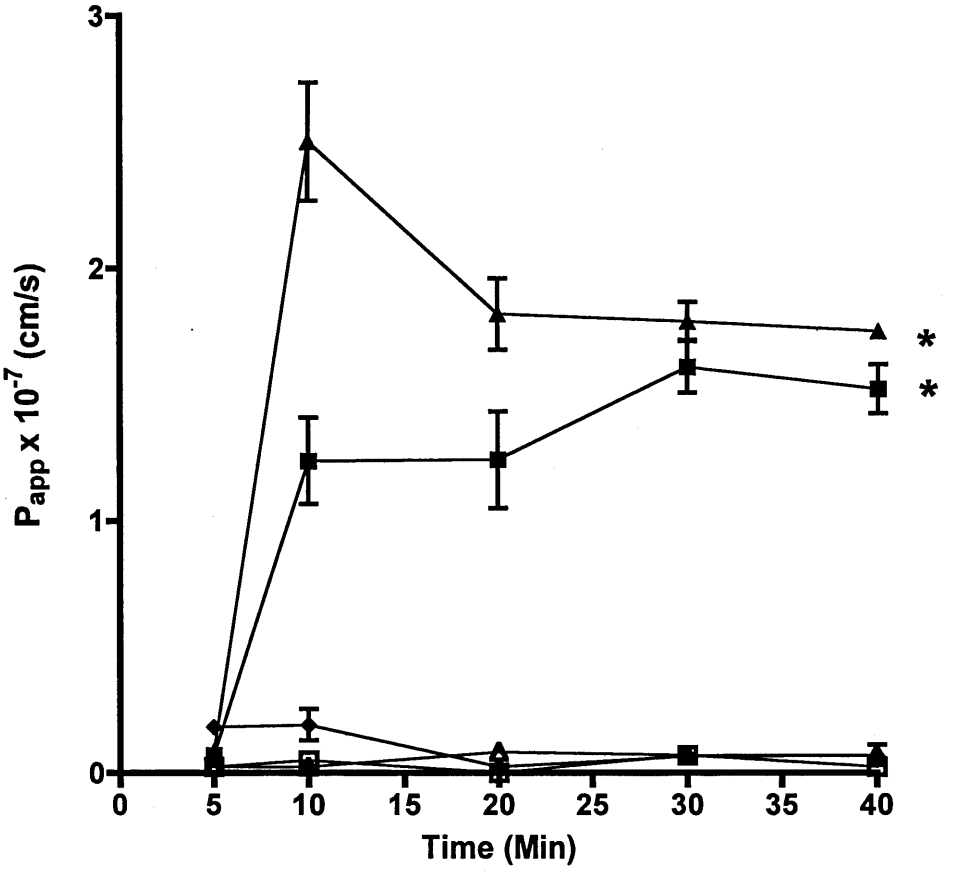


Figure 5.7 Effects of C10 on the apparent permeability coefficient ($P_{app}$) of FD-70K in Caco-$2_{BBe}$ monolayers. Control (△), FD-70K (◆), C10 (■), Dreverse PIK (□) and C10 and Dreverse PIK (▲). Statistical differences between the concentrations were determined at $p < 0.001$ (*) using two-way ANOVA and Bonferroni post hoc test. (Values are mean ± SD n=3, error bars are within plot symbols when not visible).

A

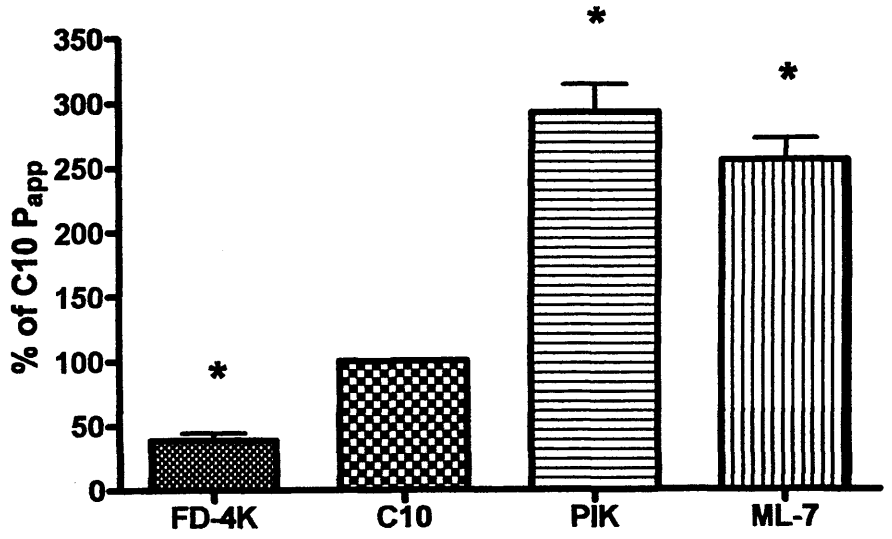


B

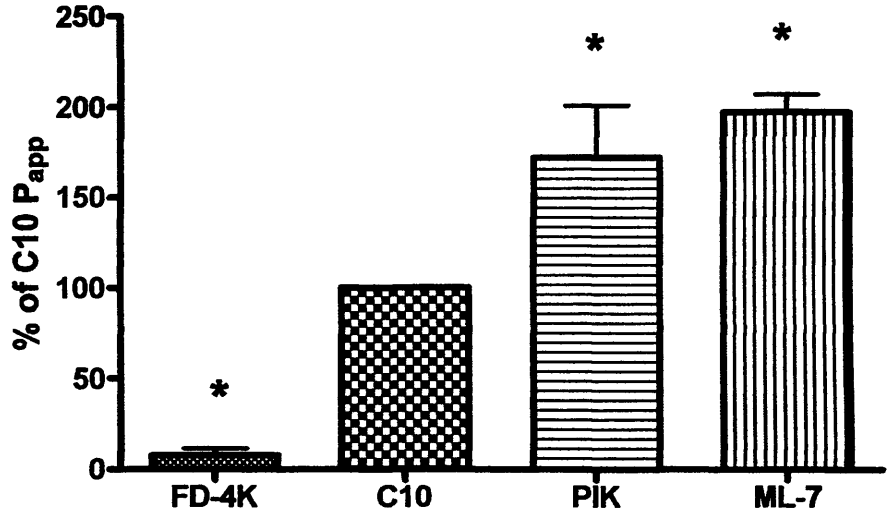


Figure 5.8 MLCK inhibitors effects on C10 increases of Caco-$2_{BBe}$ monolayer permeability to FD-4K. A) In the short-term interval, B) In the long-term interval after addition of Dreverse PIK and ML-7 at the same time as C10. Statistical analysis between treatments were determined at $p < 0.001$ (*) using one-way ANOVA and Bonferroni post hoc test. (Figure shows the percentage of the $P_{app}$ value compared with C10 without the presence of MLCK inhibitors. Values are mean ± SD n=3).

A

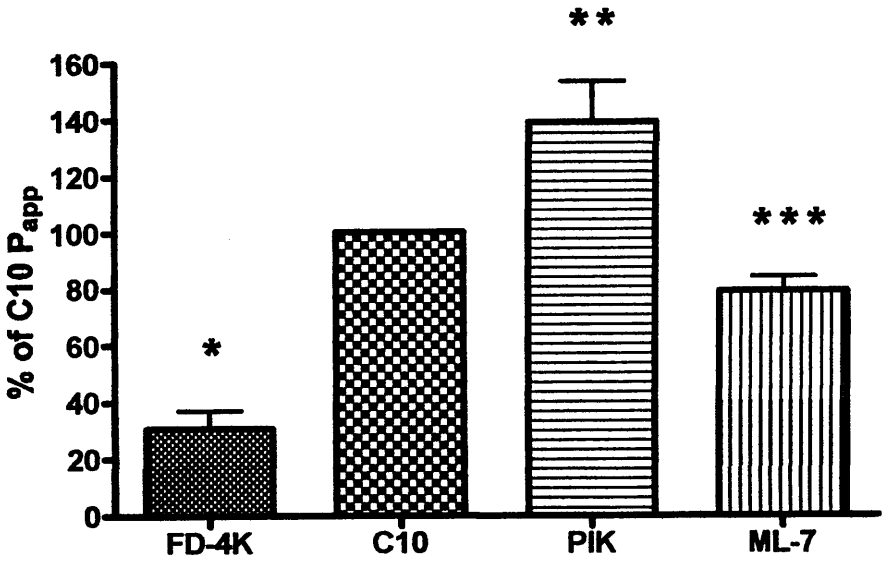


B

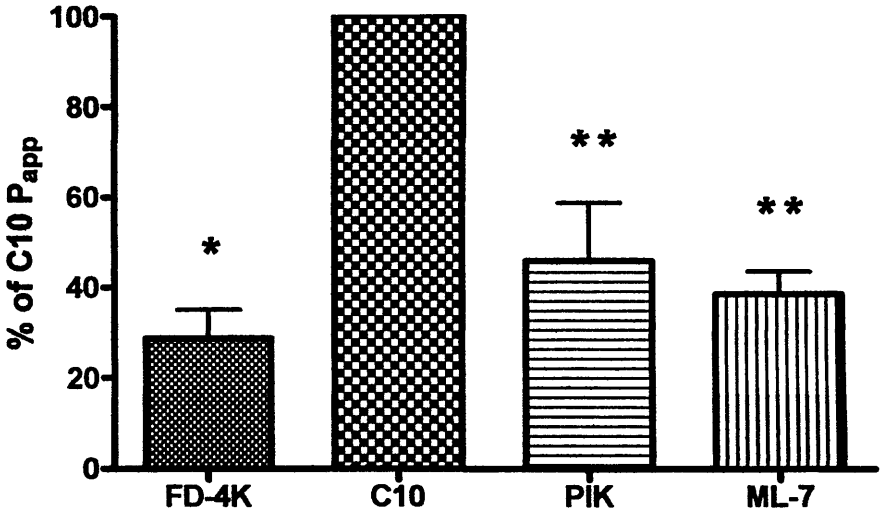


Figure 5.9 Effects of pre-incubation of Caco-$2_{BBe}$ monolayers with MLCK inhibitors on C10 increases of epithelial permeability. A) In the short-term interval, B) In the long-term interval after pre-incubation of monolayers with Dreverse PIK and ML-7. Statistical analysis between treatments were determined at $p < 0.001$ (*), $p < 0.01$ (**) and $p < 0.05$ (***) using one-way ANOVA and Bonferroni post hoc test. (Figure shows the percentage of the $P_{app}$ value compared with C10 without the presence of MLCK inhibitors. Values are mean ± SD n=3).

### 5.3.5 *MLCK inhibitors' effects on C10 increases in epithelial permeability post-incubation*

As the effects of MLCK inhibitors on C10 showed different results depending on when the inhibitors were added to the Caco-$2_{BBe}$ monolayers, Dreverse PIK and ML-7 were added at 12 min immediately after the measurement of the short-term interval. The results show that there is no significant difference between the monolayers when incubated with C10 only (figure 5.10a). However, addition of the MLCK inhibitors Dreverse PIK and ML-7 following the short-term interval resulted in significantly increasing the effects of C10 to 146 % and 198 % (figure 5.10b) when C10 was taken as 100 %. A summary of all the calculated short- and long-term $P_{app}$ values in these studies are shown in table 5.3.

### 5.3.6 *Effect of TMC on Caco-$2_{BBe}$ monolayer TER*

Incubation of Caco-$2_{BBe}$ monolayers with TMC produced a concentration dependent decrease in TER (figure 5.11). Treatment of Caco-$2_{BBe}$ monolayers with 1 %, 1.5 %, 2 % and 2.5 % TMC w/v for 2 h led to a significant decrease in TER by 53 %, 63 %, 67 % and 69 % respectively compared to the control. Incubation with 0.05 %, 0.1 % and 0.5 % TMC w/v, however, did not significantly decrease TER (23 %, 17 % and 31 % respectively when compared to the control). However, TMC caused a concentration-dependent cytotoxicity (from 0.05 – 0.5 % w/v) following 2 h incubation, with TMC displaying an $IC_{50}$ value of 0.36 % w/v (figure 5.12).

### 5.3.7 *PMA effects on Caco-$2_{BBe}$ monolayer TER*

Incubation of the monolayers with 1.62 nM and 16.2 nM PMA did not result in any significant reductions in TER, whereas 162 nM led to a significant increase in TER to approximately 130 % within 2 h of its addition to the monolayers (figure 5.13). These concentrations were used by Smith *et al.* who found that these concentrations decreased TER within 5 min (Smith, *et al* 2005). Therefore, PMA concentrations of 170 nM, 540 nM and 1.6 µM were used as Turner and colleagues' studies which showed that these concentrations of PMA increased TER (Turner, *et al* 1999). Treatment of Caco-$2_{BBe}$ monolayers with 170 nM, 540 nM and 1.6 µM PMA resulted in a significant increase in TER to approximately 130 %, 130 % and 140 % respectively when compared to control monolayers (figure 5.14).

A

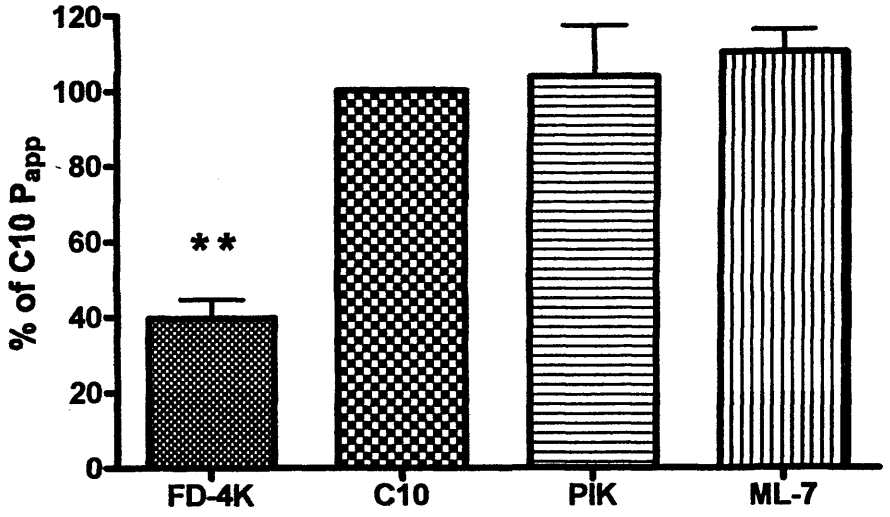


B

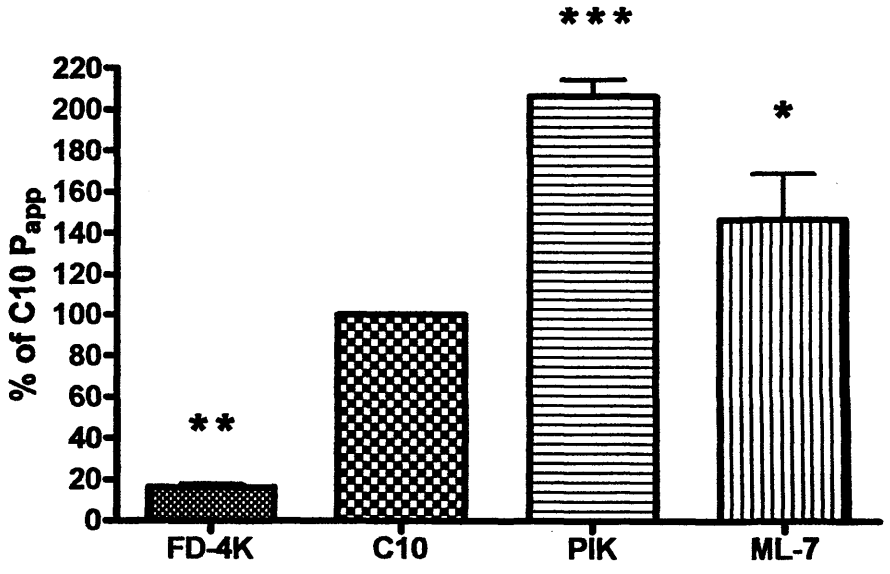


Figure 5.10 Effects of post-incubation of Caco-$2_{BBe}$ monolayers with MLCK inhibitors on C10 increased epithelial permeability. A) In the short-term interval, B) In the long-term interval after addition of Dreverse PIK and ML-7 at 12 min. Statistical analysis between treatments were determined at $p < 0.001$ (*), $p < 0.01$ (**) and $p < 0.05$ (***) using one-way ANOVA and Bonferroni post hoc test. (Figure shows the percentage of the $P_{app}$ value compared with C10 without the presence of MLCK inhibitors. Values are mean ± SD n=3).

Table 5.3 Summary of the effects of PIK and ML-7 on the short- and long-term calculated $P_{app}$ values of monolayers treated with C10*

| | Short-term interval FD-4K (± SD) | Short-term interval C10 (± SD) | Short-term interval C10 and PIK (± SD) | Short-term interval C10 and ML-7 (± SD) |
|---|---|---|---|---|
| **Simultaneously** | 39 ± 9 * | 100 | 292 ± 35 * | 252 ± 28 * |
| **Pre-incubation** | 31 ± 10 * | 100 | 139 ± 24 ** | 57 ± 18 *** |
| **Post-incubation** | 40 ± 8 ** | 100 | 104 ± 27 | 110 ± 11 |

| | Long-term interval FD-4K (± SD) | Long-term interval C10 (± SD) | Long-term interval C10 and PIK (± SD) | Long-term interval C10 and ML-7 (± SD) |
|---|---|---|---|---|
| **Simultaneously** | 8 ± 6 * | 100 | 171 ± 38 * | 196 ± 37 * |
| **Pre-incubation** | 28 ± 10 * | 100 | 45 ± 22 ** | 38 ± 9 ** |
| **Post-incubation** | 16 ± 3 ** | 100 | 198 ± 22 *** | 146 ± 38 * |

* Monolayers incubated with C10 only were taken as 100 % (values show the mean ± SD n=3). Statistical analysis between treatments were determined at $p < 0.001$ (*), $p < 0.01$ (**) and $p < 0.05$ (***) using one-way ANOVA and Bonferroni post-hoc test.

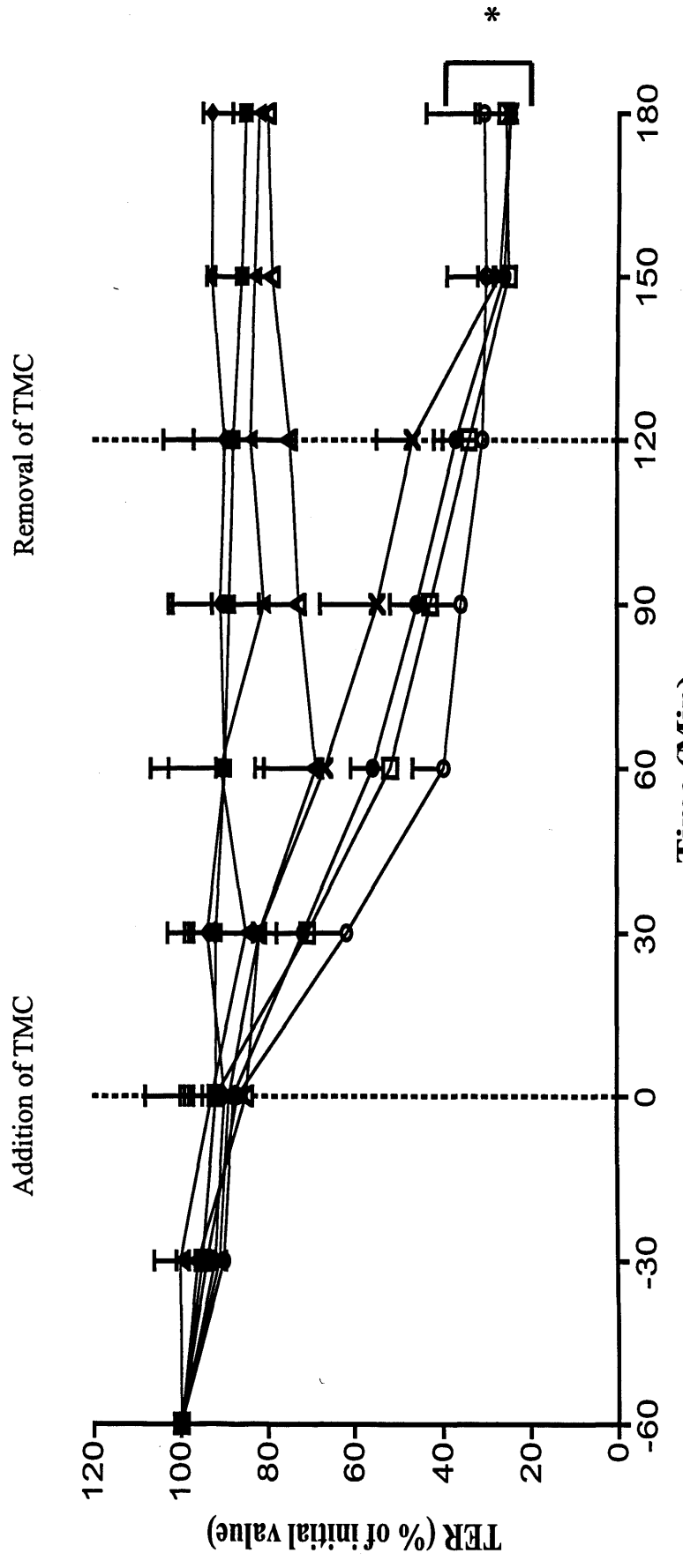


Figure 1.11 Alterations in TER following addition of TMC. Control (◆), 0.05 % (■), 0.1 % (▲), 0.5 % (△), 1 % (×), 1.5 % (●), 2 % (□) and 2.5 % (○). Statistical analysis between concentrations were determined at $p < 0.001$ (*) using the two-way ANOVA ad Bonferroni post hoc test. (Data represents mean TER normalised to the value at time -60 min ± SEM n= 3, error bars are within plot symbols when not visible). Note: resistance was monitored 60 min prior to application.

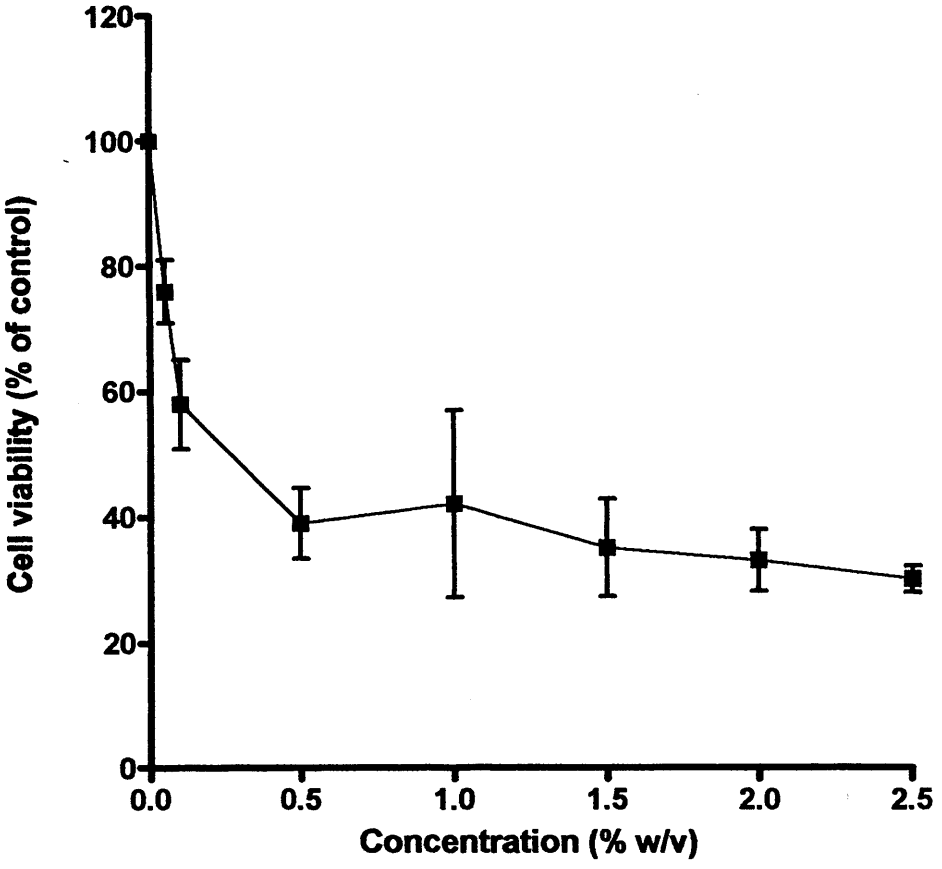


Figure 5.12 Cytotoxicity analysis of TMC. The calculated $IC_{50}$ value was 0.36 % w/v (± 0.05 SD) (Data show cell viability as percentage of untreated control cells and represent mean ± SD n=3, error bars are within plot symbols when not visible).

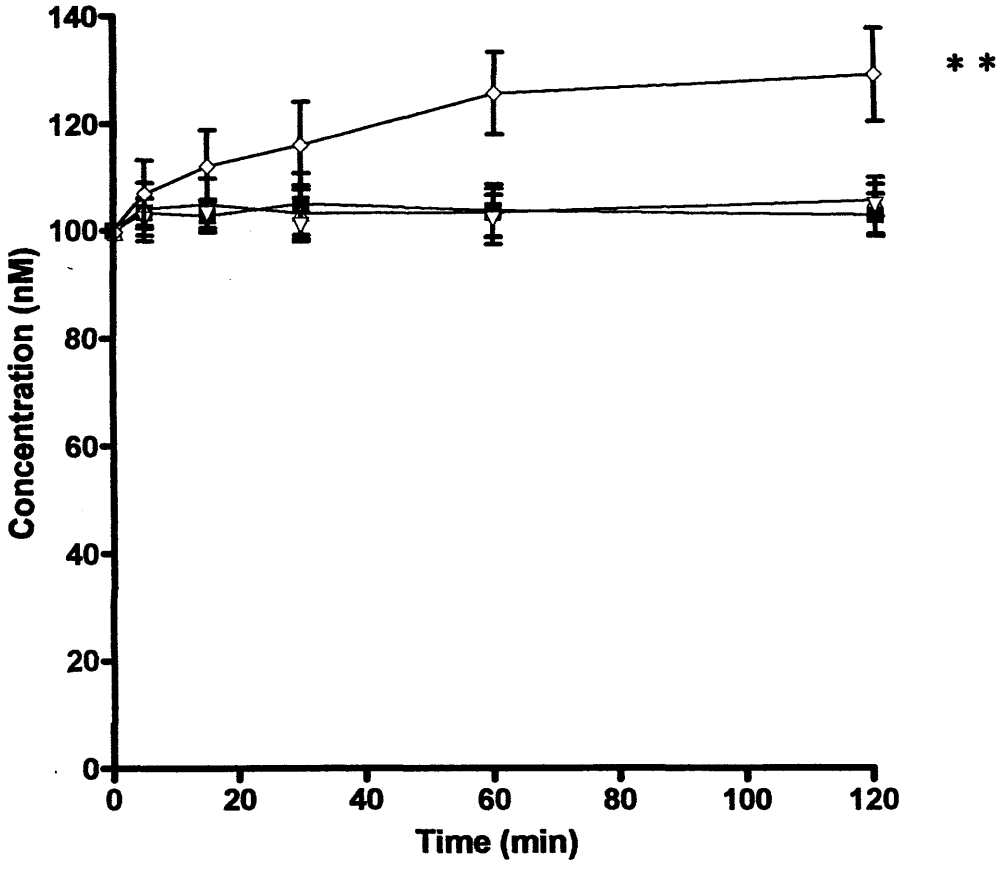


Figure 5.13 Effects of PMA on Caco-$2_{BBe}$ monolayer TER. Control (■), 1.62 nM, (◇), 16.2 nM (▲) and 162 nM (▽). Statistical analysis between concentrations were determined at $p < 0.01$ (**) using two-way ANOVA and Bonferroni post hoc test. (Data represents mean TER normalised to the value at time zero ± SD n=3, error bars are within plot symbols when not visible).

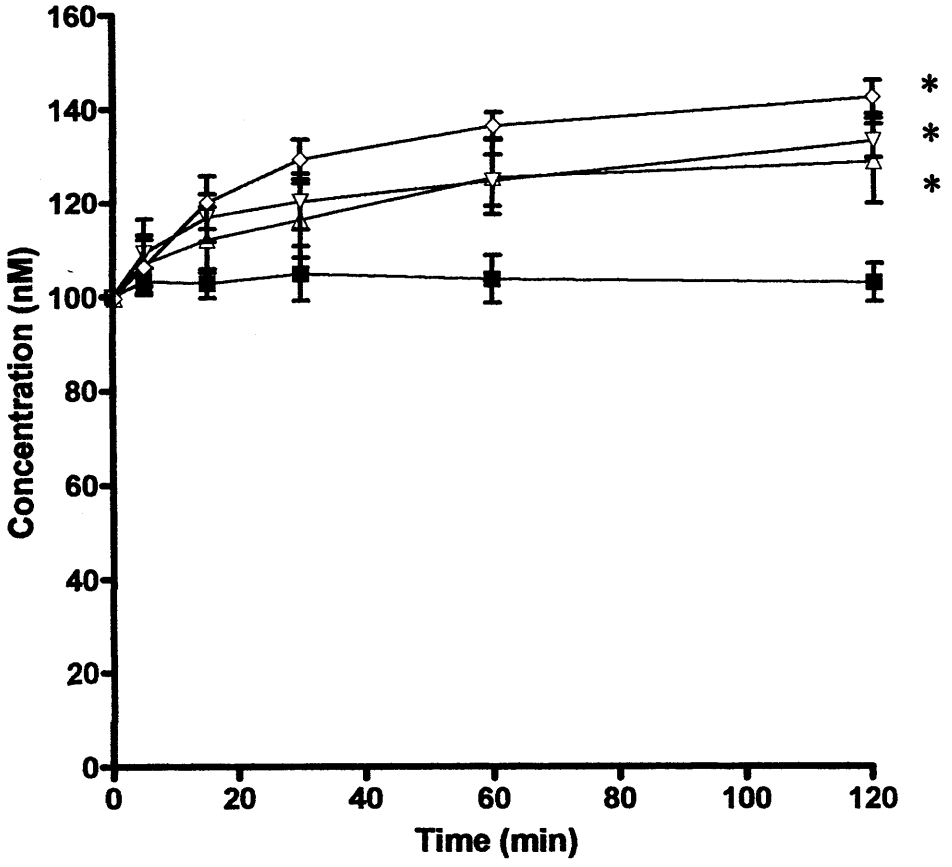


Figure 5.14 Effects of higher concentrations of PMA on Caco-$2_{BBe}$ TER. Control (■), 170 nM (△), 540 nM (▽) and 1.6 μM (◇). Statistical analysis between concentrations were determined at $p < 0.001$ (*) using two-way ANOVA and Bonferroni post hoc test. (Data represents mean TER normalised to the value at time zero ± SD n=3, error bars are within plot symbols when not visible).

## 5.4 Discussion

Sodium caprate, an absorption enhancer that has been used to increase intestinal permeability, is thought to work via MLCK activation (Hayashi, *et al* 1999, Lindmark, *et al* 1998). Myosin light chain kinase activation results in phosphorylation of MLC at $S^{19}$, which in turn commences contraction due to increased activity of myosin ATPase (Soderling & Stull 2001). This results in the opening of TJs and subsequent increases in TJ permeability (Hecht, *et al* 1996).

Lindmark and colleagues used the MLCK inhibitor ML-7 to demonstrate the importance of MLCK activity for C10 absorption enhancement effects (Lindmark, *et al* 1998). However, ML-7 is a non-specific inhibitor of MLCK as it inhibits the ATP binding site, similar motifs are found in other ATPase binding proteins (Turner, *et al* 1997). Therefore, the specific MLCK inhibitor Dreverse PIK, which is thought to inhibit MLCK by binding to its catalytic domain (Zolotarevsky, *et al* 2002), was used to confirm the importance of MLCK in C10 absorption enhancement effects.
The reductions in TER of Caco-$2_{BBe}$ monolayers incubated with C10 in these studies are comparable to Anderberg *et al.*, who found that incubating Caco-2 monolayers with 13 mM C10 resulted in an approximately 50 % decrease in TER within 1 min, followed by a $2^{nd}$ phase where the resistance decreased slowly up until 10 min. Additional reductions in resistance were not seen for the remainder of the 60 min experiment (Anderberg, *et al* 1993). The TER of the Caco-$2_{BBe}$ monolayers in these studies decreased rapidly to approximately 60 % within the first 5 min, followed by a reduction to about 50 % at 10 min. The TER then remained fairly constant for the remainder of the experiment. This established that the effect of C10 on Caco-$2_{BBe}$ monolayer resistance is comparable to those of Caco-2 monolayers.

The absorption enhancement capacity of C10 was determined by measurement of the solute size cut-off and permeability rate of the metabolically inert fluorescent markers Flu, FD-4K and FD-70K. The properties of these markers are different. According to the manufacturer's data sheets, Flu has a Mw of 376.3, while FD-4K has a Mw of 4,000 and is approximately 14 Å in diameter and exhibits the properties of an expandable coil. Meanwhile, FD-70K has a Mw of 77,000 and a diameter of approximately 60 Å and behaves as if it is highly branched.

Lindmark *et al.* determined that incubation of Caco-2 cells with C10 resulted in the $P_{app}$ of Flu being split into a short-term interval (0-12 min) and a long-term phase (12-40 min). These results compare to those found in these studies as there were 2 different phases observed. However, these results differ from Lindmark *et al.* as there was a rapid increase in $P_{app}$ in the first 10 min, followed by a decrease in $P_{app}$, although the value was still greater than that of the control monolayers. Lindmark *et al.* did not find a decrease in $P_{app}$ after 12 min but found slight increases in $P_{app}$ in the long-term interval (Lindmark, *et al* 1998). The results observed in these studies correspond to those of the decreases in TER in Caco-$2_{BBe}$ monolayers treated with C10. The TER in these experiments show a rapid decrease in TER within the first 10 min corresponding to the initial increase in $P_{app}$, followed by a slight decrease in TER at 20 min with the value remaining constant for the remainder of the experiment. This corresponds to the decrease in $P_{app}$ at 20 min followed by a plateau for the remaining 20 min. These results indicate that C10 rapidly increases paracellular permeability allowing for a rapid flux of paracellular marker, followed by a sustained opening of the TJs, which allowed a steady flux of the paracellular markers through the paracellular space.

Following 10 min incubation of monolayers with C10 and Flu, FD-4K or FD-70K, there was a significant 4-, 3- and 6-fold increase of $P_{app}$ respectively when compared to monolayers incubated with marker alone. However, monolayers incubated with C10 and Dreverse PIK with Flu, FD-4K or FD-70K led to a significant increase by 10-, 16- and 13-fold respectively when compared to the control, and a 2-, 3- and 2- fold increase compared to monolayers treated with C10 only. These results are contradictory to the previous findings by Hayashi *et al.* and Lindmark *et al.* who proposed that inhibition of MLCK reduced the permeability effects of C10. Hayashi and colleagues found that the CaM inhibitor W7 inhibited C10 effects in hamster colon cells (Hayashi, *et al* 1999), whereas Lindmark and co-workers found that both W7 and ML-7 inhibited the effects of C10 in Caco-2 cell monolayers (Lindmark, *et al* 1998). However, W7 and ML-7 are not specific inhibitors, therefore, it is possible that W7 and ML-7 have non-specific activities that cause the reduction of C10 activity that are not produced by Dreverse PIK. However, this does not explain why Dreverse PIK increases the permeability of the markers. Therefore, it was decided to measure the short- and long-term effects of C10 on the

permeability of FD-4K, using Dreverse PIK and ML-7. Fluorescein isothiocyanate-dextran 4K was chosen as a model paracellular probe as it has been widely used by others to study TJ permeability in Caco-2 cells (Kamm, *et al* 2000, Takahashi, *et al* 2002).

Inhibition of MLCK with Dreverse PIK and ML-7 resulted in C10 short-term effects on FD-4K permeability increasing to 292 % and 252 % respectively when compared to C10 alone (which was taken as 100 %). This was contradictory to results obtained by Lindmark *et al.* where MLCK inhibition by ML-7 had no effects on C10 short-term interval in Caco-2 monolayers (Lindmark, *et al* 1998). The long-term effects of C10 were also increased (although to a lesser extent than the short-term) to 171 % and 196 % when co-incubated with Dreverse PIK and ML-7 respectively. However, Lindmark *et al.* observed an approximately 50 % decrease in C10 effects when MLCK was inhibited by ML-7. Lindmark *et al.* used $^{14}$C-mannitol for the measurement of the short- and long-term intervals of C10 on epithelial permeability (Lindmark, *et al* 1998), whereas these investigations used FD-4K, which has a greater Mw and has different properties to those of $^{14}$C-mannitol which has a Mw of 182.172. However, the $P_{app}$ of Flu, FD-4K and FD-70K (shown in figures 5.4, 5.5 and 5.6) have similar patterns. Hence, the greater Mw of FD-4K compared to $^{14}$C-mannitol should not have affected the short- and long-term effects of C10. One possible reason for the differences observed in these investigations is that C10 and the MLCK inhibitors (Dreverse PIK and ML-7) were added simultaneously to the Caco-$2_{BBe}$ monolayers whereas Lindmark *et al.* did not specify when ML-7 was added. Therefore, the time at which MLCK inhibitors are added to epithelial monolayers may be important to their abilities to inhibit C10 effects. Therefore, it was decided to incubate monolayers with Dreverse PIK and ML-7 before and after the addition of C10.

Pre-incubation of the Caco-$2_{BBe}$ monolayers with Dreverse PIK resulted in an increase of C10 short-term phase to 139 %. However, ML-7 reduced the activity of C10 to 79 %. These results are comparable to Lindmark and colleagues who did not observe any reductions of C10 effects when MLCK was inhibited by ML-7 (Lindmark, *et al* 1998). The long-term effects of C10 where reduced to roughly 50 % and 40 % when pre-incubated with Dreverse PIK and ML-7 respectively. Inhibition of C10 long-term effects by ML-7 in these studies are comparable to those

of Lindmark and co-workers, who found that the long-term effects of C10 were inhibited by approximately 50 % when the monolayers were incubated with ML-7 (Lindmark, *et al* 1998).

Post-addition of Dreverse PIK and ML-7 to the Caco-$2_{BBe}$ monolayers following 12 min exposure to C10 (following the short-term interval) resulted in an increase of permeability to 198 % and 146 % when incubated with Dreverse PIK and ML-7 respectively. These results show that the long-term effects of C10 are enhanced when MLCK is inhibited.

These investigations reveal that decreases of C10 effects by MLCK inhibition relies upon when the inhibitors are added to the monolayers. Additionally, Dreverse PIK and MLCK do not have different effects on permeability increases produced by C10. They also demonstrate that MLCK must be inhibited before the addition of C10 otherwise the inhibitors enhance the permeability effects of C10. One hypothesis is that C10 opens the TJ and that Dreverse PIK and ML-7 inhibit MLCK activity, thereby retaining MCLK in an active state causing rigour of the actin cytoskeleton. This results in prolonging TJ opening and subsequent increases in paracellular permeability. However, this may not be the case as 13 mM C10 causes the TER to reduce within 10 min and then plateaus at 20 to 60 min, suggesting that the TJs are open to their maximum capacity. Therefore, rigour of MLCK would not increase the permeability further in this case. However, Dreverse PIK and ML-7 cause the largest increases of FD-4K permeability in the short-term not the long-term interval when C10 and the MLCK inhibitors are added simultaneously. This suggests that inhibition of MLCK causes the permeability to increase more rapidly in the short-term phase than monolayers treated with C10 alone. It would therefore be interesting to determine the levels of MLCK and MLC phosphorylation at both the short-term and long-term intervals of C10 treatment.

Chitosans are high molecular weight cationic linear polysaccharides that are synthesised by chitin *N*-deacetylation (Schipper, *et al* 1997). The chitosan derivative TMC is currently being investiagted due to its increased solubility at wider pH and concentration ranges (Thanou, *et al* 2000). *N,N,N*-trimethyl chitosan chloride is thought to increase paracellular permeability in a manner similar to chitosan by displacement of cations from the electronegative sites of cell membranes (Kotze, *et*

*al* 1999). Chitosan has been shown to alter the distribution of F-actin, ZO-1 and occludin (Dodane, *et al* 1999). Therefore, it is hypothesised that inhibition of MLCK via Dreverse PIK may prevent the absorption enhancement effects of TMC.

The results show that TMC with 77 % quarternisation did decrease TER. However, the concentrations required were cytotoxic when assessed using the MTT assay. This was unexpected as TMC with 61.2 % quarternisation was used by Kotzé *et al.* reduced TER by 35 % at a concentration of 0.05 % w/v, and was shown to be non toxic to cells using trypan blue staining. Highly quarternised TMC has been shown to be more effective in increasing permeability than those with a lower percentage of quarternisation (Kotze, *et al* 1999). However, increased quarternisatinon has been shown to increase cytotoxicity using the MTT assay in COS-7 (monkey kidney fibroblasts) and MCF-7 (epithelial breast cancer) cell lines. In these studies, incubation of MCF-7 and COS-7 cells with 0.1 mg/ml of TMC with 76 % quarternisation for 6 h resulted in a reduction of cell viability to approximately 50 % and 5 % respectively (Kean, *et al* 2005). Caco-$2_{BBe}$ cells treated with 0.1 mg/ml TMC 77 % quarternistion for 2 h had a cell viability of approximately 60 % compared to the control. The increased cell viability could be due to the reduced time of incubation of the cells with the polymer, or the use of a different cell line. Therefore, TMC 77 % would not be suitable for increasing paracellular permeability in Caco-$2_{BBe}$ cell monolayers and hence the importance of MLCK activity in TMC increased TJ permeability could not be assessed.

The role of actin ring reorganisation in increases of permeability by chitosan is as yet still undetermined. Some groups have found that chitosan does not effect the actin ring of Caco-2 cells (Dodane, *et al* 1999, Smith, *et al* 2004). However, numerous groups have found a redistribution of F-actin from the actin ring of Caco-2 cells following incubation with chitosan chloride and glutamate respectively (Artursson, *et al* 1994, Ranaldi, *et al* 2002). Smith *et al.* found that treatment of Caco-2 cells with the PKC inhibitor (Ro318220) led to the inhibition of chitosan glutamate effects on TER (Smith, *et al* 2005). Protein kinase C has been shown to be an upstream regulator of MLC phosphorylation. Activation of PKC leads to phosphorylation of the MLCP inhibitor CPI-17 (Kitazawa, *et al* 2000). Myosin light

chain phosphatase regulates dephosphorylation of MLC; therefore, its inhibition would result in TJ opening and hence decrease TER (Huang, *et al* 2004).

Smith, *et al* compared the effects of chitosan to those of the PKC activator PMA. In these studies PMA reduced TER within 5 min of addition (Smith, *et al* 2005). Therefore, as PMA stimulates the effects of chitosan, it was decided to determine the effects of MLCK inhibition on PMA induced reductions in TER. However, the results showed that PMA did not decrease TER. Indeed, 162 nM increased TER to 130 % of the initial value, 2 h following addition. Nevertheless, Turner and colleagues found that PMA increased TER in Caco-2 cell monolayers whereas Barbosa and co-workers found that PMA did not affect TER at all (Barbosa, *et al* 2003, Turner, *et al* 1999). However, it is worth noting that Hecht *et al.* found that PMA induces acute increases in TER, whereas prolonged treatment resulted in decreases of TER thought to be caused by the down-regulation of PKC (Hecht, *et al* 1994).

Therefore, it was decided to determine the effects of PMA on TER using 170 nM, 540 nM and 1.6 μM (Turner, *et al* 1999). The results obtained from treating Caco-$2_{BBe}$ monolayers with these concentrations of PMA for 2 h resulted in the TER increasing approximately to 130 %, 130 % and 140 % of initial value. These results compare to those of Turner, *et al* whose studies showed that PMA-induced activation of PKC increased MLCK phosphorylation which resulted in a decrease in MLC phosphorylation (Turner, *et al* 1999). These results show that PMA does not decrease TER via activation of CPI-17, which inhibits MLCP resulting in increased MLC phosphorylation as hypothesised. Rather, it increases TER via inhibition of MLCK, leading to decreased MLC phosphorylation. These differences in PKC activation on TER could be due to isoform specificity. The PKC family contains at least 10 different isoforms which are classified into 3 groups, classical, novel and atypical, based on the regulatory domain structures (Nishizuka 1988). Different PKC isoforms are expressed within each cell type, and individual PKC isoforms can have opposing cellular effects. Additionally, PKC substrates are not isoform specific, with most substrates being phosphorylated by several PKC isoforms (Clarke, *et al* 2000). Phorbol 12-myristate 13-acetate (which has a structure similar to DAG) activates all classical and novel PKC isoforms (Nishizuka 1988). This could explain why PMA increases TER in some studies whilst decreasing it in

others. However Caco-2 cell lines were used in both studies and hence does not explain the conflicting results (Smith, *et al* 2005, Turner, *et al* 1999).

## 5.5 Conclusions

Myosin light chain kinase has been shown to be important in the regulation of the paracellular space (Hecht, *et al* 1996). These studies have confirmed that the absorption enhancer C10 that has been approved for human use increases permeability via MLCK activation. Prevention of the increases in permeability by Dreverse PIK and ML-7, however, were dependent on when the inhibitors were added to the monolayers. This discovery implies that C10 and Dreverse PIK could be used in conjunction with each other to increase the permeability of poorly absorbed drugs.

One drawback to the use of C10 and Dreverse PIK in combination is that it is unlikely that they will co-localise within the intestine *in vivo*. Since pre- and post-incubation of monolayers with Dreverse PIK does not enhance but decreases C10 effects, it is essential that they be delivered simultaneously. Development of drug delivery systems such as Gastrointestinal Permeation Enhancement Technology (GIPET™) may be able to overcome this problem. Gastrointestinal permeation enhancement technology are medium-chain fatty acid-based solid dosage forms, that have been shown to increase human oral bioavailability of alendronate, desmopressin and low-molecular-weight heparin when compared to unformulated controls. This is due to their ability to release the absorption enhancer and the drug together within the intestine. Therefore, it may be possible to produce C10 and Dreverse PIK with a poorly absorbed drug in enteric-coated tablets in order to increase paracellular permeability (Leonard, *et al* 2006).

The TMC in this study was cytotoxic to Caco-$2_{BBe}$. Hence, the role of MLCK in TMC ability to increase paracellular permeability could not be established. Future studies would involve the use of lower quarternised TMC which have been shown to be less cytotoxic (Kean, *et al* 2005), and hence the role of MLCK activity could be determined.

Numerous studies have shown the different effects of PMA on Caco-2 TER. However, the increased TER upon treatment of monolayers with PMA in these studies concur with those published by Turner, *et al* who found that PMA inhibited

MLCK, resulting in a decrease in MLC phosphorylation and a subsequent increase in TER. Future studies would include the use of the novel MLCP inhibitor PIP to determine whether inhibition of MLCP would prevent the increases in TER induced by PMA.

# Chapter 6

# General Discussion

## 6.1 General Discussion

The motivation behind these investigations was the determination of MLC dependent effects on TJ function through the actions of membrane-permeant peptides (figure 6.1). This was achieved by the design and synthesis of peptides that could decrease paracellular permeability associated with epithelial inflammatory conditions and increase TJ permeability for delivery of poorly absorbed drugs.

The initial objective of this project was to design a stable biologically active PIK analogue that could be used in further *in vivo* studies of intestinal inflammatory conditions. PIK represents a unique peptide-based drug candidate for the correction of paracellular defects associated with intestinal disease. However, PIK was rapidly cleaved within the intestinal lumen as initially predicted. These studies have identified 2 stable PIK analogues Dreverse PIK and D PIK, which now provide an opportunity to examine the role of MLCK modulators in various *in vivo* models of epithelial inflammation and inflammation-associated diseases such as CD (Chapter 3). *In vivo* studies are essential, as Caco-2 cell monolayers do not have a mucous layer covering the luminal side of the monolayers an important barrier to peptide absorption. However, studies by Clayburgh and colleagues have already shown PIK to be effective in preventing immune-mediated diarrhoea in mice (Clayburgh, *et al* 2005). Additional *in vivo* studies have shown that mice orally gavaged with Dreverse PIK have decreased levels of intestinal enteropooling induced by intraperitoneal injection of TNF-α, as determined by their intestinal weight to length ratios. They have also shown that TNF-α induced internalisation of occludin is prevented in mice gavaged with Dreverse PIK, suggesting that rearrangement of the TJ architecture by TNF-α is prevented. Dreverse PIK has also been demonstrated to inhibit TNF-α induced increases in MLC phosphorylation within mouse intestines. These studies show that the stable PIK analogue Dreverse PIK is effective at decreasing paracellular permeability, by preventing remodelling of the TJ proteins. Therefore, the aim of synthesising a stable PIK analogue for *in vivo* studies appears to be achieved (Jerrold Turner, personal communication).

PIK has numerous advantages over other drugs currently being used in intestinal inflammatory conditions. PIK does not require a drug delivery mechanism as it is resistant to cleavage within the intestine, plus it is able to internalise into cells

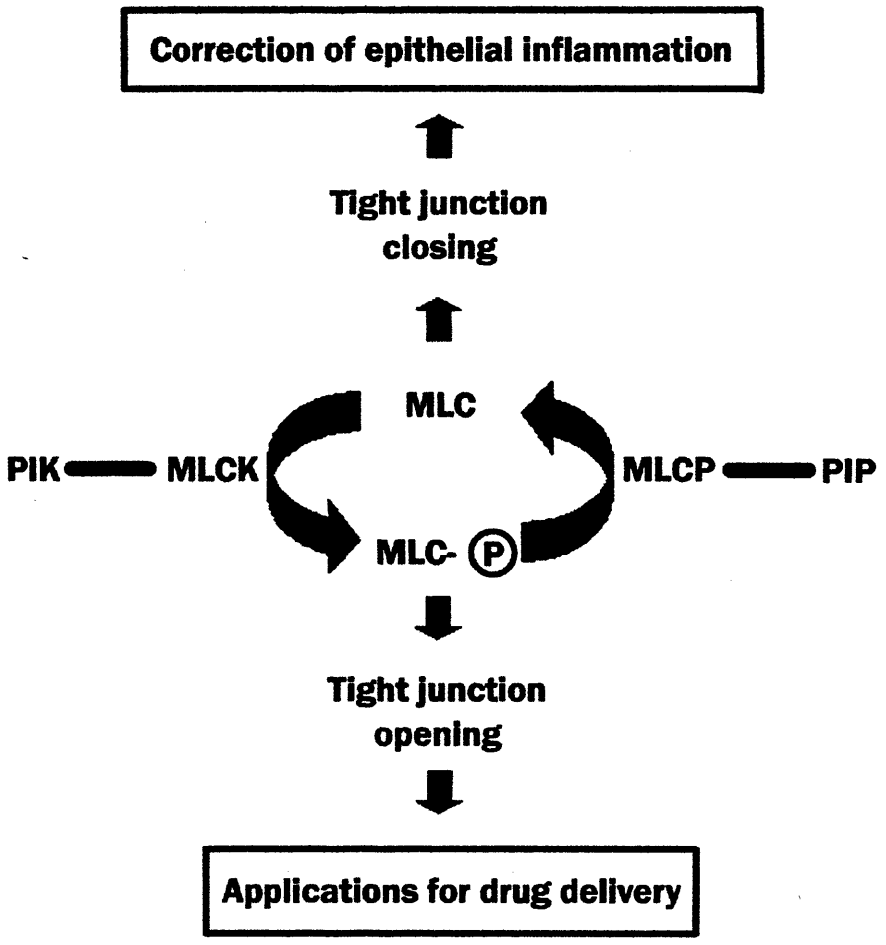


Figure 6.1 Schematic representation of the regulation of MLC phosphorylation by PIK and PIP.

due to its resemblance to the CPP TAT (Zolotarevsky, *et al* 2002). This is an unusual characteristic as the vast majority of protein and peptide therapeutics currently available are administered via injections. PIK has been shown to inhibit TJ disruption in immune-mediated diarrhoea in mice without any apparent toxicity, thought to be due to its local delivery. Therefore, it is hypothesised that PIK will have fewer side effects compared to systemic immunosuppressive therapies currently used in intestinal inflammatory disease states (Clayburgh, *et al* 2005). Thus PIK would be a local acting orally administered drug; this would be hugely beneficial as therapies for CD such as infliximab need to be administered via injections and corticosteroids have systemic side effects. One potential draw back to PIK use is the possibility that it may excessively decrease paracellular permeability. Tight junctions are involved in many physiological processes, activation of the $Na^+$-glucose co-transporter SGLT-1 results in increases in water absorption, therefore, excessive closure of TJs in the intestine could result in dehydration (Turner 2000).

It is worth noting that all studies performed using PIK so far have focused on increased intestinal permeability in cell and animal models. During the course of these PhD studies, others have investigated the role of MLCK activity in inflammatory diseases in other organs. The plasma of rats that have been inflicted by a thermal injury (burn plasma) has been shown to increase permeability across rat lung microvascular endothelial cell monolayers, which is reduced by the MLCK inhibitor ML-7. Hence inhibitors of MLCK may reduce systemic inflammation-induced endothelial dysfunction in burn patients (Tinsley, *et al* 2004). Phosphorylation of MLC is important in the regulation of corneal endothelium fluid-transport which is vital for stromal hydration, essential for tissue transparency. Histamine has been shown to increase phosphorylation of MLC via MLCK activation and partially by MLCP inhibition in corneal endothelial cells, resulting in endothelial barrier integrity breakdown. This effect was inhibited by MLCK and PKC inhibitors (Srinivas, *et al* 2006). Lipopolysaccharide exposure which is linked to cytokine production, results in infiltration of neutrophils and lung injury. Lipopolysaccharide induced lung inflammation and hyper-permeability in rats has been shown to be prevented by pre-treatment with ML-7 indicating that inhibitors of MLCK may be a relevant target for the treatment of lung injury (Eutamene, *et al* 2005). Following stroke disruption of the blood-brain barrier (BBB) results in

increased permeability of high-molecular weight compounds, leading to development of oedema and intracranial pressure. Kuhlmann, *et al* found that hypoxia increased MLC phosphorylation in bovine brain microvascular endothelial cells and that ML-7 inhibited hypoxia induced MLC phosphorylation thereby preventing BBB-disruption *in vitro* and *in vivo* (Kuhlmann, *et al* 2007).

Myosin light chain kinase activity has hence been shown to be important in inflammatory disease in other organs; especially the lungs. It is expected that in the future additional conditions were MLC phosphorylation is an important end point of hyperpermeability states will be discovered. However, Dreverse PIK and D PIK have been specifically designed for oral administration therefore, further studies would be required to determine PIK ability to cross these biological membranes and its stability in different enzymatic environments, in order to deliver the peptide to the desired target site.

The GI tract presents a significant obstacle in the delivery of oral therapeutics. The GI tract does not only constitute of a physical barrier but also consists of other barriers to oral drug delivery such as pH, mucous lining and extracellular enzymes. However, despite all the difficulties encountered there still remains a large focus in the delivery of drugs via the oral route. Advantages of this route over delivery via injections include, ease of administration and hence greater patient compliance and acceptability, also the cost of the manufacture is reduced as there is no need for sterile manufacturing facilities plus there is a reduced need for trained professionals to administer them.

Novel absorption enhancers for the delivery of poorly absorbed drugs via the oral route are continually being sought, especially with the growth in the number of new protein and peptide drugs. The vast majority of absorption enhancers have an unknown mode of action hence an absorption enhancer with a known mechanism of action would be beneficial. The second aim of this project was to design and synthesise MLCP inhibitors that could potentially increase paracellular drug delivery in a controlled and transient manner. PIP is a novel PP1 inhibitor based on CPI-17 protein PP1 active site docking motif. This novel peptide absorption enhancer has been shown to reduce TER of Caco-2 monolayers by approximately 50 %, which returned to 80 % of the initial TER 24 h following treatment. Additionally there was

no apparent cellular toxicity at the dose required for absorption enhancement (Chapter 4).

Although PIP is a promising drug candidate, it is worth noting that the studies into this inhibitor are in their infancy. PIP effects on MLC phosphorylation have yet to be determined, also relatively high concentrations of PIP are required to reduce TER compared to PIK concentrations required to increase TER. Additionally PIP in its current form would not be suitable for oral administration as it is predicted to be cleaved rapidly within the intestinal environment due the presence of numerous K and R within its sequence.

PIP has numerous advantages over other absorption enhancers as it has a known mode of action, plus it is predicted to be degraded within the intestinal cells by proteases and peptidases therefore the effects of PIP should be transient. Although many absorption enhancers increase paracellular permeability it is worth noting that this may be thought of as a mildly toxic effect, as they cause an uncontrolled passage of molecules from the intestinal lumen into circulation, consequently escaping the innate immunity function of the intestinal epithelial barriers (Ranaldi, *et al* 2002). Therefore, extensive *in vivo* studies will need to be performed to ensure that there are no adverse effects to the increases in paracellular permeability observed.

Protein phosphatase 1 does not only regulate cell contraction, it has also been shown to be important in the regulation of the cell cycle. Indeed activation of PP1 by the downregulation of Fer kinase has been shown to induce cell cycle arrest in both prostate carcinoma and breast carcinoma cell lines (Pasder, *et al* 2006). Therefore, PIP if future studies produced a specific stable analogue could potentially be used as a research molecule for prevention of cell cycle arrest in malignant cells.

Sodium caprate is one of the few absorption enhancers approved for human use, even though the exact mechanisms by which increases in absorption were unknown. Sodium caprate effects have been shown to be inhibited by the non specific MLCK inhibitor ML-7 (Lindmark, *et al* 1998). Therefore, the aim was to determine the precise role of MLCK activation in C10 absorption enhancement effects using the specific MLCK inhibitor PIK. Sodium caprate effects on absorption enhancement were significantly increased when monolayers were

simultaneously incubated with C10 and PIK or ML-7 (Chapter 5). Although when monolayers were pre-treated with MLCK inhibitors, C10 absorption enhancement effects were inhibited.

These results were unexpected as in theory increases in permeability due to increases in MLCK activity should be inhibited by PIK. These studies suggest that PIK could be administered in conjunction with C10 to increase the delivery of poorly absorbed drugs. However, on a cautionary note administration of C10 to patients should be undertaken with care, as activation of MLCK simultaneously with administration of C10 could potentially result in uncontrolled increases in paracellular permeability. This could result in the ability of noxious materials to traverse intestinal epithelial cell paracellular space and result in complications such as infections. These studies highlight the importance and complexity of MLC regulation of the TJ permeability.

*Further studies*

At the onset of this project it was hoped to determine the effects of MLC phosphorylation on paracellular permeability. Dreverse PIK and D PIK have greater stability then the parent PIK peptide whilst maintaining the biological activity and specificity. PIK has already been successfully used in an animal model of intestinal inflammatory (Clayburgh, *et al* 2005). These PIK analogues have the potential to be used in other inflammatory conditions, as studies by others have shown the importance of MLCK inhibition in the prevention of other inflammatory diseases.

These studies have designed a novel MLCP peptide inhibitor (PIP) which has been shown to increase paracellular permeability. Further studies include the assessment of PIP ability to alter MLC phosphorylation *in vitro* and in intact Caco-2 monolayers. If PIP did specifically inhibit MLCP activity, its use in *in vivo* studies would be limited due to its likely degradation within minutes of reaching the intestinal lumen rendering it inactive. Therefore, the stability of PIP would need to be assessed and subsequent synthesis of stable analogues would need to be performed.

The studies using C10 have resulted in the surprising outcome that simultaneous addition of MLCK inhibitors and C10 to monolayers increases not decrease permeability as predicted. Therefore, MLCK inhibitors and C10 could be

used in conjunction with each other to increase drug delivery of poorly absorbed drugs. Further studies would include the investigation of MLC phosphorylation state at the various points when PIK was added to the C10 treated monolayers.

*Future of peptide therapeutics*

The development of peptide therapeutics has been a long and arduous process. Issues such as low oral bioavailability, stability and high costs of manufacturing have hampered the use of peptides commercially. However, peptides have significant advantages over small molecules, including higher activity and specificity with lower toxicities. Nevertheless, the vast majority of peptide drugs still require to be delivered via injections, which have numerous disadvantages. At present there are only 2 oral and 3 nasal delivered products approved for human use in the USA. Desmopressin, 1-desamino-8-D-arginine vasopressin (DDAVP), is a 9 amino acid cyclic peptide analogue of arginine vasopressin, used as an antidiuretic that can be taken via the oral or nasal route (Fjellestad-Paulsen, *et al* 1993). Cyclosporin a lipophilic 11 amino acid cyclic polypeptide, is an immunosuppressant drug widely used following allogeneic organ transplant to reduce the activity of the patient's immune system and hence the risk of organ rejection. It is also used to treat psoriasis and rheumatoid arthritis (Italia, *et al* 2006). Synarel® (narfarelin acetate) a synthetic decapeptide analogue of gonadotropin-releasing hormone delivered via the nasal route is used to treat endometreosis. The nasal spray miacalcin® a calcitonin analogue of 32 amino acids is marketed as a treatment for osteoporosis (Brown 2005). Although, there is a limited amount of peptides delivered via non-invasive routes, there are some promising oral (Clement, *et al* 2004) and pulmonary (Cefalu 2004) insulin products in clinical trials. Therefore, it is predicted that the number of peptide drugs approved will increase in the future, although the majority of these are likely to be administered via injections.

*Summary*

The main objectives of these studies were to determine the effects of MLC phosphorylation on TJ function. These studies have shown that both MLCK and MLCP are key players in the regulation of TJ permeability. As inhibition of MLCK and MLCP by membrane-permeant peptide inhibitors resulted in the closure and

opening of TJs respectively. This project has also shown that it is possible to design stable peptide analogues that inhibit kinase and phosphatase activity. This principle could be used in the design and synthesis of other novel peptide based drugs. In conclusion, MLC phosphorylation has been proven to be a critical factor in the regulation of the paracellular space.

# References

Adessi, C. & Soto, C. (2002) Converting a peptide into a drug: strategies to improve stability and bioavailability. *Curr Med Chem,* **9,** 963-978.

Aebersold, R. & Mann, M. (2003) Mass spectrometry-based proteomics. *Nature,* **422,** 198-207.

Anderberg, E.K., Lindmark, T. & Artursson, P. (1993) Sodium caprate elicits dilatations in human intestinal tight junctions and enhances drug absorption by the paracellular route. *Pharm Res,* **10,** 857-864.

Ando-Akatsuka, Y., Saitou, M., Hirase, T., Kishi, M., Sakakibara, A., Itoh, M., Yonemura, S., Furuse, M. & Tsukita, S. (1996) Interspecies diversity of the occludin sequence: cDNA cloning of human, mouse, dog, and rat-kangaroo homologues. *J Cell Biol,* **133,** 43-47.

Arnott, I.D., Watts, D. & Satsangi, J. (2003) Azathioprine and anti-TNF alpha therapies in Crohn's disease: a review of pharmacology, clinical efficacy and safety. *Pharmacol Res,* **47,** 1-10.

Artursson, P. & Karlsson, J. (1991) Correlation between oral drug absorption in humans and apparent drug permeability coefficients in human intestinal epithelial (Caco-2) cells. *Biochem Biophys Res Commun,* **175,** 880-885.

Artursson, P., Lindmark, T., Davis, S.S. & Illum, L. (1994) Effect of chitosan on the permeability of monolayers of intestinal epithelial cells (Caco-2). *Pharm Res,* **11,** 1358-1361.

Aungst, B.J. (2000) Intestinal permeation enhancers. *J Pharm Sci,* **89,** 429-442.

Bain, J., McLauchlan, H., Elliott, M. & Cohen, P. (2003) The specificities of protein kinase inhibitors: an update. *Biochem J,* **371,** 199-204.

Balda, M.S. & Matter, K. (1998) Tight junctions. *J Cell Sci,* **111 (Pt 5),** 541-547.

Balda, M.S. & Matter, K. (2003) Epithelial cell adhesion and the regulation of gene expression. *Trends Cell Biol,* **13,** 310-318.

Balda, M.S., Whitney, J.A., Flores, C., Gonzalez, S., Cereijido, M. & Matter, K. (1996) Functional dissociation of paracellular permeability and transepithelial electrical resistance and disruption of the apical-basolateral intramembrane diffusion barrier by expression of a mutant tight junction membrane protein. *J Cell Biol,* **134,** 1031-1049.

Barbosa, L.A., Goto-Silva, L., Redondo, P.A., Oliveira, S., Montesano, G., De Souza, W. & Morgado-Diaz, J.A. (2003) TPA-induced signal transduction: a link between PKC and EGFR signaling modulates the assembly of intercellular junctions in Caco-2 cells. *Cell Tissue Res,* **312,** 319-331.

Barnes, P.J. (1998) Anti-inflammatory actions of glucocorticoids: molecular mechanisms. *Clin Sci (Lond),* **94,** 557-572.

Bazzoni, G., Martinez-Estrada, O.M., Orsenigo, F., Cordenonsi, M., Citi, S. & Dejana, E. (2000) Interaction of junctional adhesion molecule with the tight junction components ZO-1, cingulin, and occludin. *J Biol Chem,* **275,** 20520-20526.

Bonen, D.K. & Cho, J.H. (2003) The genetics of inflammatory bowel disease. *Gastroenterology,* **124,** 521-536.

Borchard, G., LueBen, H., L., de Boer, A., G., Coos Verhoef, J., Lehr, C., M. & Junginger, H.E. (1996) The potential of mucoadhesive polymers in enhancing intestinal peptide drug absorption. III: Effects of chitosan-glutamate and carbomer on epithelial tight junctions in vitro. *J Control Release,* **39,** 131-138.

Bouma, G. & Strober, W. (2003) The immunological and genetic basis of

inflammatory bowel disease. *Nat Rev Immunol,* **3,** 521-533.

Bromberg, L. & Alakhov, V. (2003) Effects of polyether-modified poly(acrylic acid) microgels on doxorubicin transport in human intestinal epithelial Caco-2 cell layers. *J Control Release,* **88,** 11-22.

Brown, L.R. (2005) Commercial challenges of protein drug delivery. *Expert Opin Drug Deliv,* **2,** 29-42.

Brozovich, F.V. (2002) Myosin light chain phosphatase: it gets around. *Circ Res,* **90,** 500-502.

Carty, E. & Rampton, D.S. (2003) Evaluation of new therapies for inflammatory bowel disease. *Br J Clin Pharmacol,* **56,** 351-361.

Cefalu, W.T. (2004) Concept, strategies, and feasibility of noninvasive insulin delivery. *Diabetes Care,* **27,** 239-246.

Cenac, N., Garcia-Villar, R., Ferrier, L., Larauche, M., Vergnolle, N., Bunnett, N.W., Coelho, A.M., Fioramonti, J. & Bueno, L. (2003) Proteinase-activated receptor-2 induced colonic inflammation in mice: possible involvement of afferent neurons, nitric oxide, and paracellular permeability. *J Immunol,* **170,** 4296-4300.

Chen, F., Castranova, V., Shi, X. & Demers, L.M. (1999) New insights into the role of nuclear factor-kappaB, a ubiquitous transcription factor in the initiation of diseases. *Clin Chem,* **45,** 7-17.

Chorev, M. & Goodman, M. (1995) Recent developments in retro peptides and proteins--an ongoing topochemical exploration. *Trends Biotechnol,* **13,** 438-445.

Clarke, H., Marano, C.W., Peralta Soler, A. & Mullin, J.M. (2000) Modification of tight junction function by protein kinase C isoforms. *Adv Drug Deliv Rev,* **41,** 283-

301.

Clayburgh, D.R., Barrett, T.A., Tang, Y., Meddings, J.B., Van Eldik, L.J., Watterson, D.M., Clarke, L.L., Mrsny, R.J. & Turner, J.R. (2005) Epithelial myosin light chain kinase-dependent barrier dysfunction mediates T cell activation-induced diarrhea in vivo. *J Clin Invest,* **115,** 2702-2715.

Clement, S., Dandona, P., Still, J.G. & Kosutic, G. (2004) Oral modified insulin (HIM2) in patients with type 1 diabetes mellitus: results from a phase I/II clinical trial. *Metabolism,* **53,** 54-58.

Denker, B.M. & Nigam, S.K. (1998) Molecular structure and assembly of the tight junction. *Am J Physiol,* **274,** F1-9.

Derossi, D., Joliot, A.H., Chassaing, G. & Prochiantz, A. (1994) The third helix of the Antennapedia homeodomain translocates through biological membranes. *J Biol Chem,* **269,** 10444-10450.

Dharmsathaphorn, K., McRoberts, J.A., Mandel, K.G., Tisdale, L.D. & Masui, H. (1984) A human colonic tumor cell line that maintains vectorial electrolyte transport. *Am J Physiol,* **246,** G204-208.

Dodane, V., Amin Khan, M. & Merwin, J.R. (1999) Effect of chitosan on epithelial permeability and structure. *Int J Pharm,* **182,** 21-32.

Donnenberg, M.S., Kaper, J.B. & Finlay, B.B. (1997) Interactions between enteropathogenic Escherichia coli and host epithelial cells. *Trends Microbiol,* **5,** 109-114.

Ebnet, K., Schulz, C.U., Meyer Zu Brickwedde, M.K., Pendl, G.G. & Vestweber, D. (2000) Junctional adhesion molecule interacts with the PDZ domain-containing proteins AF-6 and ZO-1. *J Biol Chem,* **275,** 27979-27988.

Elliott, G. & O'Hare, P. (1997) Intercellular trafficking and protein delivery by a herpesvirus structural protein. *Cell,* **88,** 223-233.

Eto, M., Kitazawa, T. & Brautigan, D.L. (2004) Phosphoprotein inhibitor CPI-17 specificity depends on allosteric regulation of protein phosphatase-1 by regulatory subunits. *Proc Natl Acad Sci U S A,* **101,** 8888-8893.

Eto, M., Kitazawa, T., Yazawa, M., Mukai, H., Ono, Y. & Brautigan, D.L. (2001) Histamine-induced vasoconstriction involves phosphorylation of a specific inhibitor protein for myosin phosphatase by protein kinase C alpha and delta isoforms. *J Biol Chem,* **276,** 29072-29078.

Eto, M., Senba, S., Morita, F. & Yazawa, M. (1997) Molecular cloning of a novel phosphorylation-dependent inhibitory protein of protein phosphatase-1 (CPI17) in smooth muscle: its specific localization in smooth muscle. *FEBS Lett,* **410,** 356-360.

Eutamene, H., Theodorou, V., Schmidlin, F., Tondereau, V., Garcia-Villar, R., Salvador-Cartier, C., Chovet, M., Bertrand, C. & Bueno, L. (2005) LPS-induced lung inflammation is linked to increased epithelial permeability: role of MLCK. *Eur Respir J,* **25,** 789-796.

Fanning, A.S., Jameson, B.J., Jesaitis, L.A. & Anderson, J.M. (1998) The tight junction protein ZO-1 establishes a link between the transmembrane protein occludin and the actin cytoskeleton. *J Biol Chem,* **273,** 29745-29753.

Farquhar, M.G. & Palade, G.E. (1963) Junctional complexes in various epithelia. *J Cell Biol,* **17,** 375-412.

Fasano, A. (1998) Novel approaches for oral delivery of macromolecules. *J Pharm Sci,* **87,** 1351-1356.

Fauchere, J.L. & Thurieau, C. (1992) Evaluation of the stability of peptides and

pseudopeptides as a tool in peptide drug design. *Advances in Drug Reasearch,* **23,** 127-159.

Fiocchi, C. (1998) Inflammatory bowel disease: etiology and pathogenesis. *Gastroenterology,* **115,** 182-205.

Fischer, D., Li, Y., Ahlemeyer, B., Krieglstein, J. & Kissel, T. (2003) In vitro cytotoxicity testing of polycations: influence of polymer structure on cell viability and hemolysis. *Biomaterials,* **24,** 1121-1131.

Fix, J.A. (1996) Oral controlled release technology for peptides: status and future prospects. *Pharm Res,* **13,** 1760-1764.

Fjellestad-Paulsen, A., Hoglund, P., Lundin, S. & Paulsen, O. (1993) Pharmacokinetics of 1-deamino-8-D-arginine vasopressin after various routes of administration in healthy volunteers. *Clin Endocrinol (Oxf),* **38,** 177-182.

Fujino, S., Andoh, A., Bamba, S., Ogawa, A., Hata, K., Araki, Y., Bamba, T. & Fujiyama, Y. (2003) Increased expression of interleukin 17 in inflammatory bowel disease. *Gut,* **52,** 65-70.

Furuse, M., Hirase, T., Itoh, M., Nagafuchi, A., Yonemura, S., Tsukita, S. & Tsukita, S. (1993) Occludin: a novel integral membrane protein localizing at tight junctions. *J Cell Biol,* **123,** 1777-1788.

Fuss, I.J., Neurath, M., Boirivant, M., Klein, J.S., de la Motte, C., Strong, S.A., Fiocchi, C. & Strober, W. (1996) Disparate CD4+ lamina propria (LP) lymphokine secretion profiles in inflammatory bowel disease. Crohn's disease LP cells manifest increased secretion of IFN-gamma, whereas ulcerative colitis LP cells manifest increased secretion of IL-5. *J Immunol,* **157,** 1261-1270.

Futaki, S., Goto, S. & Sugiura, Y. (2003) Membrane permeability commonly shared

among arginine-rich peptides. *J Mol Recognit,* **16,** 260-264.

Gailly, P., Gong, M.C., Somlyo, A.V. & Somlyo, A.P. (1997) Possible role of atypical protein kinase C activated by arachidonic acid in Ca2+ sensitization of rabbit smooth muscle. *J Physiol,* **500 (Pt 1),** 95-109.

Gassler, N., Rohr, C., Schneider, A., Kartenbeck, J., Bach, A., Obermuller, N., Otto, H.F. & Autschbach, F. (2001) Inflammatory bowel disease is associated with changes of enterocytic junctions. *Am J Physiol Gastrointest Liver Physiol,* **281,** G216-228.

Gong, M.C., Fuglsang, A., Alessi, D., Kobayashi, S., Cohen, P., Somlyo, A.V. & Somlyo, A.P. (1992) Arachidonic acid inhibits myosin light chain phosphatase and sensitizes smooth muscle to calcium. *J Biol Chem,* **267,** 21492-21498.

Gonzalez-Mariscal, L., Betanzos, A. & Avila-Flores, A. (2000) MAGUK proteins: structure and role in the tight junction. *Semin Cell Dev Biol,* **11,** 315-324.

Gonzalez-Mariscal, L., Betanzos, A., Nava, P. & Jaramillo, B.E. (2003) Tight junction proteins. *Prog Biophys Mol Biol,* **81,** 1-44.

Gratecos, D. & Fischer, E.H. (1974) Adenosine 5'-O(3-thiotriphosphate) in the control of phosphorylase activity. *Biochem Biophys Res Commun,* **58,** 960-967.

Hanada, T. & Yoshimura, A. (2002) Regulation of cytokine signaling and inflammation. *Cytokine Growth Factor Rev,* **13,** 413-421.

Harhaj, N.S. & Antonetti, D.A. (2004) Regulation of tight junctions and loss of barrier function in pathophysiology. *Int J Biochem Cell Biol,* **36,** 1206-1237.

Harrington, L.E., Mangan, P.R. & Weaver, C.T. (2006) Expanding the effector CD4 T-cell repertoire: the Th17 lineage. *Curr Opin Immunol,* **18,** 349-356.

Hartshorne, D.J. & Hirano, K. (1999) Interactions of protein phosphatase type 1, with a focus on myosin phosphatase. *Mol Cell Biochem,* **190,** 79-84.

Hartshorne, D.J., Ito, M. & Erdodi, F. (1998) Myosin light chain phosphatase: subunit composition, interactions and regulation. *J Muscle Res Cell Motil,* **19,** 325-341.

Haskins, J., Gu, L., Wittchen, E.S., Hibbard, J. & Stevenson, B.R. (1998) ZO-3, a novel member of the MAGUK protein family found at the tight junction, interacts with ZO-1 and occludin. *J Cell Biol,* **141,** 199-208.

Hayashi, M., Sakai, T., Hasegawa, Y., Nishikawahara, T., Tomioka, H., Iida, A., Shimizu, N., Tomita, M. & Awazu, S. (1999) Physiological mechanism for enhancement of paracellular drug transport. *J Control Release,* **62,** 141-148.

Hayashi, Y., Senba, S., Yazawa, M., Brautigan, D.L. & Eto, M. (2001) Defining the structural determinants and a potential mechanism for inhibition of myosin phosphatase by the protein kinase C-potentiated inhibitor protein of 17 kDa. *J Biol Chem,* **276,** 39858-39863.

Hecht, G., Pestic, L., Nikcevic, G., Koutsouris, A., Tripuraneni, J., Lorimer, D.D., Nowak, G., Guerriero, V., Jr., Elson, E.L. & Lanerolle, P.D. (1996) Expression of the catalytic domain of myosin light chain kinase increases paracellular permeability. *Am J Physiol,* **271,** C1678-1684.

Hecht, G., Robinson, B. & Koutsouris, A. (1994) Reversible disassembly of an intestinal epithelial monolayer by prolonged exposure to phorbol ester. *Am J Physiol,* **266,** G214-221.

Hemmings, H.C., Jr., Greengard, P., Tung, H.Y. & Cohen, P. (1984) DARPP-32, a dopamine-regulated neuronal phosphoprotein, is a potent inhibitor of protein phosphatase-1. *Nature,* **310,** 503-505.

Hidaka, H., Sasaki, Y., Tanaka, T., Endo, T., Ohno, S., Fujii, Y. & Nagata, T. (1981) N-(6-aminohexyl)-5-chloro-1-naphthalenesulfonamide, a calmodulin antagonist, inhibits cell proliferation. *Proc Natl Acad Sci U S A,* **78,** 4354-4357.

Hilgers, A.R., Conradi, R.A. & Burton, P.S. (1990) Caco-2 cell monolayers as a model for drug transport across the intestinal mucosa. *Pharm Res,* **7,** 902-910.

Hilsden, R.J., Meddings, J.B. & Sutherland, L.R. (1996) Intestinal permeability changes in response to acetylsalicylic acid in relatives of patients with Crohn's disease. *Gastroenterology,* **110,** 1395-1403.

Hochman, J. & Artursson, P. (1994) Mechanisms of absorption enhancement and tight junction regulation. *J Control Release,* **29,** 253-267.

Hollander, D. (1988) Crohn's disease--a permeability disorder of the tight junction? *Gut,* **29,** 1621-1624.

Huang, F.L. & Glinsmann, W.H. (1976) Separation and characterization of two phosphorylase phosphatase inhibitors from rabbit skeletal muscle. *Eur J Biochem,* **70,** 419-426.

Huang, Q.Q., Fisher, S.A. & Brozovich, F.V. (2004) Unzipping the role of myosin light chain phosphatase in smooth muscle cell relaxation. *J Biol Chem,* **279,** 597-603.

Hugot, J.P., Chamaillard, M., Zouali, H., Lesage, S., Cezard, J.P., Belaiche, J., Almer, S., Tysk, C., O'Morain, C.A., Gassull, M., Binder, V., Finkel, Y., Cortot, A., Modigliani, R., Laurent-Puig, P., Gower-Rousseau, C., Macry, J., Colombel, J.F., Sahbatou, M. & Thomas, G. (2001) Association of NOD2 leucine-rich repeat variants with susceptibility to Crohn's disease. *Nature,* **411,** 599-603.

Ichikawa, K., Hirano, K., Ito, M., Tanaka, J., Nakano, T. & Hartshorne, D.J. (1996) Interactions and properties of smooth muscle myosin phosphatase. *Biochemistry,* **35,**

6313-6320.

Inohara, N., Ogura, Y. & Nunez, G. (2002) Nods: a family of cytosolic proteins that regulate the host response to pathogens. *Curr Opin Microbiol,* **5,** 76-80.

Irvine, E.J. & Marshall, J.K. (2000) Increased intestinal permeability precedes the onset of Crohn's disease in a subject with familial risk. *Gastroenterology,* **119,** 1740-1744.

Italia, J.L., Bhardwaj, V. & Kumar, M.N. (2006) Disease, destination, dose and delivery aspects of ciclosporin: the state of the art. *Drug Discov Today,* **11,** 846-854.

Ito, M., Nakano, T., Erdodi, F. & Hartshorne, D.J. (2004) Myosin phosphatase: structure, regulation and function. *Mol Cell Biochem,* **259,** 197-209.

Itoh, M., Furuse, M., Morita, K., Kubota, K., Saitou, M. & Tsukita, S. (1999a) Direct binding of three tight junction-associated MAGUKs, ZO-1, ZO-2, and ZO-3, with the COOH termini of claudins. *J Cell Biol,* **147,** 1351-1363.

Itoh, M., Morita, K. & Tsukita, S. (1999b) Characterization of ZO-2 as a MAGUK family member associated with tight as well as adherens junctions with a binding affinity to occludin and alpha catenin. *J Biol Chem,* **274,** 5981-5986.

Jones, S.W., Christison, R., Bundell, K., Voyce, C.J., Brockbank, S.M., Newham, P. & Lindsay, M.A. (2005) Characterisation of cell-penetrating peptide-mediated peptide delivery. *Br J Pharmacol,* **145,** 1093-1102.

Kahns, A.H., Buur, A. & Bundgaard, H. (1993) Prodrugs of peptides. 18. Synthesis and evaluation of various esters of desmopressin (dDAVP). *Pharm Res,* **10,** 68-74.

Kamm, W., Jonczyk, A., Jung, T., Luckenbach, G., Raddatz, P. & Kissel, T. (2000) Evaluation of absorption enhancement for a potent cyclopeptidic alpha(nu)beta(3)-

antagonist in a human intestinal cell line (Caco-2). *Eur J Pharm Sci,* **10,** 205-214.

Kean, T., Roth, S. & Thanou, M. (2005) Trimethylated chitosans as non-viral gene delivery vectors: cytotoxicity and transfection efficiency. *J Control Release,* **103,** 643-653.

Kitazawa, T., Eto, M., Woodsome, T.P. & Brautigan, D.L. (2000) Agonists trigger G protein-mediated activation of the CPI-17 inhibitor phosphoprotein of myosin light chain phosphatase to enhance vascular smooth muscle contractility. *J Biol Chem,* **275,** 9897-9900.

Kotze, A.F., Luessen, H.L., de Leeuw, B.J., de Boer, B.G., Verhoef, J.C. & Junginger, H.E. (1997) N-trimethyl chitosan chloride as a potential absorption enhancer across mucosal surfaces: in vitro evaluation in intestinal epithelial cells (Caco-2). *Pharm Res,* **14,** 1197-1202.

Kotze, A.F., Thanou, M.M., Luebetaen, H.L., de Boer, A.G., Verhoef, J.C. & Junginger, H.E. (1999) Enhancement of paracellular drug transport with highly quaternized N-trimethyl chitosan chloride in neutral environments: in vitro evaluation in intestinal epithelial cells (Caco-2). *J Pharm Sci,* **88,** 253-257.

Kucharzik, T., Walsh, S.V., Chen, J., Parkos, C.A. & Nusrat, A. (2001) Neutrophil transmigration in inflammatory bowel disease is associated with differential expression of epithelial intercellular junction proteins. *Am J Pathol,* **159,** 2001-2009.

Kuhlmann, C.R., Tamaki, R., Gamerdinger, M., Lessmann, V., Behl, C., Kempski, O.S. & Luhmann, H.J. (2007) Inhibition of the myosin light chain kinase prevents hypoxia-induced blood-brain barrier disruption. *J Neurochem.* **102,** 501-507.

Kunzelmann, K. & Mall, M. (2002) Electrolyte transport in the mammalian colon: mechanisms and implications for disease. *Physiol Rev,* **82,** 245-289.

Lapierre, L.A. (2000) The molecular structure of the tight junction. *Adv Drug Deliv*

*Rev,* **41,** 255-264.

Lee, V.H. (1988) Enzymatic barriers to peptide and protein absorption. *Crit Rev Ther Drug Carrier Syst,* **5,** 69-97.

Lee, V.H., Yamamoto, A. & Kompella, U.B. (1991) Mucosal penetration enhancers for facilitation of peptide and protein drug absorption. *Crit Rev Ther Drug Carrier Syst,* **8,** 91-192.

Leonard, T.W., Lynch, J., McKenna, M.J. & Brayden, D.J. (2006) Promoting absorption of drugs in humans using medium-chain fatty acid-based solid dosage forms: GIPET. *Expert Opin Drug Deliv,* **3,** 685-692.

Lindmark, T., Kimura, Y. & Artursson, P. (1998) Absorption enhancement through intracellular regulation of tight junction permeability by medium chain fatty acids in Caco-2 cells. *J Pharmacol Exp Ther,* **284,** 362-369.

Lindmark, T., Soderholm, J.D., Olaison, G., Alvan, G., Ocklind, G. & Artursson, P. (1997) Mechanism of absorption enhancement in humans after rectal administration of ampicillin in suppositories containing sodium caprate. *Pharm Res,* **14,** 930-935.

Liu, Y., Nusrat, A., Schnell, F.J., Reaves, T.A., Walsh, S., Pochet, M. & Parkos, C.A. (2000) Human junction adhesion molecule regulates tight junction resealing in epithelia. *J Cell Sci,* **113 (Pt 13),** 2363-2374.

Lofberg, R. (2003) Review article: medical treatment of mild to moderately active Crohn's disease. *Aliment Pharmacol Ther,* **17 Suppl 2,** 18-22.

Lukas, T.J., Mirzoeva, S., Slomczynska, U. & Watterson, D.M. (1999) Identification of novel classes of protein kinase inhibitors using combinatorial peptide chemistry based on functional genomics knowledge. *J Med Chem,* **42,** 910-919.

Ma, T.Y., Hoa, N.T., Tran, D.D., Bui, V., Pedram, A., Mills, S. & Merryfield, M. (2000) Cytochalasin B modulation of Caco-2 tight junction barrier: role of myosin light chain kinase. *Am J Pathol Gastrointest Liver Physiol,* **279,** G875-G885.

Ma, T.Y., Hollander, D., Tran, L.T., Nguyen, D., Hoa, N. & Bhalla, D. (1995) Cytoskeletal regulation of Caco-2 intestinal monolayer paracellular permeability. *J Cell Physiol,* **164,** 533-545.

Ma, T.Y., Iwamoto, G.K., Hoa, N.T., Akotia, V., Pedram, A., Boivin, M.A. & Said, H.M. (2004) TNF-alpha-induced increase in intestinal epithelial tight junction permeability requires NF-kappa B activation. *Am J Physiol Gastrointest Liver Physiol,* **286,** G367-376.

Madara, J.L. (1998) Regulation of the movement of solutes across tight junctions. *Annu Rev Physiol,* **60,** 143-159.

Mahato, R.I., Narang, A.S., Thoma, L. & Miller, D.D. (2003) Emerging trends in oral delivery of peptide and protein drugs. *Crit Rev Ther Drug Carrier Syst,* **20,** 153 214.

Mall, M., Gonska, T., Thomas, J., Hirtz, S., Schreiber, R. & Kunzelmann, K. (2002) Activation of ion secretion via proteinase-activated receptor-2 in human colon. *Am J Physiol Gastrointest Liver Physiol,* **282,** G200-210.

Manjarrez-Hernandez, H.A., Amess, B., Sellers, L., Baldwin, T.J., Knutton, S., Williams, P.H. & Aitken, A. (1991) Purification of a 20 kDa phosphoprotein from epithelial cells and identification as a myosin light chain. Phosphorylation induced by enteropathogenic Escherichia coli and phorbol ester. *FEBS Lett,* **292,** 121-127.

Matsuzawa, F., Aikawa, S.I., Ohki, S.Y. & Eto, M. (2005) Phospho-pivot modeling predicts specific interactions of protein phosphatase-1 with a phospho-inhibitor protein CPI-17. *J Biochem (Tokyo),* **137,** 633-641.

May, G.R., Sutherland, L.R. & Meddings, J.B. (1993) Is small intestinal permeability really increased in relatives of patients with Crohn's disease? *Gastroenterology,* **104,** 1627-1632.

Miret, S., Abrahamse, L. & de Groene, E.M. (2004) Comparison of in vitro models for the prediction of compound absorption across the human intestinal mucosa. *J Biomol Screen,* **9,** 598-606.

Mitchell, D.J., Kim, D.T., Steinman, L., Fathman, C.G. & Rothbard, J.B. (2000) Polyarginine enters cells more efficiently than other polycationic homopolymers. *J Pept Res,* **56,** 318-325.

Mitic, L.L. & Anderson, J.M. (1998) Molecular architecture of tight junctions. *Annu Rev Physiol,* **60,** 121-142.

Mosmann, T. (1983) Rapid colorimetric assay for cellular growth and survival: application to proliferation and cytotoxicity assays. *J Immunol Methods,* **65,** 55-63.

Murthy, K.S. (2005) Signaling for Contraction and Relaxation in Smooth Muscle of the Gut. *Annu Rev Physiol.*

Murthy, K.S., Zhou, H., Grider, J.R. & Makhlouf, G.M. (2003) Inhibition of sustained smooth muscle contraction by PKA and PKG preferentially mediated by phosphorylation of RhoA. *Am J Physiol Gastrointest Liver Physiol,* **284,** G1006-1016.

Nakamura, R.M., Matsutani, M. & Barry, M. (2003) Advances in clinical laboratory tests for inflammatory bowel disease. *Clin Chim Acta,* **335,** 9-20.

Nishizuka, Y. (1988) The molecular heterogeneity of protein kinase C and its implications for cellular regulation. *Nature,* **334,** 661-665.

Nusrat, A., Chen, J.A., Foley, C.S., Liang, T.W., Tom, J., Cromwell, M., Quan, C. & Mrsny, R.J. (2000a) The coiled-coil domain of occludin can act to organize structural and functional elements of the epithelial tight junction. *J Biol Chem,* **275,** 29816-29822.

Nusrat, A., Turner, J.R. & Madara, J.L. (2000b) Molecular physiology and pathophysiology of tight junctions. IV. Regulation of tight junctions by extracellular stimuli: nutrients, cytokines, and immune cells. *Am J Physiol Gastrointest Liver Physiol,* **279,** G851-857.

Ogura, Y., Bonen, D.K., Inohara, N., Nicolae, D.L., Chen, F.F., Ramos, R., Britton, H., Moran, T., Karaliuskas, R., Duerr, R.H., Achkar, J.P., Brant, S.R., Bayless, T.M., Kirschner, B.S., Hanauer, S.B., Nunez, G. & Cho, J.H. (2001) A frameshift mutation in NOD2 associated with susceptibility to Crohn's disease. *Nature,* **411,** 603-606.

Ohama, T., Hori, M., Sato, K., Ozaki, H. & Karaki, H. (2003) Chronic treatment with interleukin-1beta attenuates contractions by decreasing the activities of CPI-17 and MYPT-1 in intestinal smooth muscle. *J Biol Chem,* **278,** 48794-48804.

Ohki, S., Eto, M., Kariya, E., Hayano, T., Hayashi, Y., Yazawa, M., Brautigan, D. & Kainosho, M. (2001) Solution NMR structure of the myosin phosphatase inhibitor protein CPI-17 shows phosphorylation-induced conformational changes responsible for activation. *J Mol Biol,* **314,** 839-849.

Owens, S.E., Graham, W.V., Siccardi, D., Turner, J.R. & Mrsny, R.J. (2005) A strategy to identify stable membrane-permeant peptide inhibitors of myosin light chain kinase. *Pharm Res,* **22,** 703-709.

Pappenheimer, J.R. & Reiss, K.Z. (1987) Contribution of solvent drag through intercellular junctions to absorption of nutrients by the small intestine of the rat. *J Membr Biol,* **100,** 123-136.

Pasder, O., Shpungin, S., Salem, Y., Makovsky, A., Vilchick, S., Michaeli, S., Malovani, H. & Nir, U. (2006) Downregulation of Fer induces PP1 activation and cell-cycle arrest in malignant cells. *Oncogene,* **25,** 4194-4206.

Patterson, R.L., van Rossum, D.B., Nikolaidis, N., Gill, D.L. & Snyder, S.H. (2005) Phospholipase C-gamma: diverse roles in receptor-mediated calcium signaling. *Trends Biochem Sci,* **30,** 688-697.

Pauletti, G.M.T., Gangwar, S., Siahaan, T.J., Aube, J. & Borchardt, R.T. (1997) Improvement of oral peptide bioavailability: Peptidomimetics and prodrug strategies. *Adv Drug Deliv Rev,* **27,** 235-256.

Pearson, R.B., Woodgett, J.R., Cohen, P. & Kemp, B.E. (1985) Substrate specificity of a multifunctional calmodulin-dependent protein kinase. *J Biol Chem,* **260,** 14471-14476.

Peterson, M.D. & Mooseker, M.S. (1992) Characterization of the enterocyte-like brush border cytoskeleton of the C2BBe clones of the human intestinal cell line, Caco-2. *J Cell Sci,* **102 (Pt 3),** 581-600.

Podolsky, D.K. (2002) Inflammatory bowel disease. *N Engl J Med,* **347,** 417-429.

Pooga, M., Hallbrink, M., Zorko, M. & Langel, U. (1998) Cell penetration by transportan. *Faseb J,* **12,** 67-77.

Quaroni, A. & Hochman, J. (1996) Development of intestinal cell culture models for drug transport and metabolism studies. *Adv Drug Deliv Rev,* **22,** 3-52.

Ranaldi, G., Marigliano, I., Vespignani, I., Perozzi, G. & Sambuy, Y. (2002) The effect of chitosan and other polycations on tight junction permeability in the human intestinal Caco-2 cell line(1). *J Nutr Biochem,* **13,** 157-167.

Rampton, D.S. (1999) Management of Crohn's disease. *Bmj,* **319,** 1480-1485.

Reinhardt, R.L., Kang, S.J., Liang, H.E. & Locksley, R.M. (2006) T helper cell effector fates--who, how and where? *Curr Opin Immunol,* **18,** 271-277.

Richard, J.P., Melikov, K., Vives, E., Ramos, C., Verbeure, B., Gait, M.J., Chernomordik, L.V. & Lebleu, B. (2003) Cell-pentrating peptides a reevaluation of the mechanism of cellular uptake. *The Journal of Biological Chemistry,* **278,** 585-590.

Rizzello, F., Gionchetti, P., Venturi, A. & Campieri, M. (2003) Review article: medical treatment of severe ulcerative colitis. *Aliment Pharmacol Ther,* **17 Suppl 2,** 7-10.

Romagnani, P., Annunziato, F., Baccari, M.C. & Parronchi, P. (1997) T cells and cytokines in Crohn's disease. *Curr Opin Immunol,* **9,** 793-799.
Rutgeerts, P.J. (2001) Review article: the limitations of corticosteroid therapy in Crohn's disease. *Aliment Pharmacol Ther,* **15,** 1515-1525.

Saitou, M., Fujimoto, K., Doi, Y., Itoh, M., Fujimoto, T., Furuse, M., Takano, H., Noda, T. & Tsukita, S. (1998) Occludin-deficient embryonic stem cells can differentiate into polarized epithelial cells bearing tight junctions. *J Cell Biol,* **141,** 397-408.

Sawada, T., Ogawa, T., Tomita, M., Hayashi, M. & Awazu, S. (1991) Role of paracellular pathway in nonelectrolyte permeation across rat colon epithelium enhanced by sodium caprate and sodium caprylate. *Pharm Res,* **8,** 1365-1371.

Schipper, N.G., Olsson, S., Hoogstraate, J.A., deBoer, A.G., Varum, K.M. & Artursson, P. (1997) Chitosans as absorption enhancers for poorly absorbable drugs 2: mechanism of absorption enhancement. *Pharm Res,* **14,** 923-929.

Schipper, N.G., Varum, K.M. & Artursson, P. (1996) Chitosans as absorption enhancers for poorly absorbable drugs. 1: Influence of molecular weight and degree of acetylation on drug transport across human intestinal epithelial (Caco-2) cells. *Pharm Res,* **13,** 1686-1692.

Schirmbeck, R., Riedl, P., Zurbriggen, R., Akira, S. & Reimann, J. (2003) Antigenic epitopes fused to cationic peptide bound to oligonucleotides facilitate Toll-like receptor 9-dependent, but CD4+ T cell help-independent, priming of CD8+ T cells. *J Immunol,* **171,** 5198-5207.

Schneeberger, E.E. & Lynch, R.D. (2004) The tight junction: a multifunctional complex. *Am J Physiol Cell Physiol,* **286,** C1213-1228.

Schwarze, S.R., Ho, A., Vocero-Akbani, A. & Dowdy, S.F. (1999) In vivo protein transduction: delivery of a biologically active protein into the mouse. *Science,* **285,** 1569-1572.

Shanahan, F. (2002) Crohn's disease. *Lancet,* **359,** 62-69.

Shimazaki, T., Tomita, M., Sadahiro, S., Hayashi, M. & Awazu, S. (1998) Absorption-enhancing effects of sodium caprate and palmitoyl carnitine in rat and human colons. *Dig Dis Sci,* **43,** 641-645.

Simon, D.B., Lu, Y., Choate, K.A., Velazquez, H., Al-Sabban, E., Praga, M., Casari, G., Bettinelli, A., Colussi, G., Rodriguez-Soriano, J., McCredie, D., Milford, D., Sanjad, S. & Lifton, R.P. (1999) Paracellin-1, a renal tight junction protein required for paracellular Mg2+ resorption. *Science,* **285,** 103-106.

Smith, J., Wood, E. & Dornish, M. (2004) Effect of chitosan on epithelial cell tight junctions. *Pharm Res,* **21,** 43-49.

Smith, J.M., Dornish, M. & Wood, E.J. (2005) Involvement of protein kinase C in chitosan glutamate-mediated tight junction disruption. *Biomaterials,* **26,** 3269-3276.

Soderling, T.R. & Stull, J.T. (2001) Structure and regulation of calcium/calmodulin-dependent protein kinases. *Chem Rev,* **101,** 2341-2352.

Somlyo, A.P. (1997) Signal transduction. Rhomantic interludes raise blood pressure. *Nature,* **389,** 908-909, 911.

Somlyo, A.P. & Somlyo, A.V. (2003) Ca2+ sensitivity of smooth muscle and nonmuscle myosin II: modulated by G proteins, kinases, and myosin phosphatase. *Physiol Rev,* **83,** 1325-1358.

Spring, K.R. (1998) Routes and mechanism of fluid transport by epithelia. *Annu Rev Physiol,* **60,** 105-119.

Srinivas, S.P., Satpathy, M., Guo, Y. & Anandan, V. (2006) Histamine-induced phosphorylation of the regulatory light chain of myosin II disrupts the barrier integrity of corneal endothelial cells. *Invest Ophthalmol Vis Sci,* **47,** 4011-4018.

Stancovski, I. & Baltimore, D. (1997) NF-kappaB activation: the I kappaB kinase revealed? *Cell,* **91,** 299-302.

Stevenson, B.R. & Keon, B.H. (1998) The tight junction: morphology to molecules. *Annu Rev Cell Dev Biol,* **14,** 89-109.

Stevenson, B.R. & Paul, D.L. (1989) The molecular constituents of intercellular junctions. *Curr Opin Cell Biol,* **1,** 884-891.

Stull, J.T., Hsu, L.C., Tansey, M.G. & Kamm, K.E. (1990) Myosin light chain kinase phosphorylation in tracheal smooth muscle. *J Biol Chem,* **265,** 16683-16690.

Suenaert, P., Bulteel, V., Lemmens, L., Noman, M., Geypens, B., Van Assche, G., Geboes, K., Ceuppens, J.L. & Rutgeerts, P. (2002) Anti-tumor necrosis factor treatment restores the gut barrier in Crohn's disease. *Am J Gastroenterol,* **97,** 2000-

2004.

Suzuki, T., Futaki, S., Niwa, M., Tanaka, S., Ueda, K. & Sugiura, Y. (2002) Possible existence of common internalization mechanisms among arginine-rich peptides. *J Biol Chem,* **277,** 2437-2443.

Takahashi, Y., Kondo, H., Yasuda, T., Watanabe, T., Kobayashi, S. & Yokohama, S. (2002) Common solubilizers to estimate the Caco-2 transport of poorly water-soluble drugs. *Int J Pharm,* **246,** 85-94.

Tanaka, M., Ikebe, R., Matsuura, M. & Ikebe, M. (1995) Pseudosubstrate sequence may not be critical for autoinhibition of smooth muscle myosin light chain kinase. *Embo J,* **14,** 2839-2846.

Tang, V.W. & Goodenough, D.A. (2003) Paracellular ion channel at the tight junction. *Biophys J,* **84,** 1660-1673.

Terrak, M., Kerff, F., Langsetmo, K., Tao, T. & Dominguez, R. (2004) Structural basis of protein phosphatase 1 regulation. *Nature,* **429,** 780-784.

Thanou, M., Verhoef, J.C. & Junginger, H.E. (2001) Oral drug absorption enhancement by chitosan and its derivatives. *Adv Drug Deliv Rev,* **52,** 117-126.

Thanou, M.M., Kotze, A.F., Scharringhausen, T., Luessen, H.L., de Boer, A.G., Verhoef, J.C. & Junginger, H.E. (2000) Effect of degree of quaternization of N-trimethyl chitosan chloride for enhanced transport of hydrophilic compounds across intestinal caco-2 cell monolayers. *J Control Release,* **64,** 15-25.

Tinsley, J.H., Teasdale, N.R. & Yuan, S.Y. (2004) Myosin light chain phosphorylation and pulmonary endothelial cell hyperpermeability in burns. *Am J Physiol Lung Cell Mol Physiol,* **286,** L841-847.

Toms, C. & Powrie, F. (2001) Control of intestinal inflammation by regulatory T cells. *Microbes Infect,* **3,** 929-935.

Tsukita, S. & Furuse, M. (1999) Occludin and claudins in tight-junction strands: leading or supporting players? *Trends Cell Biol,* **9,** 268-273.

Turner, J.R. (2000a) 'Putting the squeeze' on the tight junction: understanding cytoskeletal regulation. *Semin Cell Dev Biol,* **11,** 301-308.

Turner, J.R. (2000b) Show me the pathway! Regulation of paracellular permeability by Na(+)-glucose cotransport. *Adv Drug Deliv Rev,* **41,** 265-281.

Turner, J.R., Angle, J.M., Black, E.D., Joyal, J.L., Sacks, D.B. & Madara, J.L. (1999) PKC-dependent regulation of transepithelial resistance: roles of MLC and MLC kinase. *Am J Physiol,* **277,** C554-562.

Turner, J.R., Rill, B.K., Carlson, S.L., Carnes, D., Kerner, R., Mrsny, R.J. & Madara, J.L. (1997) Physiological regulation of epithelial tight junctions is associated with myosin light-chain phosphorylation. *Am J Physiol,* **273,** C1378-1385.

VanRenterghem, B., Browning, M.D. & Maller, J.L. (1994) Regulation of mitogen-activated protein kinase activation by protein kinases A and C in a cell-free system. *J Biol Chem,* **269,** 24666-24672.

Vergnolle, N. (2000) Review article: proteinase-activated receptors - novel signals for gastrointestinal pathophysiology. *Aliment Pharmacol Ther,* **14,** 257-266.

Vives, E., Brodin, P. & Lebleu, B. (1997) A truncated HIV-1 Tat protein basic domain rapidly translocates through the plasma membrane and accumulates in the cell nucleus. *J Biol Chem,* **272,** 16010-16017.

Wang, W. (1996) Oral protein drug delivery. *J Drug Target,* **4,** 195-232.

Ward, P.D., Tippin, T.K. & Thakker, D.R. (2000) Enhancing paracellular permeability by modulating epithelial tight junctions. *PSTT,* **3,** 346-358.

Wender, P.A., Mitchell, D.J., Pattabiraman, K., Pelkey, E.T., Steinman, L. & Rothbard, J.B. (2000) The design, synthesis, and evaluation of molecules that enable or enhance cellular uptake: peptoid molecular transporters. *Proc Natl Acad Sci USA,* **97,** 13003-13008.

Wilcox, E.R., Burton, Q.L., Naz, S., Riazuddin, S., Smith, T.N., Ploplis, B., Belyantseva, I., Ben-Yosef, T., Liburd, N.A., Morell, R.J., Kachar, B., Wu, D.K., Griffith, A.J. & Friedman, T.B. (2001) Mutations in the gene encoding tight junction claudin-14 cause autosomal recessive deafness DFNB29. *Cell,* **104,** 165-172.

Williams, F.M. (1985) Clinical significance of esterases in man. *Clin* Pharmacokinet, **10,** 392-403.

Wittchen, E.S., Haskins, J. & Stevenson, B.R. (1999) Protein interactions at the tight junction. Actin has multiple binding partners, and ZO-1 forms independent complexes with ZO-2 and ZO-3. *J Biol Chem,* **274,** 35179-35185.

Woodley, J.F. (1994) Enzymatic barriers for GI peptide and protein delivery. *Crit Rev Ther Drug Carrier Syst,* **11,** 61-95.

Youakim, A. & Ahdieh, M. (1999) Interferon-gamma decreases barrier function in T84 cells by reducing ZO-1 levels and disrupting apical actin. *Am J Physiol,* **276,** G1279-1288.

Yuhan, R., Koutsouris, A., Savkovic, S.D. & Hecht, G. (1997) Enteropathogenic Escherichia coli-induced myosin light chain phosphorylation alters intestinal epithelial permeability. *Gastroenterology,* **113,** 1873-1882.

Zolotarevsky, Y., Hecht, G., Koutsouris, A., Gonzalez, D.E., Quan, C., Tom, J.,

Mrsny, R.J. & Turner, J.R. (2002) A membrane-permeant peptide that inhibits MLC kinase restores barrier function in in vitro models of intestinal disease. *Gastroenterology,* **123,** 163-172.

Zweibaum, A., Pinto, M., Chevalier, G., Dussaulx, E., Triadou, N., Lacroix, B., Haffen, K., Brun, J.L. & Rousset, M. (1985) Enterocytic differentiation of a subpopulation of the human colon tumor cell line HT-29 selected for growth in sugar-free medium and its inhibition by glucose. *J Cell Physiol,* **122,** 21-29.

# Appendix

**Publications**

Owens, S.E., Graham, W.V., Siccardi, D., Turner, J.R. & Mrsny, R.J. (2005) A strategy to identify stable membrane-permeant peptide inhibitors of myosin light chain kinase. *Pharm Res*, **22**, 703-709.

**Abstracts presented orally**

Owens, S.E., Graham, W.V., Siccardi, D., Turner, J.R. & Mrsny, R.J. Welsh School of Pharmacy Postgraduate Research Day (2005). A strategy to identify stable membrane-permeant peptide inhibitors of myosin light chain kinase (oral presentation).

Owens, S.E. & Mrsny, R.J. Cardiff Institute of Tissue Engineering and Repair Annual Meeting (2004). Synthesis of a stable epithelial tight junction myosin light chain kinase inhibitor (oral presentation).

**Abstracts presented as posters**

Owens, S.E., Graham, W.V., Siccardi, D., Turner, J.R. & Mrsny, R.J. 32nd Annual Meeting and Exposition of the Controlled Release Society (2005). A strategy to identify stable membrane-permeant peptide inhibitors of myosin light chain kinase (poster presentation).

Owens, S.E & Mrsny, R.J. Welsh School of Pharmacy Postgraduate Research Day (2004). Assessment of the degradation of a tight junction myosin light chain kinase inhibitor (poster presentation).